

University of South Wales



2064849

NMR STUDIES OF MODEL MEMBRANES
INTERACTION WITH METAL IONS, IONOPHORES
AND GENERAL ANAESTHETICS

IAN CLIVE JONES, B.Sc.

A THESIS SUBMITTED TO THE COUNCIL FOR NATIONAL
ACADEMIC AWARDS FOR THE DEGREE OF
DOCTOR OF PHILOSOPHY

DEPARTMENT OF SCIENCE
THE POLYTECHNIC OF WALES
MAY 1984

DECLARATION

This thesis has not been nor is being currently submitted for the award of any other degree or similar qualification.

I. C. Jones

I. C. JONES

ACKNOWLEDGEMENTS

I would like to thank Dr. G. R. A. Hunt, my director of studies, for his encouragement and excellent guidance throughout this project. I would also like to thank all the staff of the science department, both technical and academic, for their assistance during my studies.

NMR STUDIES ON MODEL MEMBRANES. INTERACTION WITH METAL IONS, IONOPHORES
AND GENERAL ANAESTHETICS

I. C. JONES

ABSTRACT

Nuclear magnetic resonance spectroscopy in conjunction with lanthanide probe ions was used to investigate the interaction of phospholipid vesicles with membrane active compounds such as ionophores, anaesthetics, surfactants and metal ions.

In chapter 1 an introduction to the NMR technique and current progress in the field of model and biological membranes was given. In chapter 2 it was shown that pulsed NMR techniques gave insight to the effects of calcium, magnesium and lanthanide ions on the motional and physical properties of phospholipid molecules in vesicles.

Membrane permeability induced by both carrier and channel type ionophores was studied in chapter 3. The kinetics of Pr^{3+} transport induced by alamethicin 30, A23187, bile salts and phospholipase A_2 was investigated by following time dependent changes in the ^1H -NMR spectrum of phospholipid vesicles. The mechanisms involved in the permeability induced by the bile salts and phospholipase was shown to be critical when considering liposomes as carriers of therapeutic drugs delivered by the oral route.

The observation that ethanol and diethyl ether increased the degree of fusion and permeability induced by channels, while chloroform inhibited them suggested a common locus of action on the properties and structure of channel-associated water. These results were discussed in terms of the current theories of general anaesthesia. The influence of cholesterol on the transport properties of alamethicin in the absence and presence of ethanol and chloroform also emphasized the importance of hydrogen-bonds.

The preparation of large unilamellar vesicles by detergent removal gave rise to leaky vesicles. This was attributed to the incomplete removal of detergent by the dialysis method. More efficient methods for their preparation were discussed.

TABLE OF CONTENTS

	Page
LIST OF TABLES	viii
LIST OF FIGURES	ix
LIST OF ABBREVIATIONS	xv
 <u>CHAPTER 1</u>	
<u>GENERAL INTRODUCTION</u>	
1.1 Biomembranes	1
1.1.1 Composition	1
1.1.1 Membrane proteins	2
1.1.3 Membrane lipids	4
1.1.3.1 Structure of membrane lipids	4
1.1.3.2 Lyotropic and polymorphic properties of phospholipids	8
1.1.3.3 Order, fluidity and phase transitions	11
1.1.3.3.1 Types of motion in lipid bilayers	12
1.1.3.3.2 Factors influencing the phase transition temperature	19
1.1.3.3.3 The pre-transition	25
1.1.4 Structural Organisation – Membrane models	27
1.1.5 Model membranes	33
1.1.5.2 Spherically closed bilayers	34
1.1.5.2.1 Liposomes	34
1.1.5.2.2 Vesicles	35
1.1.5.2.3 Large unilamellar vesicles	36
1.1.6 Asymmetry in membranes	37
1.2 NMR of membranes	40
1.2.1 NMR theory in brief	40

1.2.2	NMR in the study of biomembranes	45
1.2.3	Use of lanthanide shift reagents in conjunction with NMR	49
1.2.4	Lanthanides as calcium probes	50
1.3	Ionophores and membrane permeability	52
1.3.1	Carrier type ionophores	55
1.3.2	Channel forming ionophores	57
1.4	Non bilayer phases	60
1.5	General anaesthetics	69
1.5.1	Molecular mechanisms of general anaesthesia . . .	70
1.5.1.1	Hydrophilic theories	70
1.5.1.2	Critical volume hypothesis	72
1.5.1.3	Lipid fluidity theories	73
1.5.1.4	Lipid phase transition theories	73
1.5.1.5	Degenerate protein perturbation hypothesis	74
1.5.1.6	Other theories	75
1.6	Cholesterol and membranes	76
<u>CHAPTER 2</u>	<u>CATION – MEMBRANE INTERACTIONS BY NMR</u>	
2.1	Introduction	82
2.1.1	Spin-lattice and spin-spin relaxation	84
2.1.2	Relaxation and molecular mobility.	86
2.1.3	The NMR timescale	87
2.2	Materials and methods	91
2.2.1	Chemicals	91
2.2.2	Preparation of vesicles	91
2.2.3	NMR spectroscopy	92
2.2.4	Sizing of sonicated vesicles	92

2.2.5	Variable temperature experiments	93
2.3	Results and Discussion	94
2.3.1	Determination of size and number of vesicles . . .	94
2.3.2	Cation membrane interaction by NMR relaxation studies	100
<u>CHAPTER 3</u>	<u>MEMBRANE PERMEABILITY</u>	
3.1	Introduction	114
3.2	Materials and Methods	129
3.2.1	Chemicals	129
3.2.2	Preparation of vesicles	130
3.2.3	Methods of introducing membrane active substances to vesicular solutions	130
3.2.4	Vesicles prepared by cosonication of DPPC and alamethicin 30	131
3.2.5	Method of lysing DPPC vesicles	132
3.2.6	Ionophore mediated transport of paramagnetic lanthanide ions as monitored by ^1H -NMR	132
3.2.7	Calibration graphs	133
3.3	Experimental Results	137
3.3.1	Alamethicin mediated transport of paramagnetic ions into phospholipid vesicles	137
3.3.1.1	Alamethicin channel stoichiometry in DPPC and egg PC vesicles	140
3.3.1.2	Activation energy for alamethicin transport in DPPC and egg PC vesicles	144
3.3.1.3	Alamethicin transport in mixed lipid vesicles . .	144
3.3.1.4	Calcium antagonists and alamethicin channels . . .	153
3.3.2	The phase transition and membrane permeability . .	155

3.3.3	The effect of bile salts and phospholipase A ₂ on egg PC vesicles	159
3.4	Discussion	172
3.4.1	Alamethicin mediated transport in DPPC and egg PC vesicles	172
3.4.1.1	The effect of mixed lipids on alamethicin transport	177
3.4.1.2	The effects of the calcium antagonists on alamethicin transport	179
3.4.2	Membrane permeability induced at the phase transition	180
3.4.3	Effects of bile salts and phospholipase A ₂ on egg PC vesicles	181
<u>CHAPTER 4</u>	<u>GENERAL ANAESTHETICS</u>	
4.1	Introduction	187
4.2	Materials and Methods	190
4.2.1	Chemicals	190
4.2.2	Incubations with phospholipid vesicles	190
4.2.3	Analysis of membrane fusion	191
4.3	Experimental Results	193
4.3.1	The effect of general anaesthetics on the ¹ H-NMR spectrum and phase transition of DPPC vesicles . .	193
4.3.2	The effects of general anaesthetics on vesicular lysis induced at the phase transition	196
4.3.3	The effects of general anaesthetics on channel mediated transport by alamethicin and on carrier mediated transport by A23187 and ionomycin	199

4.3.4	The effect of ethanol and chloroform on the activity of bile salts in egg PC vesicles	201
4.3.5	The effect of general anaesthetics on channel mediated transport and fusion in mixed lipid vesicles and on chemically induced fusion of DPPC vesicles	204
4.3.6	Effect of diazepam on alamethicin and phase transition channels in DPPC vesicles	208
4.4	Discussion	212
<u>CHAPTER 5</u>	<u>CHOLESTEROL AND MEMBRANES</u>	
5.1	Introduction	219
5.2	Materials and Methods	223
5.2.1	Chemicals	223
5.2.2	Preparation of vesicles	223
5.2.3	Lysis and transport processes	223
5.3	Experimental Results	225
5.3.1	The effect of cholesterol on alamethicin induced transport in DPPC and egg PC vesicles	225
5.3.2	The effect of ethanol and chloroform on the alamethicin transport rates in DPPC/cholesterol and egg PC/cholesterol vesicles	225
5.3.3	The effect of cholesterol on the transport and lytic rates induced by bile salts in egg PC vesicles	233
5.4	Discussion	236
5.4.1	Effect of cholesterol on the alamethicin transport rate	236

5.4.2	Effect of ethanol and chloroform on the alamethicin transport rate in vesicles containing cholesterol	238
5.4.3	Effect of cholesterol on bile salt activity . . .	239
<u>CHAPTER 6</u>	<u>THE PREPARATION AND USE OF LARGE UNILAMELLAR VESICLES</u>	
6.1	Introduction	242
6.2	Materials and Methods	246
6.2.1	Chemicals	246
6.2.2	Experimental procedure	246
6.3	Experimental Results	248
6.4	Discussion	252
<u>CHAPTER 7</u>	<u>GENERAL CONCLUSION</u>	255
REFERENCES	257

APPENDIXES

A. CALCULATION OF THE % LYSIS FROM THE O:I RATIO AND
CALCULATION OF THE % FUSION FROM THE PEAK WIDTH OF THE
HYDROCARBON SIGNAL.

B. POSTER PAPERS AND ORAL COMMUNICATIONS PRESENTED AT
MEETINGS.

C. PUBLISHED PAPERS

Hunt G R A and Jones I C (1982). Lanthanide ion transport
across phospholipid vesicular membranes: a comparison of
alamethicin 30 and A23187 using ¹H-NMR spectroscopy.
Bioscience Reports, 2, 921-928.

Hunt G R A and Jones I C (1983). A ^1H -NMR investigation of the effects of ethanol and general anaesthetics on ion channels and membrane fusion using unilamellar phospholipid membranes. *Biochimica et Biophysica Acta*, 736, 1-10.

Hunt G R A and Jones I C (1984). Application of ^1H -NMR to the design of liposomes for oral use. Synergistic activity of bile salts and pancreatic phospholipase A_2 in the induced permeability of small unilamellar phospholipid vesicles. *Journal of Microencapsulation* (in press).

Hunt G R A, Jones I C and Veiro J A (1984). Phosphatidic acid regulates the activity of the channel-forming ionophores alamethicin, melittin and nystatin. A ^1H -NMR study using phospholipid membranes. *Bioscience Reports*, 4, 403-413.

LIST OF TABLES

<u>TABLE NO.</u>		<u>PAGE</u>
1.1a	Lipid classes	5
1.1b	Fatty acid composition	5
1.2	Factors influencing the phase transition temperature	22
1.3	Properties of various nuclei used in NMR studies of lipid membrane systems	46
3.1	Alamethicin transport rates in mixed lipid vesicles	151
3.2	Transport rates induced by phospholipase A ₂ and bile salts in egg PC vesicles	171
4.1	Effects of the general anaesthetics on the chemical shift, line width and relaxation times of the ¹ H-NMR signals from DPPC vesicles	194
4.2	Effect of various concentrations of ethanol and diazepam on the alamethicin transport rate in DPPC vesicles	211

LIST OF FIGURES

<u>FIGURE NO.</u>		<u>PAGE</u>
1.1	Structure of membrane lipids	6
1.2	Lyotropic properties of lipids	9
1.3	Lipid motion in bilayers	13
1.4	Fatty acid configurations	16
1.5	Phase transition	26
1.6	Davson-Danielli and Robertson models of membranes	29
1.7	Fluid Mosaic model of membranes	32
1.8	Diagrammatic representations of nuclear magnetization	43
1.9	Non bilayer phases in membranes	65
1.10	Metamorphic mosaic model of membranes	68
2.1	Principles in the measurement of T_1	88
2.2	Relation between rate of molecular motion and relaxation times	89
2.3	^1H -NMR spectra of DPPC vesicles in the presence of various ions	95
2.4	Temperature dependence of the methylene relaxation times in DPPC vesicles	101
2.5	The effects of Pr^{3+} and calcium on the temperature dependence of the methylene T_1	102
2.6	The effects of dysprosium, calcium and magnesium on the temperature dependence of the methylene T_1	104

2.7	The effects of Pr^{3+} and calcium on the temperature dependence of the methylene T_2 . .	105
2.8	The effects of dysprosium, calcium and magnesium on the temperature dependence of the methylene T_2	106
2.9	Effect of Pr^{3+} and Dy^{3+} on the temperature dependence of the inner and outer head group T_1	108
2.10	Effect of Pr^{3+} and Dy^{3+} on the temperature dependence of the inner and outer head group T_2	109
2.11	Effects of dysprosium, calcium and magnesium on the temperature dependence of the outer head group T_1	110
2.12	Effects of dysprosium, calcium and magnesium on the temperature dependence of the outer head group T_2	111
2.13	Effect of dysprosium, calcium and magnesium on the temperature dependence of the inner head group T_1	112
2.14	Effect of dysprosium, calcium and magnesium on the temperature dependence of the inner head group T_2	113
3.1	Various structures proposed for alamethicin .	116
3.2	Structure of the calcium antagonists and bile salts	122
3.3	Calibration graph for DPPC at 50°C	134

3.4	Calibration graph for egg PC at 37°C with Pr ³⁺ and Dy ³⁺	135
3.5	¹ H-NMR spectra monitoring the transport of Pr ³⁺ into DPPC vesicles	138
3.6	Effect of incubation on the rate of alamethicin transport	139
3.7	Effects of alamethicin disposition on its transport rate	141
3.8	Transport rate obtained by various alamethicin concentrations in DPPC and egg PC vesicles	142
3.9	Stoichiometry plot for alamethicin	143
3.10	Transport rates obtained by alamethicin at various temperatures in DPPC and egg PC vesicles	145
3.11	Arrhenius plot for alamethicin transport . .	146
3.12	Alamethicin transport in mixed DPPC/egg PC vesicles	147
3.13	Pr ³⁺ transport by alamethicin in mixed lipid vesicles	148
3.14	Dy ³⁺ transport by alamethicin in mixed lipid vesicles	149
3.15	¹ H-NMR spectrum of alamethicin transport in egg PC/PA vesicles	152
3.16	Effect of verapamil on alamethicin transport.	154
3.17	Effect of Niphedipine on alamethicin transport	156

3.18	^1H -NMR monitoring lysis of vesicles	157
3.19	Effect of Triton X100 on the degree of lysis in DPPC vesicles	158
3.20	^1H -NMR spectra showing the effects of glycocholate on egg PC vesicles	160
3.21	Transport rates induced by various bile salts in egg PC vesicles	162
3.22	Rates of lysis induced by bile salts in egg PC vesicles	163
3.23	Stoichiometry plot for glycocholate	164
3.24	^1H -NMR spectra following the action of phospholipase A_2	166
3.25	Transport rates induced by various concentrations of phospholipase A_2 in egg PC vesicles	167
3.26	Effects of bile salts on 28 units of phospholipase A_2 in egg PC vesicles	168
3.27	Effects of bile salts on 2 and 7 units of phospholipase A_2 in egg PC vesicles	169
4.1	The effects of general anaesthetics on the phase transition temperature of DPPC vesicles	195
4.2	Effect of the general anaesthetics on the lysis induced at the phase transition in DPPC vesicles	197
4.3	Effects of the general anaesthetics on lysis induced at the phase transition in DPPC vesicles in the presence of Triton X100 . . .	198

4.4	Effect of the general anaesthetics on the transport rate induced by alamethicin	200
4.5	Effect of the general anaesthetics on the transport rate induced by A23187 and ionomycin	202
4.6	The effects of the general anaesthetics on the transport and lytic rates induced by glycocholate in egg PC vesicles	203
4.7	The effects of ethanol and chloroform on non bilayer phase mediated transport and fusion in egg PC/PE vesicles	205
4.8	The effects of ethanol and chloroform on on non bilayer phase mediated transport and fusion in egg PC/CL vesicles	206
4.9	The effects of the general anaesthetics on the fusion of DPPC vesicles induced by Triton X100 and PEG	207
4.10	The effects of diazepam and ethanol on the degree of lysis induced at the phase transition	209
4.11	The effects of diazepam and ethanol on the alamethicin induced transport rate	210
5.1	¹ H-NMR spectrum of DPPC/25 mole % cholesterol vesicles	224
5.2	Effects of cholesterol on the alamethicin induced transport rate in DPPC vesicles	226

5.3	Effect of cholesterol on the alamethicin induced transport rate in egg PC vesicles . . .	227
5.4	Effect of ethanol and chloroform on the transport rate induced by alamethicin in DPPC/25 mole % cholesterol	228
5.5	Effects of ethanol and chloroform on the transport rate induced by alamethicin in DPPC/40 mole % cholesterol	230
5.6	Effect of ethanol and chloroform on the transport rate induced by alamethicin in egg PC/25 mole % cholesterol	231
5.7	Effect of ethanol and chloroform on the transport rate induced by alamethicin in egg PC/40 mole % cholesterol	232
5.8	Effect of cholesterol on the transport rate induced by various bile salts	234
5.9	Effect of cholesterol on the lytic rates induced by various bile salts	235
6.1	Electron micrograph of large unilamellar vesicles	249
6.2	^{31}P -NMR spectrum of large and small unilamellar vesicles	250
6.3	^{31}P -NMR spectrum of large unilamellar vesicles in the presence of 100 mM Pr^{3+} . . .	251

LIST OF ABBREVIATIONS

AIB	α - Amino isobutyric acid
Ala	Alanine
ATP	Adenosine triphosphate
ATPase	Adenosine triphosphatase
BLM	Black lipid membranes
CL	Cardiolipin
CSA	Chemical shift anisotropy
DPPC	Dipalmitoyl phosphatidylcholine
DSC	Differential scanning calorimetry
[Dy] _i	Intravesicular concentration of dysprosium ions
EIM	Excitability inducing material
EM	Electron microscopy
ESR	Electron spin resonance
Gln	Glutamine
Glu	Glutamic acid
Gly	Glycine
H _I	Hexagonal I phase
H _{II}	Hexagonal II phase
H-bonds	Hydrogen bonds
HPLC	High performance liquid chromatography
I	NMR signal from the vesicle inner monolayer head groups
Leu	Leucine
LUV	Large unilamellar vesicles
Lyso PC	1-Acyl lyso phosphatidylcholine
NMR	Nuclear magnetic resonance
O	NMR signal from the vesicle outer monolayer head groups

PA	Phosphatidic acid
PC	Phosphatidylcholine
PE	Phosphatidylethanolamine
PEG	Polyethylene glycol
PG	Phosphatidylglycerol
Phol	Phenyl alaninol
PI	Phosphatidylinositol
PLA ₂	Phospholipase A ₂
[Pr] _i	Intravesicular concentration of praseodymium ions
Pro	Proline
PS	Phosphatidylserine
SM	Sphingomyelin
T _c	Phase transition temperature
T _p	Pre-transition temperature
T ₁	Spin-lattice relaxation time
T ₂ or T ₂ [*]	Spin-spin relaxation time
Val	Valine

CHAPTER 1

GENERAL INTRODUCTION

1.1 Biomembranes

Biological membranes have been recognised to be complex structures with numerous functional roles, the properties of which keep living cells in harmony with their environment (Jain 1972, Houslay and Stanley 1982). For the past three decades the complexity of biological membranes has attracted the attention of intrigued scientists from a variety of disciplines and has resulted in the present expanding field of membranology. The greatest problem facing membranologists is that of correlating membrane structure and composition to their functional roles in living cells. Only by accomplishing this relationship may one then begin to understand more fully the interactions of biological membranes with various physiologically active molecules such as hormones, neurotransmitters, antibody-complement, metal ions and drugs.

Probably the main reason for the current excitement in the field of membranology is to be found in the great technical developments in instrumentation during the 1950's and 1960's which allowed more and more specific questions to be asked of more and more complex structures.

1.1.1 Composition

Cell membranes were first recognised by Schleiden and Shwann in 1839 and in 1840 Bowman with his sketches of the sarcolemma had depicted the biological membrane as an anatomical entity (Robertson 1981). By the end of the last century the work of Bernstein on the cellular penetrating properties of lipid soluble substances inspired Overton to predict that a barrier of lipid surrounded the protoplasm

(Hendler 1971). In the period 1932-34 surface tension experiments on egg membranes revealed a much lower value than predicted for pure lipid membranes and was referred to as the Devaux effect. This property in conjunction with the observation that spontaneous association of water soluble proteins occurred with monolayers of lipid led to the speculation that proteins were included in cell membranes.

It is currently accepted that biological membranes are composed mainly of an association between varying amounts of lipid and protein, with carbohydrate being present in small amounts. The protein:lipid ratio varies from 80% protein in metabolically active membranes to 20% in insulating role membranes such as myelin (Hendler 1971), whilst more balanced quantities (Foot et al 1982) are found in rat brain synaptosomes (64%), rabbit muscle microsomes (54%) and human erythrocytes (60%).

1.1.2 Membrane Proteins

Membrane proteins have been characterised by using the anionic detergent sodium dodecyl sulphate (SDS) which disaggregates them from their associated lipids, the mixture then being electrophoresed on polyacrylamide gel (Gomperts 1977). The quantity of associated anionic detergent allows the proteins to be separated according to their size.

The requirement of detergent for the solubilization of various proteins led to the conclusion that a considerable area of their surface had to be apolar in character. Dialysis experiments have shown that these proteins are unstable without bound detergent or lipid molecules and the area of their hydrophobic surface has been measured using radioactively labelled detergents (Houslay and Stanley 1982). This evidence in conjunction with freeze-fracture etch studies on biological

membranes (Bayer and Remsen 1970) led to membrane proteins being classified as either peripheral or integral. Proteins which may be washed off the membrane using low and high ionic strength buffers are called peripheral or surface proteins (for example, cytochrome C), whereas those requiring detergent or organic solvent for extraction are called integral or intrinsic proteins (for example, glycophorin).

Enzyme hydrolysis and radioactive labelling experiments have shown that some integral proteins span the membrane implying that they have hydrophilic amino acids residues on both sides of the membrane separated by a hydrophobic sequence embedded in the hydrocarbon region (Singer and Nicolson 1972). The only unfavorable contacts between the hydrophobic peptide and the hydrocarbon region of the membrane lipids are the carbonyl and amino groups of the peptide linkages. The studies of Glaser and Singer (1971) suggested that this problem is solved by intramolecular hydrogen bonding (H-bonding) which stabilize the peptides in helical or globular conformation. Singer and Nicolson (1972) using the above evidence proposed a difference in the role between integral and peripheral proteins and postulated that only integral proteins are critical to the structural integrity of the membrane.

Protein lipid interactions have been extensively studied by nuclear magnetic resonance (NMR) and electron spin resonance (ESR) spectroscopy in model and biological membranes. This is mainly due to the possibility that a specific annulus lipid is associated with protein activity (Racker 1972, Chapman 1982, Sandermann 1978, Katsikas and Quinn 1981). The different results obtained by the NMR and ESR methods are a consequence of time scales and are outlined in chapter 2.

1.1.3 Membrane Lipids

Cell membranes in animals generally contain three types of lipids; phospholipids, glycolipids and sterols. A lipid analysis of rat brain synaptosomal membranes (Table 1.1a) shows the quantitative contribution of these lipid classes. They are all amphipathic molecules since each contains a hydrophilic head group and hydrophobic tail (Fig 1.1), giving them a common property in that they can be isolated from non-lipid material by extraction with a mixture of chloroform and methanol. They can then be separated into their various classes by chromatographic procedures. For a comprehensive review on animal cell lipid composition and extraction refer to Rouser et al (1968).

1.1.3.1 Structure of Membrane Lipids

The phospholipids are the most abundant lipids, there being three main types; glycerol phospholipids, sphingolipids and plasmalogens. The simplest phospholipid is phosphatidic acid (PA) which is a phosphorylated 1,2 diglyceride. The other glycerol phospholipids are most commonly named using "phosphatidyl" as a general term to indicate derivatives of PA. The structures of some glycerol phospholipids are illustrated in Fig 1.1a.

The hydrophobic moiety of these lipids is derived from two long chain fatty acid molecules, R_1 and R_2 which are esterified to the glycerol molecule at position 1 and 2 respectively. R_1 and R_2 may range in length from 12 to 24 carbon atoms. R_1 is generally saturated whilst R_2 , depending on its length, may contain up to six olefinic double bonds. Naturally occurring unsaturated fatty acids almost always contain cis double bonds. The variety of fatty acid chain length and unsaturation is illustrated in Table 1.1b which shows the fatty acid

Table 1.1

a. Lipid Classes Present in Rat Brain Synaptosomes

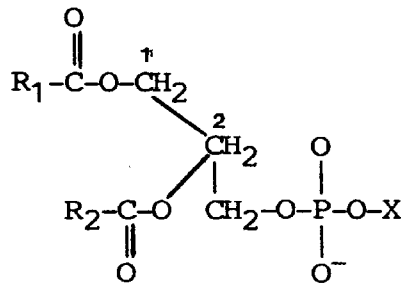
<u>Lipid</u>	<u>Amount Present(% wt/wt)</u>
Cholesterol	18.6
Glycolipids	0.9
Phosphatidyl choline	33.9
Phosphatidyl ethanolamine	28.2
Phosphatidyl serine	} 11.8
Phosphatidyl inositol	
Sphingomyelin	3.0

b. Fatty Acid Content of Rat Brain Synaptosomal Phospholipids

<u>Chain length and degree of unsaturation</u>	<u>Trivial name of fatty acid</u>	<u>Fatty acid content(% wt/wt)</u>		
		<u>PC</u>	<u>PE</u>	<u>PS+PI</u>
16:0	Palmitic	50.7	7.5	3.6
16:1	Palmitoleic	1.0	0.3	0.3
18:0	Stearic	12.6	23.7	40.8
18:1	Oleic	24.2	6.6	7.2
18:2	Linoleic	0.6	0.2	-
20:4	Arachidonic	5.6	18.0	10.0
22:6	-	3.4	32.9	32.2

Fig. 1.1

a) Structure of membrane lipids



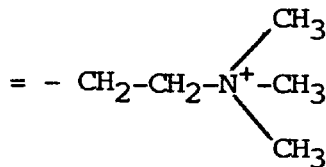
General structure of a
glycerol phospholipid

net charge at
neutral pH

X = - H

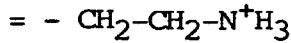
Phosphatidic acid
(PA)

negative



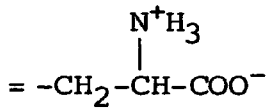
Phosphatidylcholine (PC)
(Lecithin)

neutral



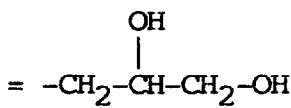
Phosphatidylethanolamine
(PE)

neutral



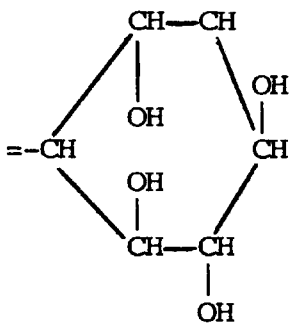
Phosphatidylserine (PS)

negative



Phosphatidylglycerol (PG)

negative

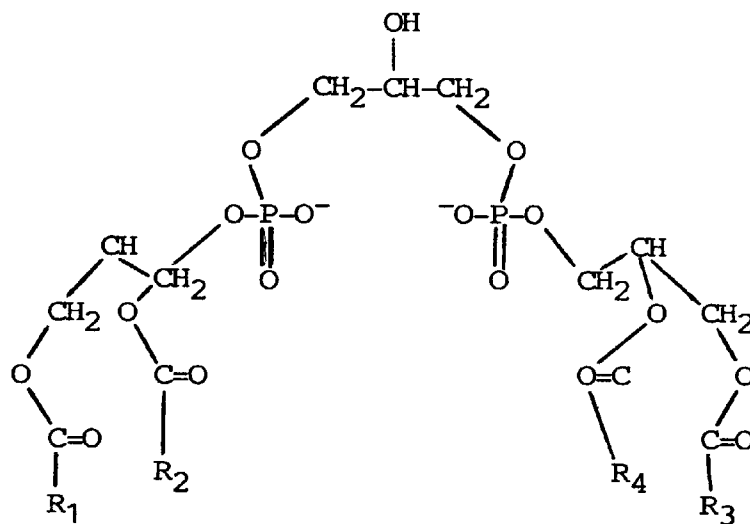


Phosphatidylinositol (PI)

negative

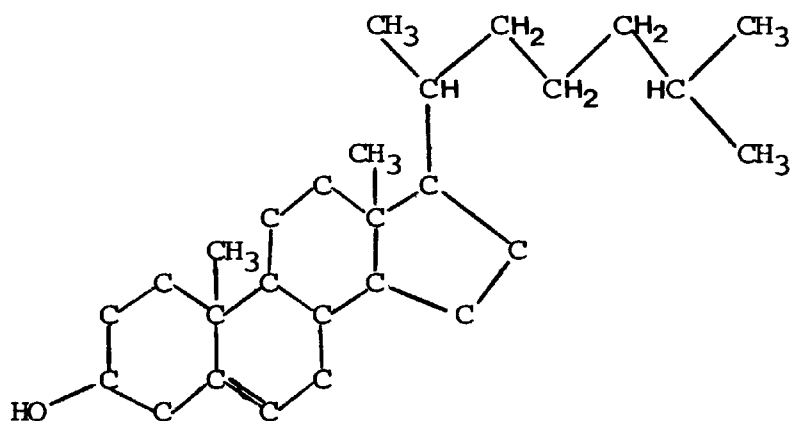
Lysolecithin is PC less the fatty acid esterified to the 2 position.

Fig 1.1 (cont.)



Dipalmitoylglycerol
Cardiolipin (CL)

b.
Structure of cholesterol



analysis of the phospholipids present in rat brain synaptosomal membranes (Cotman et al 1969).

The head groups of the glycerol phospholipids are polar containing the negative charge of the phosphate hydroxyl (pK 1-2) together with the charges and the polar groups of the bases. They vary in size, shape and can be charged or neutral at physiological pH (Fig 1.1a). The variability of head group and acyl chain moieties therefore give phospholipids a large range of properties.

Phosphatidyl choline (PC) is the predominant phospholipid in most mammalian membranes. It is a neutral zwitterion with its acyl chains most commonly being made up from esters of palmitic, stearic and oleic acids (Table 1.1a and 1.1b). Phosphatidyl ethanolamine (PE) is also a neutral zwitterion at physiological pH but above pH 9 the protonated amino group dissociates to give a negatively charged molecule. Phosphatidyl serine (PS) carries a net negative charge at neutral pH due to the positive amino group and negatively charged carboxyl and phosphate groups. Phosphatidyl glycerol (PG) and cardiolipin (CL) are negatively charged due to their phosphate groups.

1.1.3.2 Lyotropic and Polymorphic Properties of Phospholipids

By varying the concentration of phospholipids in water a variety of polymorphic phases are produced (Bangham 1968). Generally at low concentrations ($<10^{-6}\text{M}$), phospholipids give rise to monolayers at the air water interface (Fig 1.2a). The critical micellar concentration (cmc) is found to be very low for lipids ($10^{-6} - 10^{-5}\text{M}$) with the phospholipids having a natural tendency to aggregate into a number of defined phases above this concentration.

In the presence of less than 30% aqueous phase the phospholipids

Fig 1.2

Lyotropic Properties of Phospholipids

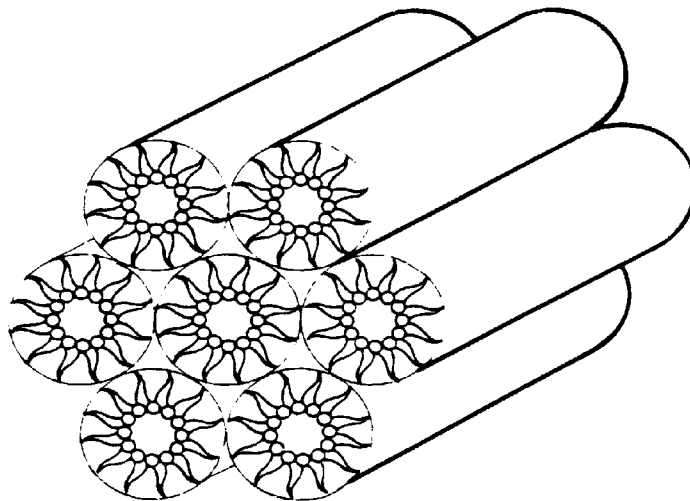
a. Monolayer at an air/water interface

AIR



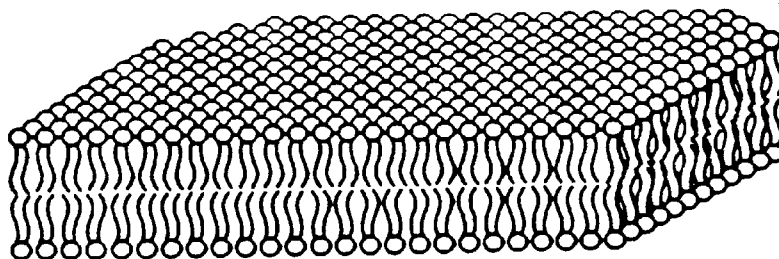
WATER

b.



HEXAGONAL PHASE

c.



BILAYER

aggregate as extended hexagonal structures in two dimensional arrays. The structural details of hexagonal phases were considered by analogy with soaps which have been extensively studied by X-ray diffraction methods (Luzzati 1968). There are two types of hexagonal phase which are referred to as hexagonal I (H_I) and hexagonal II (H_{II}) phases. However the majority of phospholipids take up the H_{II} phase which is composed of water filled, extended tubular structures (the tubes in hexagonal arrays) with the internal surface of the tubes lined with polar head groups (Fig 1.2b). With higher concentrations of water a lamellar or smectic mesophase is developed. Here the phospholipids form a bimolecular leaflet (bilayer) where the hydrated polar headgroups are at the lipid water interface while the hydrocarbon moieties occupy the centre of the bilayer (Fig 1.2c).

These phases are a consequence of the amphipathic nature of the phospholipids with the phase adopted being dependent on the lipid structure, ionic strength, pH and temperature (Cullis and De Kruijff 1979). Luzzati and coworkers established that the relative size of the hydrophilic and hydrophobic moieties was the most important factor in determining the adoption of a certain phase (Luzzati 1968, Luzzati et al 1966, Luzzati and Tardieu 1974). A relatively large hydrophilic group promotes conformations with large surface to volume ratios and vice versa. The stability of each phase is therefore influenced by head-group size and charge as well as the length and degree of unsaturation of the acyl chain moieties.

In this study the main concern lies with the bilayer phase but H_I and H_{II} phases are included when non bilayer phases are considered. The bilayer phase is adopted by lipids such as PC which has head group and

acyl chain moieties of comparable size (cylindrical). The H_{II} phase is preferred by lipids such as CL which possesses a head group moiety which is much smaller in cross section than its acyl chain moieties (cone shaped), whilst the micellar and H_1 phases are adopted by lipids such as lysolecithin (lyso PC) which has a head group moiety which is larger in cross section than its acyl chain moiety (inverted cone shape). Further discussions of non bilayer effects which have relevance to this study are given in section 1.4, chapter 3 and chapter 4.

1.1.3.3 Order, Fluidity and Phase Transitions

The order and fluidity of the constituent molecules of biological membranes are major factors in determining their functional properties (Lee 1975, Levine et al 1972, Seelig 1977, Jacobs and Oldfield 1981). When discussing these factors emphasis is largely placed on the lipid component since the most fruitful studies have been performed using simple lipid bilayers. Although the presence of proteins and other membrane components perturb the lipid bilayer, there is much evidence to suggest that the state of the lipids in these model systems is of relevance to the study of biological membranes.

Order can be described as an angular distribution of molecules (or groups within molecules) about a preferred molecular (or group) orientation. Order gives a measure of the degree of motional flexibility of a molecule or of various groups within a molecule (Seelig 1977, Jacobs and Oldfield 1981, Smith 1977, Smith 1979). These deviations from the more stable molecular conformations give rise to time averaged fluctuations a measure of which is given by order parameters obtained by techniques such as 2H -NMR and ESR. In 2H -NMR a order parameter value (S) is obtained from the quadrupole splitting which arises from the

orientation of the ^2H nucleus with respect to the molecular symmetry axis and to the degree of anisotropic motion (Seelig 1977, Jacobs and Oldfield 1981).

Fluidity refers to the rate of molecular motions such as rotations and translocations. Correlation times for these molecular motions are usually obtained by NMR relaxation time studies (T_1 and T_2). These values are dependent on the rate of molecular motion (Jacobs and Oldfield 1981) and are further discussed in section 1.2 and chapter 2.

X-ray studies revealed two phases for membrane lipids in lamellar form (Bangham 1968, Luzzati 1968, Luzzati et al 1966). Subsequent infra red studies showed that these phases were temperature dependent (Chapman et al 1967). The fluid form present at higher temperatures is referred to as the liquid crystal phase ($L\alpha$), whilst the stiffer form present at lower temperature is called the gel phase ($L\beta'$). The factors which influence the temperature at which this thermotropic gel to liquid crystal phase transition occurs are outlined in section 1.1.3.3.2.

The order and fluidity in each phase is determined by the types of motion that the lipid molecules can undergo.

1.1.3.3.1 Types of Motion in Lipid Bilayers

Phospholipids have several possible modes of motion (Fig 1.3) which determine the order and fluidity of the bilayer.

a. Translocation of the lipid molecules in the plane of the bilayer

Phospholipids can undergo lateral diffusion in the plane of the bilayer when they are in the liquid crystal phase. This property contributes to the fluidity of the bilayer, with the faster rates of lateral diffusion corresponding to more fluid bilayers. ESR and ^1H -NMR

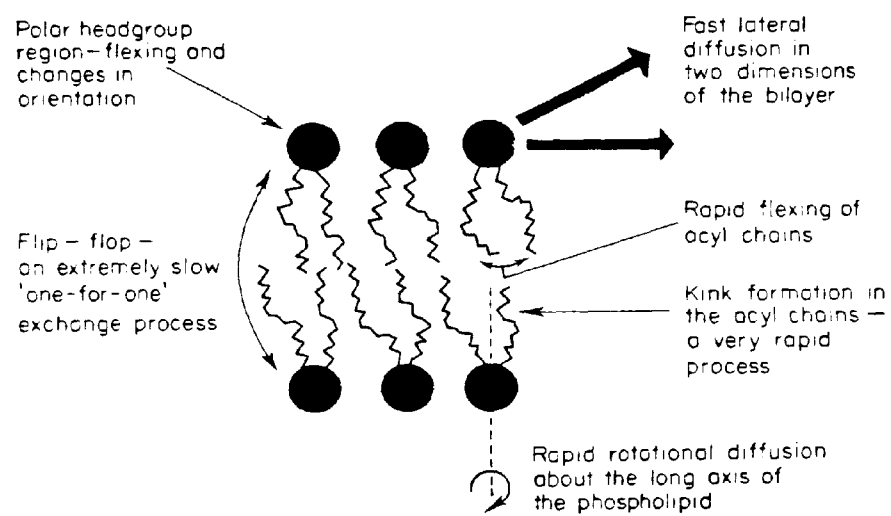


Fig 1.3 Modes of mobility of lipid molecules in the bilayer.

give self diffusion coefficients of the order of $10^{-8} \text{ cm}^2\text{s}^{-1}$ (Trauble and Sackmann 1972, Lee et al 1973). These values correspond to an interchange frequency of adjacent molecules of 10^7 times per second. Interestingly these measurements indicate that lipid molecules are capable of redistributing themselves rapidly over the surface of the membrane at a rate of 1000 nm/second and could therefore travel the length of an E. coli bacterium in about one second.

Phillips et al (1969) have shown that the fluidity of the acyl chains in lipid bilayers is approximately half that of long chain hydrocarbon solutions, and suggest that this difference is due to intermolecular interactions within the lipid bilayer.

A variety of models have been postulated to explain the molecular mechanism where by lipids undergo lateral diffusion. Perhaps the most plausible of these mechanisms is the one which involves migration of lipid molecules into vacant lattice sites (Lee et al 1974). Positron annihilation techniques have also detected the existence of vacancies in fluid bilayers and it is suggested that these could form transient pores to provide not only a means for lateral diffusion but a route for water diffusion across the bilayer (Houslay and Stanley 1982).

b. Internal motion within the lipid molecule

NMR relaxation measurements are capable of estimating the rates of rotation about the carbon-carbon (C-C) bonds within the fatty acyl chains, glycerol backbone and head group components of phospholipids in liquid crystal bilayers. The ^{13}C -NMR relaxation times for sonicated vesicles show very clearly that there is a gradient of internal motions within lipid molecules present in bilayers. There is a significant increase in mobility about C-C bonds on moving away from the glycerol

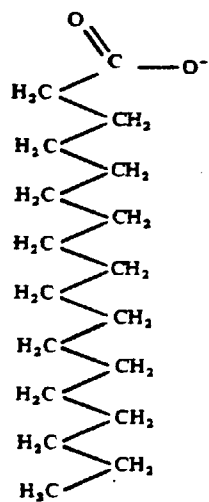
backbone, with the increase being most dramatic towards the terminal end of the fatty acyl chains, which are clearly undergoing extremely rapid motion (Jacobs and Oldfield 1981, Levine et al 1973). In part this pronounced motion is due to the motion of all the C-C bonds between it and the immobilized glycerol backbone (Levine et al 1972).

This flexibility gradient within lipid bilayers is described in terms of an order parameter (S) which measures the time averaged orientation of groups within the bilayer. ESR studies show that phospholipids with longer fatty acyl chains give rise to smaller S values which corresponds to an increasing amplitude of motion along the acyl chains (Hubbel and McConnell 1971, Seelig 1970). However S values obtained by ^2H -NMR (Seelig 1977) and T_1 's from ^{13}C -NMR (Lee 1975) are relatively constant over the the first 8-10 methylene groups from the glycerol moiety, and then change very rapidly as the carbon number increases. The discrepancy between NMR and ESR is attributed to the different time scales involved and to the spin label perturbing the bilayer in the latter. It is therefore the NMR data which gives a more realistic assessment of the microviscosity at various depths within the bilayer. In fact ^{13}C -NMRT $_1$ values show that the change in fluidity (rate of segmental motion) is confined to a narrow region in the centre of a fatty acyl chain (Lee 1975, Seelig 1977)

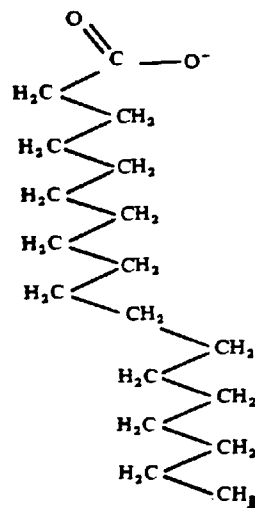
The order parameter yields quantitative estimation of the relative probabilities of possible C-C bond rotations along the fatty acyl chains. Each single bond rotation is a transition between stable rotational isomers, the trans (t) and gauche (g) conformations, with gauche being higher in energy. The creation of gauche conformers in the fatty acyl chains can give rise to large angular deviations from the all trans linear arrangement (Fig 1.4a) because a gauche isomer involves a

Fig 1.4 The rotational isomers of saturated fatty acyl chains

All Trans



One Gauche Rotomer



bond rotation of 120° from the more stable trans isomer. A rotation to the right is a g^+ isomer and a rotation to the left is a g^- isomer. The separate identification of these two forms is only possible by spectroscopic methods operating in the frequency region 10^{10} /sec because of the rapid interconversion of the different rotomers of the acyl chains.

In the gel phase the acyl chains are linear due to an all trans configuration (t_0) which gives the most ordered state. In the liquid crystal state there is less order towards the centre of the bilayer due to the decrease in t_0 and increase in t_{60} and g_{60} , where the subscripts 0 and 60 refer to the $-\text{CH}_2-\text{CH}_2-$ bond angle with respect to the plane of the bilayer. Order parameters obtained by ^2H NMR suggest that the formation of rotational isomers in the fatty acyl chains is not a simple process of isolated gauche isomer formation, but a cooperativity of isomer formation is involved in the all trans chains so that rotomers can form and at the same time disrupt the overall packing as little as possible (Seelig 1977).

One possible chain-chain interaction is the suggested formation of the so called "kink" structure which involves either a g^+tg^- sequence or a g^-tg^+ sequence of isomers (Fig 1.4a). The prominent feature of either conformational sequence is a shift of about 1.5\AA of a part of the chain sideways to its long molecular axis and at the same time the chain is shortened by one methylene unit (Lee 1975). The kink is not static but fluctuates up and down the chain with a certain life time. The formation of such kinks is found to be more probable in the central regions (C_8-C_{14}) of the chains (Seelig 1977, Seelig and Niederberger 1974).

c. Transfer of lipid molecules from one side of the bilayer to the other - (flip-flop)

This is a one for one exchange mechanism and thus the total amount of molecules in each monolayer remains constant. ESR studies have indicated that the rate of flip-flop is relatively slow. For spin labelled phospholipids in egg PC vesicles the rate of flip flop is of the order of once every 24 hours (Kornberg and McConnell 1971). More rapid flip-flop rates have been observed in natural membranes and in mixed lipid vesicles (McNamee and McConnell 1973, Cullis et al 1980a), where it is suggested they provide a mechanism of carrier mediated transport of ions in the form of inverted micelles (see section 1.4).

d. Axial rotation of whole lipid molecules

As well as motions about C-H and C-C bonds, lipid molecules undergo fast axial rotations in the liquid crystal phase (Seelig 1970). The axial rotation has been demonstrated for steroid spin labels of similar cross sectional area to phospholipids, and indicates that rotation takes place at about 10^8 times / second (Marsh 1975). The rates for spin labelled fatty acids and phospholipids give similar values (Seelig 1970, Hubbel and McConnell 1971). These factors therefore contribute to fluidity of membranes.

e. Flexing of acyl chains

This concerted pendulum like motion of the acyl chains affects the order of the methylene groups especially towards the centre of the bilayer. The order depends on the degree of swing whilst the rate or period of flexing effects the fluidity of the bilayer (Jacobs and Oldfield 1981).

1.1.3.3.2 Factors Influencing the Phase Transition Temperature

When anhydrous phospholipid is examined in the presence of increasing amounts of water the marked endothermic gel to liquid phase transition temperature (T_c) falls to a limiting value which becomes independent of water concentration (Chapman 1975, Levine 1973). The initial amount of water causes a reduction in the dispersion forces responsible for the tight packing of the solid phospholipid. When the limiting temperature, T_c , is reached water that can be frozen appears on the differential scanning calorimetry (DSC) curve at 0°C. Since biological membranes are invariably in a high state of hydration it is always this limiting value T_c that is referred to when discussing lipid bilayers. However the bound water that is not frozen is very important to natural membranes since it contributes strongly to the stability of the bilayer.

Only bilayers composed of a single type of phospholipid undergo a well defined phase transition. The transition in large unilamellar vesicles and multilamellar liposomes occurs over a temperature width of 1-2°C, but a much broader temperature range is observed in small vesicles (Lee 1975, also see chapter 2). At T_c a change of state occurs between the crystalline gel phase and the fluid liquid crystal phase. This is associated with a change in conformational freedom experienced by the fatty acyl chains (Chapman et al 1967). The hydrocarbon chains are said to have "melted" in the liquid crystal phase.

The temperature at which T_c takes place depends on :

- a. The length and degree of unsaturation of the fatty acyl chains (Chapman et al 1967).
- b. The size and charge of the polar head groups (Boggs 1980).
- c. Ionic concentration (Chapman and Urbina 1974, Trauble and Eibl

1974). This is considered further in chapter 2.

d. Concentration of sterols such as cholesterol (Lee 1975, Chapman 1975). This is discussed in section 1.6.

a.

In general T_c increases with increasing length of the fatty acyl chain and decreases with increasing unsaturation (Table 1.2a). In DSC a narrow transition is shown by a narrow endothermic peak at the transition temperature of phospholipid bilayers containing one or two similar fatty acyl chains. This is exemplified by dipalmitoyl phosphatidylcholine (DPPC) liposomes having a narrow peak at 41°C whilst egg PC liposomes have a broader phase transition due to the heterogeneous fatty acyl chain content.

DSC and ESR studies have shown that the variation in T_c is due to the degree of interaction between the hydrocarbon constituents of the bilayer interior (Phillips et al 1969, Phillips et al 1972a). In the gel phase (L_β') the phospholipid adopts a bilayer structure in which the all trans fatty acyl chains (Fig 1.4a) are packed in highly ordered hexagonal arrays with the chains perpendicular to the bilayer plane (Shimshick and McConnell 1973a). However in phosphatidyl cholines and glycerols the long axis of the fatty acyl chains are tilted between $30-40^\circ$ to the normal of the bilayer plane - L_β' (Fig 1.5, Chapman 1975). The motion of these chains are highly anisotropic and restricted. In this phase the phospholipids do not undergo lateral diffusion or form rotational isomers.

The hydrocarbon C-C bonds are restricted in motion by steric hindrance and Van der Waals interactions of adjacent fatty acyl chains. The magnitude of these intermolecular interactions increases with

increase in saturated fatty acyl chain length, with a corresponding higher temperature required for disrupting the ordered arrays of the gel phase (Table 1.2a). However the inclusion of only one cis double bond imparts an overall bend of about 30° to the region between the double bond and the terminal methyl (Fig 1.4b). The inclusion of such bent molecules in the bilayer gives the lipid a greater molecular volume with increased mobility of acyl chains and head groups as is indicated by NMR relaxation studies (Jacobs and Oldfield 1981). However ^2H -NMR order parameters for the region of the chain before and after the double bond is similar to the values obtained from fully saturated chains, but the double bond region has values corresponding to higher order than in saturated chains. This suggests a local rigidity induced by the cis double bond which may also give reduced motional freedom to adjacent methylene segments in the neighboring acyl chains (Seelig 1977).

The effect of a cis double bond is reflected in the T_c values of mono-unsaturated phospholipids which are on average 50°C lower than their corresponding saturated phospholipids (Table 1.2a) and it is probably this property of unsaturated lipids that maintains biological membranes in a fluid state at physiological conditions. From bacterial membranes, DSC studies have shown that T_c is affected by the growth temperature and culture medium (Gomperts 1977). It is also found to be dependent on the position to which the fatty acyl chains are esterified (Table 1.2a, Boggs 1980). X-ray diffraction, neutron diffraction and ^2H -NMR studies have shown that this can be attributed to the configuration of the glycerol moiety which allows the fatty acyl chain esterified at the 1 position to penetrate deeper in to the bilayer than the same chain esterified at the 2 position (Hitchcock et al 1974, Buldt et al 1978). Therefore corresponding segments of the two acyl chains are positioned

Table 1.2

Factors influencing the phase transition temperature

a. Fatty acid chain length and degree of unsaturation for diacyl phosphatidyl cholines.

<u>Fatty acid chain</u>	<u>T_c (°C)</u>
12:0	0.0
14:0	23.0
16:0	41.5
18:0	54.0
20:0	64.0
22:0	75.0
1(16:0),2(14:0)	27.3
1(14:0),2(16:0)	35.3
1,2 16:1 _{cis}	-36.0
1,2 18:1 _{cis}	-22.0
1,2 18:1 _{trans}	9.5

b. Head group and pH.

<u>Phospholipid</u>	<u>Charge on the head group</u>	<u>T_c (°C)</u>	<u>pH</u>
DPPC	+ -	41	7
DPPE	+ -	63	7
	-	41	12
DPPS	- - +	55	7
	+ -	72	2
DPPG	-	41	7
	0	61	2
DPPA	-1/2	72	4
	-	69	7
	- -	46	11
	0	63	1

at slightly different distances from the bilayer surface. ^2H -NMR studies show that this property causes the acyl chains to experience different fluctuating motions (Seelig 1977).

The studies above indicate that at the transition temperature the gel phase melts and there is a 50% increase in surface area occupied by each lipid molecule (Levine 1973). This is mainly due to kink formation as outlined in section 1.1.3.3.1b. Spin label studies have shown that this increase in volume and motion is accompanied by a reduction in bilayer thickness by 0.7nm which gives rise to a large internal expansion (Sackmann et al 1973).

^1H -NMR studies have shown that water binding changes at the phase transition. This has been attributed to the increase in surface area occupied by the lipids (Lee 1975). The spaces arising from the decreased packing density in the glycerol region are taken up by water molecules which penetrate to the second methylene of the hydrocarbon region and possibly further in the light of later results (see chapter 3 and 4).

b.

The size and charge of the head group moiety of a phospholipid also determines the amount of bound water and effects the value of T_c . The transition temperature is thus dependent on the surface charge density. If the head groups are ionised the surface charge increases whilst the surface potential decreases. These phenomena are pH dependent with ionised head groups generally lowering both T_c (Table 1.2b) and the magnitude of the enthalpy change (Boggs 1980, Forsyth et al 1977). This has been associated with the lipid packing in the bilayer. The bulkiness

of water-associated head groups affects the packing efficiency of the fatty acyl chains, thus affecting their inter-molecular interaction. Closely packed lipids (in the case of small neutral head groups) require less surface area which restricts the motion of the fatty acyl chains. This situation gives rise to a more ordered state than less closely packed lipids.

The presence of charged head groups gives rise to inter and intra-molecular H-bonding. It is found that at pH values where lipids can participate in inter-molecular H-bonding the transition temperature is at its maximum value (Boggs 1980). PE and PS have higher T_c values than PC, which is attributed to their ability to form H-bonds between the negatively charged phosphate or acidic carboxylic groups and the protonated amine (Boggs 1980, Trauble and Eibl 1974). PA has two dissociable protons and T_c is at its maximum value at pH 4 when the first proton is 50% dissociated. This gives maximum opportunity for H-bonding. At pH 1 PA is fully protonated and T_c is reduced by 9°C. At pH 11 the second proton dissociates and T_c is decreased by 25°C from its value at pH 7. This is clearly a result of repulsion between the negatively charged head groups giving a greater molecular area and increased mobility (Boggs 1980).

^2H -NMR shows that PE and PS head groups have lower affinity towards water and have greater motional restriction than PC head groups at pH 7 (Gally et al 1975, Seelig and Seelig 1977). In this respect it is suggested that the hydrated choline head group assumes a preferred orientation normal to the bilayer plane, whereas the ethanolamine head group (H-bonded to a neighboring head group) prefers an orientation parallel to the surface of the membrane (Phillips et al 1972b). However

neutron diffraction, ^2H -NMR and X-ray studies imply that the orientation of the choline head group in the liquid crystal and gel phases is parallel to the bilayer surface and is undergoing rapid rotation around an axis perpendicular to the bilayer surface (Seelig 1977, Worcester and Franks 1976). However the latter orientation may be affected by the presence of cations (see chapter 2).

1.1.3.3.3 The Pre-transition

DSC and ESR studies reveal that PC's and PG's unlike other types of phospholipids exhibit a rather broad first order transition with a small endothermic event that proceeds the larger endothermic phase transition (Houslay and Stanley 1982, Lee 1975). This event is referred to as the pretransition and constitutes a defined structural change in the bilayer (Fig 1.5).

The gel phase in synthetic PC's has two forms. X-ray analysis shows that at temperatures below T_p the lipids of the bilayer form a one dimensional lamellar lattice with the acyl chains fully extended and tilted with respect to the plane of the bilayer (L_{β}'). This angle of tilt appears to be temperature dependent and falls to a minimum of 30° at the pretransition temperature (T_p), where a structural transformation to a two dimensional monoclinic lattice (P_{β}') occurs which is referred to as the boundary or ripple phase (Janiak et al 1976). This phase consists of a lipid lamellar distorted by a periodic ripple (Fig 1.5). The acyl chains remain tilted in this way until the main transition is reached, when they assume a liquid like conformation with the lattice reverting to a one dimensional lamellar structure (Janiak et al 1976).

Rippled structures have been reported for a variety of synthetic lecithins by freeze fracture and electron microscopy when quenched from

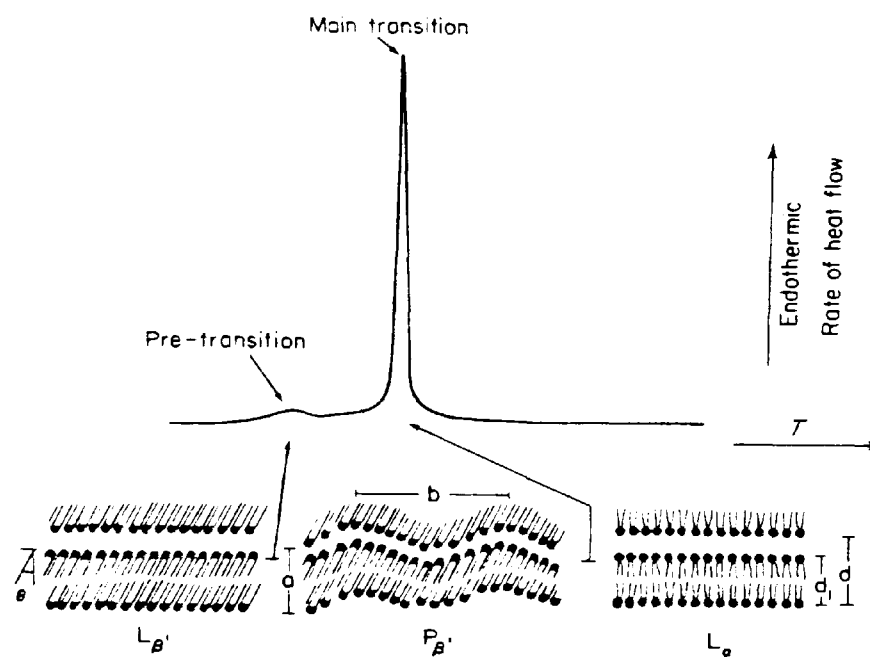


Fig 1.5 The Pre-transition of phosphatidylcholines as detected by DSC (from Janiak et al 1976).

a temperature below T_c (Gulik-Krzywicki 1975). DSC studies indicate that the pretransition exhibits a compositional dependence with it first being observed at 20% hydration. This corresponds to an hydration shell of eleven water molecules per lecithin head group (Hauser et al 1976). It is suggested that the formation of a structured water matrix surrounding the lecithin head group is a requirement for the existence of a pretransition and thus prevents the head groups from packing with maximum interaction. PE's are much less hydrated and have highly ordered head groups which explains the lack of a pretransition in these bilayers.

There is however much controversy concerning the nature of the structural change at the pretransition. One other suggestion to the above concept is that the pretransition is associated with a conformational change in the fatty acyl chains from a tilted to a perpendicular orientation (Gally et al 1975, Seelig and Seelig 1977, Rand et al 1975). Chapman and coworkers have suggested that the pretransition is associated with increased mobility of the head group moiety (Ladbroke and Chapman 1969, Chapman and Chen 1972), a possibility which is also implied by the ^1H -NMR studies of Hunt and Tipping (1978), although the latter studies were done in the presence of 5 mM Pr^{3+} .

1.1.4 Structural Organisation - Membrane Models

Numerous models have been postulated over the past 60 years in an attempt to explain natural membrane processes at molecular levels. To date these representations have largely been unsuccessful but each postulated model has stimulated new ideas for the development of more plausible models.

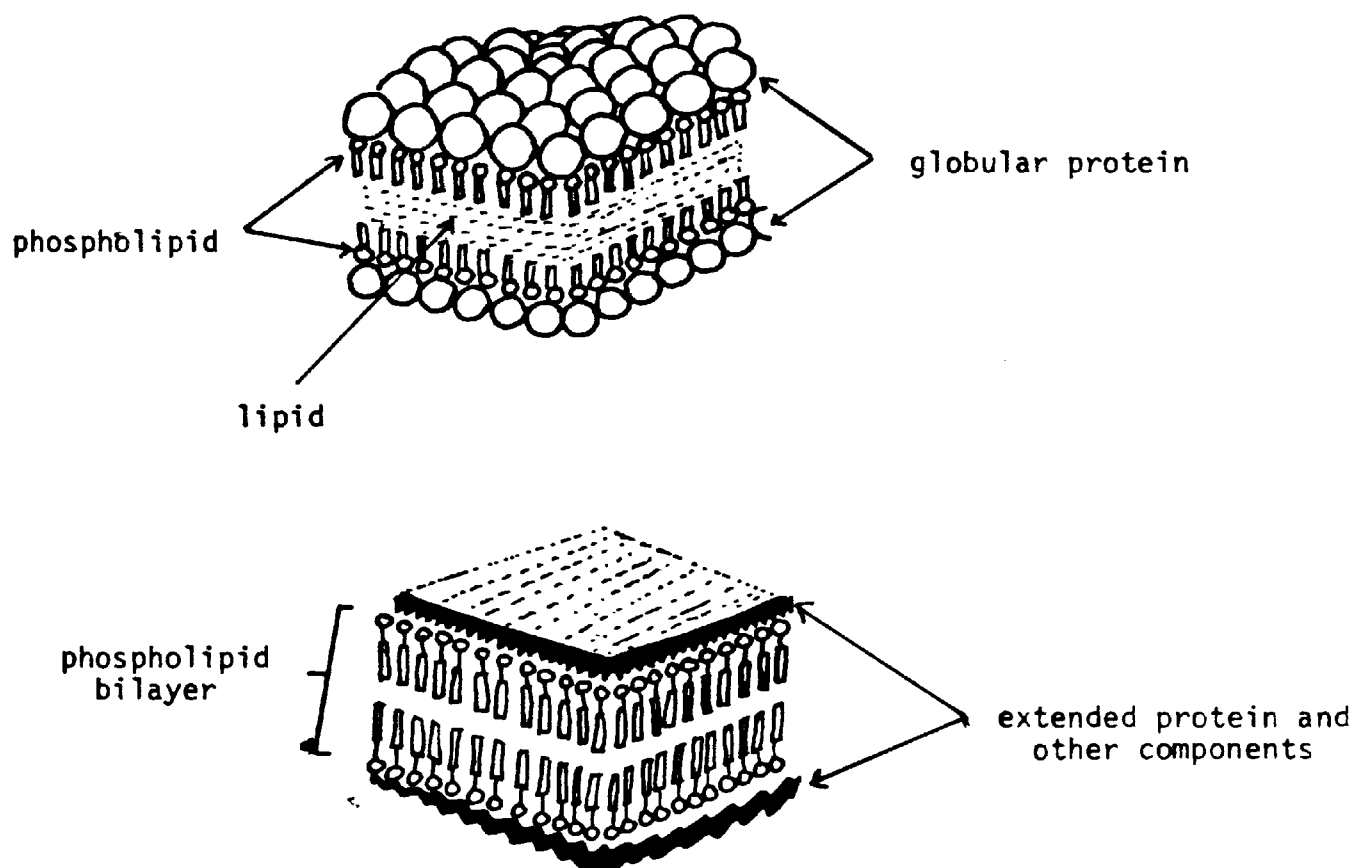
The surface tension experiments of Langmuir in 1917 allowed him to calculate the areas occupied by various fatty acids and in 1913 Fricke calculated the thickness of the erythrocyte membrane (from capacitance experiments) to be 33\AA and was therefore of molecular dimensions (Robertson 1981). On the bases of these results Groter and Grendel in 1925 reported that lipid extracted from the erythrocyte membrane spread as a monolayer at an air-water interface (Fig 1.2a). They calculated the surface area of the acetone extracted lipid as a monolayer and the surface area of the erythrocyte in a dried film preparation. Although Bar et al (1966) revealed that the erythrocyte lipids were not completely extracted and the surface area of the erythrocyte membrane was underestimated, Gorter and Grendel obtained the correct ratio of 2:1 as the two errors cancelled each other (Quinn 1976). This led them to the conclusion that the erythrocyte membrane was in the form of a lipid bilayer in which the hydrocarbon chains occupy the centre of the bilayer with the head groups facing outwards (Fig 1.2c)

Between 1932 and 1935 surface tension studies revealed lower values for cell membranes and lipid - protein films than for pure lipid films. These results led to the first membrane model of Danielli and Davson in which they proposed that membranes are composed of globular proteins attached to the polar phospholipid head groups on each side of the bilayer and with a lipid core sandwiched between each lipid monolayer (Fig 1.6a, Quinn 1976).

The use of electron microscopy in the late 1950's revealed information about membrane ultrastructure. This showed that membranes which had been fixed, stained and sectioned gave a trilaminar appearance and therefore supported the bilayer hypothesis of cell membranes.

Fig. 1.6

a. DANIELLI-DAVIDSON MODEL



b. UNIT MEMBRANE MODEL OF ROBERTSON

Electron microscope (EM) and X-ray studies of Robertson on myelin sheath and Swann cells inspired him to modify the Danielli - Davson model and postulated his unit-membrane hypothesis in 1962 (Fig 1.6b). In its original form this model suggested that all membranes in the cells of all species conformed to a basic structure (Robertson 1981).

This model differed from the earlier model of Danielli and Davson in the following ways:

- a. The protein coating the phospholipid head groups are in an extended β structure rather than in a globular configuration.
- b. The non lipid components are asymmetrically distributed across the membrane.
- c. The absence of an unspecified lipid layer sandwiched between the two lipid monolayers. This factor brings the dimensions of the lipid bilayer into line with more accurate measurements of membrane thickness obtained by EM and X-ray diffraction.

Although this model was widely acclaimed for several years as a viable model of membrane structure, certain inconsistencies became apparent when membranes other than myelin were examined, particularly membranes containing a high proportion of protein where there is insufficient lipid to form a continuous bilayer over the entire membrane (Singer 1973). It also suggested that only hydrophilic interactions between membrane proteins and lipid head groups were present and that extensive hydrophobic interactions between the two are excluded. However the use of rather drastic procedures needed to disrupt membranes and to extract lipid-free proteins was incompatible with the model and therefore both hydrophobic and hydrophilic interactions must be included.

These phenomena and new evidence from freeze fracture in conjunction with EM, immunofluorescence, ESR and DSC led to Singer and Nicolson (1972) proposing their Fluid Mosaic Model (Fig 1.7). Probably the most convincing evidence for this model came from freeze fracture studies, a technique which reveals the interior hydrophobic faces of the membrane. Using this method Branton was the first to view intra membrane particles (IMP) in erythrocyte membranes (Robertson 1981). IMP's were subsequently found to be present in a range of other membranes and were attributed to integral proteins crossing the mid plane of the membrane (Singer and Nicolson 1972).

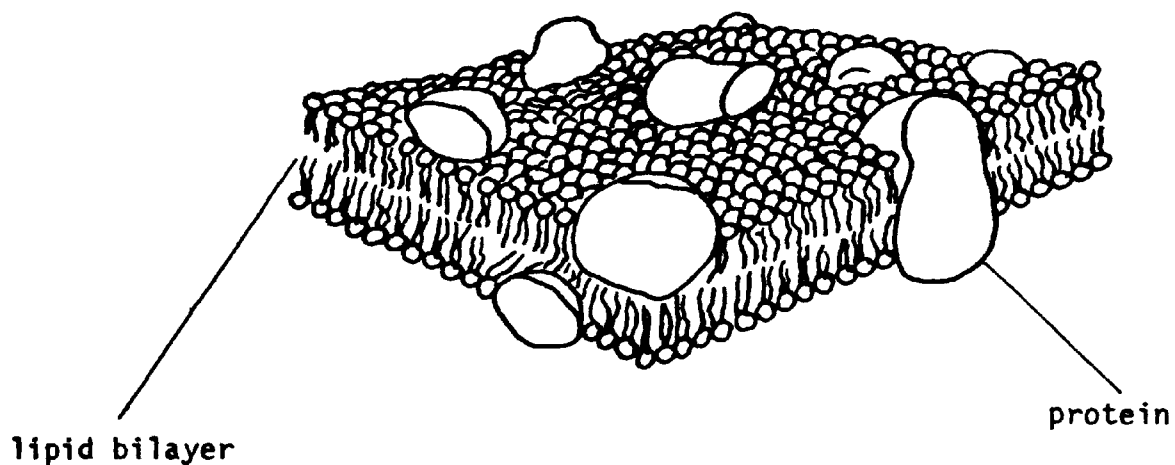
In the fluid mosaic model integral proteins were thought to be helical or globular structures having amphipathic properties and hence were embedded into the bilayer to varying degrees. This allows the hydrophobic amino acids to interact with the lipid acyl chains and the hydrophilic residues to interact electrostatically with the polar head groups on one side or both sides of the bilayer. Peripheral proteins interact electrostatically with the polar head groups only.

The model considers the structure to be fluid in the sense that lipids and to a lesser extent protein molecules can undergo lateral and rotational diffusion in the plane of the membrane. Evidence for this was obtained by the X-ray diffraction and immunofluorescence studies of Frye and Edidin on human and mouse cell membranes (Singer and Nicolson 1972). It was also proposed that proteins required a specific annulus lipid for their activity and that although a slow rate of lipid flip-flop was observed membrane asymmetry is maintained.

However the fluid mosaic model has various drawbacks especially when considering physiological processes such as fusion (in exocytosis

Fig. 1.7

FLUID MOSAIC MODEL



The Singer-Nicolson model for membrane structure. Proteins are predominantly globular and amphipathic, with their hydrophilic end protruding from the membrane and their hydrophobic ends embedded in the bilayer lipids. Proteins are embedded on one or the other side of the bilayer, others pass entirely through the bilayer. Some of the latter presumably contain transport pores.

and endocytosis), flip-flop, transbilayer transport and protein insertion. These phenomena are better explained by the presence of non bilayer phases (see section 1.4) as suggested in the metamorphic mosaic model of Cullis and De Kruijff (1979).

1.1.5 Model Membranes

One of the ways in which the importance and role of individual membrane components have been most clearly illustrated has been by the development of model membranes. These are synthetic structures of defined lipid or lipid-protein composition. Although they have been subjected to a great deal of criticism (Conrad and Singer 1981) their potential as good models has led to the physical characterisation of their constituent molecules and they have been extensively used as baselines for investigations into their possible functional roles in biological membranes (Bangham et al 1974).

Two types of lipid systems have been developed, namely planar lipid bilayers (Jain 1972) and spherically closed bilayers (Bangham et al 1974, Szoka and Papahadjopoulos 1980), the former being referred to as Black Lipid Membranes (BLM).

1.1.5.1 Black Lipid Membranes

A considerable technical advance in protein-free model membranes was made by Muller et al (1962) when they reported a method for preparing BLM's separating two aqueous phases. BLM's are formed when a lipid dispersion in a non polar solvent (usually decane) is spread (beneath a saline solution) across an aperture several millimeters in diameter drilled through a septum of some non polar material such as polytetrafluoroethylene (White et al 1976). Bilayers spontaneously formed in this way appear black since no light is reflected. They have been used

extensively but have one drawback in that the bilayers may contain solvent molecules. However methods have been developed that give rise to BLM's that contain very little solvent (White 1974, Montal and Muller 1972). Substances to be tested for their effects on the membrane are injected into the saline on one side of the membrane. This system has an advantage over other models in that a potential difference can be set up rather easily and therefore BLM's can be made to mimic neurotransmission that takes place in neuronal cells (White et al 1976).

1.1.5.2 Spherically Closed Bilayers

Principally these include three types of structures.

- a. Multilamellar liposomes, referred to as liposomes.
- b. Unilamellar vesicles, referred to as vesicles.
- c. Large unilamellar vesicles.

1.1.5.2.1 Liposomes

Bangham et al (1965) reported that lecithin from cellular origin spontaneously reforms into bilayers in the presence of water. EM has shown these structures to be particles composed of multiple concentric lamellae with an aqueous compartment separating each bilayer from its neighbour (Papahadjopoulos and Miller 1967). The spaces between the bilayers is determined by a balance of the Van der Waals forces of attraction and the electrostatic hydration repulsion forces between each bilayer.

Liposomes are prepared by first drying a solution of phospholipid to a thin film on the inner surface of a preparation flask. Aqueous solution is then added and the vessel is hand or mechanically shaken

above the thermotropic transition temperature of the lipid until the lipid has gone into suspension. The resultant milky solution contains liposomes of variable sizes which range in diameter from about 500 to 5000 nm.

Since their discovery, liposomes have been extensively studied by various techniques (Bangham et al 1974). Some of these studies include facilitated and non facilitated permeability (Young and Gomperts 1977, Blok et al 1975), enzyme entrapment (Steger and Desnick 1977), drug delivery (Ryman and Tyrrell 1980, Gregoriadis 1981), hydrolysis by phospholipases (Op Den Kamp et al 1975), protein reconstitution (Korenbrod 1977) and anaesthetic interaction (Papahadjopoulos 1972). Such studies have shown the potential of this model system.

1.1.5.2.2 Vesicles

The solubility studies of Saunders et al (1962) showed that ultrasonic irradiation (sonication) of phospholipid dispersions gave rise to stable, optically clear solutions. Subsequent EM studies by Bangham et al (1974) revealed that the structures formed by sonication were small vesicles of about 50 nm in diameter and enclosed an aqueous space. Huang (1969) rigorously characterised vesicular preparations and introduced the method of molecular sieve chromatography on Sepharose 4B columns for the purpose of obtaining a population of vesicles of uniform size.

Vesicles can be prepared in two ways, namely solvent evaporation and ultrasonication of liposomes (Bangham et al 1974). Solvent evaporation has not proved very popular but consists of layering a solution of the phospholipid (in an organic solvent) onto an aqueous phase and then removing the solvent with a stream of nitrogen. In the

second and most popular technique a liposome solution is sonicated with a bath or probe type sonicator under an inert atmosphere of nitrogen for as long as it is needed to clarify the suspension (Finer et al 1972). It is essential that the sonication is performed at a temperature above the lipid phase transition, since sonication below this temperature produces vesicles with defective bilayers (Lawaczeck et al 1975,1976).

The vesicular system is ideal for spectroscopic and permeability studies and has been extensively used (Bangham et al 1974, Szoka and Papahadjopoulos 1980). The small size of these vesicles implies a tight bilayer curvature corresponding to a ratio of the outer to inner surface area of about 2 in 25 nm diameter vesicles (de Kruijff et al 1975). This results in a different surface curvature for the inner and outer monolayers. Structural differences such as molecular packing may therefore give rise to the observed asymmetric distribution of lipids across the bilayer in vesicular preparations of mixed lipids (Litman 1975, Michaelson et al 1973, Brenden et al 1975). This phenomenon is further discussed in section 1.1.6.

1.1.5.2.3 Large Unilamellar Vesicles

Unilamellar vesicles which have a diameter greater than 100 nm are referred to as large unilamellar vesicles (luv). A preparative method for luv's was first reported by Reeves and Dowben (1969) which depended on a low phospholipid to water ratio. Subsequently a wide range of techniques have been developed for the preparation of luv's of various sizes (Szoka and Papahadjopoulos 1980) and are further considered in chapter 6.

1.1.6 Asymmetry in Membranes

Studies on erythrocyte membranes revealed that the constituent lipids and proteins are not distributed evenly between the inner and outer leaflets of the bilayer (Bretscher 1973). Consequently membrane asymmetry has been found in the majority of biological membranes and has been regarded as a prerequisite for membranes to carry out their functional roles (Rothman and Lenard 1977, Bergelson and Barsukov 1977, Houslay and Stanley 1982, chapter 4).

A greater understanding of membrane asymmetry (especially with respect to the lipid component) has been obtained from studies employing lipid vesicles. The use of NMR and chemical labelling showed that small vesicles composed of binary mixtures of PC with other lipids are normally asymmetrically distributed. Some negatively charged phospholipids (PI, PS, PA) and zwitterionic PE, accumulate predominantly in the inner monolayer, whilst PG and sphingomyelin (SM) prefer the outer monolayer (Berdn et al 1975b, Bergelson and Barsukov 1977). Cholesterol is also found to be asymmetrically distributed (de Kruijff et al 1976).

Primarily these observations have been attributed to the difference in curvature between the inner and outer monolayers of the small vesicular bilayers (Berdn et al 1975a). As a consequence the packing densities of the lipid molecules in the two layers are different and lipids with different charge and space requirements distribute unevenly between the two monolayers. On such a basis, in a mixture of neutral and charged phospholipids the latter would tend to accumulate in the outer monolayer where the inter molecular charge repulsion is smaller (Israelachvili et al 1977). But charged phospholipids accumulate in the inner monolayer and therefore charge repulsion is not

the only contributing factor. A more important factor is thought to be the size and geometry of the lipid molecules (Bergelson and Barsukov 1977, section 1.1.3.2) the ideas of which are based on the following principles.

In small vesicles the area available for polar head groups and hydrocarbon chains of lipid molecules are different in the inner and outer monolayers. For a molecule in the inner monolayer the methyl ends of the fatty acyl chains can occupy an area 1.5 times that covered by the head group, where the opposite is true for molecules in the outer monolayer (Sheetz and Chan 1972). These factors thus suggest that lipids having a head group area greater than the area occupied by the hydrocarbon chains should best be accommodated in the outer monolayer, whilst molecules with polar head groups smaller than the acyl chain area should occupy the inner monolayer. Lipids with identical head groups but with different fatty acyl chains can be expected to distribute asymmetrically with the more unsaturated species preferring the outer monolayer, due to their larger effective head group volume with respect to molecules with saturated acyl chains (Yeagle et al 1976).

Relief from strain may be achieved by combining lipids of different shapes. Such a consideration may explain why cholesterol (having a small head group) is frequently found together with PC and SM (both of which have relatively large polar head groups). Since cholesterol is known to condense the molecular area of lecithins, especially the more loosely packed unsaturated species, the preference of cholesterol for the inner monolayer (in small vesicles) is explained by the shape of the cholesterol being slightly tapered towards the hydroxyl end and by the assumption that in such small vesicles

tightening of the inner monolayer is thermodynamically more profitable than such action on the outer monolayer (De Kruijff et al 1976, Bergelson and Barsukov 1977).

1.2 NMR of Membranes

In nuclear magnetic resonance (NMR) spectroscopy signals are observed from individual nuclei within a molecule. The nature of these signals are dependent on the chemical environment of each of the nuclei and therefore the technique is sensitive to the structure and conformation of molecules. The technique holds the advantage over the majority of other physical methods in that it does not involve perturbation of the sample (by spin label or other physical methods) and therefore gives realistic information regarding molecular structure and conformation in their native environments.

NMR theory is extensively covered in several books, for example, Knowles et al (1976), Gadian (1981), Akitt (1973) and Lee et al (1974).

1.2.1 NMR Theory in brief

Certain atomic nuclei such as the hydrogen nucleus ^1H , the phosphorus nucleus ^{31}P and the carbon nucleus ^{13}C , possess a property known as spin. Associated with the spin is a magnetic property so that the nucleus in question can be regarded as a tiny bar magnet with its axis along the axis of rotation. Nuclei such as ^1H which have a spin quantum number $I=1/2$, can have one of two orientations with respect to an applied magnetic field, B_0 , a low energy orientation in which the magnetic dipole moments of the nuclei are aligned in the direction of B_0

and a higher energy orientation in which they are aligned against the applied field.

In reality the moments do not align parallel to the field, but instead will precess about the field with a characteristic angular frequency ω_0 , the Larmor frequency. Examples for single and multiple nuclear systems are shown in Fig 1.8 a and b respectively. The two orientations have slightly different energies and the energy difference between the two states is

proportional to the magnitude of the applied field. The population of the nuclei in the various energy states are determined by the Boltzmann distribution, so that at a thermal equilibrium characteristic of the temperature T , the relative numbers of n^+ and n^- in the spin $+1/2$ (lower energy) and $-1/2$ (higher energy) states are given by

$$n^-/n^+ = \exp(-\Delta E/KT)$$

where K = Boltzmann constant. Normally the populations differ by less than 1 part in 10^4 , hence the low sensitivity of the NMR technique.

Transitions between the energy states can be induced by applying an oscillating magnetic field of frequency ν_0 that satisfies the equation:

$$E = h\nu_0$$

where E is the energy separation of the levels. It is found that:

$$\nu_0 = \gamma\beta_0/2$$

where γ is the magnetogyric ratio of the nucleus, and ν_0 is the resonance frequency. γ varies from one nuclear isotope to another and this is why ^1H , ^{13}C and ^{31}P -NMR for example are all performed at different frequencies in a given field. The nuclear magnetic dipoles interact very weakly with the applied field which accounts for the low value of the energy separation ΔE , lack of sensitivity and of characteristic NMR frequencies.

Absorption of energy from the oscillating field B_1 relies on there being a population difference between adjacent states; if the populations were equal there would be equal number of transitions in both directions resulting in no net absorption of energy and no signal. The small energy difference between the two states therefore leads to a very weak absorption of energy as indicated above, and is responsible

for the inherently low sensitivity of NMR.

In NMR experiments single nuclei are not studied but rather a sample containing a large number (typically 10^{18}) of nuclei. These nuclear dipole moments all precess randomly about B_0 in the same direction. Since there is no preferential orientation in the plane perpendicular to B_0 (the xy plane) the net component of magnetic moment in the xy plane is zero. However there is a net magnetization (defined as magnetic moment per unit volume) along the z axis (represented in Fig 1.8) since there are slightly more nuclei orientated with the field than against it.

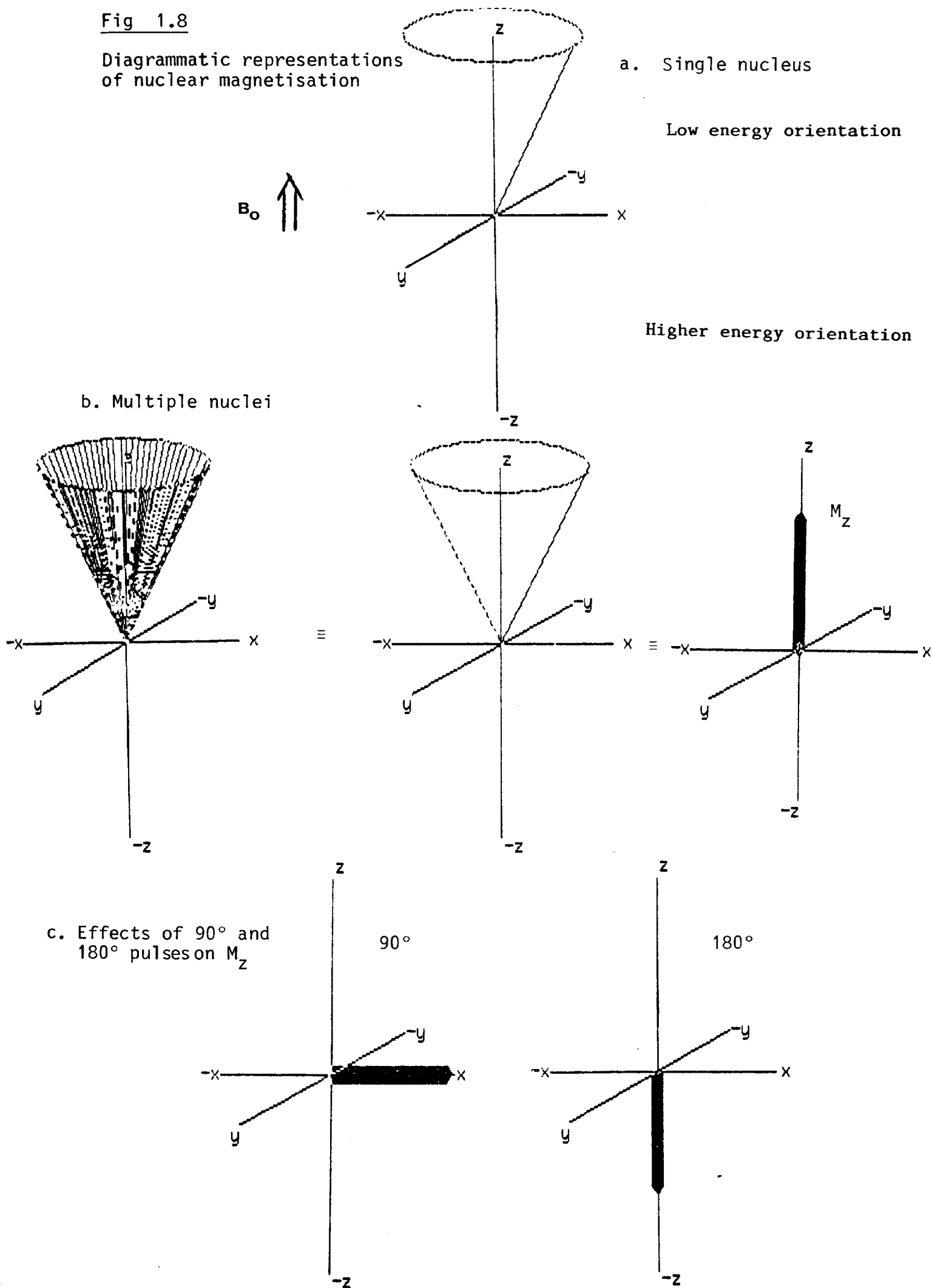
In order to detect the magnetization set up in a sample by way of B_0 , it is necessary to tilt the magnetization towards or into the xy plane. This is accomplished by means of a radiofrequency field B_1 applied in the xy plane. This causes the nuclear magnetization to precess about B_1 . The pulse duration determines the degree to which the nuclear magnetization is tilted towards the xy plane. The application of a radiofrequency field causes the nuclear magnetization to precess in phase, thus generating a net magnetization M_{xy} in the xy plane.

A pulse that tilts the nuclear magnetization from the z direction into the xy (detection) plane is known as a 90° pulse and a pulse that tilts the magnetization into the negative z direction is referred to as a 180° pulse (see Fig 1.8).

In 1966 Ernst and Anderson showed that by use of Fourier Transformation (FT) the radiofrequency pulse approach could give high resolution spectra equivalent to those obtained in continuous wave NMR. Pulse NMR has the advantage over continuous wave NMR in that all the resonances can be excited simultaneously. This is accomplished by pulsing

Fig 1.8

Diagrammatic representations
of nuclear magnetisation



the sample with a radiofrequency pulse of short duration (Typically 10 - 60 μ s) which gives a large range in frequency (from the uncertainty relationship $\Delta\nu = 1/t$). Following the application of the pulse the nuclei precess freely at their own characteristic Larmor frequency about the field B_0 . The coherence of the precession gradually disappears owing to the inherent frequency distribution resulting from spin-spin relaxation processes and the magnetization M_{xy} decays with its characteristic time constant T_2 . If additional factors such as field inhomogeneity contribute to line broadening, the decay is even more rapid. The observed decay is then characterized by the time constant T_2^* where $T_2^* < T_2$.

It is usually necessary to accumulate a large number of free induced decays (FID) to improve the signal to noise ratio. The radiofrequency is applied, the FID observed and the process repeated at chosen time intervals until a sufficient signal to noise ratio is obtained. The time interval between consecutive pulses is affected by a process known as saturation. The effect of a 90° pulse is to "sample" the z component of magnetization M_z that exists immediately prior to the pulse. Just after the first 90° pulse M_z is zero, and if M_z is still zero after a time T a second 90° pulse applied at this time would produce no further signal. Such a situation is known as saturation.

However mechanisms exist whereby M_z returns to the equilibrium value that existed prior to the application of the first radiofrequency pulse. This return to equilibrium is known as relaxation. It is often an exponential process and is characterized by the time constant T_1 which is known as the spin-lattice (longitudinal) relaxation time. On this basis maximum sensitivity would be obtained if the time period between successive pulses was long enough to allow M_z to return to its

equilibrium value (this is a time equivalent to $5T_1$). If the next pulse is initiated before this time the result is a greatly attenuated signal because the equilibrium magnetization along the z axis has not yet been established. It has been shown that after a few pulses a steady state builds up, that is a situation arises where the effect of the pulse and the spin-lattice relaxation are balanced and each pulse leads to the same, but considerably reduced, signal. The loss in signal strength can be made less severe by lowering the value of the pulse flip angle (that is an angle less than 90°) so that a large fraction of the longitudinal magnetization is unaffected by the pulse (Wehrli and Wirthlin 1978). The relaxation processes T_1 and T_2 , give information on various aspects of molecular motion and are further considered in chapter 2.

1.2.2 NMR in the study of biomembranes

Phospholipid membranes can be examined from two view points. In the first the membrane is considered as a collection of phospholipids with particular macroscopic properties, for example permeability barrier properties and thermodynamic properties such as phase behaviour and transitions. The second viewpoint is a molecular or microscopic one, which examines the structural and motional properties of the various parts of the phospholipid molecule. Both aspects are amenable to study by NMR methods.

The properties of the most commonly employed nuclei are presented in Table 1.3. This shows an overview of these nuclei and details some of their more obvious advantages and disadvantages, typically measured parameters and the types of information that can be obtained.

The application of proton NMR to biological membranes has been hindered by two major problems: an inability to obtain resolved spectra

Table 1.3

Properties of various nuclei used in NMR studies of lipid membrane systems (from Browning 1981)

Nucleus	Relative ^a sensitivity	Measured parameters	Advantages	Disadvantages	Common applications
¹ H	1,000	High resolution spectra Chemical shift T_1 T_2 ^b	High sensitivity Natural abundance	Reasonable spectra only with small vesicles or micelles Several relaxation mechanisms Overlapping resonances	Dynamic properties of phospholipids Lipid diffusion
² H	9	Powder spectra Quadrupole splitting T_1	Direct determination of order parameters Measurable in cells and dispersed lipids T_1 dominated by one mechanism Low natural abundance	Need for selective deuteration Low sensitivity	Ordering properties of phospholipids Dynamic properties of phospholipids Phospholipid hydration
¹³ C	16	High resolution spectra Chemical shift T_1	Natural abundance T_1 dominated by one mechanism	Reasonable spectra only with small vesicles or micelles Without selective enrichment: overlapping resonances	Dynamic properties of phospholipids Lipid asymmetry
¹⁹ F	830	High resolution and powder spectra Chemical shift CSA ^c T_1	Chemical shift is sensitive to positional isomers Order parameters can be obtained High sensitivity Measurable in cells and in dispersed lipids	Need for selective fluorination Two factors contribute to the line shape complicating the analysis High power proton decoupling is difficult	Ordering properties of phospholipids Lipid asymmetry
³¹ P	66	High resolution and powder spectra Chemical shift CSA T_1 NOE ^d	Natural abundance Chemical shift anisotropy is sensitive to head-group environment and phase properties of the bulk lipids Measurable in cells and in dispersed lipids	Individual lipid classes cannot be resolved in mixed systems unless sonicated	Quantitation of lipid composition Lipid asymmetry Phase properties Headgroup conformation and dynamics (NOE CSA)

^aAt constant field.

^b T_1 and T_2 are the spin-lattice and spin-spin relaxation times, respectively.

^cCSA is the chemical shift anisotropy.

^dNOE is the nuclear Overhauser effect.

and the lack of an easily characterizable physical parameter. However high resolution proton NMR spectra can be obtained from small vesicles. There have been two reasons suggested for the appearance of a high resolution spectrum: (a) difference in Brownian tumbling rate for the different particle size (that is for vesicles and liposomes) and (b) difference in molecular packing and therefore molecular motion in the two types of dispersions. However Stockton and Smith indicate that the molecular packing in the bilayers of small vesicles is similar to that in LUV (Stockton and Smith 1976). Horwitz et al (1973), Sheetz and Chan (1972) and Chapman et al (1968) have conflicting views on the relative contributions of the above given reasons to the difference in linewidth in sonicated and unsonicated lipids.

Hunt (1980a) and Degani (1978) used dynamic ^1H -NMR methods to examine how ionophores effect the transport of ions across the membranes of small vesicles. Using DPPC vesicles and lanthanide reagents Hunt (1980a) found that Pr^{3+} caused a downfield shift of 67% of the choline methyl proton resonance intensity. He found that the nigericin-type ionophore A23187 causes the downfield shift of the inner choline signal. The rate of downfield shift and broadening of this signal yielded information about the transport rate. A plot of the rate against the ionophore concentration is shown to give information about ionophore-cation stoichiometry.

Sonicated lipid vesicles give rise to high resolution ^{13}C -NMR signals (Smith 1979). One advantage of this nucleus is that the chemical shift difference between signals are larger than those of the corresponding proton resonances, resulting in better resolution, thus allowing the observation of individual signals arising from the various

carbons within the phospholipid molecule. The approach has been well exploited and relaxation studies have provided important dynamic information (Burns and Roberts 1980). Relaxation times are easily measured and a dipole-dipole relaxation mechanism is generally dominant. Thus an analysis of dynamic aspects can proceed on the basis that only one relaxation mechanism is contributing.

Selective enrichment with ^{13}C has also been used to avoid problems with overlapping resonances, for example the methylene carbons of the fatty acyl chains. Since the natural abundance of ^{13}C is low (about 1%), essentially only the labelled carbon is observed. Growth of yeast-like fungus on $[1-^{13}\text{C}]$ glucose led to ^{13}C -labelled phospholipids (Smith et al 1978) and well resolved resonances from the fatty acyl chains were observed. Since labelling only occurred in every second carbon, overlapping resonances did not occur and the lack of ^{13}C - ^{13}C coupling sharpened the signals.

Phosphorus NMR has proved to be a very powerful technique in membrane studies, because many natural lipids contain ^{31}P and thus there is no need for elaborate labelling. In small vesicle preparations sharp lines can be observed and the chemical shift is sensitive to the head group environment (De Kruijff and Cullis 1976). This has been used used advantageously in lipid asymmetry studies and in an assay of phospholipid compositions in natural membranes (Bergelson 1977, London and Feigenson 1979, Berden et al 1975a, De Kruijff et al 1975, 1976). The technique is sensitive to both motion and the conformation of the phosphate group and complicating dipole-dipole contributions to the line shapes are not apparent. An additional feature of ^{31}P -NMR which has accounted for most of its popularity is the determination of different phospholipid phase structures. Lamellar, hexagonal and micellar phases

have distinctive spectral shapes allowing quantification of the amounts of the various phases present (Cullis and De Kruijff 1979, Cullis et al 1983). Thus ^{31}P -NMR can provide information which was available only by freeze fracture and X-ray techniques.

1.2.3 Use of lanthanide reagents in conjunction with NMR

Lanthanide shift reagents (LSR) are used in NMR spectroscopy to reduce the equivalence of nuclei by altering their magnetic environment (Hinckley 1969). LSR function by co-ordinating to suitable donor atoms in the compound under study, thereby expanding their co-ordination shell and forming a new complex in solution. Owing to magnetic interactions with the metal ion in the complexed substrate, the NMR signal positions of associated nuclei in the substrate differ from those in the uncomplexed state. The equilibrium in solution is rapid on the NMR time scale (see chapter 2) so that only a single average chemical shift is recorded for each nucleus in the different environments (Mayo 1973).

The lanthanide series is formed by the successive incorporation of electrons in the 4f inner shell. The magnetic properties of the lanthanide ions vary sensitively to the number of 4f electrons. Amongst the lanthanide ions Pr^{3+} , Eu^{3+} and Yb^{3+} ions, with short electron spin relaxation times ($T_s < 10^{-12}$ s), induce shifts of NMR frequencies of substrates without appreciable line broadening. Gd^{3+} and Eu^{2+} ions, with long relaxation times ($T_s > 10^{-10}$ s), enhance relaxation rates without inducing appreciable shift. The ions Dy^{3+} and Ho^{3+} , with intermediate electron spin relaxation times, induce shifts and also enhance relaxation rates.

The functional shift (ΔL) of the NMR frequency (ν) induced by paramagnetic ions may be expressed as a sum of three terms including the

complex formation shift (Δ_{CFS}), the contact shift (Δ_{CS}) and pseudocontact shift (Δ_{PCS})

$$\Delta C = \nu / \nu_0 = \Delta_{\text{CFS}} + \Delta_{\text{CS}} + \Delta_{\text{PCS}}$$

Complex formation shift arise from the paramagnetic ion inducing changes in the electronic state of the substrate nuclei. The hyperfine interaction of the delocalized unpaired electrons of the 4f atomic orbital of the lanthanide probe with the magnetic moment of the atomic nuclei in the substrate cause shifts in the magnetic nuclear frequencies (through-bond or contact shift). The lanthanide induced contact shifts are proportional to $1/T$ and occur in ^{31}P nuclei of phospholipids.

The pseudocontact shift of lanthanide ions are obtained from the local magnetic field at the substrate nucleus induced by the magnetic moment of lanthanide ion, that is a through space effect. The magnetic moment is derived from magnetic susceptibility, and the local magnetic field induced by such a magnetic moment is averaged over all orientations of the lanthanide complex with respect to the external magnetic field. For an indepth treatment of the above properties the reader is referred to a review by Inagaki and Migazawa (1981).

1.2.4 Lanthanides as calcium probes

Metal ions exert significant effects on the structural and functional properties of cell membranes (Dos Remedios 1981, Lee 1975, Forsen and Lindman 1981). Some of them, for example the transition metal ions occur in trace quantities, whereas others like sodium, potassium, magnesium and calcium are much more abundant (Dos Remedios 1981). The latter are ions with closed electronic shells and are therefore devoid of spectrscopic properties suitable for studying their macromolecular environment. The chemical properties of the lanthanides show only a

gradual variation along the series which results from the well known ionic radius contraction, and thus renders them good probes for studying biological systems.

The ionic radius of calcium (0.99 \AA) is well within the range of ionic radii of the lanthanides ($1.061\text{--}0.848 \text{ \AA}$) and the possibility of isomorphous replacement has been emphasized. The question of charge difference has been shown to be of less importance than size in isomorphous replacement (Williams 1970). The lanthanides also possess the same co-ordination number and the same sensitivity to steric effects as calcium.

1.3 Ionophores and Membrane Permeability

Biological membranes are found to be permeable towards various ions and molecules, for example K^+ , Na^+ , Ca^{2+} and glucose where conductance values of between 10^{-3} and 10^{-1} mhos cm^{-2} have been obtained for these ions in a majority of plasma membranes (Eisenberg et al 1977). These values are much too high to be explained by simple diffusion processes based on the partition coefficient of the permeant into the membrane. The hydrocarbon region of the membrane has a high dielectric constant, with the energy required to bring a small ion such as Na^+ or K^+ from the aqueous solution into the membrane is many times the mean thermal energy (Lee 1975, Lauger 1972). Therefore mechanisms exist within the membrane framework which drastically reduce the activation energy for ion transport.

The permeability of biological membranes is associated with various types of protein present within the membrane, which have a high specificity for the types of ions they transport. In many cases ions are transported down their concentration gradient by the process of facilitated diffusion. This process is susceptible to saturation kinetics and Fick's diffusion law is not obeyed. Another method of transport involves ions being pumped against a concentration gradient. This process is energy coupled, the energy being in the form of ATP.

The Ca^{2+} ATPase of the sarcoplasmic reticulum controls relaxation and muscle contraction by governing the calcium concentration in the sarcoplasm (Hokin 1981). The Na^+, K^+ ATPase maintains the potassium and sodium ion distribution across membranes and plays a major role in restoring membrane potential after nerve impulse propagation (Hokin 1981). However interpretations of the molecular mechanisms of these transport proteins in their native membranes have been hampered by the

complex nature of both membrane and transport protein. Even reconstitution of various purified membrane proteins into liposomes and BLM s has not led to the elucidation of the molecular mechanism of transport by these proteins (Hokin 1981, Shamoo and Murphy 1979, Gomez-Poyou and Gomez-Lojero 1977). A recent report emphasised that in order to investigate transmembrane transport mechanisms the development of a range of physical methods is required which can probe the membrane system at the molecular level (Hokin 1981).

The use of various antibiotic compounds of relatively low molecular weight (200-2000) in conjunction with model lipid membranes and physical techniques has resulted in a greater understanding of transport processes at the molecular level. Pressman and coworkers first reported in 1964, that certain streptomyces metabolites including valinomycin and gramicidin at nanomolar concentrations could initiate the energy linked accumulation of alkali ions by mitochondria. Subsequently valinomycin was also shown to uncouple oxidative phosphorylation (Gomez-Payou and Gomez-Lojero 1977) and was shown to transport potassium into mitochondria. However the mode of action of these antibiotic ionophores did not start to be formulated until studies were initiated by Muller and Rudin in 1967 who used these ionophores with planer lipid membranes (Gomez-Payou and Gomez-Lojero 1977).

Lipid membranes such as BLM s and liposomes have a very low electrical conductivity (10^{-8} mhos cm^{-2}) and are therefore highly impermeable to ions (Lee 1975). In the presence of ionophores the conductivity is greatly increased. The permeability induced by these compounds has been attributed to two types of mechanism. One possible mechanism is represented by a mobile carrier molecule which binds a

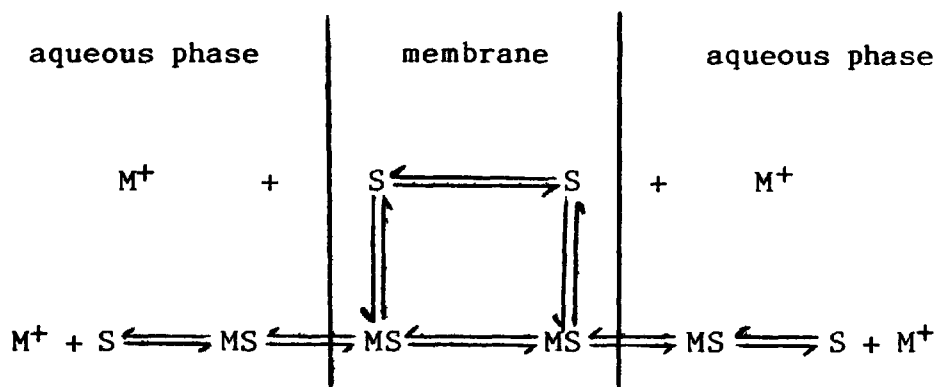
dehydrated ion at the membrane - solution interface and then migrates to the opposite interface where it releases the ion into the aqueous solution. The second class of ionophore forms hydrophilic pores which transverse the membrane. These are usually water filled channels which allow the passage of hydrated or dehydrated ions from one side of the membrane to the other. Both carriers and channels therefore provide a similar service in that they reduce the activation energy of translocating an ion across the membrane.

These two mechanisms are distinguished mainly by conductance measurements in BLMs. These show that carrier mediated transport only takes place in membranes in the liquid crystal phase, whereas channel mediated transport can take place in both the liquid crystal and gel phases (Ovchinnikov et al 1974, Lee 1975). Conductances from channel-formers give rise to fluxes of about 10^8 ions/second. The conductance for carrier mediated ionophores is limited by the diffusion coefficient of the ionophore into the lipid matrix (Lauger 1972), that is by the rate at which the ionophore - ion complex and individual ionophore molecules can shuttle from one side of the membrane to the other. For carriers to give rise to similar fluxes as channels a diffusion coefficient of 10^{-5} cm²/second would be required which is far too high especially for charged complexes where values of 10^4 ions/second have been measured (Hall 1978).

Structural determination by X-ray crystallography and NMR on both types of ionophores reveals that they are mainly amphipathic in nature. This property allows the hydrophobic and hydrophilic groups of the ionophore to simultaneously interact with the membrane hydrocarbon core and aqueous medium respectively.

1.3.1 Carrier Type Ionophores

A model for carrier mediated transport is represented below:



Two types of reactions are possible and an ion (M^+) can therefore find its way across the membrane by two distinct pathways. It can combine with the carrier (S) in the aqueous phase (homogeneous reaction), remain complexed long enough to enter the surface of the membrane and then move across to the opposite surface and thence into the opposite aqueous phase where it dissociates from the carrier. Alternatively it can combine with the carrier at the membrane surface (heterogeneous reaction), move complexed across the membrane and released by the carrier at the opposite surface. In both cases the free carrier has to diffuse back to get another ion.

Studies with mitochondrial membranes showed that the antibiotics valinomycin, macrotetralide actins and enniatins all show properties of an ion carrier (Pressman 1968). These molecules have been shown to increase cation permeability across phospholipid bilayers by many orders of magnitude (Stark and Benz 1971). Valinomycin and enniatin B depsipeptides are built up of alternating sequences of amino acids and hydroxy acids whereas the macrotetralide, nonactin is cyclic with four ether and four ester bonds (Fenton 1980).

All these ionophores form complexes with the alkali ions in organic solvent with a high degree of specificity being shown (Lauger 1972). In non polar media valinomycin forms a compact bracelet conformation with hydrophobic chains directed towards the exterior whilst the carbonyl oxygen atoms of the ester linkages are directed towards the internal cavity. This gives the complexed ion an ideal masking environment for transport across the membrane. Valinomycin shows a 10000 : 1 preference for K^+ over Na^+ although their ionic radii are not too dissimilar ($K^+ - 0.133nm$, $Na^+ - 0.095nm$). This emphasises the relationship between precision of fit of the ion into the polar oxygen lined cavity and specificity of an ionophore towards an ion.

The valinomycin type ionophores mentioned above are electrically neutral at physiological pH and form 1 : 1 complexes with alkali metal ions (Stark and Benz 1971). As a consequence a charged complex is formed which requires a higher activation energy for transversing a membrane.

The nigericin family of ionophores represents a second group of carrier ionophores. All are non cyclic and in general contain tetrahydrofuran and tetrahydropyran rings and a carboxylic function. The carboxyl group dissociates under complexing conditions and its charge neutralizes that of the complexed ion giving rise to neutral complexes which are electrically insensitive. The polar groups at either end of the molecule can take part in both inter and intramolecular H-bonding to give cyclic conformations on complexation (Gomez-Poyou and Gomez-Lojero 1977).

X537A differs in its properties to nigericin in that it can transport both monovalent and divalent cations across membranes. This reduced selectivity arises from increased structural flexibility thus

allowing 1 : 1 and 2 : 1 complexes to be formed. However A23187, another carboxylate ion carrier shows little tendency to transport monovalent cations and shows good selectivity towards divalent cations. This ionophore has been widely used for calcium transport in biological and model membranes and has been used to trigger many calcium dependent processes within cells (Gomez-Puyou and Gomez-Lojero 1977).

Another important class of ionophores are those which contain a β -diketone group. Examples of such ionophores include ionomycin and the synthetic fluronated β -diketone, NaFod. The latter has been shown to transport Pr^{3+} and Ca^{2+} across phospholipid membranes and to stimulate potassium dependent efflux from human erythrocytes (Hunt 1980a, Gomperts et al 1981). Its importance lies with its relatively inexpensive synthesis and in its potential for variation.

1.3.2 Channel Forming Ionophores

BLM studies showed that molecules such as gramicidin, alamethicin, excitability inducing material (EIM), monazomycin and the polyene antibiotics filipin, nystatin and amphotericin B all facilitate ion transport across membranes by the formation of aqueous channels. For such channels the permeability decreases with increasing ionic radius and the conductance is proportional to the n^{th} power of the ionophore concentration (Gomez-Puyou and Gomez-Lojero 1977). In BLM s they are observed to give rise to discrete conductance jumps (Gorden and Haydon 1972, Eisenberg et al 1973) in both gel and liquid crystal phases (Lee 1975).

Gramicidin, an antibiotic polypeptide of molecular weight 1860 and having alternating D and L amino acids, has been extensively characterised in lipid membranes (Gorden and Haydon 1972, Gomperts

1977). Its mechanism of action, established from conductance studies, indicate that the functional form of the peptide is a dimer and that this dimer forms a channel that spans the bilayer. Its conductance is selective for a few monovalent cations such as sodium and potassium with specificity arising from a pore diameter of 0.4 nm (Clement and Gould 1981).

Studies with erythrocytes, A. ladlawii and lipid liposomes indicate that the polyene ionophores nystatin and amphotericin B require the presence of cholesterol in a molar ratio of 1 : 1 to form channels. A large number of ionophore molecules (10-14) have been calculated for each channel with cholesterol stabilizing their cylindrical packing (Gomperts 1977).

Other channel formers when incorporated into BLMs can simulate the action potential observed in excitable membranes such as neurone and muscle membranes. Examples of such voltage dependent ionophores include alamethicin, EIM, monazomycin and haemocyanin. EIM a membrane protein extracted from Enterobacter cloacae was the first substance isolated that could induce voltage dependent channels (Lattore and Alvarez 1981, Gomperts 1977). It is a cation selective channel and rates of 10^8 ions/second have been obtained in lecithin BLMs in the presence of 100 nM KCl and a transmembrane potential of 100mV (Lattore and Alvarez 1981). However full characterization of this protein channel has not been established due to its structural complexity.

The studies of Mueller and Rudin (1968) on lecithin - cholesterol BLMs first showed that the conductance of the polypeptide antibiotic alamethicin was voltage dependent. Subsequently it has become one of the best characterised channels with respect to its structure and electrical properties in BLMs. The conductance is mainly found to be

dependent on the applied voltage (transmembrane potential), alamethicin concentration, ionic strength and membrane composition (Lattore and Alvarez 1981). The channel conductance shows a steep current-voltage curve and a strong high power dependence (4-10) on concentration (Hall 1981). The channels do not turn on immediately with the application of a voltage but show time delayed turn on characteristics suggestive of one or more intermediate states between the closed and open states. Alamethicin monomers are rod like in shape and are thought to form channels by aggregating together like staves in a barrel (Bauman and Mueller 1974, Boheim and Kolb 1978).

Ionic permeability of lipid membranes is also induced by lowering the temperature to a value corresponding to the lipid phase transition temperature (Lee 1975). In general when lipids are in the liquid crystal phase the passive diffusion of ions is very low and decreases with temperature. However $^{23}\text{Na}^+$ studies with DPPC vesicles showed that this permeability property changes with the onset of the lipid phase transition with a maximum value occurring at the transition mid-point (Lee 1975, Papahadjopoulos et al 1973). It is generally agreed that the permeability increase is due to transbilayer channels opening up in the membrane. Many theories have been proposed for this phenomenon but the mechanism by which it occurs is still under discussion and is outlined in chapter 3.

1.4 Non Bilayer Phases

The fluid mosaic model proposed by Singer and Nicolson (1972) suggests that the lipid component is responsible for the bilayer structure of membranes. However, a single phospholipid species such as PC could satisfy such structural requirements. The observation that a typical mammalian cell membrane contains one hundred or more distinctly different lipids implicitly suggests that lipids play other functional roles.

Evidence in support of the suggestions that protein activity may be controlled by local variation in local fluidity or by a specific annulus lipid, have been regarded as inconclusive (Warren et al 1975, Roelofsen and Schatzmann 1977, Cullis and de Kruijff 1979). In addition to this a number of membrane mediated processes such as cell fusion (in exo and endocytosis), transmembrane lipid exchange (flip-flop), facilitated transport and protein insertion are difficult to reconcile with an inviolate bilayer structure. These factors consequently alerted attention to the possibility that non bilayer phases were involved in membrane structure (de Grip et al 1979, Cullis et al 1980a, Burnell et al 1980a).

The foundations for these ideas were laid down by Luzzati and coworkers (1966, 1968, 1974) who employed X-ray diffraction techniques to study crystal symmetry and dimension and hence the various polymorphic phases in lipid water systems (see section 1.1.3.2). They reported that the experimental conditions (concentration and temperature) under which these polymorphic transitions were observed are not too different to those that exist in living cells and therefore it is not unreasonable to assume that analogous reversible structural changes may take place in vivo under the influence of other parameters

of more direct biological significance.

Recently the techniques available to study lipid polymorphism have been significantly extended by the introduction of NMR (particularly ^{31}P -NMR) methodology (Cullis and McLaughlin 1977, Cullis and Hope 1978) which may be usefully applied to both model and biological membranes. The increasing sophistication in freeze fracture techniques has also provided a complementary and independent method to directly visualize the macromolecular structures assumed by lipids. In addition, due to the improvements in lipid isolation and synthesis, well defined model systems are now available which allow less ambiguous assessments of the potential properties of lipids in biological membranes.

The use of ^{31}P -NMR in detecting lipid polymorphism is dependent on various factors. It exhibits a large chemical shift anisotropy (CSA) which for bilayers in large structures ($> 200\text{nm}$ in diameter) is only partially averaged out by the rapid rotation of the lipid molecules about their long axis and by their lateral diffusion in the plane of the bilayer (Cullis and McLaughlin 1977). In the presence of broad band proton decoupling these bilayers give a broad ^{31}P -NMR with a low field shoulder and a high field peak separated by an effective CSA ($\Delta\sigma_{\text{CSA}}^{\text{EFF}}$) of about -40 ppm. In contrast the H_{II} phase spectrum shows a low field peak and a high field shoulder and a reduction in the CSA of about 20 ppm due to the fast diffusion of the lipid molecules around the small (20 \AA in diameter) aqueous channel. Isotropic motion occurs in small vesicles, micelles, inverted micelles and cubic phases since lateral diffusion of the lipid molecules contributes to averaging over all orientations leading to a relatively narrow symmetric ^{31}P -NMR spectrum.

^{31}P -NMR studies have demonstrated that many lipids adopt the H_{II} phase at physiological temperatures but prefer the bilayer phase at lower temperatures. Unsaturated PE from eucaryotic cells, E. coli or from synthetic origin (Cullis and De Kruijff 1978a, Burnell et al 1980a, Tilcock and Cullis 1982), monogalactosyldiacylglycerol from chloroplasts and monoglucosyldiacylglycerol from A. laidlawii (De Kruijff et al 1979) all adopt the H_{II} phase at physiological temperatures. The tendency for other naturally occurring lipids like CL and PA to form the H_{II} phase has proved to be dependent on pH and the presence of divalent ions such as Ca^{2+} and Mg^{2+} (Cullis et al 1978a, Cullis and De Kruijff 1979, Verkleij et al 1982, Rand and Sengupta 1972).

Negatively charged phospholipids have also been found to adopt the H_{II} phase in the presence of the local anaesthetics, dibucane and chlorpromazine (Verkleij et al 1982, Cullis et al 1978a). That cytochrome C promotes H_{II} phase in CL membranes (de Kruijff and Cullis 1980) has suggested a mechanistic role for such a phase in the mitochondrial membrane. Moreover the H_{II} phase can be induced by gramicidin (van Echteld et al 1981, 1982) and can be modulated in the presence of cholesterol (Cullis et al 1978b). It is also found to appear in complex mixtures of synthetic lipids (Cullis and De Kruijff 1979) and in lipid extracts from biological membranes (Burnell et al 1980, Cullis et al 1980b and De Grip et al 1979).

^{31}P -NMR studies on PE/PC/cholesterol and PC/CL(Ca^{2+}) bilayers revealed an isotropic phase intermediate in chemical shift between the bilayer and the H_{II} phase signals (Cullis et al 1978 and De Kruijff et al 1979). The narrow symmetrical signal obtained indicates effective isotropic motion of phospholipid molecules similar to that expected in an inverted micelle. Freeze fracturing of the PC/CL samples reveal

bilayers with numerous small particles and pits of diameter 100 Å and 70 Å which correspond to the expected size of an inverted micelle composed of CL and PC (De Kruijff et al 1979a). Thus it has been suggested that the isotropic ^{31}P -NMR signals in such bilayers originate from inverted micelles sandwiched in between the two monolayers of the bilayer. The isotropic motion comes from tumbling of the inverted micelle in the bilayer, lateral diffusion of the lipids in the inverted micelle, the curved monolayers surrounding the inverted micelle and exchange of lipids between the inverted micelle and each monolayer. The equilibrium between lipid in the bilayer and inverted micelle phases is thought to be very rapid, at a rate of 10^5 – 10^6 per second (Cullis and De Kruijff 1978b, De Kruijff et al 1979a).

The lipidic particles from freeze fracture have been envisaged as intermediary structures between lamellar and H_{II} phases (Cullis and De Kruijff 1979). H_{II} phases consisting of lipid cylinders with hydrophilic cores (Section 1.1.3.2) give rise to distinct fracture planes which follow the apolar interfaces and result in a fracture face with a ribbed appearance, whilst liquid crystal bilayer phases exhibit smooth fracture faces. Studies on the H_{II} to lamellar transition in PE bilayers and CL bilayers reveal lipidic particle within H_{II} tubes as well as at the smooth fracture faces of the bilayers. These have been complemented by the appearance of the isotropic signal in the ^{31}P -NMR spectrum (Cullis et al 1978a, De Kruijff et al 1982, Van Ventie and Verkleij 1981).

The presence of such lipidic particles were found to be influenced by the presence of cryoprotectants (Sen et al 1982) as well as environmental factors such as temperature, divalent cations and pH

(Cullis and De Kruijff 1979, Verkleij et al 1982). It is suggested that these effects may be caused by influencing the forces existing between lipid molecules, in particular the H-bonding between lipid head groups and water (Sen et al 1982).

Much evidence has been obtained to indicate a role for these lipid particles (inverted micelles) in membrane events such as lipid flip-flop, transmembrane ion transport and membrane fusion (Cullis and De Kruijff 1979). Lipid flip-flop has been observed in a number of systems. ^{31}P -NMR studies revealed that PA formed in the outer monolayer of small PC vesicles (by the action of phospholipase D) is exchanged with PC in the inner monolayer (De Kruijff and Baken 1978). Glycophorin, when incorporated into small or large unilamellar vesicles greatly promotes the lyso PC and PC flip-flop rates (Van Zoelen et al 1978, Van der Steen et al 1981, De Kruijff et al 1978). ^{13}C -NMR studies indicate that flip-flop of PC and lyso PC occur in both large unilamellar vesicles and in rat sarcoplasmic reticulum preparations (De Kruijff and Wirtz 1977, Gerritsen et al 1979, De Kruijff et al 1979b, Van den Besselar et al 1979).

In PS/PC membranes the PS concentration in the inner monolayer is found to increase at lower pH (that is, a decrease in negative charge on PS) whilst the addition of calcium to PC/CL large unilamellar vesicles induces rapid flip-flop with characteristic lipidic particles and isotropic signal being shown by freeze fracture and ^{31}P -NMR respectively (Gerritsen et al 1980, De Kruijff et al 1979a). A possible mechanism for such lipid flip-flop phenomena has been explained by transitory formation of intrabilayer inverted micelles as illustrated in Fig 1.9a (Cullis and De Kruijff 1978b).

The low activation energy (from the low enthalpy changes

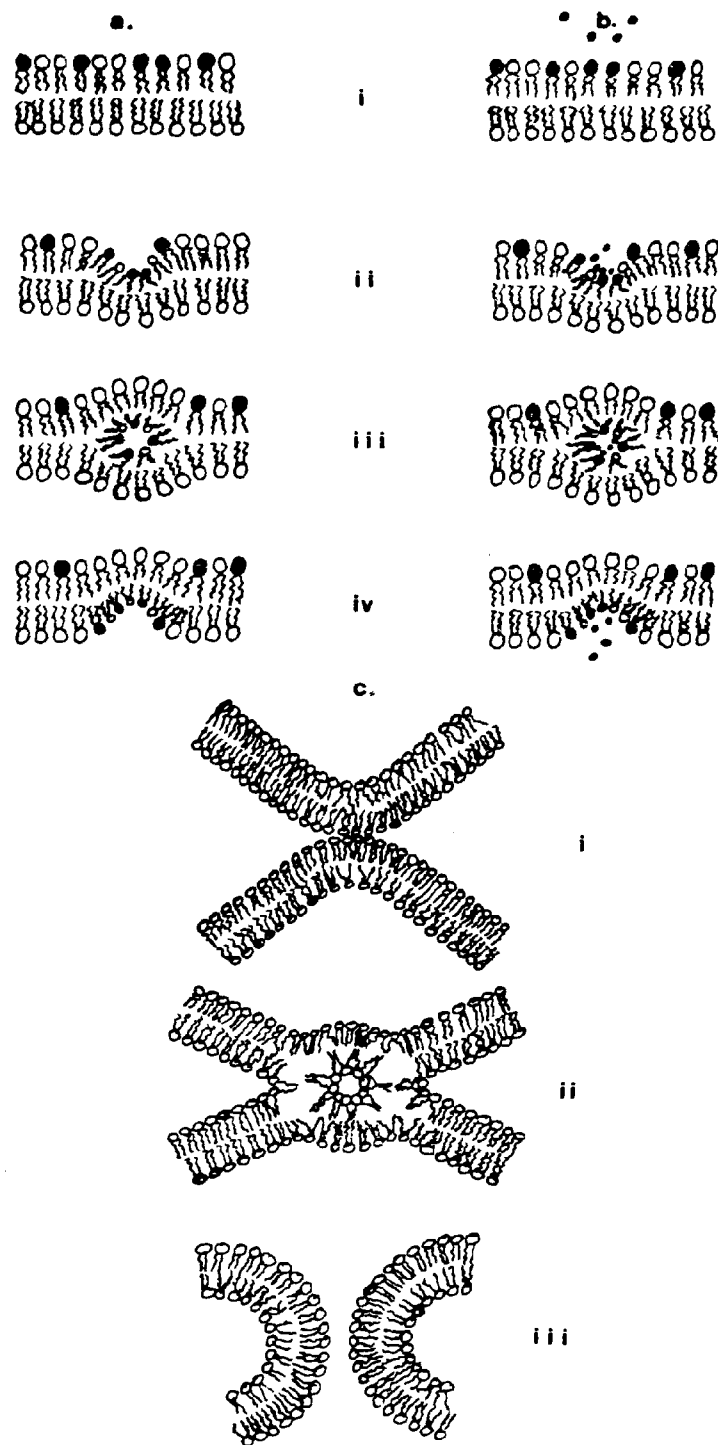


Fig 1.9

Membrane processes mediated by the formation of inverted micelles.

- A possible mechanism of lipid 'flip-flop' phenomena in biomembranes. In (i) "non-bilayer" lipid in one monolayer is redistributed across the membrane via formation of an intermediary 'inverted' phase as indicated in (ii) and (iii).
- A model of facilitated transport of divalent cations via formation of an intermediate intrabilayer inverted micellar cation-phospholipid complex (iii).
- A possible sequence of events involved in membrane fusion. In (i) two neighbouring vesicular bilayers form polar contact points. This allows joining of the bilayers to take place in (ii) which proceeds via an inverted micelle (as shown) or H_{II} type rod. (iii) shows the intermixing of the two aqueous compartments of both vesicles.

calculated during the bilayer to H_{II} transition in PE systems) required for such lipid rearrangement suggests that lipid molecules in the inverted micelles are in exchange with the surrounding bilayer lipid on either side of the membrane. In general these phenomena have only been observed in bilayers which contain lipid capable of inducing non-bilayer phases and have included molecules such as unsaturated fatty acids (Cullis and De Kruijff 1978b).

Various studies with model and biological membranes have shown a correlation between the ability of divalent cations to induce the H_{II} phase and the ability of such lipids to facilitate transmembrane ion transport (Tyson et al 1976, Cullis et al 1980, Gerritsen et al 1980, Mandersloot et al 1981, Noordam et al 1980, Nayar et al 1982, Mirghani 1982). A proposed mechanism involved the formation of an inverted micelle as illustrated in Fig 1.9 b. It is suggested that local compositional fluctuations or agents which induce the H_{II} phase could cause a bilayer invagination, possibly allowed by micelle formation. When the inverted micelle subsequently dissolves in the opposite monolayer, transport of lipids and polar molecules via the aqueous compartment occurs. Further net transport is envisaged if the lipid carrier is able to return to its original monolayer to initiate other transport cycles (Cullis and De Kruijff 1979). Therefore this mechanism suggests a method in which lipid molecules act as ionophores with simultaneous lipid flip-flop. Such a mechanism has been associated with the ability of the inner mitochondrial membrane to sequester calcium ions in vivo (Cullis and De Kruijff 1979).

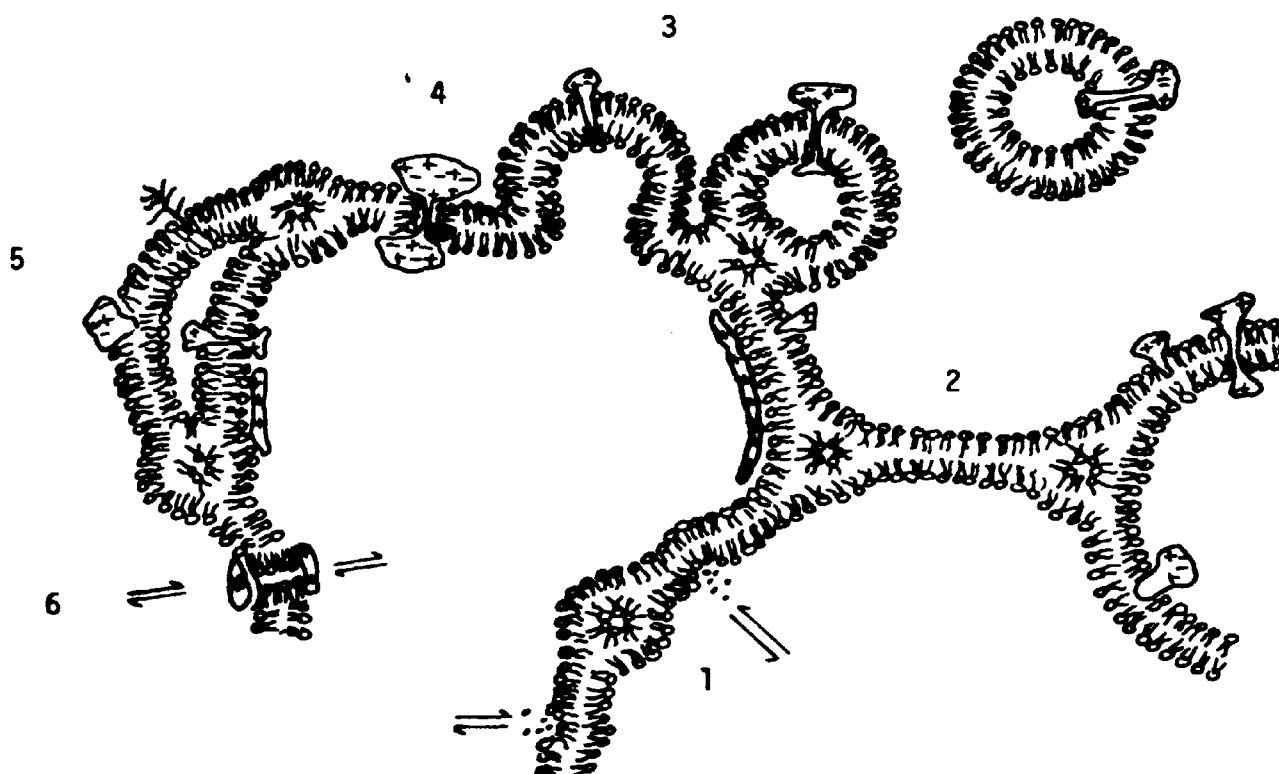
Probably the most convincing evidence for the role of inverted micelles in membrane events comes from their suggested

involvement in membrane fusion. Initial studies employing ^{31}P -NMR on erythrocyte membranes showed that very low concentrations of membrane fusing agents were sufficient to induce H_{II} phase in parts of the membrane (Cullis and Hope 1978). Further, it has been observed that unilamellar vesicles composed of a mixture of bilayer and H_{II} phase preferring lipids will fuse when they are subjected to conditions in which the tendency to form the H_{II} phase is increased (Verkleij et al 1979, 1980). Lipid particles are often present at the site of fusion. The proposed mechanism involves inverted micelle formation between the outer monolayers of two adjacent bilayers (Fig 1.9 c) and is thought to be analogous with the process occurring during exocytosis, endocytosis and cell-cell fusion (Cullis and De Kruijff 1979).

However, it has been emphasised that in the light of both the high heterogeneity of lipid composition and lipid asymmetry it is unlikely that one type of lipid is required for such membrane fusion. The role of PS in membrane fusion can only be valid for exocytosis or other fusion events from the cytoplasmic side, since PS is almost exclusively found in the inner monolayer of plasma membranes (Berden et al 1975a). A proposed mechanism involves binding of calcium to PS in the inner monolayer and thus diminishing the bilayer stabilizing power it has over PE (Tilcock et al 1981). Therefore fusion is triggered by calcium indirectly promoting the non-bilayer phase behaviour of PE.

The accumulation of evidence for the existence of non-bilayer phases in biological membranes led to the proposal of the metamorphic mosaic model by Cullis et al (1980a) as illustrated in Fig 1.10. The validity of the concepts which the model entails has been questioned and is currently a matter of debate (Miller 1980, Hui et al 1981, Hui and Stewart 1981, Thayer&Kohler 1981, Duzgunes et al 1981).

Fig.1.10 DYNAMIC MODEL OF MEMBRANE STRUCTURE
PROPOSED BY CULLIS ET AL.



A metamorphic mosaic model of biological membranes illustrating various structures and processes suggested by the ability of lipids to assume nonbilayer configurations. In part 1 transbilayer transport of polar molecules (e.g., divalent cations) is facilitated by intermediary formation of inverted micelles, whereas part 2 indicates membrane continuity between membrane bound compartments. In section 3 a process of budding off of a membrane bound vesicle is illustrated. The protein in region 4 is shown to assume a transmembrane configuration without the requirement for an apolar sequence of amino acids. The protein penetrates the membrane through a (short) cylinder of phospholipid. In the region 5 compartmentalization is depicted within a continuous membrane system, whereas part 6 indicates possibilities of transmembrane transport where hexagonal (H_2) phase lipids form an aqueous pore through the membrane. This lipid configuration is stabilized in an orientation perpendicular to the plane of the surrounding bilayer by doughnut shaped proteins with hydrophilic and hydrophobic sides, which could also serve as selectivity filters.

1.5 General Anaesthetics

The range of drugs that are capable of producing anaesthesia exhibit wide variations in chemical structure (Janoff and Miller 1982). They do not have common features of chemical structure which suggests lack of highly specific interactions with receptor sites. They are relatively unspecific in their action in the sense that a sufficient concentration of any one will produce the same type of depression of activity of all neurones (Richards 1980). Their type of action therefore differs from that of drugs that selectively depress responsiveness of cells by acting at specific receptor sites.

Many anaesthetic agents are chemically unreactive or are unable to form ionic, dipole or hydrogen bonds but they are capable of interacting with other molecules through Van der Waals bonds or have an effect on hydrophobic bonds (Janoff and Miller 1982, Richards 1980). Theories to account for the production of anaesthesia have proposed the interaction of anaesthetic molecules with membrane lipids, with membrane proteins or with water molecules associated with membrane structure (Richards 1980, Pauling 1961, Miller 1961). These theories raise fundamental questions of anaesthetic activity. Firstly how can drugs which have no chemical specificity produce such a specific response as the depression of neuronal activity? Secondly, if this specificity is related to some physical property possessed by all anaesthetics, then why are not all the living cells of an organism equally affected?

Currently there is no evidence that the changes in synaptic efficiency that occurs during anaesthesia are secondary to metabolic changes occurring within the cell. The effects are therefore best explained by direct interaction between anaesthetics and the various components of the neuronal membranes that subserve synaptic transmission

(Richards 1980). It has been assumed, as an initial working hypothesis, that all general anaesthetics work essentially the same way (the unitary hypothesis of anaesthesia). Because of the extraordinary wide range of substances that possess anaesthetic properties, much experimental effort has concentrated on regularities observed in correlations between the physical properties of anaesthetics and their anaesthetic potency. These physical properties include lipid solubility, hydrate dissociation pressure, Van der Waal's constants, molar refractivity and molar polarisation (Miller 1961, Pauling 1961, Seeman 1972, Richards 1980). As a result of these studies many mechanisms have been proposed for anaesthetic action.

1.5.1 Molecular Mechanisms of General Anaesthesia

1.5.1.1 Hydrophilic Theories

In 1961 Pauling and Miller independently proposed that the site of action of anaesthetics lay in the aqueous phase of the central nervous system (Pauling 1961, Miller 1961). Although the two theories differ in detail, both sought to relate anaesthetic potency to the stability of gas hydrates (clathrates) which many anaesthetics can form in aqueous solution. Pauling suggested that anaesthetic molecules are incorporated into clathrates and that it is these which block the passage of ions and hence perturb neuronal channels. He showed that anaesthetics were capable of forming two types of clathrates, depending on the anaesthetic in question. He correctly predicted that the effect of the two anaesthetics on an animal would be additive rather than synergistic, given the anaesthetics involved the different clathrate types (Pauling 1961).

Miller suggested that anaesthetics, being hydrophobic, increased

the degree of ordered water molecules in the vicinity of the neuronal membranes (Miller 1961). Further support for this theory came from studies on the abolition of the righting reflex in Italian crested newts, taking this as the end-point of anaesthesia (Richards 1980). They showed that the partial pressure of the anaesthetic at which this point was reached correlated reasonably well with the hydrate dissociation pressure at 0°C, but the correlation with the olive oil/gas partition coefficient was closer (Richards 1980).

The main drawback to the Pauling-Miller hypothesis is that many clathrates or gas hydrates are not stable under the conditions in which anaesthesia is produced. Pauling therefore suggested that additional stabilization was provided by components of the cell membrane such as hydrophobic side chains of certain amino acids.

In contrast to these clathrate theories which advocate the promotion of Ice I-like hydrophobic hydration by anaesthetics, Eyring and co-workers (Kamaya et al 1980) proposed the destruction of Ice III like electrostrictive hydration. Their NMR studies showed that the action of inhalation anaesthetics at clinical levels on DPPC bilayers was confined to the head group region (Shieh et al 1976). They indicate that the presence of a dipolar moment in a hydrophobic molecule greatly enhances anaesthetic activity and that the action is directed to the water membrane interface.

Alternatively, Brockerhoff (1982) proposes that bilayer-hydrogen belts formed from hydrogen bond acceptors (carbonyl groups) and donors (hydroxyl groups) are highly co-operative and manipulation of their composition changes their hydrogen bonded structure. Proteins participate in this hydrogen bonded network and he suggests that this

participation is restructured when the hydrogen belt is modified by the incorporation of anaesthetic. This could form or break hydrogen bonds, thereby changing the conformation of a protein. The theory also allows the possibility that anaesthetics may hydrogen bond immediately to a protein and thus disrupt its hydrogen belt.

1.5.1.2 Critical Volume Hypothesis

Mullins considered that the most important aspect of an anaesthetic was the volume it occupied within the membrane phase (Mullins 1954). He predicted that equinarcotic effects should occur at equal volume occupations of anaesthetics within the membrane phase, on the basis that large molecules would cause greater perturbations in the membrane than small molecules.

Recent observations by Miller and co-workers on the reversal of anaesthesia by pressure (Richards 1980) led to the proposal that the anaesthetic dissolved in some hydrophobic region of the cell, presumably lipid, causing that region to expand and thereby impairing some vital functions. From the amount of pressure required to reverse the various doses of anaesthetics they calculated that during anaesthesia the hydrophobic region should expand by about 0.4% (v/v). These predictions were later verified by Seeman and Roth in their studies with erythrocyte membranes (Richards 1980). These findings were consistent with the critical volume hypothesis. Their work provided evidence that the site of action increases its volume when anaesthetics are bound, but allows no inference to be made about the nature of the site itself.

1.5.1.3 Lipid Fluidity Theories

Metcalfe and co-workers using NMR techniques found that benzyl alcohol increased the fluidity of biological membranes (Seeman 1972). This observation was later extended by Trudell and co-workers to include clinically important anaesthetics such as halothane (Richards 1980, Janoff and Miller 1982). It was subsequently proposed that anaesthetics cause membrane expansion by increasing the disorder of the fatty acid chains of phospholipids in membrane bilayers. However, Boggs et al and Rosenberg et al have shown that concentrations of anaesthetics sufficient to cause general anaesthesia or which block the conduction of impulse along a nerve (local anaesthesia) have little or no effect on the fluidity of model membranes and synaptosomal membranes (Richards 1980, Janoff and Miller 1980).

Roth and Seeman hypothesised that the increased fluidity induced by anaesthetics (with accompanying membrane expansion) disrupted the normal function of membrane proteins. This was based on the observation that anaesthetics increase membrane thickness which affects the operations of ion channels (Haydon et al 1977). However, the evidence for such increases are limited and are still unclear (Richards 1980).

1.5.1.4 Lipid Phase Transition Theories

Anaesthetics have been found to lower the phase transition temperature of phospholipids (Jain and Wu 1977, Richards 1980, Vanderkooi et al 1977) as is shown in chapter 4. On this basis Trudell has suggested that anaesthetics may work by decreasing the T_c of phospholipids which exist in the membrane in a condition of lateral phase separation (Richards 1980). This is achieved by the anaesthetic fluidising the gel state phospholipids which increases the lateral

pressure that they exert on membrane proteins and thus inhibiting their function.

Alternatively, Lee (1976) has suggested that sodium channels of nerves are maintained in an operational conformation by an annulus of rigid lipid molecules and that anaesthetics fluidise this lipid, so causing the channel to relax into an inactive conformation. However, both these hypotheses are considered unlikely since no phase transitions are apparent in mammalian membranes (due to their high cholesterol and variable fatty acid contents) and that recent ^2H -NMR studies indicate that bulk and annulus lipid exchange at a rate faster than 10^3 per second (Rice et al 1979).

1.5.1.5 Degenerate Protein Perturbation Hypothesis

Studies investigating the effect of temperature on anaesthetic action indicate that anaesthetic potency increased as the temperature decreased (Richards 1980). This suggests that anaesthetic potency does not always correlate with lipid solubility. Such observations indicate that membrane proteins were a more plausible site for anaesthetic action. Further, different isomers of the same anaesthetic show different anaesthetic activities indicating a specific action associated with specific binding sites present on membrane proteins (Richards 1980). To affect the function of a protein the binding of an anaesthetic must result in a conformational change that impairs normal activity, or in the restriction of the normal conformational changes associated with activity. Evidence supporting this comes from studies showing cooperative binding of anaesthetics to specific sites (Richards 1980, Janoff and Miller 1982).

1.5.1.6 Other Theories

Krjnevic questioned the axiom that anaesthetics must act on the plasmamembrane (Richards 1980). He argues that the total area of the mitochondrial membrane is 30 times that of the plasma membrane and so anaesthetics must have a considerable effect here. Any effect on the mitochondria will be effected in terms of cellular function. A disruption of mitochondrial action would lead to a decrease in ATP levels which feeds the Na^+/K^+ pump and contributes to the membrane potential. Thus disruption of mitochondrial function would lead to eventual depolarization and a dampening of overall neuronal excitability. However such activity would be expected in cells other than neurones and is therefore an unlikely mechanism of anaesthetic action.

These molecular mechanisms are further considered in chapter 4 where the action of general anaesthetics on the membrane permeability of lipid vesicles is investigated.

1.6 Cholesterol and Membranes

Cholesterol is an extremely important constituent of many biological membranes where it often constitutes some 6-50 mole % of the total lipid pool (see Section 1.1.3). Cellular membranes such as liver plasma membranes, erythrocyte and myelin membranes contain high levels of cholesterol in cholesterol:phospholipid molar ratios of 0.83, 0.9 and 1.32 respectively (Demel and De Kruijff 1976).

The structure of cholesterol is shown in Fig 1.1b. It consists of a rigid sterol ring region some 1.1 nm long with a β hydroxyl group attached to one end. At the other end is a highly flexible carbon chain some 0.8 nm long. Many studies have shown that cholesterol inserts itself into phospholipid bilayers with its hydroxyl group proximal to the carbonyl oxygens of the fatty acyl chains and its hydrocarbon side chain situated in a region towards the apolar core of the bilayer (Worcester and Franks 1976, McIntosh 1978, Brokerhoff 1974, De Kruijff 1978). It is therefore considered that the hydroxyl group on cholesterol can to some extent participate in H-bonding with the carbonyl oxygens of the fatty acyl chains. In this position X-ray diffraction & ^2H -NMR studies have shown that the sterol ring region of cholesterol extends as far as C_{12} of the fatty acyl chains whilst its aliphatic side chain extends to the same depth in the bilayer as the phospholipid acyl chains (Houslay and Stanley, Chapter 2, 1982, McIntosh 1978).

ESR, ^1H , ^{13}C and ^2H -NMR studies on lecithin bilayers above their phase transition show that the addition of cholesterol causes an increase in bilayer thickness and a reduction in the surface area of each monolayer (Smith 1979, Oldfield and Chapman 1971, Darke et al 1972). Increase in the bilayer thickness is attributed to a reduction

in the number of gauche rotamer segments (see Section 1.1.3.3.1) and a corresponding increase in the number of trans rotamer segments (Smith 1979). This condensing property of cholesterol has been demonstrated in bilayers formed of PE, PA, PG and sphingomyelin, with the degree of condensation being dependent on chain length and unsaturation (Demel and De Kruijff 1976). However, these effects are severely reduced in bilayers containing lipid analogues which lack the carbonyl group, supporting the concept that a specific interaction occurs between cholesterol and phospholipids (Houslay and Stanley 1982).

Taylor and co-workers (1982) employing ^2H -NMR with ^2H labelled cholesterol showed that the sterol ring region of cholesterol when present in phospholipid bilayers has a high degree of order which is greatest at a high membrane cholesterol concentration or at low temperatures. Relaxation times, T_1 and T_2 reveal slower motions for cholesterol than for the phospholipid acyl chains and is attributed to the large bulk and inflexibility of the cholesterol sterol ring system. T_1 and T_2 measurements on the methyl groups of the alkyl side chain indicate that this region has greater flexibility than the sterol ring system. This is attributed to the availability of motional degrees of freedom, through rotation about the methyl three-fold symmetry axes and the C-C bonds of the alkyl chain.

Cholesterol has then a condensing effect on the acyl chain region of fluid phospholipid bilayers producing a more ordered rigid structure. However, NMR, ESR, X-ray diffraction and DSC studies show that it has an opposite effect on bilayers in the gel phase (Darke et al 1972, Oldfield and Chapman 1971, Demel and De Kruijff 1976). They indicate that in the gel state the phospholipids do not pack together to form a solid phase

excluding cholesterol, but instead cholesterol remains intimately associated with the phospholipids and thus preventing their acyl chains adopting the all trans configuration which allows them to pack together. This leads to a decrease in the fraction of acyl chains found in the all trans state at temperatures below T_c and hence an increase in bilayer fluidity (Demel and De Kruijff 1976, Stockton and Smith 1976). ^1H -NMR studies show that the addition of cholesterol to dioleoyl PC or egg PC causes a significant reduction in the rates of lateral diffusion (Cullis 1976), but with no significant change in the activation energy for diffusion (Lee 1975). This suggests that the reduction in diffusion coefficient is an entropy effect consistent with the maintenance of increased order during the diffusion necessary to avoid unfavourable cholesterol-cholesterol contact.

DSC studies show that increasing the cholesterol content in DPPC bilayers results in the phase transition being gradually broadened and shifted to lower temperatures (Ladbroke et al 1968). Spin label and laser Raman studies show that 50 mole % cholesterol results in a very broad phase transition and gives rise to a bilayer which gradually changes over a wide temperature range going from a relatively ordered structure to a relatively disordered state (Lippert and Peticolas 1971, Shimshick and McConnell 1973b).

Cholesterol at different concentrations has been found to induce new phases in DPPC bilayers. Above 5 mole % cholesterol overcomes the tendency of the acyl chains in DPPC bilayers to tilt to the bilayer normal and therefore a new phase L_β is formed where the fatty acyl chains align extended parallel to the bilayer normal (Lentz et al 1980, Hui and He 1983). For temperatures below T_c for high concentrations of cholesterol a new phase is produced for which the detailed molecular

structure is unknown, but it seems to be considerably disordered (Lentz et al 1980). Cholesterol concentrations below 20 mole % abolish the formation of the ripple phase, P_{β}' with a corresponding abolition of the thermal pretransition (Lentz et al 1980, Copeland and McConnell 1980).

In the fluid state the maximum concentration of cholesterol that bilayers can accommodate before a pure cholesterol phase separates out depends very much on the nature of the head groups of the phospholipids present and their associated fatty acyl chains. The maximum level occurs at 50 mole % cholesterol but in the case of sphingomyelin or highly unsaturated PC the value can rise to 67 mole % (Demel et al 1977). Such studies have shown that cholesterol prefers to interact with phospholipids in a sequence, $SM \gg PS = PG > PC \gg PE$. When mixtures of phospholipids with identical head groups but different acyl chains are present the cholesterol associates preferentially with the more fluid species (Lee 1975, De Kruijff et al 1974). However its affinity for SM is so great that this interaction is favoured even when other types of lower melting point phospholipids are present (Demel et al 1977). Such interactions are attributed to the overall geometry of cholesterol and the phospholipid as well as the interaction through the 3 β hydroxyl group.

The interaction of cholesterol with various phospholipids has been shown to determine the phase adopted by membranes (Cullis and De Kruijff 1978b, Cullis and Hope 1980, Tilcock et al 1982). ^{31}P -NMR studies have shown that in soya PE bilayers cholesterol lowers the temperature at which the bilayer to H_{II} phase transition takes place, indicating a destabilisation of the bilayer phase (Cullis and De Kruijff 1978a, Tilcock et al 1982). A similar effect is observed in membranes

composed of PE/PC, but cholesterol is found to stabilize the bilayer phase in PE/DPPC membranes. It is considered that either cholesterol associates with PC in PC/PE membranes to give a cone shaped complex which forms a H_{II} phase or cholesterol induces lateral segregation of PC allowing the free PE to adopt the H_{II} phase (Cullis and De Kruijff 1978a). Such properties explain why biological membranes high in PE content contain little or no cholesterol and thus stabilize membrane structure and integrity.

High levels of SM are inevitably associated with a high cholesterol content as is the case in the erythrocyte membrane. Pure SM membranes at 60°C give rise to an isotropic signal in the ^{31}P -NMR spectrum but in the presence of 50 mole % cholesterol only a bilayer phase is apparent (Cullis and Hope 1980). A comparison between SM/PE, PC/PE and DPPC/PE membranes in the presence of cholesterol indicate that SM is by far the most effective lipid for stabilising the bilayer phase (Cullis and Hope 1980). The increased cholesterol content of the membranes of intimal cells of arterial walls during the initial stages of atherosclerosis is associated with a complementary increase in SM which may therefore be stabilising membrane structure.

The stoichiometry of the phospholipid - cholesterol complex is not agreed on, and phospholipid : cholesterol molar ratios of 1:1, 2:1, and 4:1 have been proposed. Studies employing ^1H -NMR, X-ray diffraction and phase contrast microscopy suggest a 1:1 molar ratio (Phillips and Finer 1974, Hunt and Tipping 1978, Demel and De Kruijff 1976, Darke et al 1972). The ^1H -NMR studies indicate that the 1:1 complex begins to change when the lecithin acyl chains are more than 20°C above their T_c since more methylene groups have increased mobility (Darke et al 1972). DSC and X-ray analysis studies indicate that lyso PC interacts with

cholesterol in a 1:1 molar ratio, suggesting that cholesterol interacts only with one acyl chain at any one time (Demel and De Kruijff 1976). However X-ray diffraction (Engelman and Rothman 1972), NMR (Darke et al 1972) and DSC studies (Demel and De Kruijff 1976) indicate an abrupt change in the physical properties of bilayers when 33 mole % cholesterol is present and thus suggesting a molar ratio of 2:1. Other studies show that such abrupt changes occur at 20 mole% and thus favouring a phospholipid : cholesterol ratio of 4:1 (Lentz et al 1980, Presti and Chan 1982, Opella et al 1976, Hui and He 1983).

³¹P-NMR studies show that cholesterol incorporated into gel phase bilayers cause a significant increase in the polar head group motion (Cullis et al 1976). However when incorporated into fluid bilayers only a marginal increase in head group freedom is observed (Demel and De Kruijff 1976). This incorporation of cholesterol into fluid bilayers is thought to be responsible for the increase in hydration of the bilayer, with the extent of hydration being dependant on the phospholipid. In the absence of cholesterol the degree of hydration depends on the intermolecular forces between the head groups, and thus to the extent to which these charged groups are accessible to water. PE bilayers exhibit a greater increase in hydration than do PC bilayers since PE head groups are more tightly associated and exhibit a much reduced motional freedom compared to PC head groups.

The distribution of cholesterol and its effect on protein activity and membrane permeability are dealt with later in chapter 5.

CHAPTER 2

CATION MEMBRANE INTERACTION BY NMR

2.1 Introduction

The interaction of cations particularly divalent cations such as calcium, with phospholipids in natural and model membrane systems has received a great deal of attention (Hauser et al 1975, Hunt and Tipping 1978, Chrzeszczyk et al 1981). Such interactions are believed to play an important role in membrane structure and function. Calcium for example, has long been known to stabilize the electrically excitable membranes of nerve and muscle; in the presence of an increased concentration of calcium in the extravesicular fluid the membrane is depolarized to a greater degree to elicit an action potential. This is thought to be induced by calcium adsorbing to the outer surface of the membrane thereby creating a positive surface potential. Many studies have indicated that calcium binding to negatively charged lipids is involved in membrane fusion events (see section 1.4, Cullis and De Kruijff 1979).

It is generally accepted that calcium binds strongly to negatively charged phospholipids but there is some controversy as to whether divalent ions bind to neutral phospholipids such as PC. Some reports indicate that calcium does not interact with PC (Rojas and Tobias 1965, Hauser and Davson 1967) but recent studies employing NMR (Hauser et al 1975, 1977), radiotracers and X-ray diffraction (Lis et al 1981) leave little doubt that calcium interacts with the phosphate groups of PC monolayers and bilayers, imparting a change to them. Resulting small changes in the head group orientation and flexibility may therefore significantly alter the electrical properties of the membrane surface, producing in turn, changes in the physiological or biochemical characteristics to the membrane (Hauser et al 1977).

Lanthanide binding to model membranes has also been extensively studied, due to their resemblance to calcium (Westman and Eriksson 1979). Bergelson et al (1970) and Bystrov et al (1972) have shown that the "inner" and "outer" choline ^1H -NMR signals of sonicated lecithin can be separated by salts of paramagnetic ions such as lanthanides and manganese added extravesicularly. This allows perturbations of the inner and outer monolayers to be monitored separately.

The interaction of cations with lipid bilayers has been shown to have important effects on the packing of the lipid molecules in the bilayer. The effect of ions on the temperature of the gel to liquid-crystal phase transition has been used to probe this phenomena. Using DPPC vesicles and variable temperature ^1H -NMR techniques, Hunt and Tipping (1978) studied the effects of Pr^{3+} and Ca^{2+} or Mg^{2+} or K^+ , on the phase transition temperature of this lipid. By measuring the widths of their NMR signals they showed that interaction of metal ions with the head groups of one monolayer is transmitted to the other monolayer and alters the temperature and extent of the phase transition and the pre-transition observed in each monolayer. One disadvantage in this study is the relatively high concentration of Pr^{3+} ions (required to obtain separate O and I signals) which compete with the other ions when they are present and thus possibly suppressing their full effects. In the current study the technique used by Hunt and Tipping (1978) is extended by the use of spin lattice relaxation measurements and Dy^{3+} ions which can be used at a much lower concentration than Pr^{3+} to obtain separate O and I signals.

2.1.1 Spin-lattice and spin-spin relaxation

Following the perturbation of magnetization by a 90° pulse, processes occur whereby M_z and M_{xy} (see section 1.2) return to their equilibrium values of M_0 and zero respectively. The relaxation processes taking place are very important because of their critical role in the theory and practice of NMR spectroscopy.

The return of M_z to its equilibrium value is termed spin lattice relaxation and is characterised by the time constant T_1 known as the spin lattice relaxation time. The term spin lattice is used because the process involves an exchange of energy between the nuclear spins and their molecular frame work, which is regarded as the lattice independent of the physical state of the system. The return of the nuclear spins to equilibrium is often an exponential process.

The relative populations of the spin states can be altered in a well defined way by the application of a resonant B_1 field in the xy plane. In a similar manner any fluctuating magnetic field which has a component in the xy plane that oscillates at the resonant frequency will induce transitions between the spin states of the nuclei. If these fluctuating fields are associated with the lattice, there will be an exchange of energy until the nuclear spins are in thermal equilibrium with the lattice.

Fluctuating magnetic fields may be set up when two different nuclei X and A both of spin $1/2$, are present within a molecule. Since X has a dipole moment it produces a field at A that has a component B_{xy} in the xy plane. If the molecule is tumbling round in solution the relative orientation of A and X change randomly. As a result B_{xy} also fluctuates. If there are any components of molecular motion that happen to fluctuate at the resonance frequency, then these can cause relaxation of nucleus

A. The two nuclei do not have to be in the same molecule; for example , diffusion of molecules can modulate fields and therefore lead to relaxation. Relaxation stimulated by this interaction between neighboring nuclear magnetic dipole moments is termed dipole-dipole relaxation.

The frequency distribution of a rapidly tumbling molecule can be expressed in terms of the spectral density $J(\omega)$, and under any circumstances it is given by

$$J(\omega) = \frac{\tau_c}{1 + \omega^2 \tau_c^2}$$

where τ_c is known as the correlation time. τ_c expresses the characteristic time scale of the molecular motion. For example water molecules in solution have a correlation time of 3×10^{-12} s. ATP might be expected to have a correlation time of about 10^{-10} s and an enzyme of molecular weight 20,000 might have a correlation time of about 10^{-8} s. The relaxation mechanism is most efficient when the molecular motion is equal to the resonance frequency.

The return of M_{xy} to its equilibrium value is termed spin-spin relaxation and is characterized by a time constant T_2 known as the spin-spin or transverse relaxation time. The term spin-spin is used because the relaxation process involves interactions between neighboring nuclear spins, without any exchange of energy with the lattice.

The magnetization M_{xy} precess coherently about the z axis. However for a spread in frequencies the different nuclei will precess at slightly different frequencies, and the nuclear dipoles will lose phase coherence and "fan out", the net effect being that the M_{xy} decays. The greater the frequency spread the more rapidly M_{xy} decays. If T_2

represents the time constant of the decay of M_{xy} that results from spin-spin relaxation, then:

$$1/T_2 = \pi\Delta\nu_{1/2}$$

where $\Delta\nu_{1/2}$ is the corresponding resonance line width at half height. Spin-spin relaxation therefore involves processes which cause an inherent broadening of the resonance line widths.

2.1.2 T_1 T_2 and molecular mobility

Fluctuating magnetic fields are responsible for both spin-spin and spin-lattice relaxation, but the timescales of these fluctuations determine their relative contributions to the two types of relaxation. In particular slow motions contribute only to spin-spin relaxation, whereas components of motion at the resonance frequency contribute to both spin-spin and spin-lattice relaxation. However the two nuclei A and X (as described above) can undergo simultaneous transitions. Both nuclei can undergo transitions in the same direction if there is a component of molecular motion of frequency equal to the sum of the Larmor frequencies of the two nuclei. Such a process contributes to spin-lattice relaxation and hence by lifetime-broadening to spin-spin relaxation. If A and X are like nuclei they can also undergo spin-spin exchange in which a downward transition of one nucleus is accompanied by a simultaneous upward transition of the other without any exchange of energy with the lattice. Such a process does not affect T_1 , but it does affect the lifetimes of the nuclear spin states and therefore contribute to T_2 .

A small ratio of $T_2 : T_1$ is common in the NMR of biological material. This is largely because the correlation times (see Fig 2.2) of biological molecules are long as a result of their large size. In

addition there are other mechanisms that tend to affect linewidths more strongly than T_1 ; these include scalar coupling and chemical exchange.

A method for the measurement of T_1 is known as the inversion recovery and is illustrated in Fig 2.1 and 2.2. The double pulse sequence used is shown in Fig 2.1a. The application of a 180° pulse inverts the magnetization so that it is directed along the negative z axis. The magnetization relaxes back towards its equilibrium position M_0 with the time constant T_1 and a 90° pulse applied after a time T (PI*** in Fig 2.1) samples the value to which M_z has relaxed after this time. Following signal detection the system is allowed to return to equilibrium by waiting for a time t_D equal to at least $4T_1$ and the sequence is then repeated until sufficient signal to noise ratio is obtained. The accumulated signal is Fourier Transformed in the usual way and the whole procedure is repeated for a variety of different PI*** values. T_1 is then obtained from a plot of $\ln(M^\infty - M\tau)$ against T which should be a straight line of gradient $1/T_1$.

If factors other than relaxation contribute towards resonance linewidths, then the spin-spin relaxation time T_2 can be obtained from the relationship:

$$1/T_2 = \pi\Delta\nu_{1/2}$$

however effects such as B_0 inhomogeneity often make additional contributions to the observed linewidths.

2.1.3 The NMR timescale

This property is explained by reference to studies involving protein-lipid interaction as measured by NMR and ESR. The perturbations of lipid dynamics by intrinsic proteins if measured on one timescale (for example 10^{-8} s using ESR and spin labelled molecules) may show a

Fig 2.1 Principles in the measurement of T_1

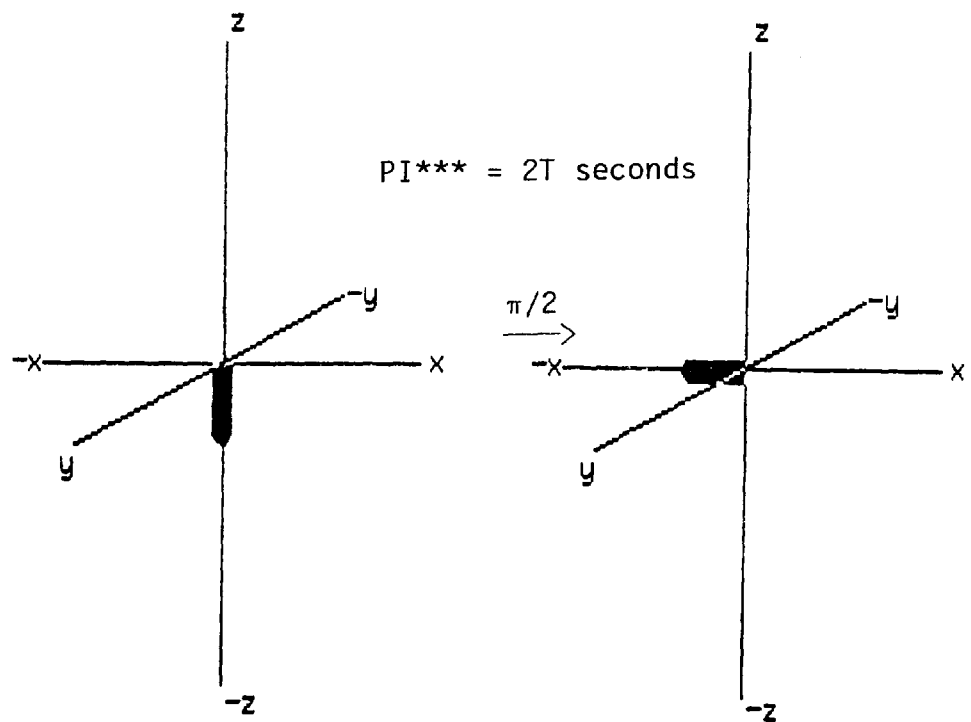
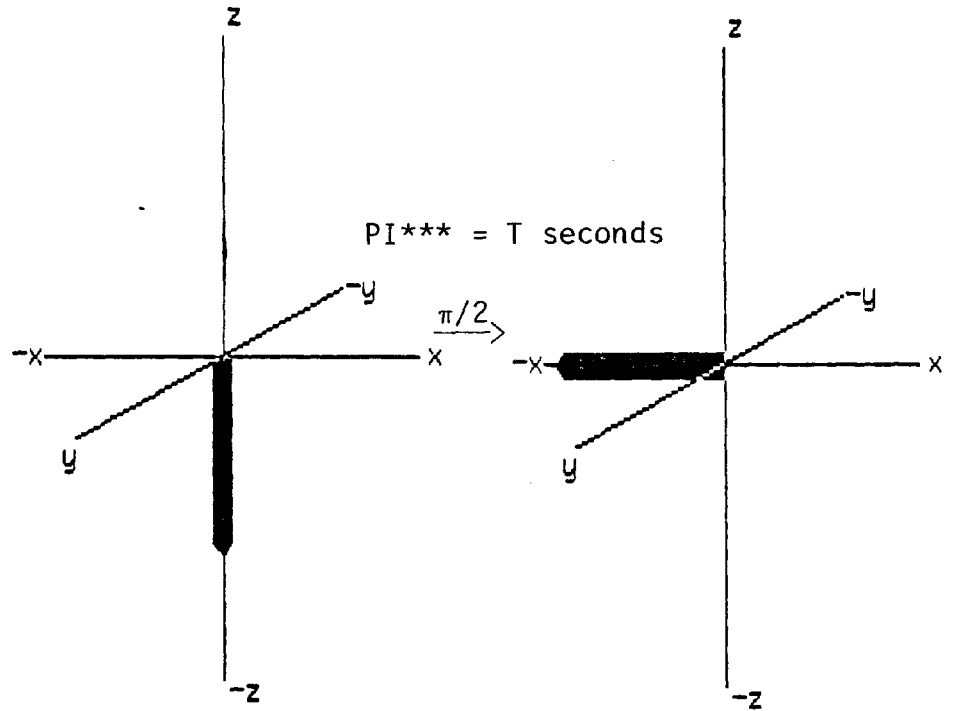
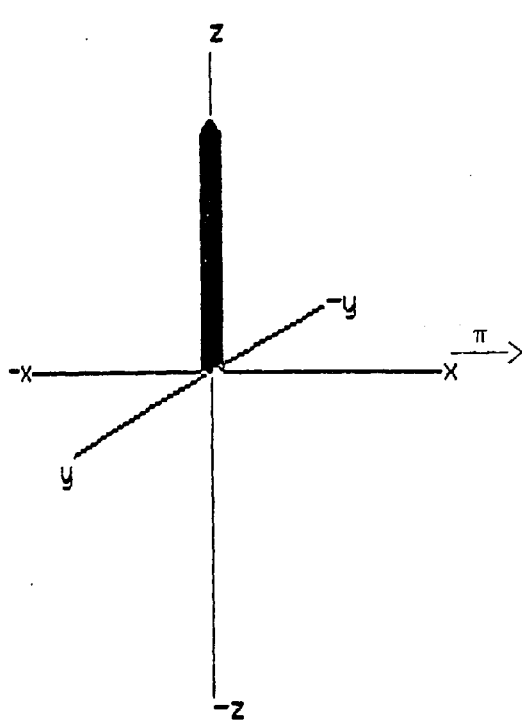
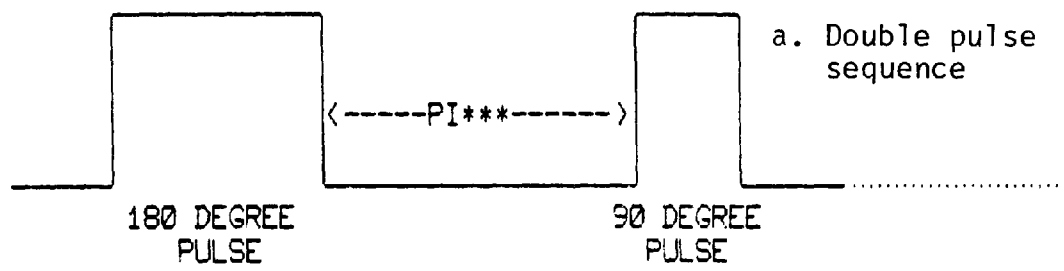


Fig 2.1 (continued)

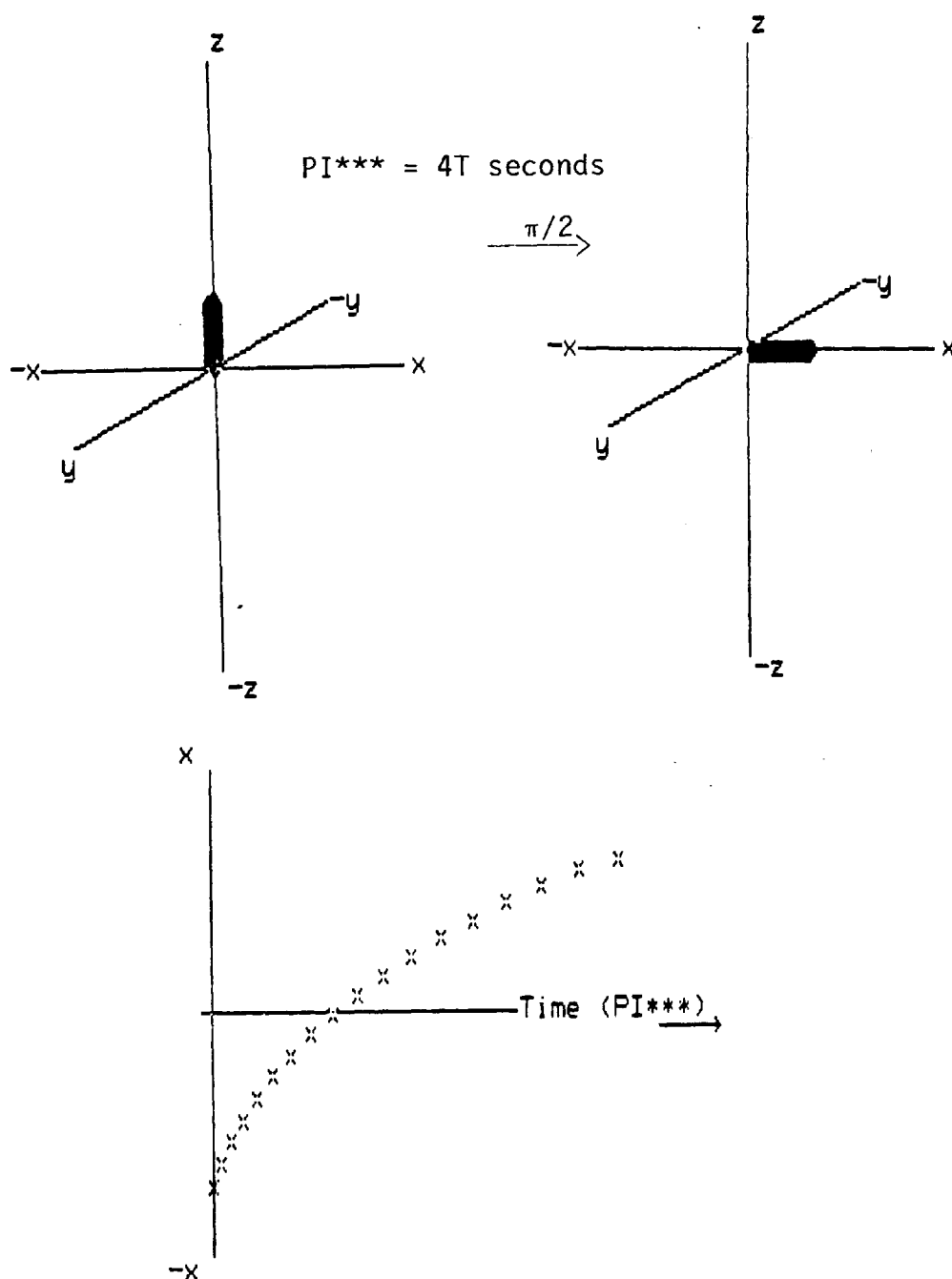
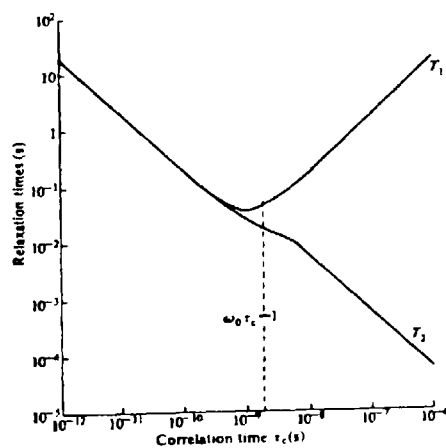


Fig 2.2 Diagram showing how relaxation times vary with correlation time



molecule to be rigid, whereas on another timescale (for example 10^{-5} s using NMR methods) the same molecule can appear to be mobile. If NMR and ESR are used to monitor three lipid states (liquid-crystal, boundary lipid and gel phase lipid), the ESR views the rigid gel state of lecithin below T_c to be similar to the motional properties to the rigid or ordered boundary lipid of an intrinsic protein. However the ^2H -NMR view of a terminal methyl labelled lecithin boundary lipid is even more disordered than the lipid above its phase transition temperature.

The differences between NMR and ESR therefore result from an exchange rate of the order of 10^{-5} - 10^{-7} Hz. This exchange rate is fast enough to produce an exchange narrowed NMR spectrum but would be slow compared to the ESR timescale, and would account for different ESR spectra of boundary and bulk lipid (McLaughlin et al 1981, 1982, Seelig et al 1982).

2.2 Materials and Methods

2.2.1 Chemicals

Dipalmitoyl phosphatidylcholine (DPPC) was purchased from Lipid Products, South Nutfield, Redhill and was used without further purification. A stock solution in chloroform/methanol was prepared (10 mg/ml) and was stored at -5°C . The chloroform used was purified by passing it through a preactivated (500°C overnight) 10 x 50 cm. alumina column, followed by distillation. 1% AnalaR methanol was added to prevent phosgene formation.

Deuterium oxide ($^2\text{H}_2\text{O}$ (D_2O) - 99.8% Gold Label) was obtained from Aldrich, Gillingham, Dorset. Praseodymium chloride ($\text{PrCl}_3 \cdot 6\text{H}_2\text{O}$) was obtained from Lancaster Synthesis, Morecambe, Lancs; and dysprosium chloride ($\text{DyCl}_3 \cdot 3\text{H}_2\text{O}$) from Koch-Light, Colnbrooke, Bucks. Calcium chloride ($\text{CaCl}_2 \cdot 2\text{H}_2\text{O}$) and magnesium chloride ($\text{MgCl}_2 \cdot \text{H}_2\text{O}$) were purchased from BDH, Poole, Dorset. Solutions of the three compounds were prepared in D_2O such that 5-10 μl in 1 ml of sample gave the required concentration.

2.2.2 Preparation of vesicles

The vesicles were prepared by pipetting a known volume of the stock DPPC solution into a glass sonicating tube and the chloroform removed by passing a stream of nitrogen over the warm solution. Traces of methanol were removed by evacuation for 20 minutes at 2 mm Hg pressure using an electric pump. The dried lipid was then hydrated in a known volume of D_2O (preheated to about 50°C) to give a final concentration of 10 mg/ml. The solution was shaken at 50°C using a mechanical shaker to produce homogeneous milky liposomes.

The liposomes were sonicated at 50°C for approximately 5 minutes

using a DAWE Soniprobe Type 7532A fitted with a titanium microtip at a delivery of approximately 25 W. The sonicator probe tip was polished after every few sonications, a procedure which avoids contamination by titanium particles from the microtip. The homogeneous vesicle solution was kept between 50–60°C and was clear and typically bluish. 1 ml of the vesicular solution was pipetted into a dry, clean 10 mm NMR tube and placed in a thermostated water bath, set at the required temperature before NMR spectra were recorded.

2.2.3 NMR Spectroscopy

¹H-NMR spectra were obtained using a Jeol FX60Q FT NMR spectrometer operating at 60 MHz and fitted with a calibrated temperature control. Typically 10 pulse sequences were used (180 – τ – 90) with a pulse interval of about 3 seconds to minimize the HOD signal.

Spin-lattice relaxation times T_1 , were obtained by the inversion recovery method (see section 2.1.2) employing a pulse repetition time of 3 seconds and 20 different pulse interval (PI**) values (τ seconds) in the range 10 ms to 0.6 s. The pulse sequence can be summarized as:

$$[- 90 - \tau - 180 - T]_N$$

where τ is the pulse interval, T is the pulse repetition and N is the number of pulses (usually 10 pulses were used).

2.2.4 Sizing of sonicated vesicles

Vesicular dimensions were determined from the integral ratio of the outer:inner choline head group ¹H-NMR signal. This is done by assuming that the vesicles are spherical and have a bilayer thickness of 4 nm (Hutton et al 1977, Sheetz and Chan 1972).

2.2.5 Variable temperature experiments

T_1 and T_2 values were obtained from DPPC vesicles at various temperatures between 60°C and 30°C. In these studies the vesicles were allowed to equilibrate for about 15 minutes at the set temperature.

2.3 Results and Discussion

The ^1H -NMR spectrum of DPPC vesicles in the absence of ions (Fig 2.3a) reveals sharp well resolved signals corresponding to choline (C), methylene (H) and terminal acyl chain methyl groups (M). The reason for the appearance of a high resolution spectrum from small sonicated vesicles are outlined in section 1.2.2.

Fig 2.3b shows a spectrum of DPPC vesicles in the presence of 5 mM Pr^{3+} . The ratio of the areas under peaks O (outer choline head groups) and I (inner choline head groups) represent the ratio of the number of DPPC molecules in the outer and inner monolayers of the vesicles. This property allows calculation of the average diameter of the vesicles (Hutton et al 1977), the number of vesicles present in solution, and a variety of other characteristics as outlined below. The conditions that must exist in order for the NMR - paramagnetic ion technique to give accurate ratios of the inner and outer phospholipids in the vesicles are outlined by Hutton and coworkers (1977).

2.3.1 Determination of size and number of vesicles

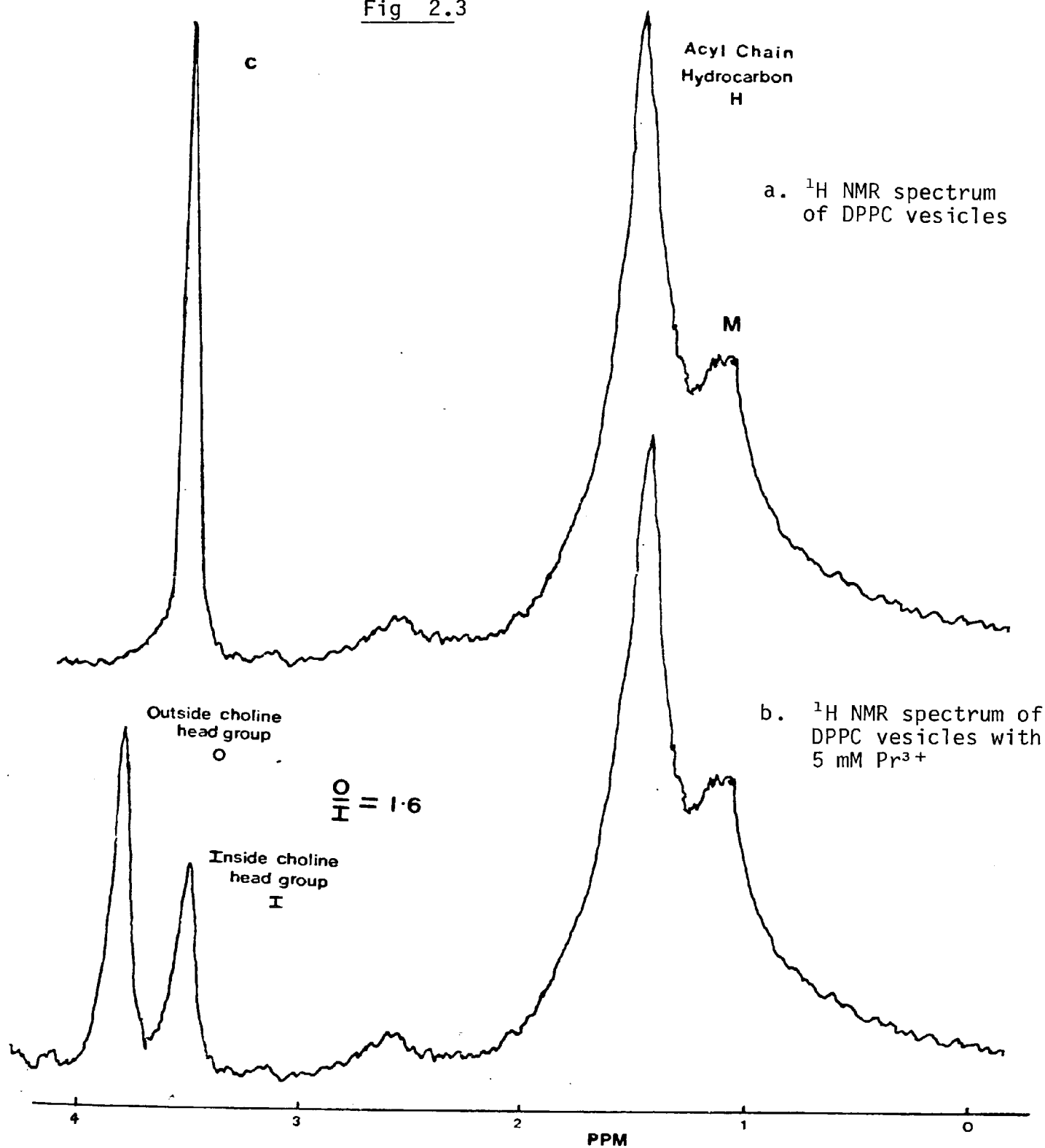
Fig 2.3 shows that the ratio of the outer choline head group signal (O) to the inner choline head group signal (I) signal is 1.6. Therefore assuming the vesicles are spherical:

$$\frac{4 \pi r_o^2}{4 \pi r_i^2} = \frac{\text{Area of signal O}}{\text{Area of signal I}} = 1.6 \quad \text{--- (i)}$$

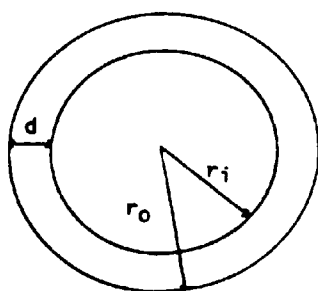
where r_o and r_i are the outer and inner radii of the vesicles respectively (Fig 2.3)

Assuming a bilayer thickness of 4 nm from X-ray crystallography (Sheetz and Chan 1972) equation (i) can be written in the form:

Fig 2.3



c. DIMENSIONS OF SINGLE BILAYER VESICLE



r_i and r_o are the internal and external radii of the vesicles, and d is the bilayer thickness.

$$\frac{r_o^2}{(r_o - 4)^2} = 1.6$$

$$0.6r_o^2 - 12.8r_o + 25.6 = 0$$

$$r_o = \frac{12.8 \pm [(12.8)^2 - 4(0.6)(25.6)]^{1/2}}{2 \times 0.6}$$

$$r_o = 2.2 \text{ nm or } r_o = 19.1 \text{ nm.}$$

The first of these values can be ignored as it is smaller than the bilayer thickness. Hence the vesicles produced have an outer diameter of 38 nm, which is confirmed by electron microscopy showing that unilamellar vesicles of homogeneous size are formed (Mirghani 1982). Thus the vesicles produced have dimensions similar to the preparations of other workers (Bystrov et al 1973, Shapiro et al 1975).

The assumption of fast exchange of lanthanide has been accepted in the literature (Bergelson 1977). A minimum limit for the exchange rate is the chemical shift separation for the bound and free phospholipid. Since separation is complete with a lipid:metal ratio as low as 0.05 (Huang 1974), the exchange rate is probably fast on the NMR timescale (see section 2.1.4).

The NMR spectrum of vesicles recorded several hours and even 2 days after the addition of paramagnetic lanthanide does not show any spectral changes, which suggests that the vesicles are quite stable and are impermeable to lanthanide cations at 50°C above T_c .

Further to the above calculations the vesicle volume and vesicle number can be calculated:

$$\begin{aligned} \text{Vesicle volume} &= \frac{4}{3} \pi r^3 \\ &= \frac{4}{3} \pi (19.1 \times 10^{-7})^3 \end{aligned}$$

$$\begin{aligned}
 &= 2.919 \times 10^{-17} \text{ cm}^3 \\
 \text{Intravesicular volume} &= \frac{4}{3} \pi (15.1 \times 10^{-7})^3 \\
 &= 1.442 \times 10^{-17} \text{ cm}^3 \\
 \text{Bilayer volume} &= \text{vesicle volume} - \text{intravesicular volume} \\
 &= 1.477 \times 10^{-17} \text{ cm}^3
 \end{aligned}$$

The total number of vesicles can be calculated on the basis of ^{31}P -NMR and sedimentation studies which shows that DPPC occupies an area of 76 \AA^2 (Chrzeszczyk et al 1977).

10 mg of DPPC (molecular weight 734) per 1 ml of D_2O is used.

Therefore:

$$\begin{aligned}
 10 \times 10^{-3} \text{ g of lipid contain } & \frac{10 \times 10^{-3} \times N_A}{734} \\
 &= 8.2 \times 10^{18} \text{ molecules}
 \end{aligned}$$

where $N_A = 6.023 \times 10^{23}$ Avogadro's number.

The number of DPPC molecules

$$\begin{aligned}
 \text{present in the outer monolayer} &= \frac{\text{Total surface area of one vesicle}}{\text{Area occupied by the hydrated head group of one molecule}} \\
 \text{of each vesicle} &= \frac{4 \times (19.1 \times 10^{-7})^2}{76 \times 10^{-16}} \\
 &= 6032 \text{ molecules.}
 \end{aligned}$$

From the O:I ratio of NMR spectrum (Fig 2.3) the number of DPPC molecules in the inner monolayer:

$$\frac{6032}{1.6} = 3770 \text{ molecules}$$

Therefore the number of molecules (inner and outer monolayers)

which are present per vesicle:

$$6023 + 3770 = 9802 \text{ molecules.}$$

$$\begin{aligned} \text{The number of vesicles present} &= \frac{\text{Total number of molecules in 1 ml}}{\text{Number of lipid molecules present in one vesicle}} \\ \text{in 1 ml} &= \frac{8.2 \times 10^{18}}{9802} \\ &= 8.366 \times 10^{14} \text{ vesicles} \end{aligned}$$

$$\begin{aligned} \text{The internal volume of all} &= \text{internal volume} \times \text{total number} \\ \text{the vesicles present in 1 ml} &= \text{of one vesicle} \times \text{of vesicles} \\ &= 1.442 \times 10^{-17} \times 8.366 \times 10^{14} \\ &= 1.21 \times 10^{-2} \text{ cm}^3 \end{aligned}$$

This represents 1.21% of the total volume (1 ml). The equilibrium number of ions can also be calculated (for use in chapter 3):

$$\begin{aligned} \text{Number of Pr}^{3+} \text{ ions / ml} &= 5 \times 10^{-6} \times N_A \\ &= 3.31 \times 10^{18} \text{ Pr}^{3+} \text{ ions} \end{aligned}$$

$$\begin{aligned} \text{The number of} &\text{internal volume} \\ \text{Pr}^{3+} \text{ ions in 1 ml} &\times \text{of each vesicle} \\ &= (3.31 \times 10^{18})(1.42 \times 10^{-17}) \\ &= 48 \text{ ions.} \end{aligned}$$

Such a value is consistent with those obtained by Ting et al (1981).

For egg PC vesicles (used in chapters 3,4 and 5) an O:I ratio of

1.6 is also obtained from the NMR spectrum. The following data is obtained for egg PC assuming a molecular weight of 767 (Koch-Light Catalogue 1977) and that an egg PC hydrated head group occupies an area of 84 \AA^2 (Cornell et al 1980):

Vesicle radius and volume are the same as DPPC vesicles.

Number of molecules in the outer monolayer = 5458

inner monolayer = 3411

Total number of molecules per vesicle = 8869

Total number of vesicles in 1 ml = 8.85×10^{14}

These figures indicate that a discrete number of ions will cross the membrane during an approach to equilibrium. The change in extravesicular Pr^{3+} concentration during such a process:

Total number of Pr^{3+} ions
transported into DPPC vesicles = $48 \times 8.336 \times 10^{14}$
= 4.02×10^{16}

The number of Pr^{3+} ions remaining = Initial number - Total number
on the outside of ions of Pr^{3+} transported
= $3.31 \times 10^{-18} - 4.02 \times 10^{16}$
= 3.2698×10^{18} ions.

This still corresponds to approximately 5 mM extravesicular Pr^{3+} and this remains effectively constant during the transport and lytic processes investigated in chapters 3, 4 and 5.

2.3.2 Cation-membrane interaction by NMR relaxation studies

Fig 2.4 indicates that both T_1 and T_2 measurements on the hydrocarbon signal can be used to detect the gel to liquid-crystal phase transition. The figure shows quite clearly the difference in the time scales involved in the spin-lattice and spin-spin relaxation times (as explained in section 2.1.2) and that both processes can detect the limits of the phase transition ($34^\circ - 42^\circ\text{C}$) to about the same extent. The absolute values of the relaxation times are a consequence of T_2 being determined by the longest correlation time, while the shorter correlation time (see Fig 2.2) dominates spin-lattice relaxation rates (Podo 1975). This suggests that the faster motional events occurring in the hydrocarbon region (for example, the equilibrium between trans and gauche rotomers - see section 1.1.3.3.1) are being affected since spin-lattice relaxation times are only sensitive to relatively fast motions.

A relatively broad transition range is exhibited by small vesicles, with an upper limit of 42°C and a lower limit of about 34°C . A slight inflection at about 36°C (Fig 2.4 and controls in Figs 2.5 and 2.7) suggests that the relaxation rates are influenced by the changes occurring during the pre-transition. The widths of these transitions are in contrast to PC liposomes or LUV, which exhibit a sharp, highly cooperative main transition with a well defined pre-transition. Small vesicles therefore show less cooperative transitions which has been attributed to the packing constraints resulting from the high radius of curvature and from the fact that the number of molecules that can act cooperatively is limited by the vesicle size (Lee 1975, Yellin and Levin 1977, Gruenewald et al 1979). This concept therefore explains why the pre-transition and main transition overlap in small vesicles.

In Fig 2.5 the values of T_1 s for the control (at temperatures

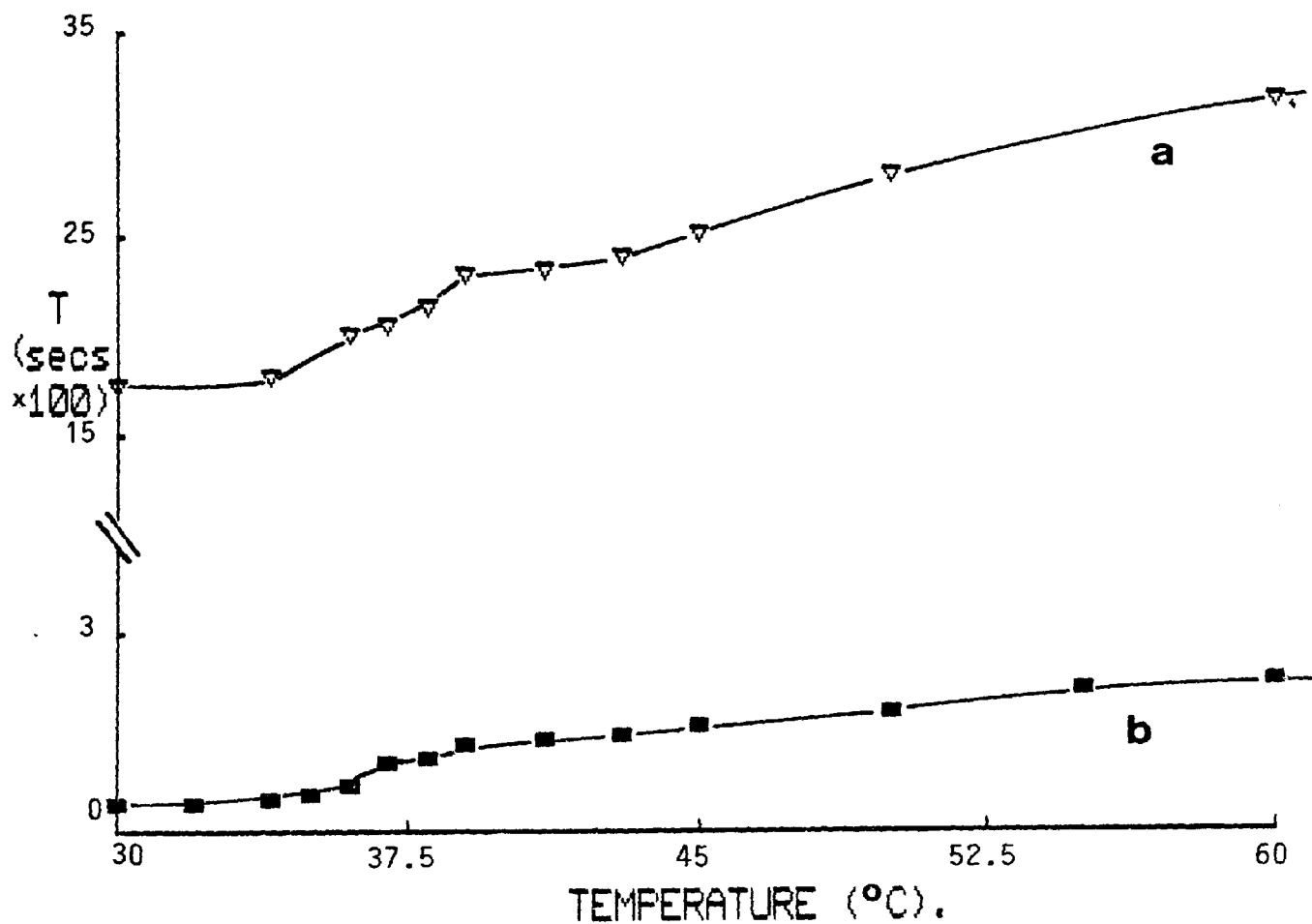


Fig 2.4 The temperature dependence of the spin-lattice relaxation time, T_1 (a), and the spin-spin relaxation time, T_2 (b), of the ^1H -NMR signal from the hydrocarbon methylene groups ($-\text{CH}_2-$) of DPPC vesicles.

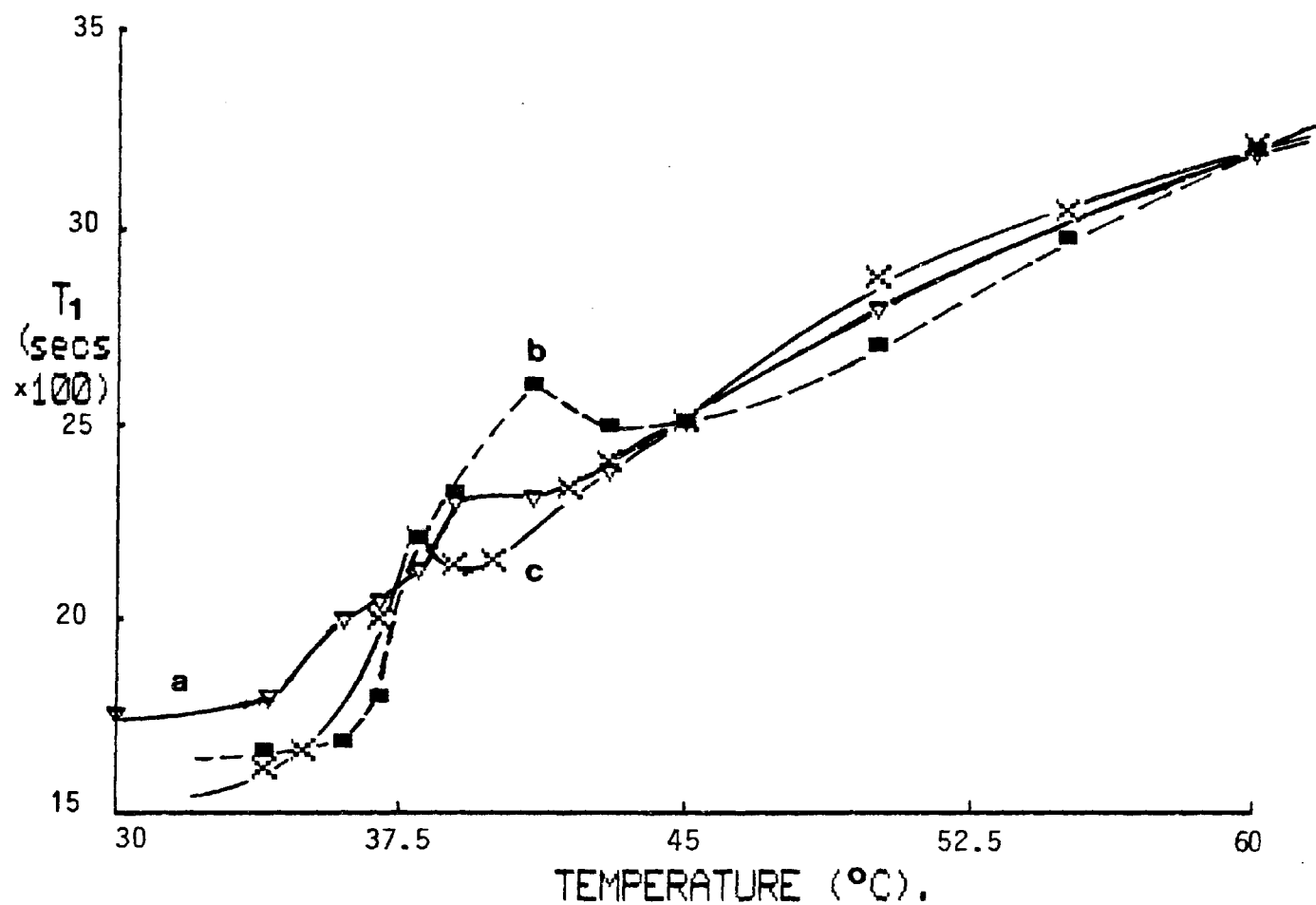


Fig 2.5 The temperature dependence of T_1 of the hydrocarbon methylenes of DPPC vesicles, (a). Vesicles in the presence of extravesicular 5 mM Ca^{2+} (b), and 5 mM Pr^{3+} (c).

above the phase transition) gradually decrease. This is a characteristic of the thermal motion of molecules, in which slower molecular motions are apparent at lower temperatures and thus causing a decrease in the values of the relaxation times. The rate at which T_1 is decreasing is seen to be slower as the temperature approaches the upper limit of the phase transition, where an abrupt decrease in the T_1 values occurs. This region corresponds to an increase in trans rotomers, which allows more inter-molecular interaction between the fatty acyl chains. This results in more efficient spin-lattice relaxation and hence the T_1 values decrease.

The effects of the cations Ca^{2+} , Pr^{3+} (Fig 2.5), Dy^{3+} , $\text{Dy}^{3+}/\text{Ca}^{2+}$ and $\text{Dy}^{3+}/\text{Mg}^{2+}$ (Fig 2.6) are most marked at or near the phase transition. These effects also appear in the T_2 measurements (Figs 2.7 and 2.8), but these effects are not as pronounced as the T_1 effects. This indicates that both fast, and to a lower extent slow motions are affected.

The characteristic elevation in the T_1 and T_2 values of the hydrocarbon protons, when extravesicular cations are present, suggests that the binding of these ions to the head group phosphates is being affected at these temperatures. There is substantial experimental evidence to suggest that cations (in particular divalent and trivalent cations) cross-link phospholipids and that the binding stoichiometry of M^{n+} : phospholipid is 1:2 (Chrzesczyk et al 1981, MacDonald et al 1976). At the onset of the phase transition the lipid molecules undergo motional changes, such as the reduction in the formation of rotational isomers (as described above). This may induce changes in the head group conformation and so altering the 2:1 stoichiometry to a 1:1. This would clearly result in greater motional freedom for the head groups and may give the whole phospholipid molecule extra motional manoeuvrability and

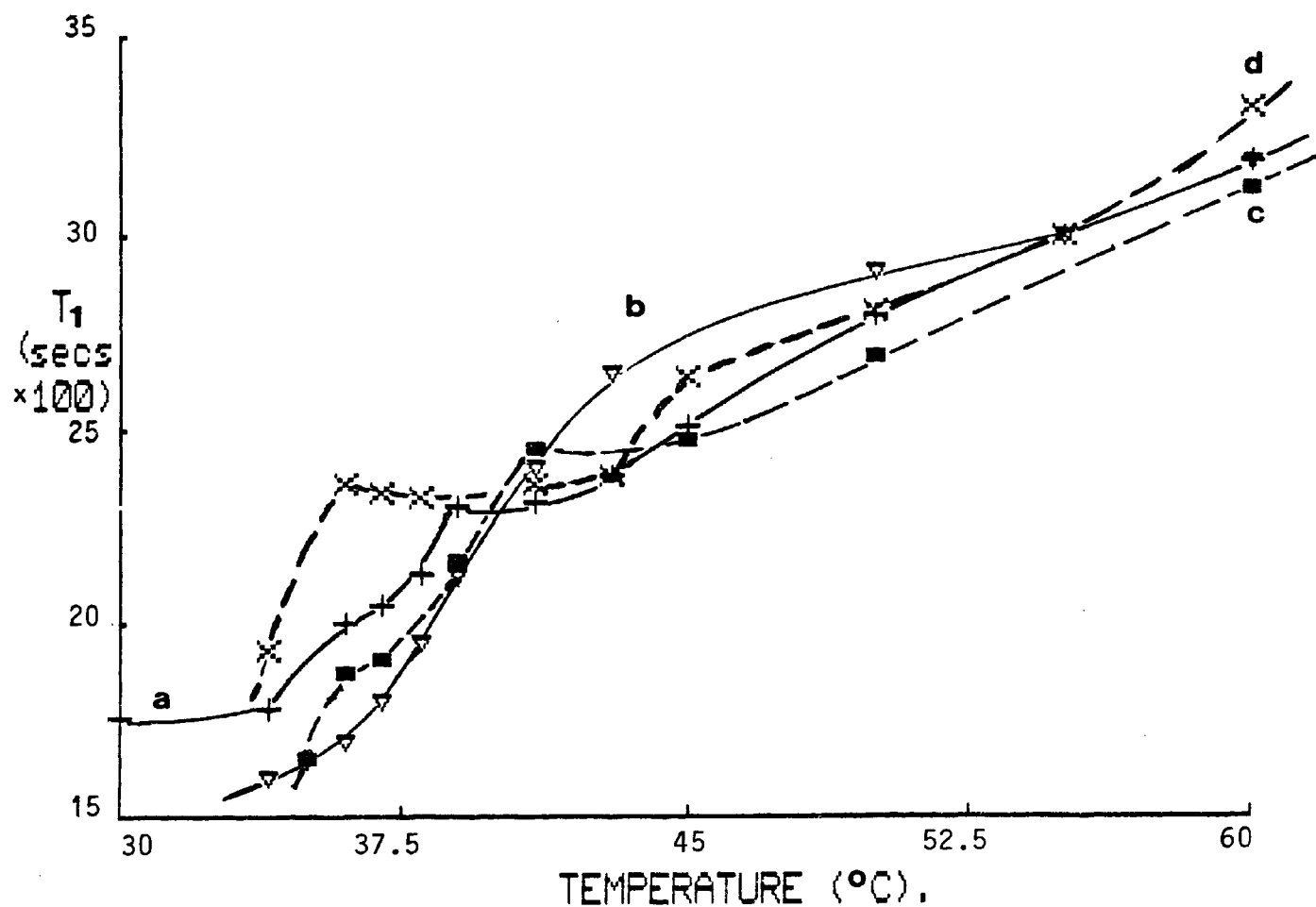


Fig 2.6 The temperature dependence of T_1 of the hydrocarbon methylenes of DPPC vesicles (a). Vesicles in the presence of extravesicular 0.15 mM Dy^{3+} (b), $0.15 \text{ mM Dy}^{3+} + 5 \text{ mM Ca}^{2+}$ (c) and $0.15 \text{ mM Dy}^{3+} + 5 \text{ mM Mg}^{2+}$ (d).

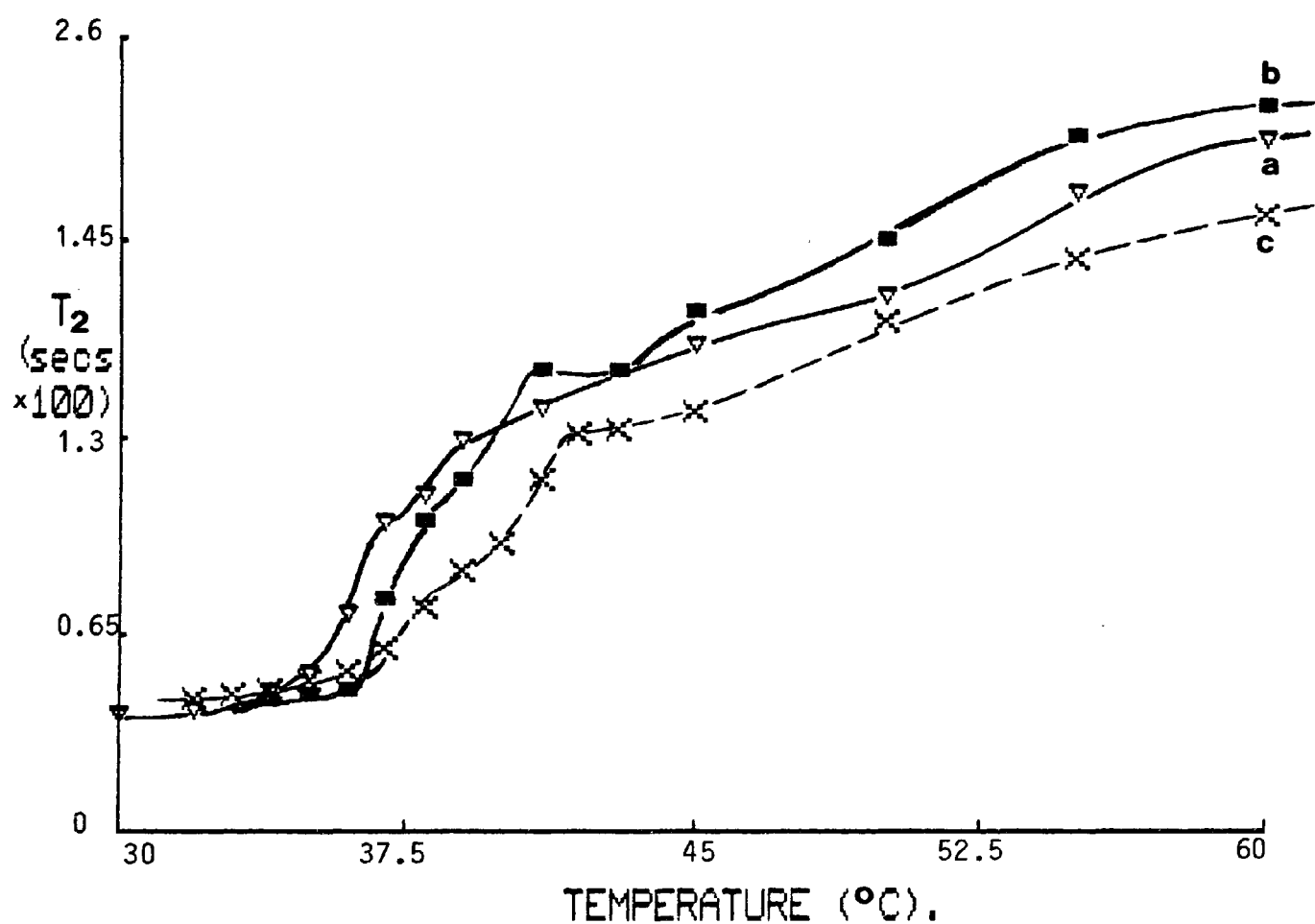


Fig 2.7 The temperature dependence of T_2 of the hydrocarbon methylenes of DPPC vesicles (a). Vesicles in the presence of extravesicular 5 mM Ca^{2+} (b) and 5 mM Pr^{3+} (c).

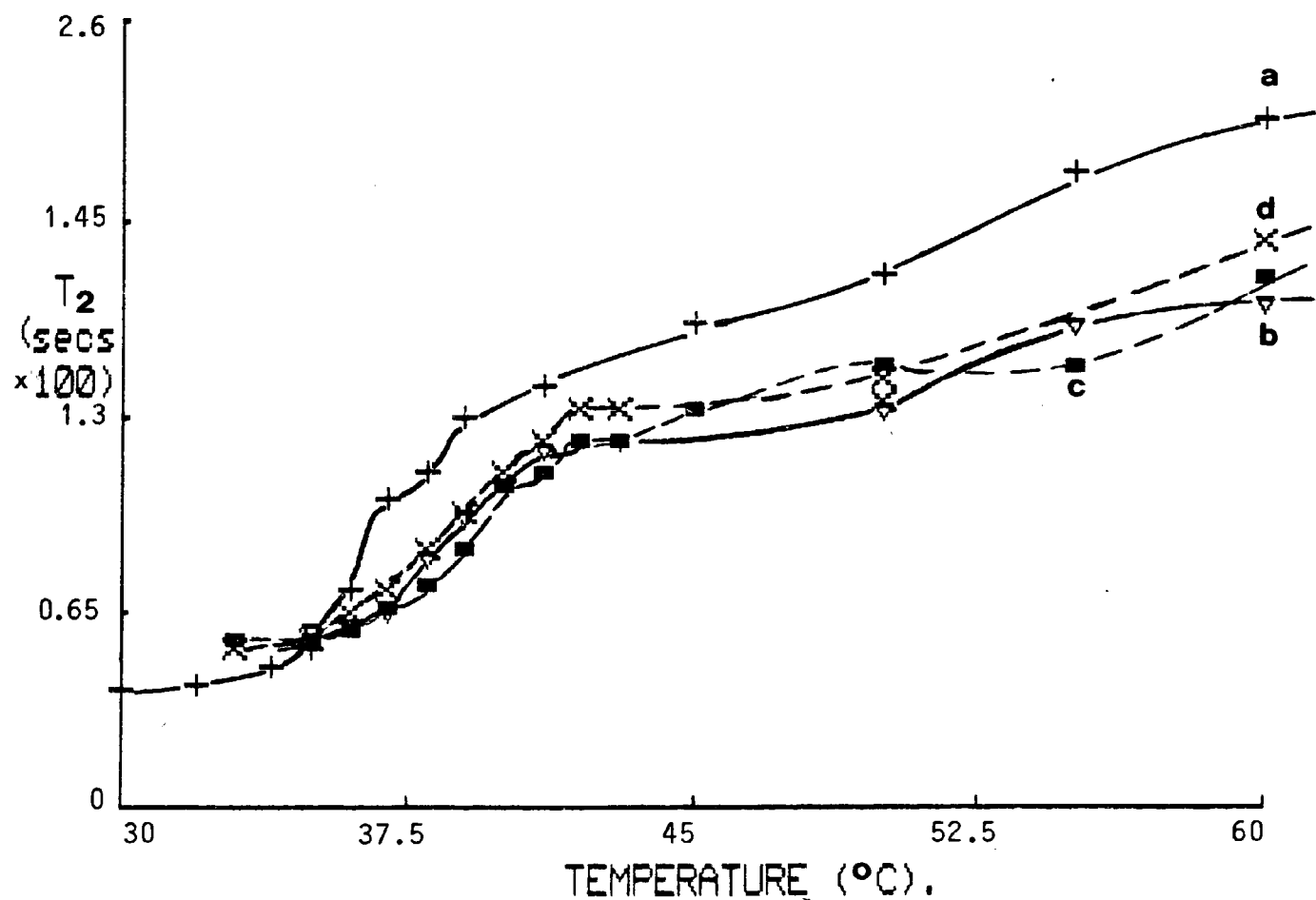


Fig 2.8 The temperature dependence of T_2 of the hydrocarbon methylenes DPPC vesicles (a). Vesicles in the presence of extravesicular 0.15 mM Dy^{3+} (b), $0.15 \text{ mM Dy}^{3+} + 5 \text{ mM Ca}^{2+}$ (c) and 0.15 mM Dy^{3+} and 5 mM Mg^{2+} (d).

thus the rise in the relaxation time values. T_1 measurements in other studies (Podo 1975) also indicate that a head group conformational change takes place which is cooperatively coupled to the freezing of the acyl chains. At lower temperatures (39–35°C) further increase in trans rotomer formation promotes increased Van der Waals interactions between the acyl chains, restricting molecular motion and hence a consequent reduction in the relaxation times.

In Figs 2.4 – 2.8 both transitions have been elevated to slightly higher temperatures (3–4°C) when cations are present. Such effects have previously been observed and it has been shown that the magnitude of temperature increase is directly related to the cation charge (Trauble and Eible 1974, Hauser et al 1976b). The effects are found to be small with neutral lipids but are much greater in charged bilayers. Thus the addition of calcium under appropriate conditions may induce an isothermal reversible phase transition which may be accompanied by an abrupt increase in the bilayer lateral compressibility.

Figs 2.9 – 2.14 show the effects of cations on the outer and inner head group relaxation times. The use of the paramagnetic ion method in this way has the advantage of allowing signals from both monolayers to be observed simultaneously in a sample of vesicles under the same conditions. The form of these plots shows that the head groups are affected by the main phase transition and also that ion (calcium and magnesium) binding to the outer phosphates greatly affect the motional properties of the head groups during and above the phase transition. The observations that cations also influence the relaxation times of the inner head groups emphasise the cooperativity that exists between the two monolayers, a property which may be of major importance in transmitting information across the bilayer.

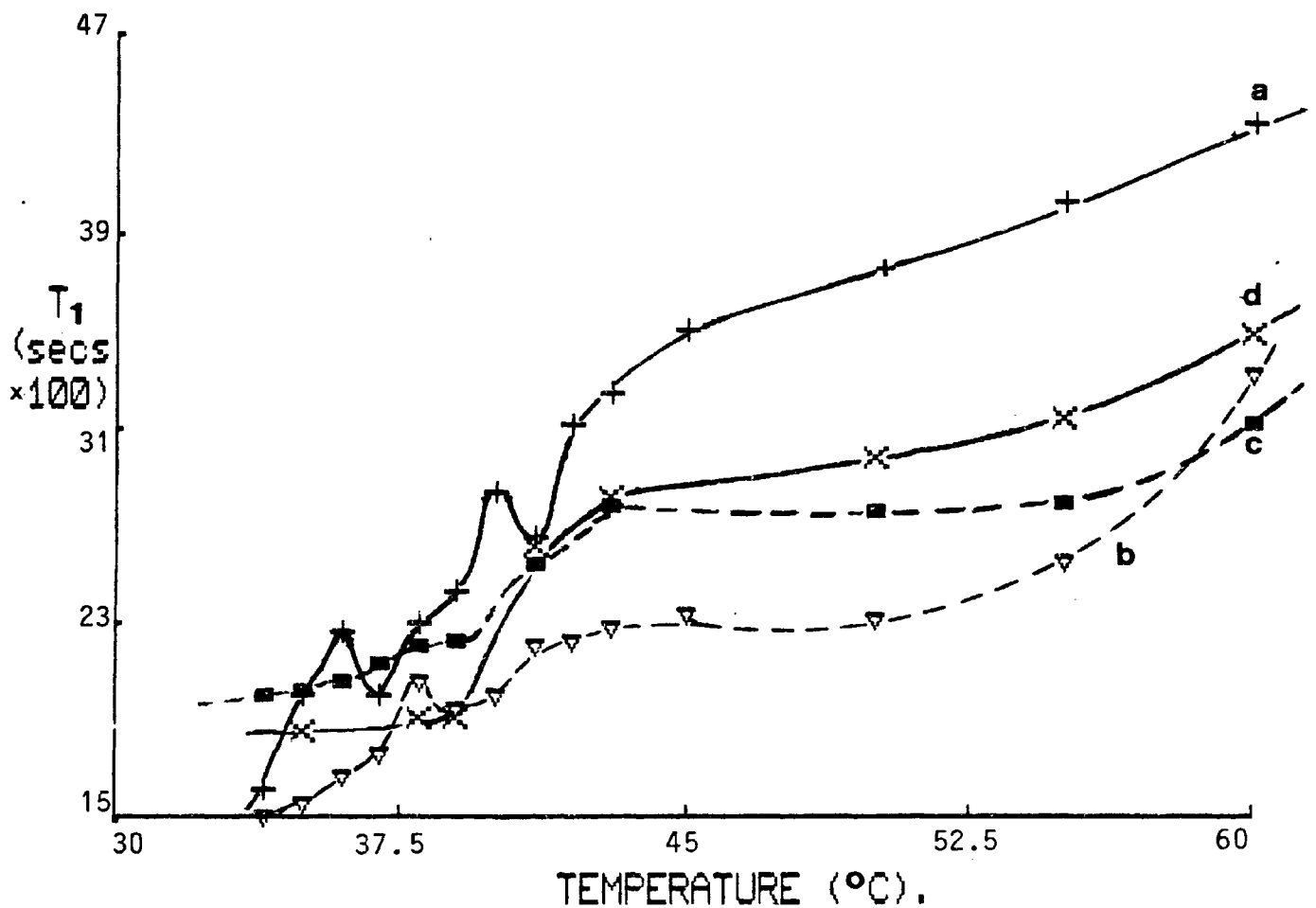


Fig 2.9 The temperature dependence of T_1 of the inner and outer head-group signals of DPPC vesicles. Vesicles in the presence of:-
 Extravesicular 5 mM Pr^{3+} : a) outer head-group; b) inner head-group.
 Extravesicular 0.15 mM Dy^{3+} : c) outer head-group, d) inner head-group

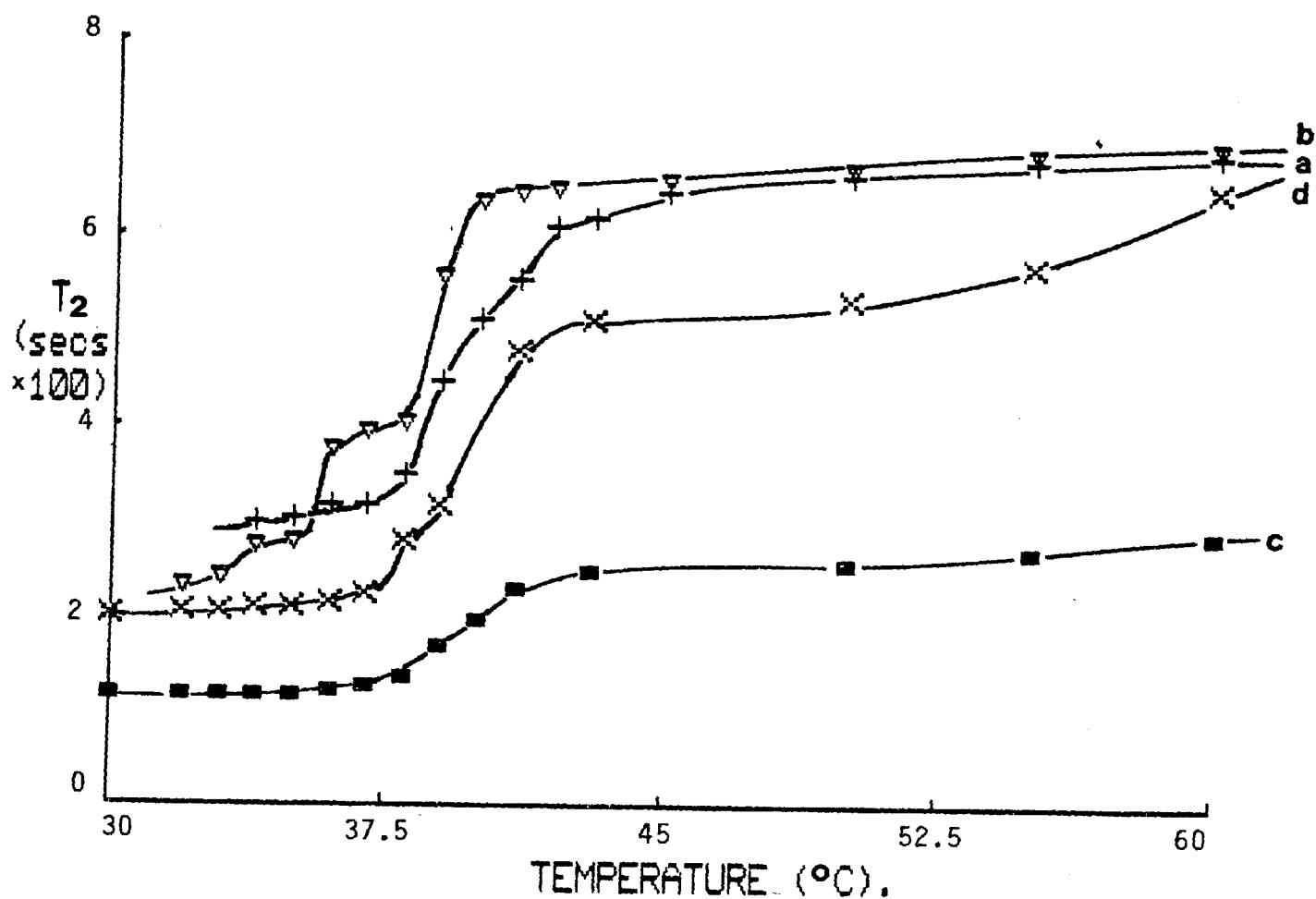


Fig 2.10 The temperature dependence of T_2 of the inner and outer head-group signals of DPPC vesicles. Vesicles in the presence of:- Extravesicular 5 mM Pr^{3+} : a) outer head-group; b) inner head-group. Extravesicular 0.15 mM Dy^{3+} : c) outer head-group, d) inner head-group

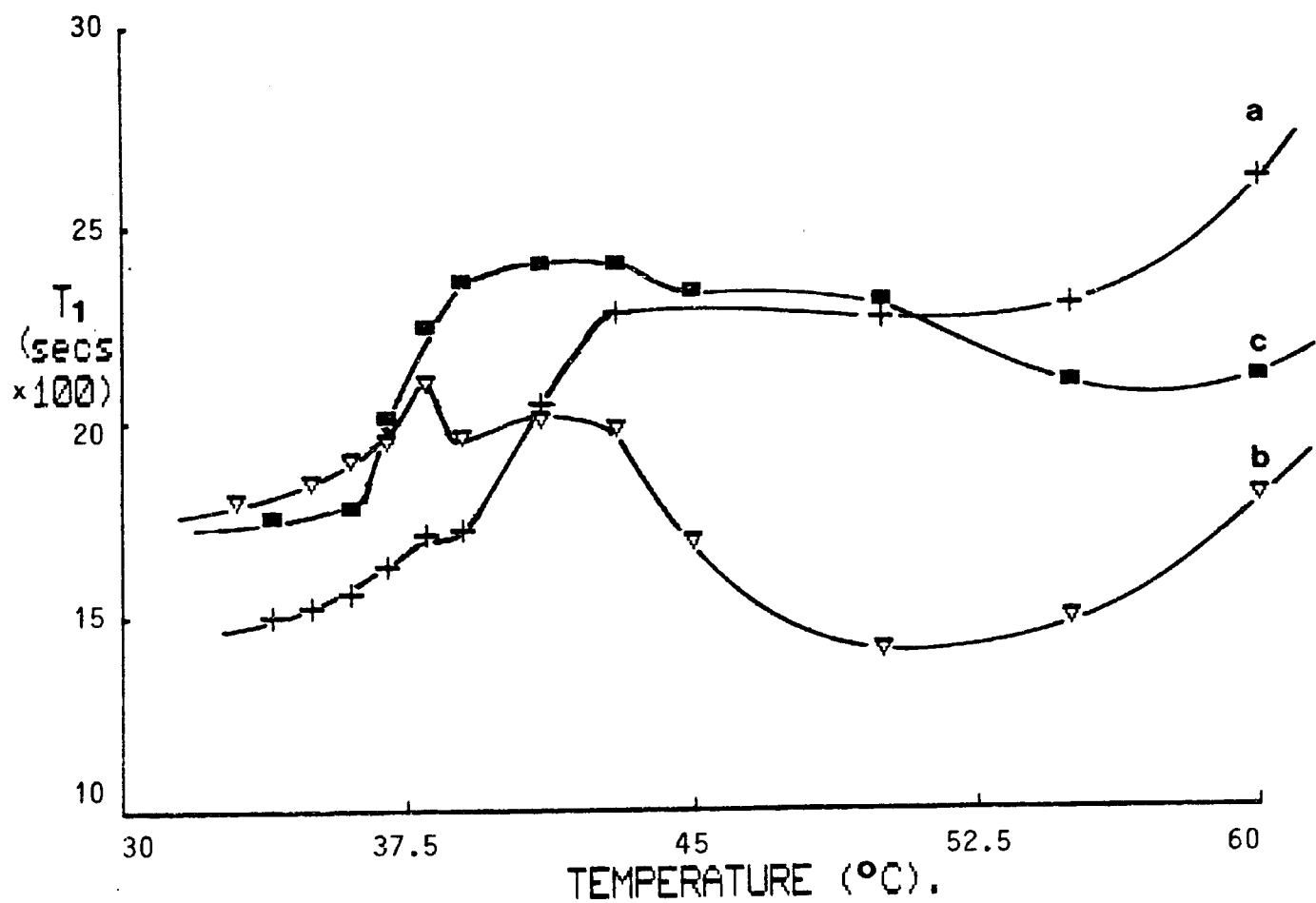


Fig 2.11 The temperature dependence of T_1 of the outer head-group signals of DPPC vesicles in the presence of:-

- a) 0.15 mM Dy^{3+} , b) 0.15 mM Dy^{3+} + 5 mM Ca^{2+} ,
 c) 0.15 mM Dy^{3+} + 5 mM Mg^{2+} .

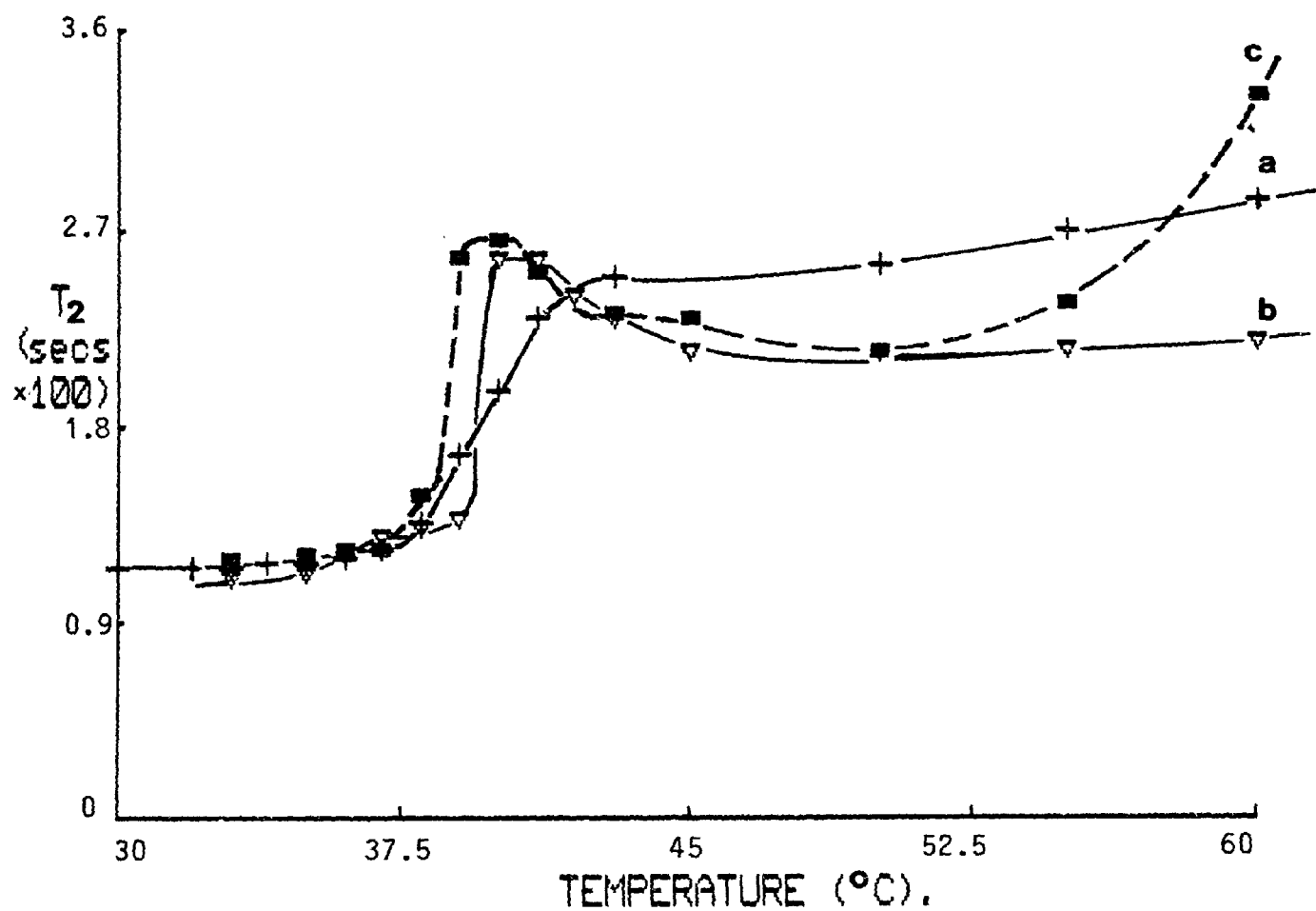


Fig 2.12 The temperature dependence of T_2 of the outer head-group signals of DPPC vesicles in the presence of:-

- a) 0.15 mM Dy^{3+} , b) 0.15 mM Dy^{3+} + 5 mM Ca^{2+} ,
- c) 0.15 mM Dy^{3+} + 5 mM Mg^{2+} .

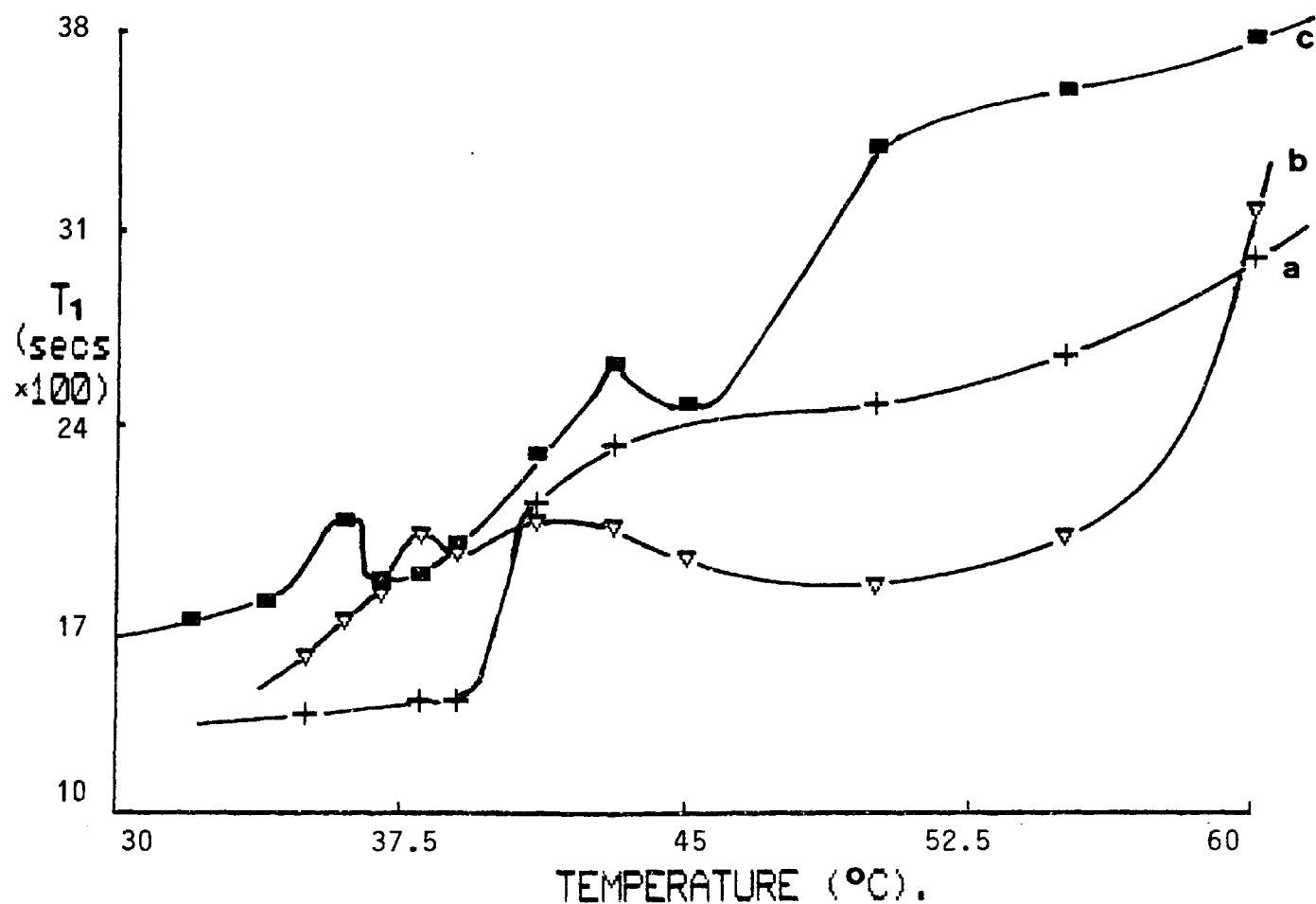


Fig 2.13 The temperature dependence of T_1 of the inner head-group signals of DPPC vesicles in the presence of:-
a) 0.15 mM Dy^{3+} , b) 0.15 mM Dy^{3+} + 5 mM Ca^{2+} ,
c) 0.15 mM Dy^{3+} + 5 mM Mg^{2+} .

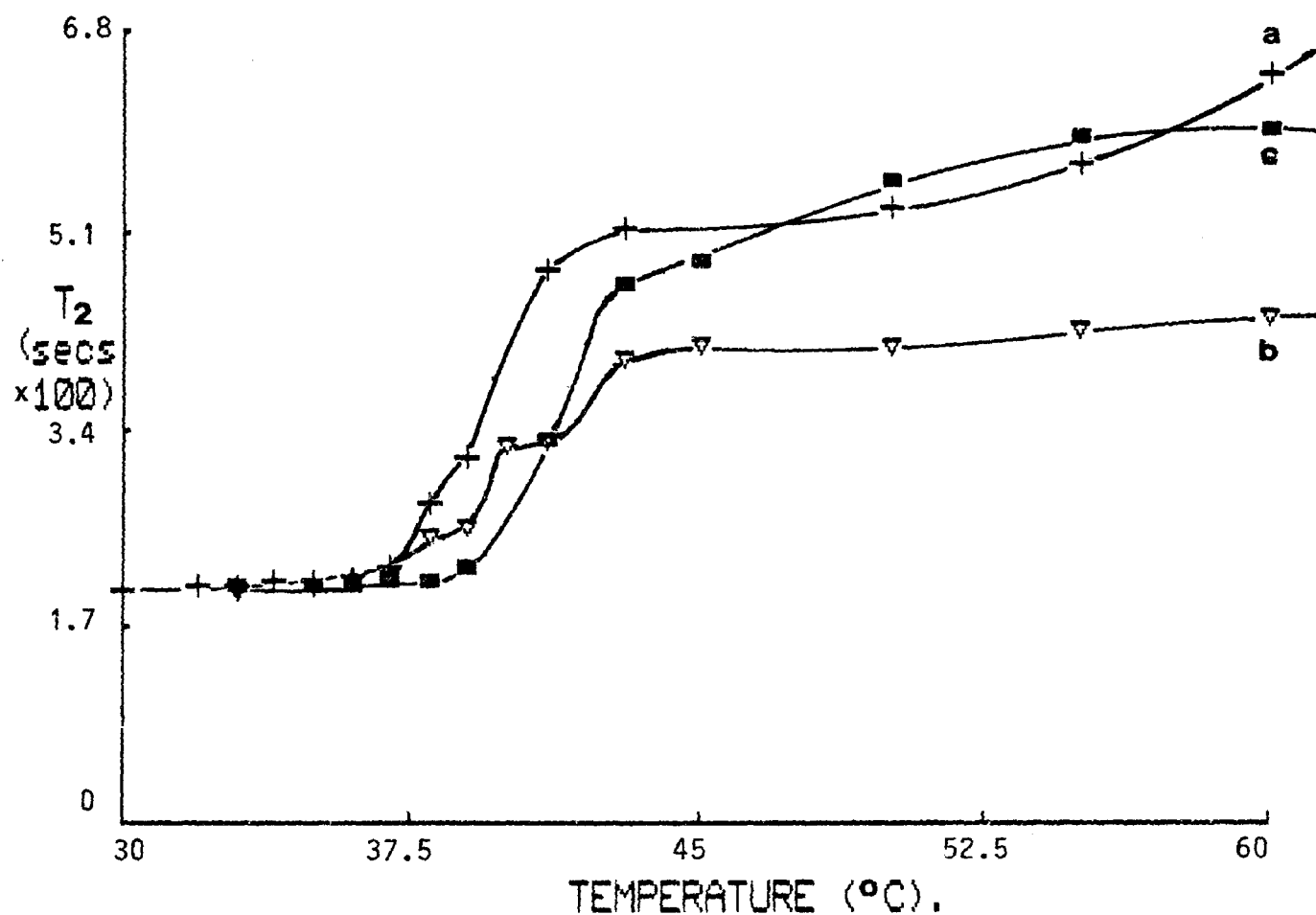


Fig 2.14 The temperature dependence of T_2 of the inner head-group signals of DPPC vesicles in the presence of:-
a) 0.15 mM Dy^{3+} , b) 0.15 mM Dy^{3+} + 5 mM Ca^{2+} ,
c) 0.15 mM Dy^{3+} + 5 mM Mg^{2+} .

CHAPTER 3

MEMBRANE PERMEABILITY

3.1 Introduction

A recent report emphasised that in order to investigate transmembrane transport mechanisms the development of physical methods is required which can probe the membrane system at the molecular level (Hokin 1981). Several groups have already begun to explore the application of NMR techniques to the problem, initially using model systems (Ting et al 1981, Pike et al 1982, Hunt 1975, Hunt et al 1978, Donis et al 1981, Grandjean and Laszlo 1982).

To monitor ion transport across membranes it is useful to distinguish between molecules that are in the inner and outer monolayers of a lipid bilayer. In the ^1H -NMR spectrum of PC vesicles this can be achieved by either, use of paramagnetic shifting cations (for example Eu^{3+} , Pr^{3+} , Dy^{3+}) as indicated in chapter 2, or by the use of paramagnetic broadening cations such as Mn^{2+} and Gd^{3+} . For the latter type the paramagnetic enhancement of the relaxation rates is such that the signals of the nuclei interacting with the paramagnetic ion broaden out and vanish into the base line. In this system cation transport can be followed simply by monitoring peak intensities as is indicated in the study of Mn^{2+} transport (Degani 1978, Degani and Lenkinsky 1980, Degani et al 1981). These phenomena make it possible to study the influence of various chemical agents, such as ionophores, on membrane permeability.

In the present study the ^1H -NMR methods developed by Hunt and coworkers are used to monitor the transmembrane transport of the paramagnetic shift ions, Pr^{3+} and Dy^{3+} into sonicated lipid vesicles. By this method information regarding the transport rate can be obtained provided that the lanthanide shift ions are used in combination with a

relatively low concentration of ionophore. This lowers the possibility of instantaneous equilibration of the probe ion into the intravesicular solution, a phenomenon which was problematic in some early studies (Chen 1978).

Alamethicin, an extracellular pore forming polypeptide was extracted from the fungus Trichoderma viridie by Meyer and Reusser in 1967 (Melling and McMullen 1975). Early attempts to establish the amino acid sequence of alamethicin led to the proposal of a cyclic structure (Fig 3.1a, Payne et al 1970, Ovchinnikov et al 1971) which was later revised to a linear branched structure (Fig 3.1b) on the basis of 270 MHz ^1H -NMR and ^{13}C -NMR studies (Martin and Williams 1976, Marshall and Balasubramanian 1979). However both these proposed structures have been prepared synthetically and were found to be deficient in membrane activity (Gisin et al 1977a, Marshall and Balasubramanian 1979).

Mellings and coworkers (1975) showed that natural alamethicin consisted of four components, referred to as factors F_{20} (2%), F_{30} (85%), F_{50} (12%) and F_{60} (1%). Field desorption mass spectroscopy and ^{13}C -NMR studies gave a linear structure for alamethicin 30 (Fig 3.1c), but a synthetic preparation of this structure only showed 10% the membrane activity obtained from natural alamethicin (Marshall and Balasubramanian 1979).

Recently natural alamethicin has been separated by HPLC into twelve closely related polypeptides (Balasabramanian et al 1981), the main ones being fraction 4 (45%), fraction 5 (10%) and fraction 6 (20%). Studies by Gisin and coworkers (1977b) on a synthetic polypeptide showing 70% the membrane activity of natural alamethicin led to the proposal that the major component of natural alamethicin was a mixture

- a.** Pro-Aib-Ala-Aib-Ala-Gln-Aib-Val-Aib-Gly-Leu-Aib-Pro-Val-Aib-Aib-Glu-Gln-OH
 {-----}
- (Payne et al 1970, Ovchinnikov 1971)
- b.** AcAib-Pro-Aib-Ala-Aib-Ala-Gln-Aib-Val-Aib-Gly-Leu-Aib-Pro-Val-Aib-Aib-Glu-Gln
 |
 Phol OH
- Martin and Williams (1976)
- c.** AcAib-Pro-Aib-Ala-Aib-(^{A₁a}_{A₁b})-Gln-Aib-Val-Aib-Gly-Leu-Aib-Pro-Val-Aib-Aib-Glu-Gln-^γPhol
 |
 α | α
 OH NH₂
- (Padney 1977)
- d.** AcAib-Pro-Aib-Ala-Aib-(^{A₁a}_{A₁b})-Gln-Aib-Val-Aib-Gly-Leu-Aib-Pro-Val-Aib-Aib-Glu-Gln-Phol
- (Gisin et al 1977, Rinehart et al 1977, Fox 1982)

Fig 3.1 Various structures proposed for alamethicin 30 .

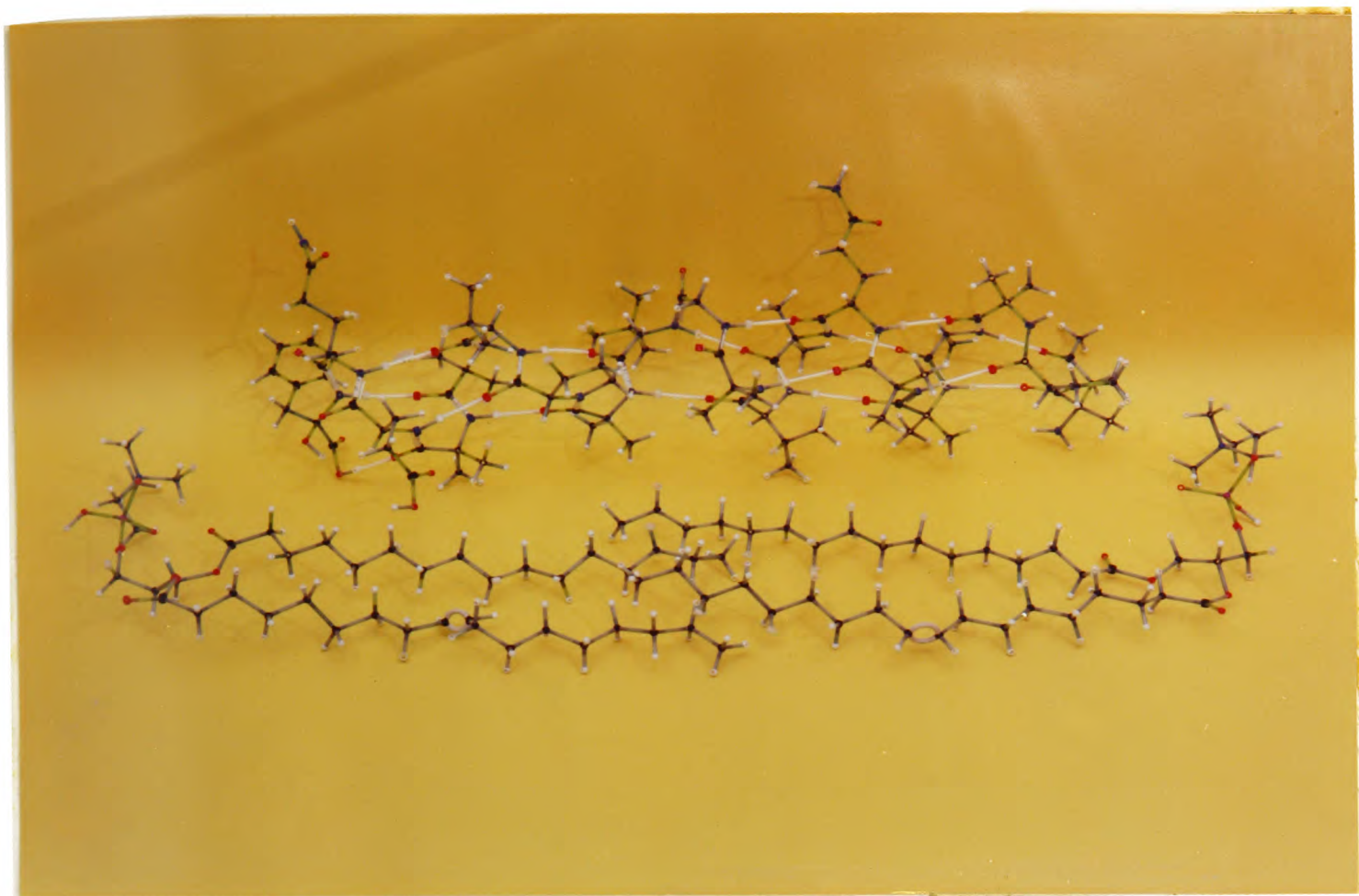


Fig 3.1(e) Indicates that alamethicin in the α -helical form is long enough to span a lipid bilayer.

(Fig 3.1d). The two structures differ only in their sixth residue and are termed alamethicin I and alamethicin II for the alanine and α - aminoisobutyric acid (methyl alanine) residues respectively. Further studies employing 600 MHz ^1H -NMR, HPLC and mass spectral techniques on natural and synthetic components of alamethicin reveal that the major component, fraction 4, to be alamethicin I and fraction 6 to be alamethicin II (Gisin et al 1981, Balasabramanian et al 1981). These structures are supported by HPLC (Marshall et al 1979), X-ray crystallography (Fox and Richards 1982) and mass spectral studies (Rinehart et al 1977) thus suggesting that alamethicin 30 is a mixture of alamethicin I (69%) and alamethicin II (31%) having molecular weights of 1962 and 1976 respectively. X-ray crystallography, circular dichroism and NMR studies indicate that alamethicin exists in a α -helical form (as a consequence of its high AIB content) which is too narrow to allow passage of ions as large as Na^+ through the helix interior (Jung et al 1979, Fox and Richards 1982, Mathew and Balaram 1983). A molecular model of alamethicin II in the α -helical conformation is shown in Fig 3.1e. This shows that alamethicin in this form is long enough to span a lipid bilayer.

The majority of alamethicin studies have been performed using natural alamethicin and BLMs, where it has been shown to induce voltage dependent channels (see section 1.3.2). Molecular models, based on electrophysiological studies, have been proposed for the formation of the alamethicin conducting channel (Boheim and Kolb 1978, Hall 1975, Baumann and Muller 1974, Muller and Rudin 1968, Eisenberg et al 1973). It has generally been postulated that in the absence of an electrical field alamethicin resides at the membrane surface and channel formation involves the voltage dependent insertion of alamethicin molecules into

the hydrocarbon region of the bilayer. After removal of the electrical field alamethicin molecules are thought to return to the membrane surface. The molecular models differ on whether the voltage dependent insertion involves preformed oligomers of alamethicin molecules (Hall 1975, Boheim and Kolb 1978) or monomers which diffuse laterally in the bilayer to form oligomeric conducting channels, similar to staves in a barrel (Baumann and Muller 1974).

However a few studies reveal that alamethicin molecules may not require a transmembrane potential to partition into the bilayer. For high aqueous concentrations of alamethicin, Eisenberg and coworkers (1973) have observed voltage dependant conductance in planar bilayers in the absence of an applied field. Recently it has been confirmed that alamethicin can transport lanthanide ions across planar lipid membranes in a manner which differs in its voltage dependence as observed for univalent ions (Goglein et al 1981).

The interaction of alamethicin with phospholipids has also been studied by a number of physical techniques. Chapman and coworkers found that alamethicin readily penetrated lipid monolayers and that increasing amounts of alamethicin decreased the intensity of the lamellar X-ray diffraction orders obtained from lipid liposomes. Hauser et al (1970) interpreted their NMR data to mean that each alamethicin molecule induces a transition of about 600 lipid molecules from the normal unilamellar state to some new form of aggregate, thus abolishing the multilamellar structure. However in subsequent NMR studies Lau and Chan (1974, 1975, 1976) conclude that alamethicin was surface active interacting primarily with the polar lipid head groups.

Recently some groups have more strongly challenged the idea that

alamethicin requires a transmembrane potential to be inserted into the bilayer. Infra- red total reflection spectroscopy has been employed to examine the interaction of alamethicin 30 with DPPC liposomes below the thermal phase transition (Fringeli and Fringeli 1979, Fringeli 1980). The data obtained indicates that under these conditions in the absence of an electric field, alamethicin spans the lipid bilayer. Using X-ray diffraction and electron density profiles McIntosh et al (1982) found that even in the absence of an electric field, alamethicin modifies both the hydrophilic and hydrophobic region of liposome bilayers both above and below the phase transition of the lipid. Furthermore, using an analogue consisting of an alamethicin molecule covalently bound to a phospholipid molecule, Latorre and coworkers (1981, Quay and Latorre 1982) were able to demonstrate voltage dependent conductance similar to that of natural alamethicin. They interpreted these results to mean that alamethicin gating does not involve the insertion of alamethicin monomers into the membrane but rather conformational changes of molecules already in the bilayer.

But for the work of Lau and Chan (1974, 1975, 1976) which was dominated by the occurrence of vesicular fusion, no detailed study of the transport properties of alamethicin in lipid vesicles has been made. In the present study the ^1H -NMR methods are used to investigate the molecular mechanism of alamethicin ion transport into lipid vesicles with no applied transmembrane potential. The initial investigations include channel stoichiometry - activation energy calculations and the effects of various experimental procedures on the transport rates.

The increase in calcium permeability of cell membranes has been associated with phosphatidate (PA) formation during the degradation of PI (Michell 1975, 1979, Michell and Kirk 1981). The mechanism of the PI

effect is unclear but a possibility involves PA directly mediating the inward movement of Ca^{2+} possibly by activation of surface membrane receptors (Putney et al 1980, Tyson et al 1976, Serhan et al 1982). Another possibility involves PA influencing the activity of calcium transporting proteins via a lipid - protein interaction (Niskizuka 1983, Dawson et al 1983).

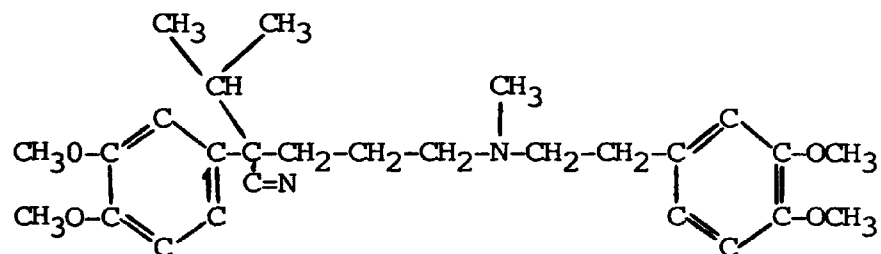
The ability of CL to adopt the H_{II} phase in the presence of divalent ions (see section 1.4) has led to the suggestion that non bilayer structures play important functional roles in the inner mitochondrial membrane, of which Ca^{2+} transport and the activity of cytochrome C are the most important ones (Cullis and De Kruijff 1979, Cullis et al 1980a). With these phenomena in mind the influence of CL on ion transport by alamethicin channels is investigated.

^{31}P -NMR studies have clearly demonstrated that the polypeptide channel former gramicidin has a strong H_{II} phase promoting ability in PE bilayers (at a lipid : gramicidin ratio of 200 : 1) and to a lesser extent in dioleoyl PC (at a lipid : gramicidin ratio of 10 : 1) bilayers (Van Echteld et al 1981, 1982). It is suggested that the H_{II} phase plays an essential role in the stability of gramicidin channels. Further evidence for a gramicidin-lipid interaction has been obtained by ^2H -NMR where gramicidin is found to promote order in annulus lipid (Rice et al 1979). The experiments carried out in the present study were therefore designed to investigate the effect of physiological concentrations of the non bilayer phase promoting lipids, PA, CL and PE, on the transport of cations by alamethicin in lipid vesicles.

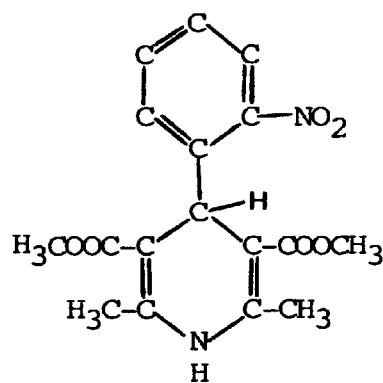
Calcium antagonistic drugs (Zsoter and Church 1983, Kates 1983, Deedwania 1982) such as verapamil and nifedipine (Fig 3.2a) represent a major development in cardiovascular pharmacology. Their main site of

Fig 3.2

a) Calcium antagonist structure.

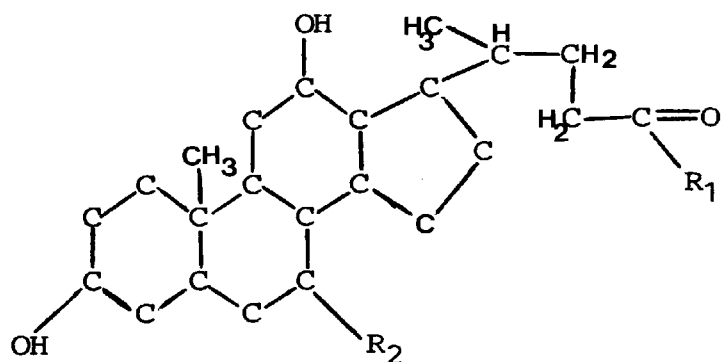


Verapamil



Nifedipine

b) Bile salt structure.



R_1 - ONa	R_2 - OH	Sodium cholate
R_1 - ONa	R_2 - H	Sodium deoxycholate
R_1 - $\text{NHCH}_2\text{COONa}$	R_2 - OH	Sodium glycholate
R_1 - $\text{NHCH}_2\text{COONa}$	R_2 - H	Sodium glycodeoxycholate

action is thought to be on the slow channels where they inhibit calcium influx into the cell. However the exact site of action and its mechanism has not yet been determined (Zsoter 1980). The possibilities include :

- a. Blocking the gate of the channel pathway.
- b. Competing with calcium at the outside gate (Flechanstein 1977).
- c. Deforming the channels or in some other way interfering with the passage of calcium (Mas Oliva and Nayer 1980, Katz and Messineo 1981).
- d. Interfering with the release of activated calcium on the inside of the cell membrane (Church and Zsoter 1980).

Most studies have set out to investigate these possibilities using relatively complex systems. Therefore in this study alamethicin 30 channels in DPPC vesicles has been used as a biologically relevant model for investigating the mechanism and site of action of the calcium antagonist drugs, verapamil and niphedipine.

Membrane permeability induced at the phase transition has been observed in planer lipid membranes (Antanov et al 1980) and in liposomes (Papahadjopoulos et al 1973). Studies on the electrical conductance of planer lipid bilayers formed of DSPC showed current fluctuations at T_c , a result that is consistent with the appearance of ionic channels in the membrane (Haydon and Hladky 1972).

The mechanism by which such channels open up in membranes at the phase transition is not clear. Some of the proposed theories include lipid domain formation, phase separation and lateral compressibility (Nagle and Scott 1978, Kanehisia and Tsong 1978, Marcelja and Wolfel 1979). Marcelja and Wolfe (1979) reject the lipid domain theory (for neutral lipids) on thermodynamic grounds and favour the concept of

lateral compressibility. This suggests that lipids in bilayers are subject to intrinsic lateral pressure which depends strongly on the interactions at the polar head group - water interface. These are thought to promote lateral density fluctuations which open up short-lived cavities in the head group region, thus entrapping metal ions. When the cavities close the ions diffuse across the hydrocarbon phase (Neagle 1978, Marcelja 1979).

Alternatively the lipid domain and phase separation concepts have been favored. During the phase transition three phases are formed (see chapter 1). When the phase transition is approached from higher temperatures, islands or clusters of gel phase lipid are formed within the bulk liquid crystal phase. The packing of the lipid molecules in such a phase is likely to be variable due to disorders in the liquid crystal phase. As T_c is approached the growth and aggregation of these lipid clusters take place in a cooperative change from fluid liquid crystal to solid gel phase. The lipid molecules in all these states exhibit different free energies (Houslay and Stanley 1982) with the lipid in the boundary phase having the highest value due to the mismatch occurring between the molecular packing of ordered and fluid domains. This mismatch in packing is thought to be responsible for the maximum in passive permeability to ions and small molecules at the phase transition.

The phase transition range in small vesicles occurs over a relatively wide range of temperature (see chapter 2) over which the different phases can coexist (in DPPC vesicles 42-32°C). Papahadjopoulos and coworkers (1973) maintain that the compressibility is at its maximum at the mid-point of T_c since the fractional area of boundary regions within the membrane is at its greatest.

The ^1H -NMR studies of Hunt (1980b) showed that lysis of DPPC vesicles occurs when they are repeatedly cycled between 60° and 38°C. He found that the population of vesicles lysing depended on the number of temperature cycles. The detergent Triton X100 was found to greatly increase the population lysing per temperature cycle, but the process was accompanied by wide-spread vesicular fusion.

The present study is aimed at quantifying the degree of vesicular lysis in DPPC vesicles which have been cycled through their entire phase transition. A comparison is then made with the effects of Triton X100. Low concentrations of Triton X100 are used (0.1mM) to eliminate the permeability induced by Triton X100 transport (Hunt 1980b) and also in an attempt to reduce vesicular fusion.

While bile salts have a well understood function in the digestive process (through their formation of mixed micelles with lipids and fats) they have also been implicated in a number of abnormal physiological changes, especially the dehydroxylated forms deoxycholate and lithocholate (Bowman and Rand 1980, Bett and Wells 1980, Martin and Marriott 1981, Hunt and Jawaharlal 1980, Hill 1977, Strange et al 1981, Coleman et al 1980). They have also been widely employed as reagents in biochemical studies (Vyvoda et al 1977, Hunt and Jawaharlal 1980).

The present study involves two aspects:

- a. Membrane damage by bile salts which has been associated with lysis of erythrocytes (Coleman et al 1980, Billington and Coleman 1978) and cancer of the large intestine (Bowman and Rand 1980, Hill 1977, Bett and Wells 1980).
- b. The use of liposomes for drug delivery via the oral route (Ryman and Tyrrell 1980, Yatvin and Lelkes 1982).

Over the past decade much concern has been concentrated on the involvement of bile salts in the development of cancer in the large bowel (Bowman and Rand 1980, Bett and Wells 1980). The lack of fibre in the gut gives rise to anaerobic conditions which alter the bacterial flora. The changes in the bacterial flora along with other dietary factors alter the bile salts in the gut to products such as the deoxy bile salts. These are found to be more carcinogenic than the trihydroxy bile salts when applied to the large bowel mucosa. The studies of Strange and coworkers (1981) suggests that the trihydroxy and dihydroxy bile salts partition into the bilayers to different degrees, hence showing different membrane activities. Coleman et al (1980) show that the resistance of membranes to bile salt attack is dependent on the lipid composition.

^1H -NMR studies have shown that bile salts possess ionophore activity in DPPC and DPPC/cholesterol vesicles (Hunt 1980b, Hunt and Jawaharlal 1980). The NMR techniques employed in these studies could distinguish between a carrier-type transport in DPPC vesicles and lysis occurring in DPPC/cholesterol vesicles. It was proposed that the carrier mechanism involves inverted micelles each formed from a mixture of lipid and four bile salt molecules in which their hydrophilic sides (see Fig 3.2b for structure) are bound inwards by H-bonds between the hydroxyl groups, leaving the hydrophobic sides facing outwards to interact with the fatty acyl chains.

In the present study the membrane-damaging capabilities of the bile salts, cholate, deoxycholate and their conjugates glycocholate and glycodeoxycholate are investigated using egg PC vesicles. In contrast to DPPC vesicles (Hunt and Jawaharlal 1980) no cholesterol was required for lytic activity.

The use of liposomes as carriers of therapeutic drugs is being widely explored at present (Ryman and Tyrrell 1980, Gregoriadis and Allison 1980, Knight 1981, Yatvin and Lelkes 1982). In particular the prospect of a more convenient method of taking insulin has attracted much attention to liposomal packing and delivery of this drug by the oral route (Patel et al 1978, Hashimoto and Kawada 1979). It has been demonstrated that liposomally entrapped insulin when given orally produces hypoglycemia in both diabetic and normal rats. Thus liposomes not only seem to protect insulin from proteolytic degradation in the stomach and intestine, but also act as structurally organised vehicles with endocrine therapeutic potential (Patel et al 1978). However only about 1% of the packed insulin reaches the target site and this has been attributed to the lack of liposomal stability in the harsh environment of the gastrointestinal tract (Rowland and Woodley 1980).

Studies on this aspect includes:

- a. The degradation of liposomally entrapped insulin in the stomach and during incubations with intestinal washings (Patel and Ryman 1977).
- b. The effect of conjugated bile salts, taurocholate and glycocholate on chromate release from liposomes (Richards and Gardner 1978).
- c. The separate actions of bile salts and pancreatic lipases on liposomes of a variety of compositions in order to explore how their stability may be improved (Rowland and Woodley 1980).

However some studies suggest that interaction between bile salts and digestive enzymes can occur in:

- a. The hydrolysis of triglyceride by lipase in milk fat globules (Blackberg et al 1981).
- b. In the hydrolysis of phospholipid by phospholipase A₂ (PLA₂) in bile salt - lipid mixed micelles (Nalbone et al 1980).
- c. The hydrolysis of triacylglycerol by pancreatic lipase in the presence of bile salt and PLA₂ (Rigler and Patton 1983).
- d. In the hydrolysis of PE/PC micelles by PLA₁ being greatly stimulated by sodium deoxycholate (Van den Bosch et al 1974).

The possibility that bile salt and phospholipase activity may be cooperative has clear implications for the design and use of liposomes by the oral route. A recent report outlines the advantages of using small unilamellar vesicles for investigating such aspects as drug targeting (Machy and Leserman 1983). Therefore this part of the study sets out to determine:

- a. The action of pancreatic PLA₂ on egg PC vesicles.
- b. Whether or not bile salts and pancreatic PLA₂ increase the permeability of egg PC vesicles in a cooperative or synergistic manner.

3.2 Materials and Methods

3.2.1 Chemicals

Egg phosphatidyl choline(PC), Bovine cardiolipin (CL) and egg phosphatidic acid (PA) were purchased from Lipid Products (South Nutfield, Surrey). Plant phosphatidyl ethanolamine (PE) was obtained from Biomedical Ltd (Canvey Island, Essex). Stock solutions in chloroform-methanol of egg PC (50 mg/ml), CL (5 mg/ml), egg PA (5 mg/ml) and plant PE (5 mg/ml) were prepared and stored at -5°C . The antioxidant tertiary butyl hydroquinone was added to the plant PE stock solution (0.2 mg/10ml).

Alamethicin 30 was obtained from PHLS Centre for Applied Microbiology and Research (Porton Down, Salisbury). Stock solutions were prepared either in D_2O (1 mg/ml) or in chloroform (2 mg/ml) and stored at 5°C and -5°C respectively. Verapamil (Mol.wt. 491) was a gift from the Abbot Research Laboratory (Queensborough, Kent). A stock solution was prepared in D_2O (5 mg/ml) and stored at room temperature. Niphedipine (Mol.wt. 346) was a gift from Bayer U.K Ltd (Haywards Heath, Sussex). A stock solution was prepared in chloroform/methanol (17.6 mg/ml) and stored in the dark at room temperature.

The bile salts cholic acid, deoxycholic acid, glycocholic acid and glycodeoxycholic acid were purchased as their sodium salt from Calbiochem (Bishops Stratford, Heartfordshire). 0.1 M stock solutions in D_2O of each bile salt was prepared and stored at room temperature. Porcine pancreatic and snake venom (naja naja) PLA_2 were purchased from Sigma (Poole, Dorset). A stock solution of pancreatic PLA_2 (900 units/mg of solid) was made up in D_2O (900 units/ml) and stored at 5°C . Triton X100 (scintillation grade) was purchased from BDH (Poole, Dorset) and an average molecular weight of 624 (9.5 oxyethylene units) was used to

calculate molarities. A stock solution was prepared in D₂O (11.7 mg/ml) and stored at room temperature.

3.2.2 Preparation of vesicles

DPPC vesicles were prepared as described in chapter 2. Egg PC vesicles were prepared by pipetting a known volume of stock PC solution into a glass sonicating vessel and the solvent removed as described for DPPC vesicles preparation. D₂O was then added to the dried lipid to give a concentration of 10 mg/ml. The solution was shaken and the resulting liposomes were sonicated for 10 minutes at 4°C under an atmosphere of nitrogen.

The mixed lipid vesicles, DPPC/50 mole % PC, egg PC/5 mole % CL, egg PC/10 mole % CL, egg PC/20 mole % PE and egg PC/5 mole % PA were prepared by pipetting the required volumes of the stock solutions into a sonicating tube. The contents of the tube was mixed and the solvent removed as described above. The required volume of D₂O was added to the dry lipid and the liposomes formed by shaking, were sonicated under nitrogen as previously described.

3.2.3 Method of introducing membrane active substances to vesicular solutions

Alamethicin 30 was introduced into 1ml of vesicular solution in a NMR tube by adding a known volume of the D₂O stock solution. This was followed by incubation for 1 hour at 50°C, after which transport was initiated by addition of Pr³⁺. In the case where no incubation time of alamethicin was required a known volume of the D₂O stock was added to 1ml of vesicular solution (containing Pr³⁺) to initiate the transport process.

The calcium antagonists verapamil and nifedipine were co-incubated with alamethicin 30 for 1 hr. Verapamil was introduced by adding a known volume of the D₂O stock solution to 1ml of vesicular solution in a NMR tube. Nifedipine was introduced by pipetting a known volume of the chloroform stock solution into an empty NMR tube and the solvent removed by a jet of nitrogen followed by evacuation for 20 minutes at 2mm Hg. 1 ml of vesicular solution and the desired quantity of alamethicin was then added to the NMR tube and incubated at 50°C with occasional shaking using a vortex mixer. After incubation for 1 hr Pr³⁺ was added to initiate transport.

The bile salts were added to a vesicular solution containing either 5mM Pr³⁺ or 0.15mM Dy³⁺ and 2mM Ca²⁺ by pipetting a known volume of stock solution, thus initiating the transport process. PLA₂ was introduced by pipetting a known volume of stock solution to a NMR tube containing lipid with either 0.15mM Dy³⁺ and 2mM Ca²⁺ or 0.15mM Dy³⁺, 2mM Ca²⁺ and bile salt, the bile salt being added about 30 seconds before PLA₂.

3.2.4 Vesicles prepared by cosonication of DPPC and alamethicin

a.

A known volume of alamethicin D₂O stock was diluted to 3.5 ml with D₂O (warmed to 50°C) and added to dried lipid in a sonicating tube. The tube was then shaken at 50°C for 30 minutes. The solution was sonicated as described for DPPC vesicle preparation. This process gives rise to a solution containing intravesicular and extravesicular alamethicin, in which transport was initiated by addition of Pr³⁺.

b.

A known volume of the chloroform alamethicin stock was mixed with a known volume of DPPC stock in a sonicating vessel. The solvent was removed and the vesicles prepared by the procedure described in chapter 2. These vesicles contained alamethicin initially situated within the bilayer. Transport was initiated by the addition of Pr^{3+} .

3.2.5 Method for lysing DPPC vesicles

Lysed vesicles were obtained by cycling the vesicular solution from 60°C to below the phase transition and back to 60°C, over a period of 20 minutes per cycle in the NMR tube, with spectra being taken before and after each series of cycles. Triton X100 was introduced by pipetting a known volume of stock into the vesicular solution containing Pr^{3+} and then incubating at 60°C for 30 minutes.

3.2.6 Ionophore mediated transport of paramagnetic lanthanide ions as monitored by ^1H -NMR

The high resolution ^1H -NMR signals obtained from lipid vesicles above the gel to liquid crystal phase transition, allows the monitoring of paramagnetic ion diffusion into small unilamellar vesicles (Hunt 1980a). The separation in signal O and I (see Fig 2.1) is due to a pseudocontact, dipolar interaction of the paramagnetic ions (which are in rapid exchange between the D_2O and the phosphate sites on the extravesicular lipid head groups) with the nearby outer choline protons. The separation of the signals O and I thus results principally in the down field shift of the extravesicular head group, signal O and such shifts are now well documented (see chapter 1 and 2, Bergelson 1978). When the lanthanide ions are transported across the lipid bilayer into the intravesicular solution the rise in intravesicular concentration of

lanthanide causes signal I to move downfield towards signal O. By measuring the change in chemical shift (Hz) of signal I with time (using the hydrocarbon signal as a reference), the rate of transport can be obtained.

3.2.7 Calibration graphs

In order to convert experimentally-observed shifts into intravesicular concentrations of lanthanide, a calibration graph is necessary.

A small known volume of lanthanide stock was diluted with D₂O to give the desired concentration. This solution was added to the dried lipid in a sonicating tube and the contents shaken at a temperature above the T_c of the lipid used, for 90 minutes using a flask shaker. The liposomes formed were sonicated as previously described. The sonicated vesicles contain equal concentrations of of lanthanide in the intravesicular and extravesicular solutions. By adding lanthanide stock the extravesicular concentration was then adjusted to 5 mM Pr³⁺ or 0.15 mM for Dy³⁺. The ¹H-NMR spectrum (at 90 MHz) was recorded and the chemical shift (Hz) of the inside choline signals, I ($\Delta\nu_1$), was measured with reference to the hydrocarbon signal. Vesicles were also prepared in D₂O only. To these vesicles extravesicular lanthanide was added to reveal signal I, the chemical shift ($\Delta\nu_2$, with reference to the hydrocarbon signal) of which corresponds to 0 mM intravesicular lanthanide. Shift values (Hz) were then derived by subtracting $\Delta\nu_1$ from $\Delta\nu_2$.

Calibration graphs were prepared from DPPC vesicles with Pr³⁺ at 50°C and egg PC vesicles with Pr³⁺ (50°C), Pr³⁺ (37°C) and Dy³⁺ (37°C) as shown in figures 3.3, 3.4a and 3.4b respectively. Chemical shifts of

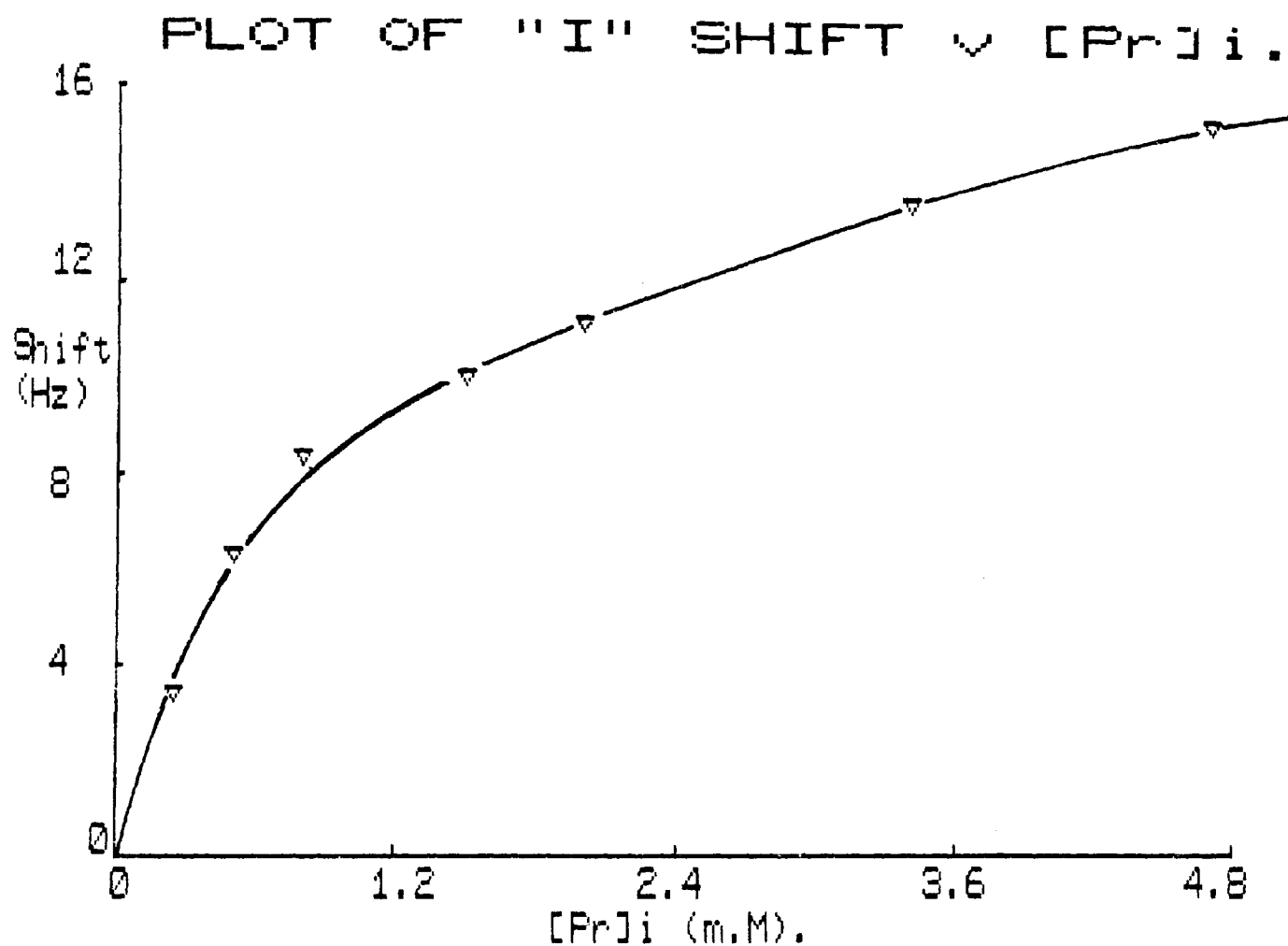
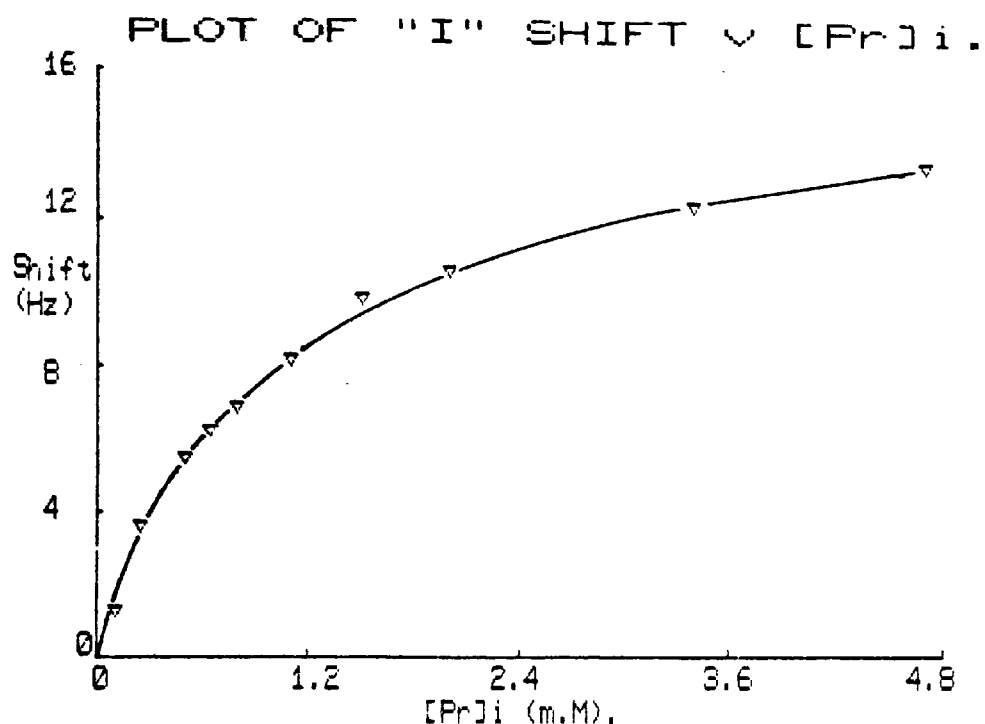


Fig 3.3 Calibration graph giving the shift of signal I, as a factor of $[Pr]_i$ in DPPC vesicles at 50°C $[Pr]_0 = 5 \text{ mM}$.

(a)



(b)

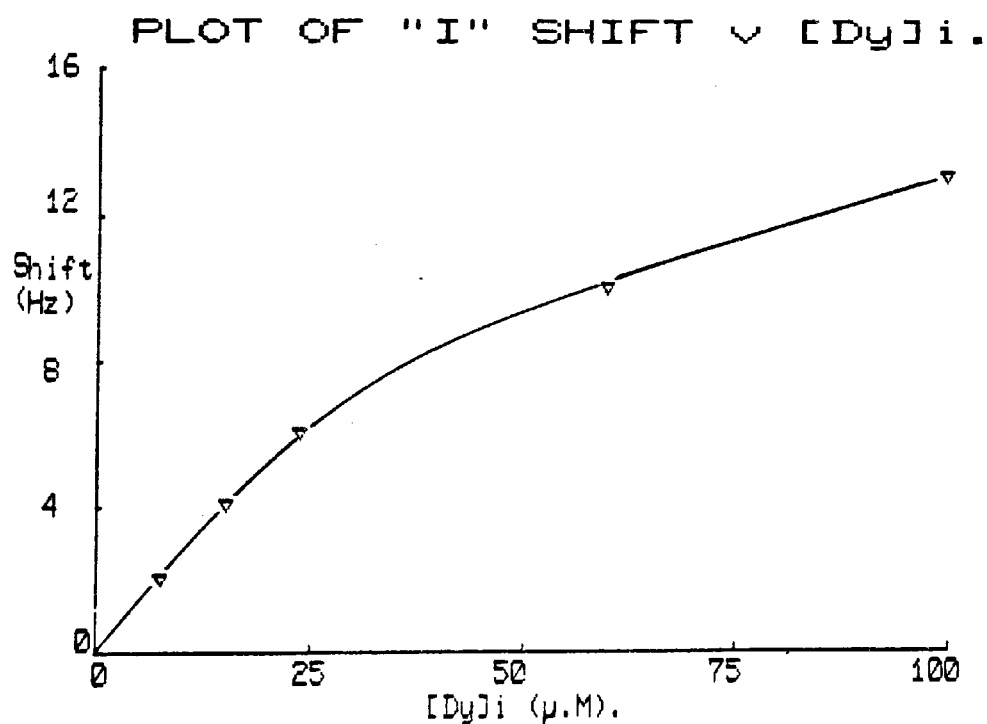


Fig 3.4 Calibration graphs giving the shift of signal I as a function of the intravesicular concentration of lanthanide ion, $[\text{Ln}]_i$, in egg PC vesicles at 37°C.

(a) Lanthanide ion - Pr^{3+} . $[\text{Pr}]_0 = 5 \text{ mM}$

(b) Lanthanide ion - Dy^{3+} . $[\text{Dy}]_0 = 150 \text{ } \mu\text{M}$

signal I obtained at 60 MHz were increased by a factor of 1.5 so as to make use of these calibration graphs.

3.3 Experimental Results

3.3.1 Alamethicin-mediated transport of paramagnetic ions into phospholipid vesicles.

Fig 3.5 show the time dependent changes in the ^1H -NMR spectrum at 50°C obtained from DPPC vesicles during a transport experiment in which alamethicin 30 ($20\text{ }\mu\text{g/ml}$) had been preincubated with the vesicles (see section 3.2). Signal I is seen to shift downfield towards signal 0 as the internal concentration of Pr^{3+} ions, $[\text{Pr}]_i$ increases. The extravesicular Pr^{3+} concentration remains effectively constant since the total internal volume of all the vesicles is only about 2% of the total volume of the sonicate (see chapter 2).

On conversion of the measured shift of signal I (Hz) into $[\text{Pr}]_i$ using the appropriate calibration graph, the corresponding plot of $[\text{Pr}]_i$ against time is shown in Fig 3.6. The linear increase in $[\text{Pr}]_i$ with time indicates that the transport rate is zero order with respect to $[\text{Pr}]_i$. The slope of the line gives the value of the zero order rate constant, which has the value of $3.33 \times 10^{-2}\text{ m mol dm}^{-3}/\text{min}$ (mM/min) in this result.

Fig 3.6 also shows that in the case where no incubation time is allowed for alamethicin, a rate of $1.8 \times 10^{-2}\text{ mM/min}$ is obtained. The difference in rates and the lack of real linearity in the data points suggests that the incubation period allows alamethicin to partition into the bilayer, hence making itself available for channel formation.

Fig 3.7 shows the transport rates at 50°C for alamethicin ($5\text{ }\mu\text{g/ml}$) in DPPC vesicles prepared by various protocols (see sections 3.2.2 and 3.2.4). The plot gives rates of 0.12×10^{-2} , 0.15×10^{-2} and $2.96 \times 10^{-2}\text{ mM/min}$ for alamethicin incubated extravesicularly, when present initially in the bilayer and when intravesicular and

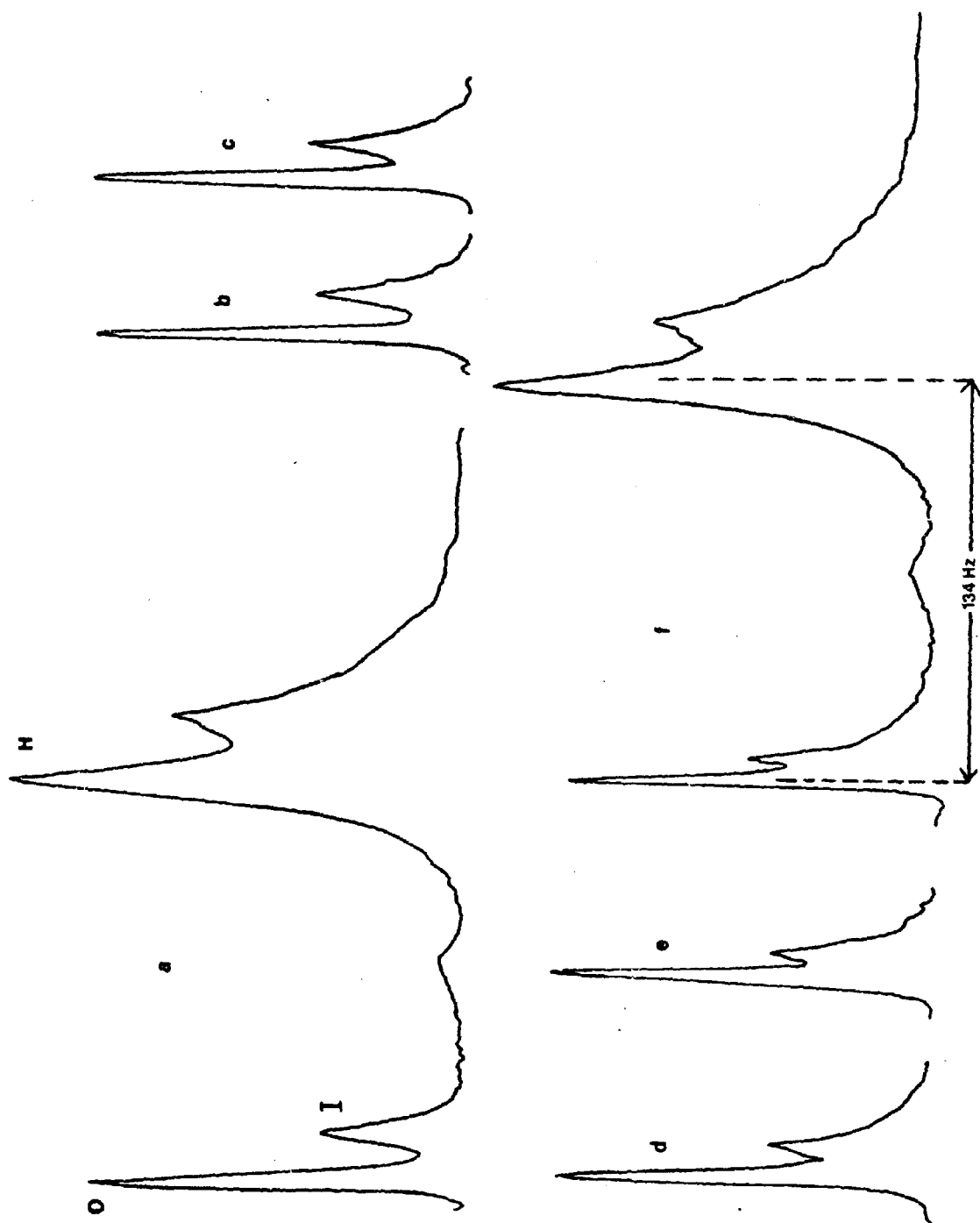


Fig 3.5 (a) The ^1H -NMR spectrum at 60 MHz of DPPC vesicles at 50°C in the presence of 5 mM extravesicular Pr^{3+} .

(b)-(f) shows the downfield movement of signal I during the transport of Pr^{3+} by alamethicin 30 (20 $\mu\text{g}/\text{ml}$). Shifts in signal I are measured with respect to signal H and are shown after (b) 4.5 mins, (c) 10 mins, (d) 15 mins, (e) 24 mins, (f) 35 mins.

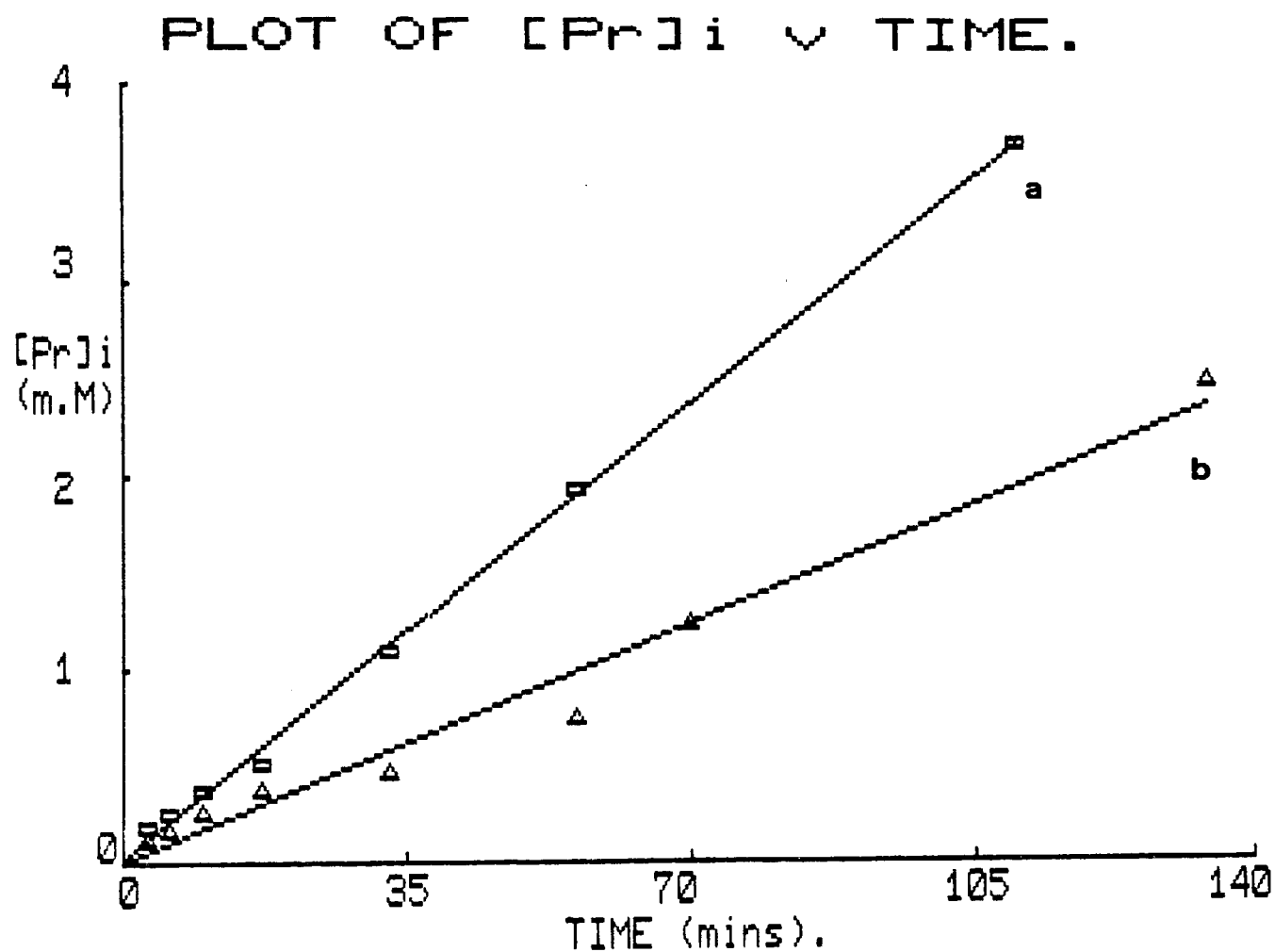


Fig 3.6

The effect of incubation on the transport rate by alamethicin in DPPC vesicles at 50°C.

(a) Alamethicin incubated. (b) No incubation time.

extravesicular, respectively. During the transport process in each of the above experiments, the peak width of the hydrocarbon signal (H) was monitored. Variations of only a few Hz were observed indicating that no appreciable fusion of vesicles occurred over the duration of the experiment (Liao and Prestegard 1980). The results are discussed below in terms of alamethicin environment and the activation energy of channel formation.

The standard protocol adopted for most of the alamethicin studies in this chapter was that of incubating extravesicularly. This method has the advantage over the other two protocols in Fig 3.7 in that variable alamethicin concentrations can be used with a single sonicate.

3.3.1.1 Alamethicin channel stoichiometry in DPPC and egg PC vesicles

To investigate the number of alamethicin molecules involved in each conducting channel, transport rates were measured at various concentrations of alamethicin in DPPC and egg PC vesicles. The results are shown in Figs 3.8a and 3.8b respectively. Fig 3.9 shows a plot of the logarithm of the rates of transport (as obtained from Fig 3.9) against the logarithm of the alamethicin concentration used. The slopes of these plots are 4.05 for DPPC vesicles and 3.85 for egg PC vesicles, which indicates that an average of 4 alamethicin molecules are involved in the formation of each channel. As a comparison a plot for the carrier mediated ionophore A23187 is included and shows a slope of 1.9 which is consistent with the $\text{Ca}(\text{A23187})_2$ complex determined by X-ray analysis (Chaney et al 1976) thus adding some weight to the reliability of the method.

In these experiments it was observed that a greater concentration

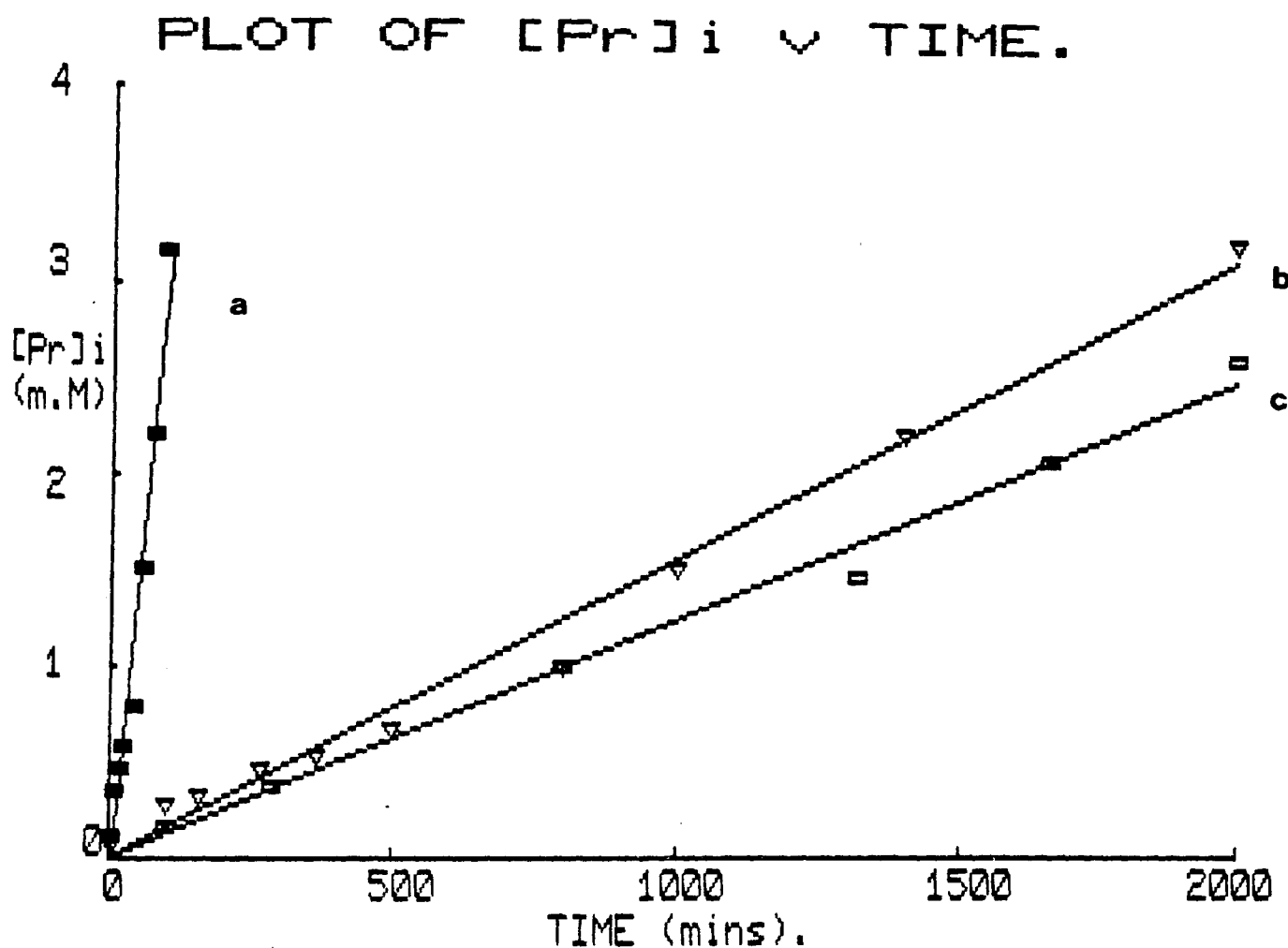


Fig 3.7

The transport rates at 50°C by alamethicin (5 µg/ml) in DPPC vesicles prepared by various protocols:

- (a) Alamethicin sonicated inside and outside vesicles (see 3.2.4.a)
- (b) Alamethicin sonicated into the lipid bilayer (see 3.2.4.b)
- (c) Alamethicin incubated extravesicularly with DPPC vesicles (3.2.2.)

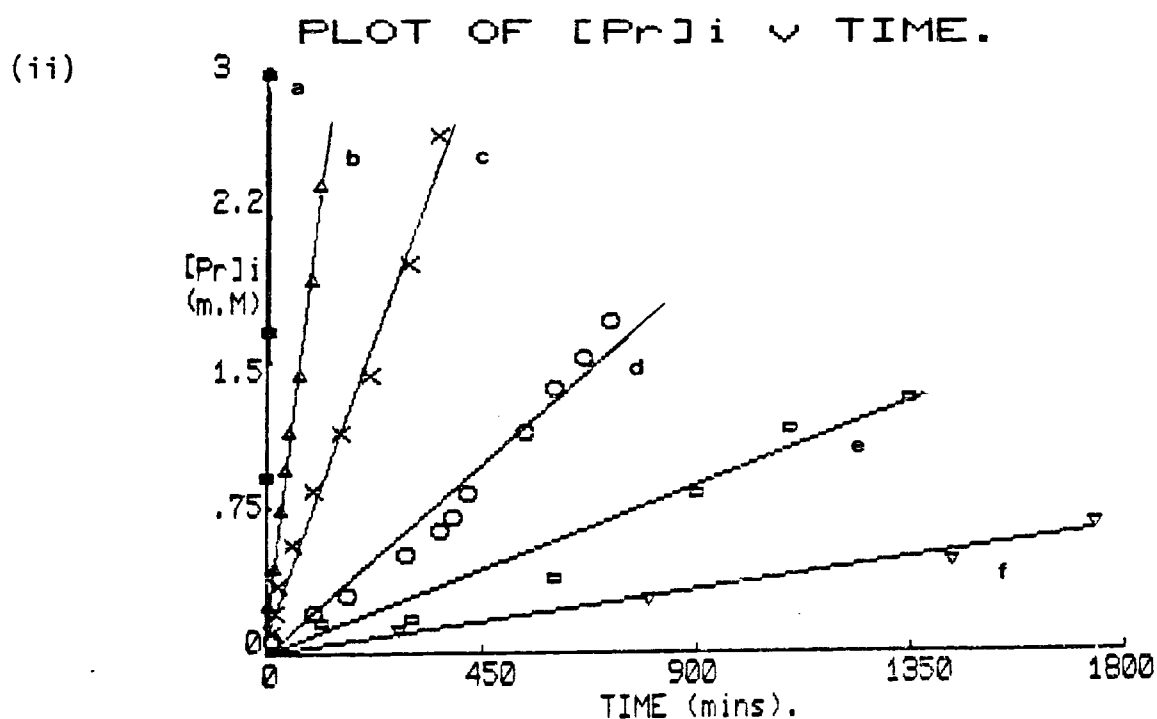
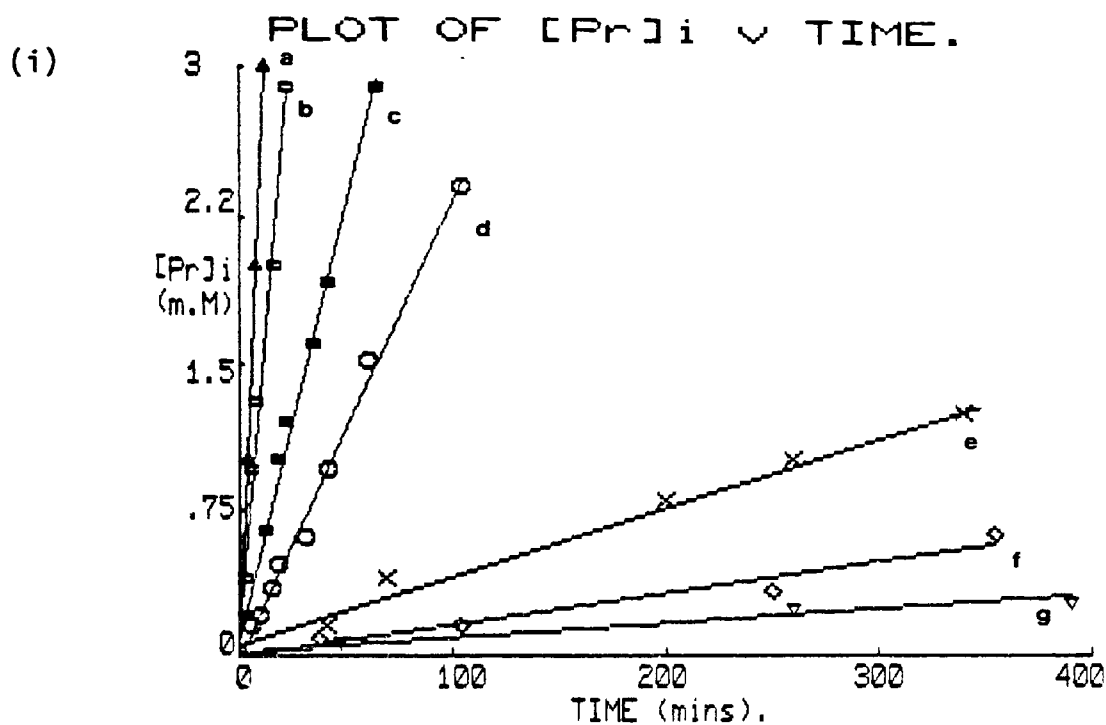


Fig 3.8 The transport rates obtained by various concentrations of a) amethicin at 50°C in:-

(i) DPPC vesicles; a $30\text{ }\mu\text{g}$, b $25\text{ }\mu\text{g}$, c $20\text{ }\mu\text{g}$, d $15\text{ }\mu\text{g}$, e $10\text{ }\mu\text{g}$, f $7.5\text{ }\mu\text{g}$, g $5\text{ }\mu\text{g}$.

(ii) Egg PC vesicles; a $120\text{ }\mu\text{g}$, b $80\text{ }\mu\text{g}$, c $60\text{ }\mu\text{g}$, d $40\text{ }\mu\text{g}$, e $30\text{ }\mu\text{g}$, f $20\text{ }\mu\text{g}$.

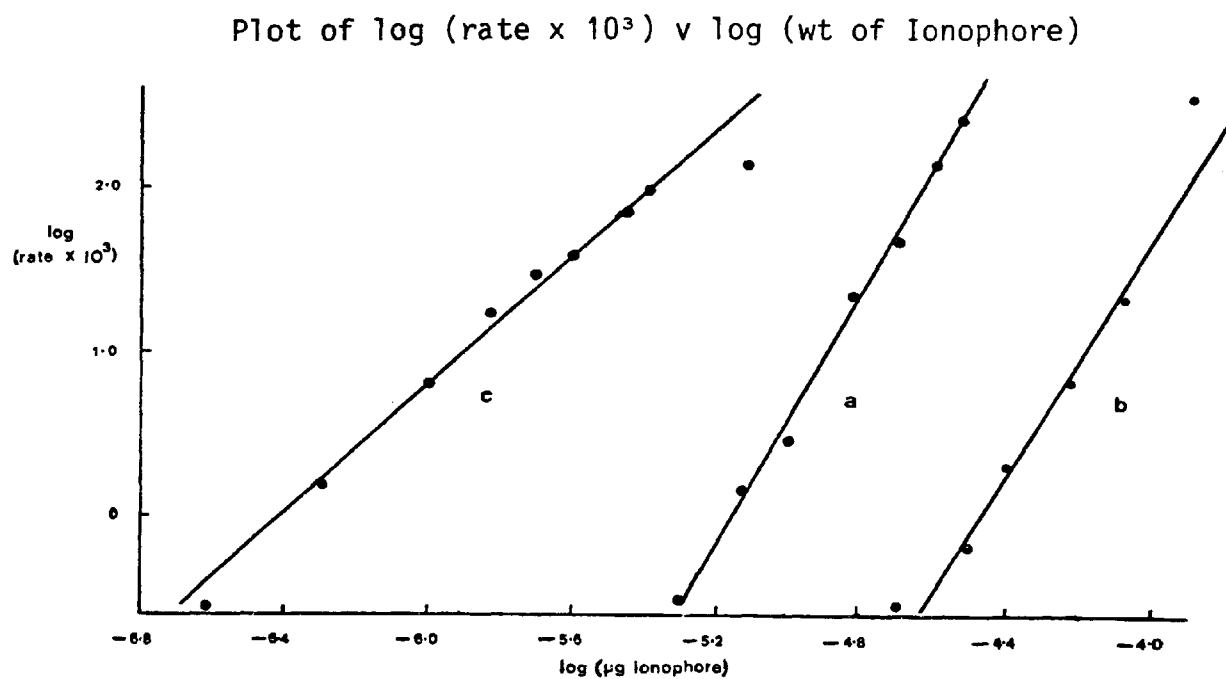


Fig 3.9 Stoichiometry plots obtained from alamethicin and A23187 transport rates.

- a. Alamethicin in DPPC vesicles (slope 4.05)
- b. Alamethicin in egg PC vesicles (slope 3.85)
- c. A23187 in DPPC vesicles (slope 1.9)

of alamethicin is required with egg PC to give a similar rate to that obtained by DPPC. Activation energy experiments were therefore carried out to probe this phenomenon.

3.3.1.2 Activation energy for alamethicin transport in DPPC and egg PC vesicles

The rate of transport of Pr^{3+} by alamethicin into DPPC and egg PC vesicles was measured at various temperatures (Fig 3.10). The Arrhenius plot, Fig 3.11, shows the log of the measured rate of transport against $1/T$, where T is the absolute temperature. The slope is equivalent to $-E/R$ where E is the activation energy and R is the universal gas constant. From Fig 3.12 a value of 58 KJ/mol and 72 KJ/mol are obtained for DPPC and egg PC vesicles respectively.

3.3.1.3 Alamethicin transport in mixed lipid vesicles

Fig 3.12 shows the rate obtained by alamethicin (20 $\mu\text{g}/\text{ml}$) in vesicles formed from egg PC/50 mole % DPPC. This has a value of 0.7×10^{-2} mM/min whereas the controls show rates of 0.03×10^{-2} mM/min for egg PC vesicles and 2.4×10^{-2} mM/min for DPPC vesicles.

The effects of CL, PE and PA on the transmembrane transport of Pr^{3+} by alamethicin (40 $\mu\text{g}/\text{ml}$) are shown in Fig 3.13(i). A similar plot monitoring the transport of Dy^{3+} is shown in Fig 3.14(i). However the 20 mole % PE sample is found to be permeable in the absence of alamethicin. The transport (rate 0.01 $\mu\text{M}/\text{min}$) is probably due to nonbilayer phase formation with transport being mediated by inverted micelles composed of PE and PC (see section 1.4). This non bilayer phase transport rate will therefore contribute to the rate when alamethicin is present (rate 0.125 $\mu\text{M}/\text{min}$). The data points for the rates obtained

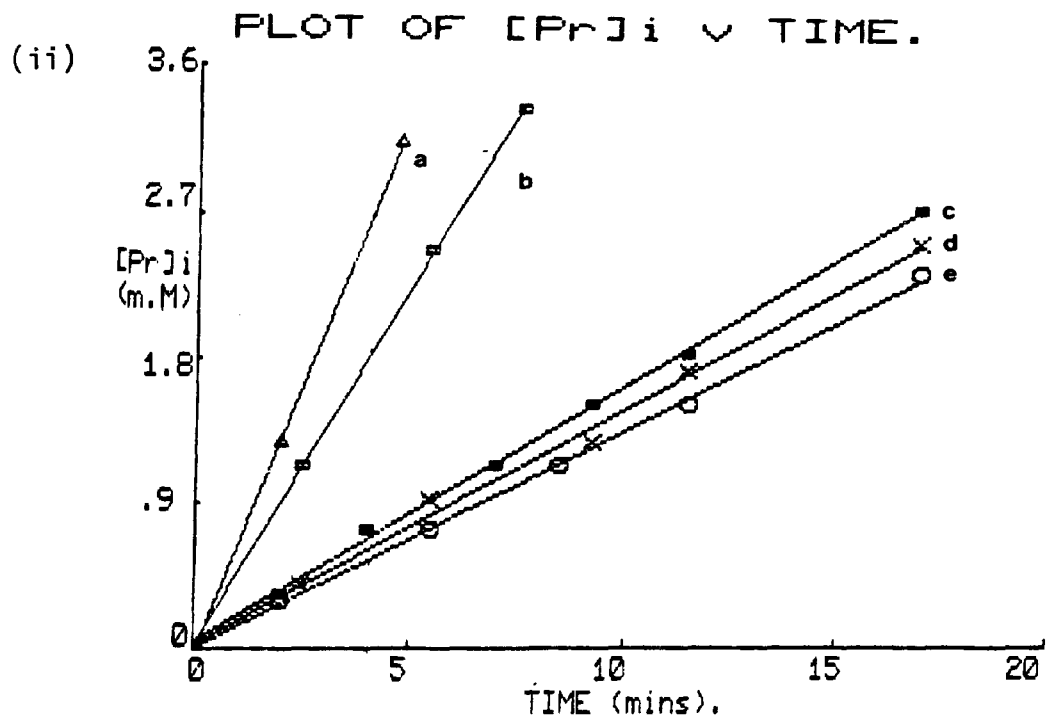
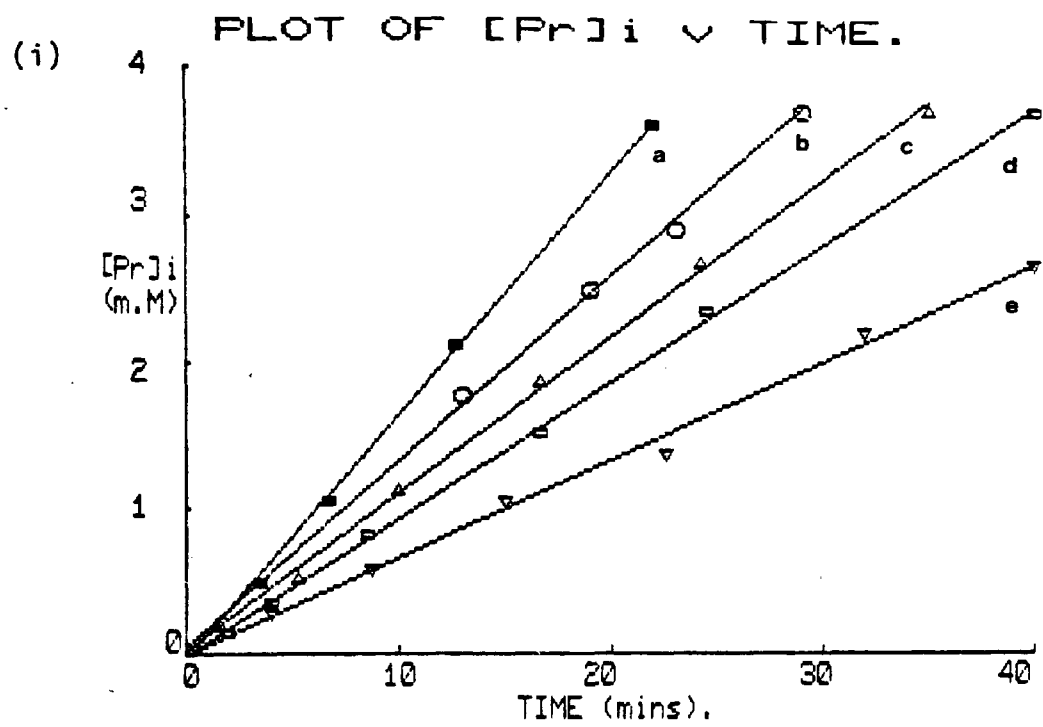


Fig 3.10 (i) The alamethicin ($20 \mu\text{g/ml}$) transport rates in DPPC vesicles at a 60° , b 55° , c 50° , d 45° , e 41° .

(ii) The alamethicin ($80 \mu\text{g/ml}$) transport rates in egg PC vesicles at a 70° , b 60° , c 50° , d 37° , e 28° .

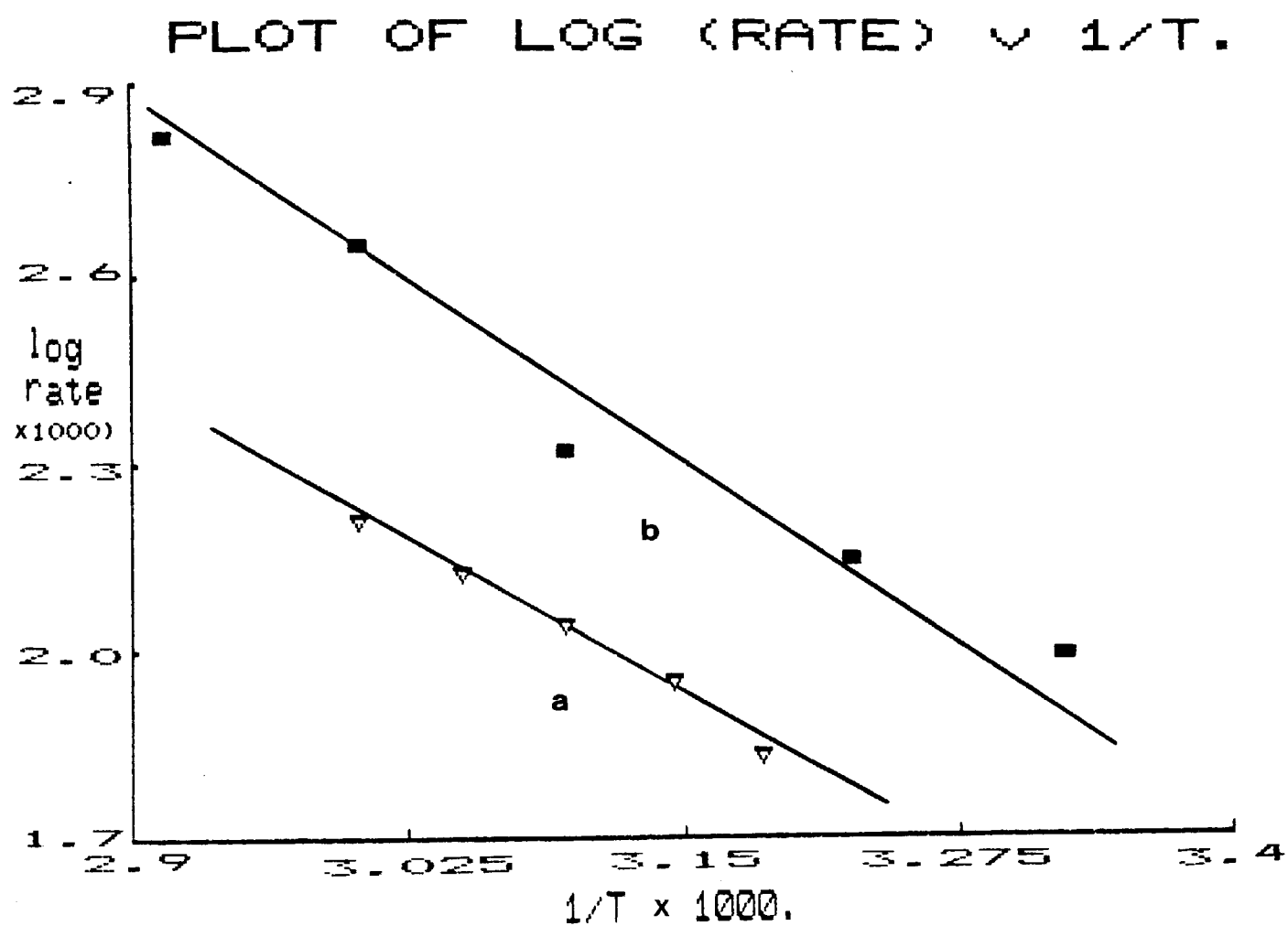


Fig 3.11 Arrhenius plot giving the activation energies of 58 kJ/mole and 72 kJ/mole for alamethicin transport in DPPC vesicles (a) and egg PC vesicles (b) respectively.

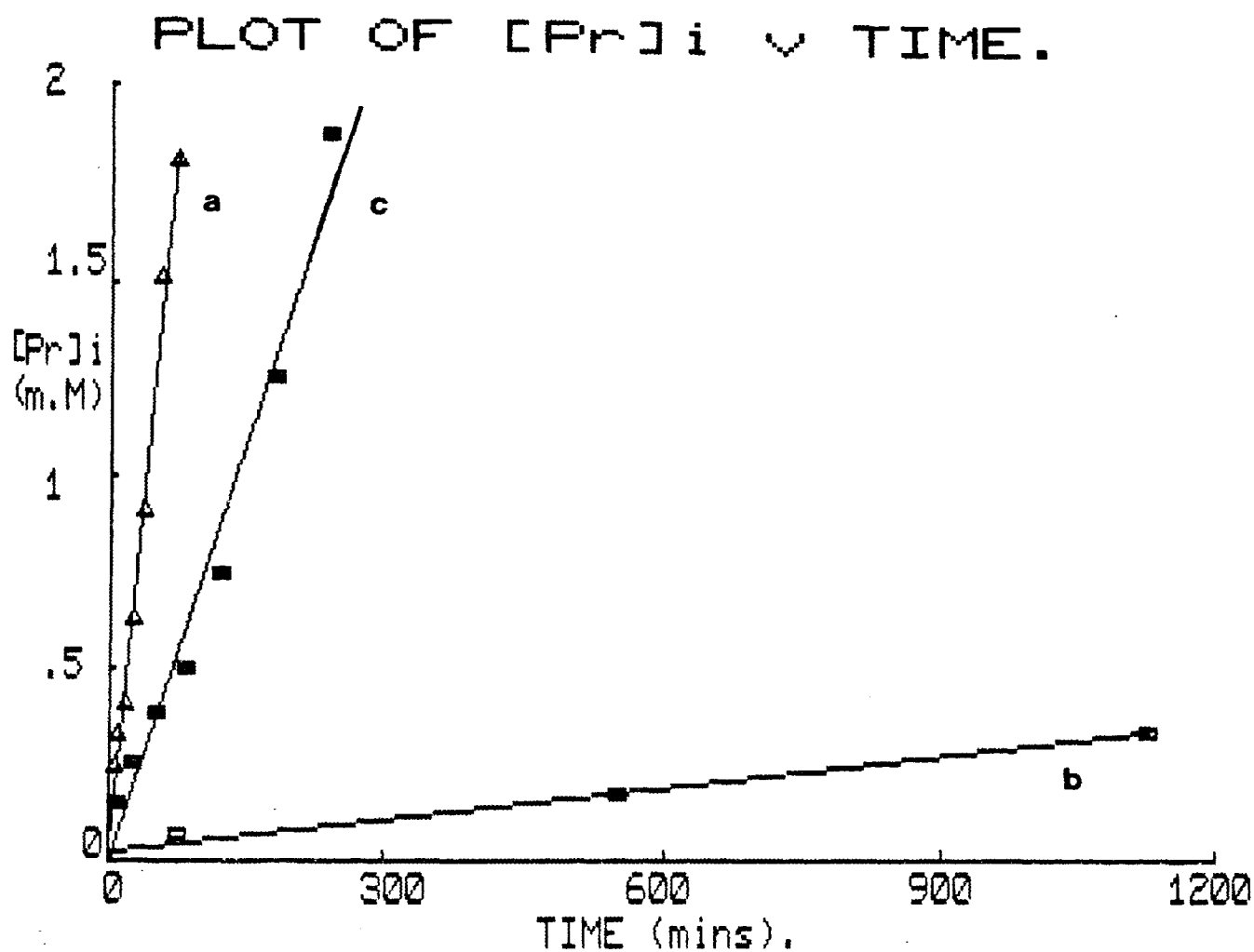


Fig 3.12 The effect of mixed lipid vesicles on the alamethicin (20 $\mu\text{g/ml}$) transport rate at 50°C

a. DPPC, b. egg PC, c. egg PC/50 mole % DPPC

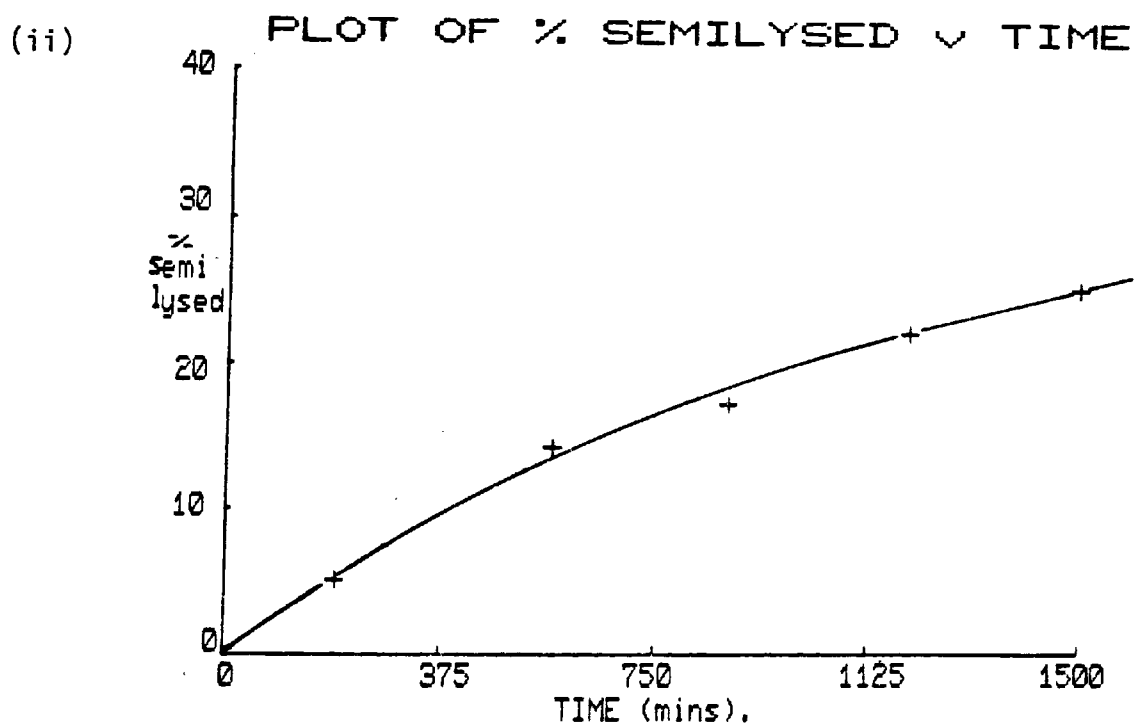
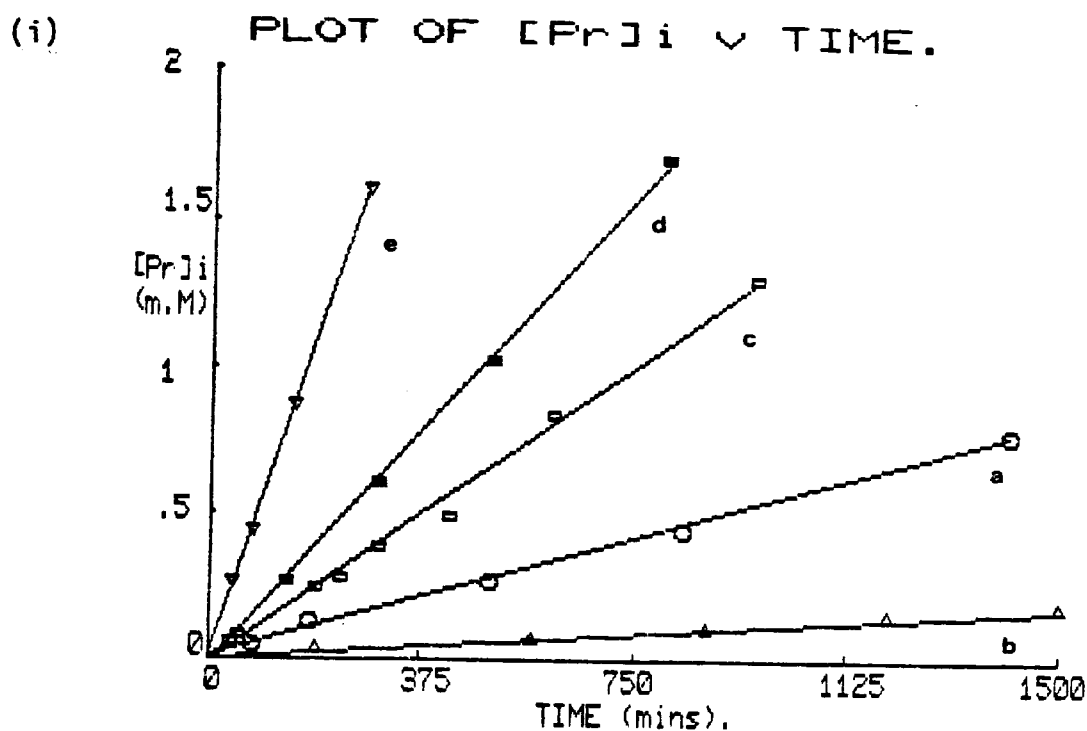
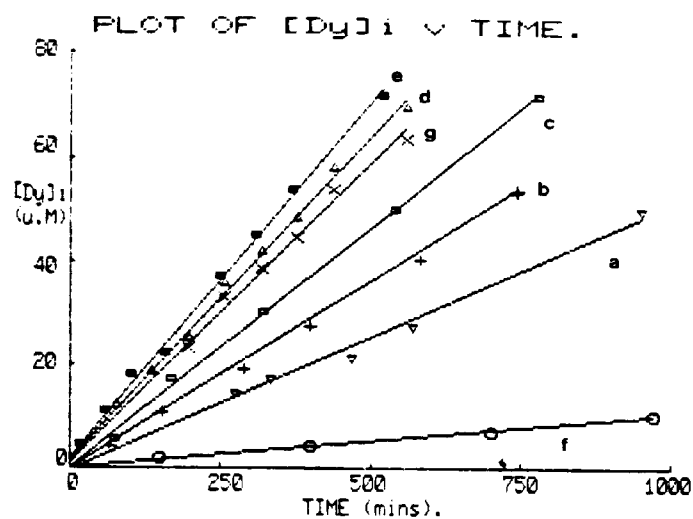


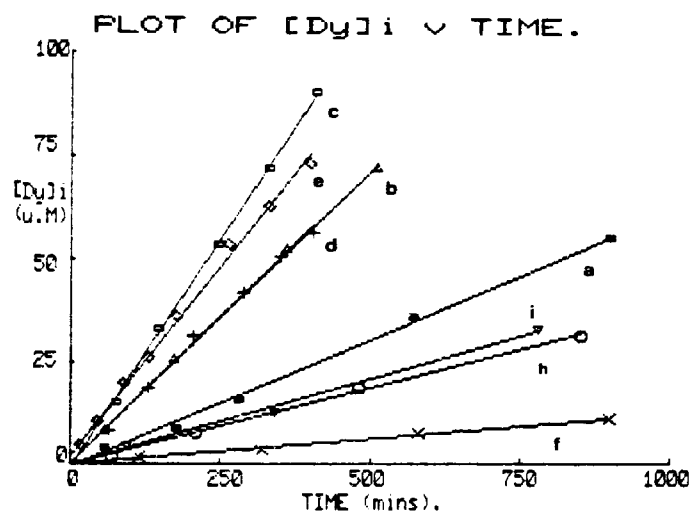
Fig 3.13

- (i) The rate of Pr^{3+} transport at $37^\circ C$ by alamethicin ($40 \mu g/ml$) in vesicles formed from: a. egg PC (control), b. egg PC/5 mole % PA, c. egg PC/5 mole % CL, d. egg PC/10 mole % CL, e. egg PC/20 mole % PE.
- (ii) The proportion of the egg PC/5 mole % PA vesicles in Fig 3.14 that are receiving bursts of $2 \text{ mM } Pr^{3+}$.

(i)



(ii)



(iii)

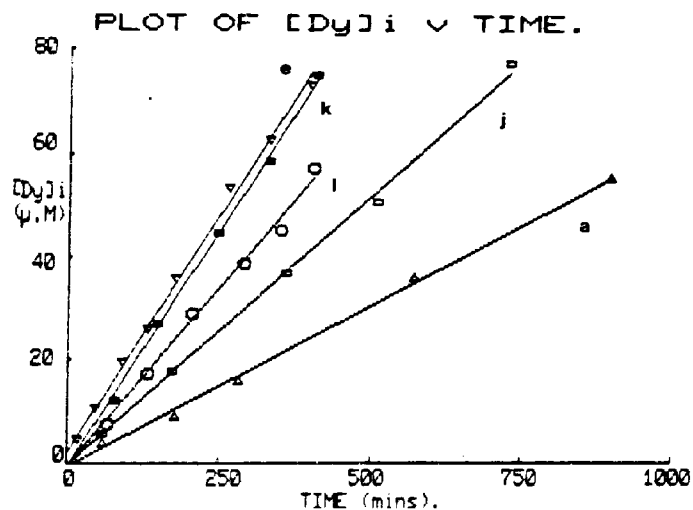


Fig 3.14

- i. The effects of various lipid compositions on the Dy^{3+} transport by alamethicin (40 μ g/ml) at 37°C.
a. Control (100% egg PC), b. egg PC/5 mole % CL, c. egg PC 10 mole % CL, d. egg PC/20 mole % PE, e. egg PC/5 mole % PA, f. egg PC/20 mole %PE with no alamethicin, g. resultant alamethicin rate from d-f (see text).
- ii. As for i. with extra vesicular Ca^{2+} (0.5 mM).
a-f as above. h. egg PC/5 mole % CL, no alamethicin, i. egg PC/10 mole % CL, no alamethicin.
- iii. As for ii., a and e as above, j. resultant rate from b-h in ii. h. resultant rate from c-i in ii. l. Resultant rate from d-f in ii. (see text).

in the presence of alamethicin are corrected (to account for the non bilayer phase transport) by subtracting the time equivalent non bilayer phase $[D_y]_i$ values. The resultant rate (0.115 $\mu\text{M}/\text{min}$) can be assumed to be due to the transport by alamethicin only.

Fig 3.14(ii) shows that nonbilayer transport is obtained with 5 mole % CL (slope h), 10 mole % CL (slope i) and 20 mole % PE (slope f) having rates of 0.037, 0.042 and 0.012 $\mu\text{M}/\text{min}$ respectively. These therefore contribute to the rates obtained when alamethicin is present where rates of 0.142, 0.221 and 0.111 $\mu\text{M}/\text{min}$ are obtained for vesicles containing 5 mole % CL (slope b), 10 mole % CL (slope c) and 20 mole % PE (slope d) respectively. In Fig 3.14 (iii) the contribution of non bilayer transport to the transport rates obtained in the presence of alamethicin has been subtracted.

The presence of 5 mole % and 10 mole % CL and 20 mole % PE cause an increase in the rate of Pr^{3+} transport by approximately 1, 10, and 3 orders of magnitude respectively (see Table 3.1). However PA has the effect of decreasing the transport rate, but it is seen from the ^1H -NMR spectra (see Fig 3.15) that a peak I' appears inbetween signals O and I. This peak corresponds to vesicles containing 2 mM Pr^{3+} and increases in intensity with time. This may be representative of vesicles in which the channel life time is long enough for a pulse of ions (approximately 2 mM Pr^{3+}) to get across the membrane. Fig 3.13(ii) shows the proportion of vesicles containing 2 mM Pr^{3+} as a function of time. Taking both mechanisms into account (transport and semilysis) and calculating the total number of intravesicular Pr^{3+} ions gives rise to a rate of 0.46×10^{-3} mM/min which is less than the control rate (from 100 % PC) of 0.54×10^{-3} mM/min. In contrast the presence of PA causes a 2.6 fold increase in the Dy^{3+} transport rate. A similar result is obtained for

	<u>Transport Rates</u>		
	Pr ³⁺	Dy ³⁺	Dy ³⁺ Ca ²⁺
	mM/min x 10 ³	μM/min x 10 ²	μM/min x 10 ²
Control (100% PC)	0.54	5.15	6.21
5 mole % CL	1.34	6.57	10.42
10 mole % CL	5.66	9.27	18.29
5 mole % PA	0.12	13.27	18.54
20 mole % PE	2.11	11.87	14.75

Table 3.1

Summary of the rates of Pr³⁺ and Dy³⁺ transport by alamethicin through vesicular bilayers formed from mixed phospholipids.

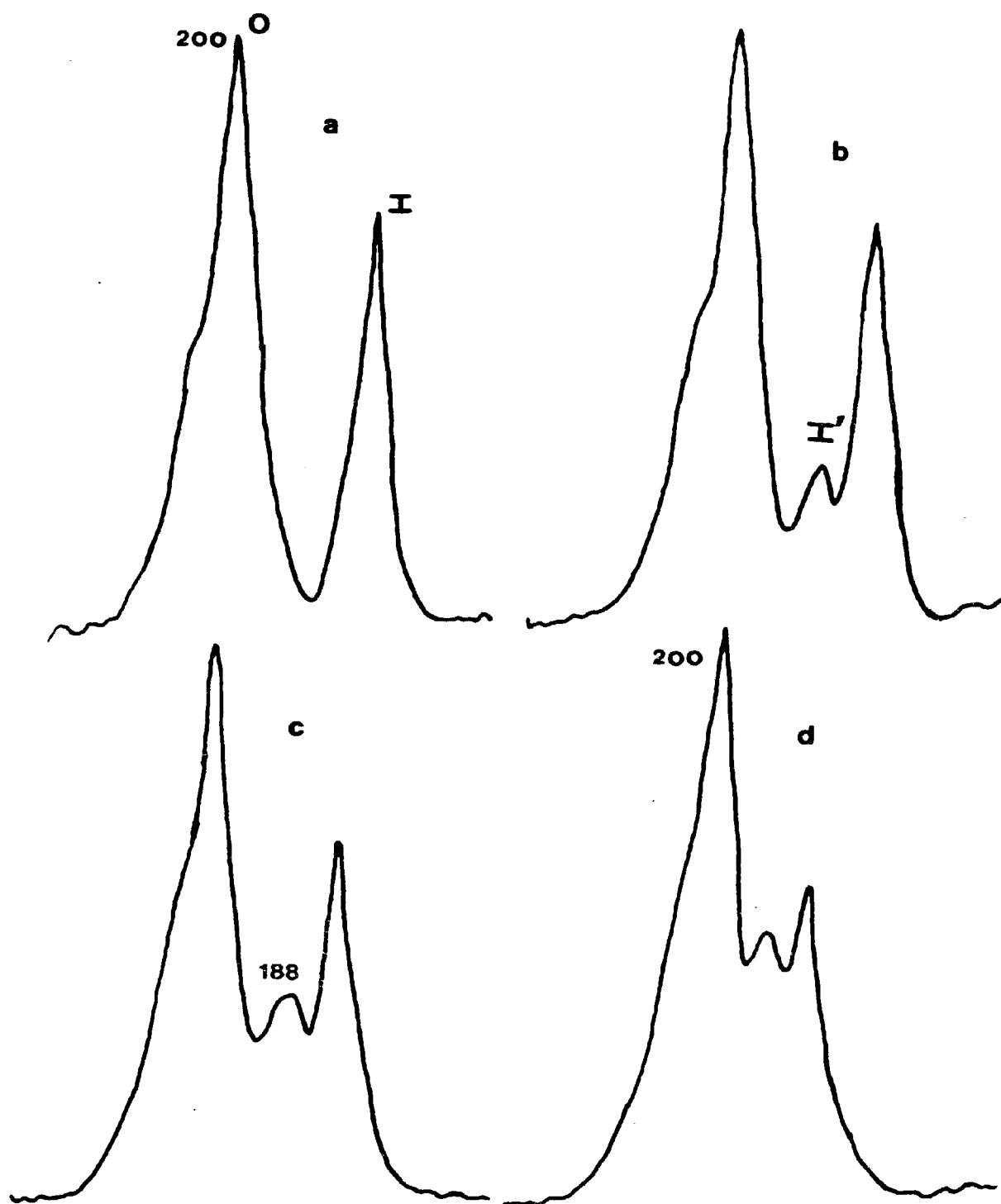


Fig 3.15 a-d show the time-dependent changes in the ¹H-NMR signals (O+I) at 90 MHz from egg PC /5 mole% PA (5 mM extravesicular Pr³⁺) with alamethicin 30 (40 µg/ml) at 37°C. These are shown after (a) 5 min (b) 190 min (c) 1500 min, (d) 2600 min. The chemical shifts are measured with reference to the hydrocarbon signal. Signal I' arises from the inside head-groups of vesicles that have partially lysed.

Dy³⁺ transport in the presence of calcium (Table 3.1). The results for Dy³⁺ transport (Fig 3.14) show that each lipid mixture used potentiates the rate.

In Fig 3.15 the addition of Pr³⁺ ions to egg PC/PA reveals that signal 0 is asymmetric; the shoulder on the lower field side of the signal probably arises from PC molecules next to PA molecules. The negative charge on PA enhances the binding of the metal ion to the adjacent PC molecules hence causing a greater downfield shift. A similar effect is seen with egg PC/CL mixtures.

These results indicate that the lipids are interacting with the alamethicin molecules and altering their channel-forming properties as discussed below.

3.3.1.4 Calcium antagonists and alamethicin channels

The following study (work done in conjunction with Z-E.M Mirghani) was based on the suggestions that calcium antagonists may affect the slow inward calcium channel and that an antagonist concentration greater than that required to block voltage-sensitive channels promote rather than inhibit the conduction rate (Middleton et al 1981, Putney 1978).

Experiments were performed with high and low molar ratios of antagonist : alamethicin, in DPPC vesicles at 50°C. The results in Fig 3.16 show that the transport rate mediated by alamethicin (20 µg/ml) is inhibited by verapamil at the lower molar ratios (2:1 and 10:1) whilst the higher ratios (20:1, 30:1 and 50:1) the transport rate is potentiated. Verapamil does show some ionophoric properties of its own (rate 0.61×10^{-2} mM/min). However this rate has been taken into account and the rates shown in Fig 3.16 resultant rates based on corrected data

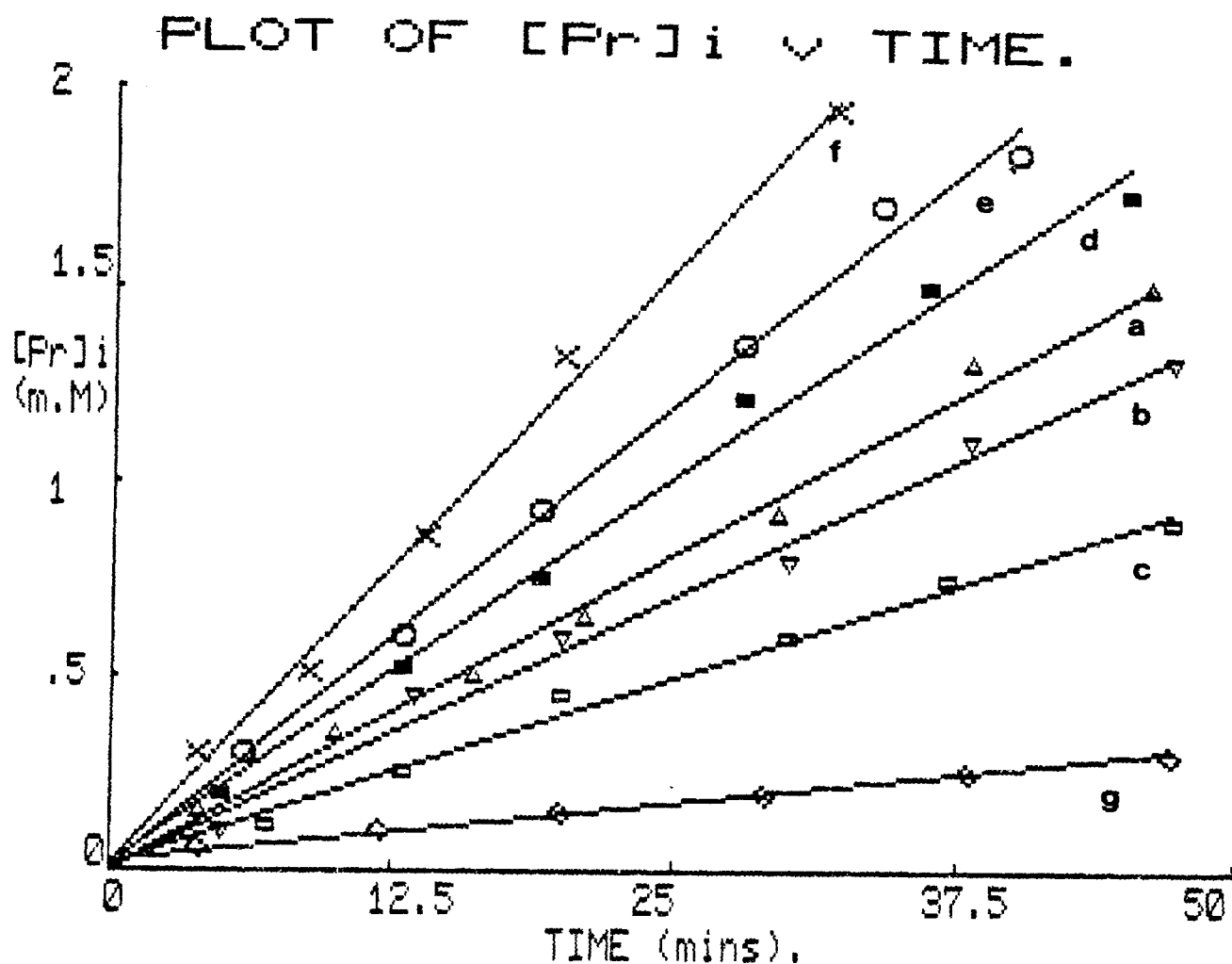


Fig 3.16 shows that at lower molar ratio verapamil inhibits the transport rate mediated by alamethicin (20 $\mu\text{g/ml}$) in DPPC vesicles, whilst at higher molar ratios the transport rate is potentiated.

a. Control (DPPC + alamethicin), b. 10 μg verapamil (2:1),
 c. 50 μg verapamil (10:1), d. 100 μg verapamil (20:1),
 e. 150 μg verapamil (30:1), f. 250 μg verapamil (50:1),
 g. 100 μg verapamil only.
 (Molar ratios = verapamil:alamethicin)

points as explained above. Nifedipine also shows a similar mode of action (Fig 3.17) but in this case the effects are seen at much lower molar ratios than that shown by verapamil.

Therefore the nature and relative concentration of antagonist with respect to alamethicin are important factors in determining whether potentiation or inhibition of transport is observed. The results are consistent with the above mentioned slow calcium channel mechanism of ion conduction (see discussion).

3.3.2 The Phase Transition and Membrane Permeability

On cycling DPPC vesicles through the phase transition (see section 3.2.5) channels are formed in the vesicles which allow rapid equilibration of Pr^{3+} ions across the bilayer. However only a fraction of vesicles lyse during each cycle. The process is demonstrated in Fig 3.18 where a sample of DPPC vesicles (with extravesicular 5 mM Pr^{3+}) has been cycled eighteen times through the phase transition (60-30-60) over a six hour period. The effect on the ratio O/I is clearly seen (1.7 \rightarrow 2.7). Addition of an extra 20 mM Pr^{3+} to the sample after lysis reveals signal I' from the inside head groups of the lysed vesicles, whilst the remaining signal I, arises from the unlysed vesicles. This also demonstrates that vesicular integrity is maintained during the lysis procedure. Thus from the changes in the O/I ratio the % lysed vesicles can be calculated (Appendix A).

Fig 3.19 shows a plot of % lysed against time where a series of cycles through the phase transition are used separated by incubation periods at 60°. In each case the vesicles are seen to be impermeable to Pr^{3+} at 60° but on passing through the phase transition (one cycle per

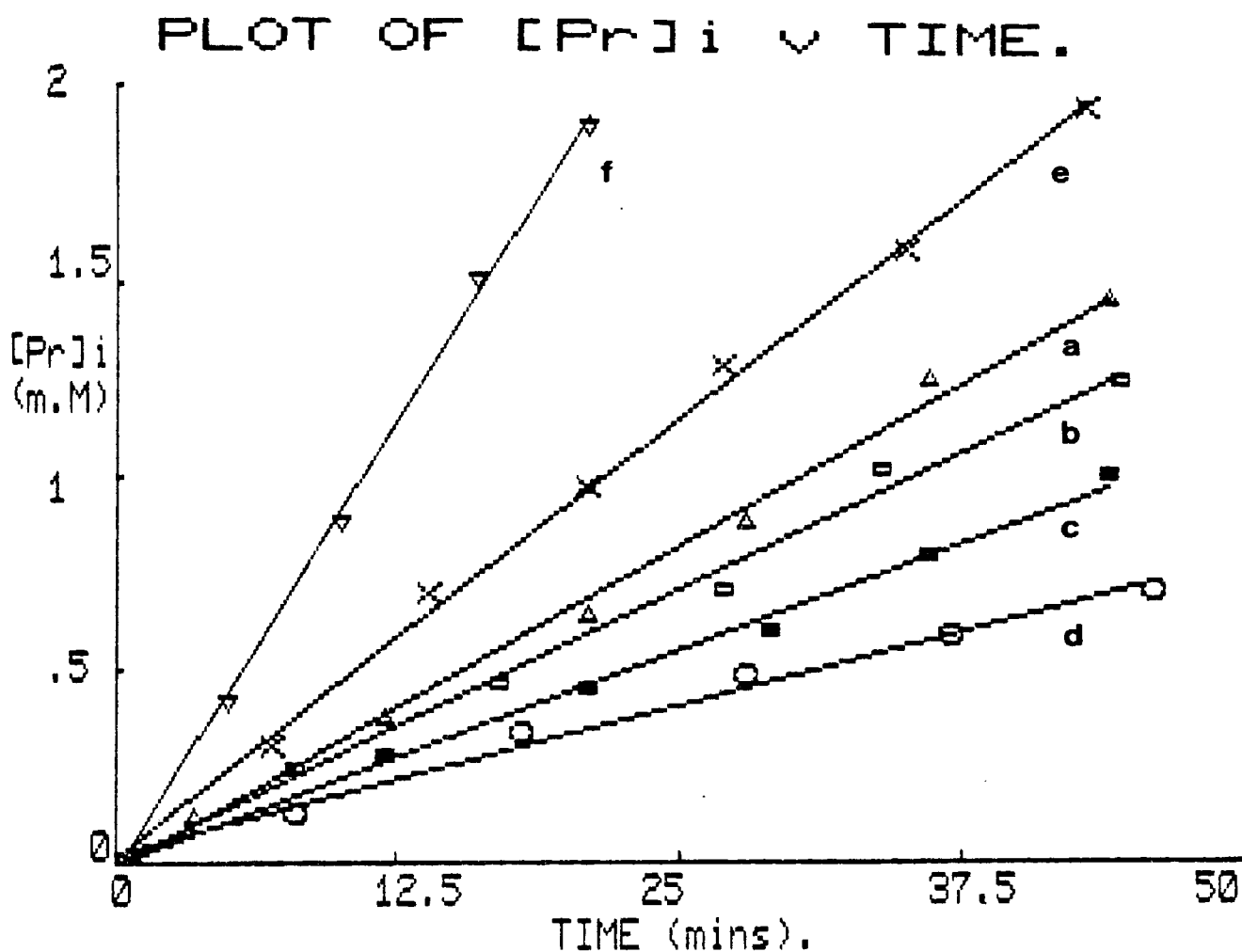


Fig 3.17 shows that low concentrations of niphedipine inhibit the rate of alamethicin mediated transport, whilst higher concentrations potentiate the rate.

a. Control (DPPC-alamethicin), b. 3.5 μ g niphedipine (1:1),
 c. 7 μ g niphedipine (2:1), d. 10.5 μ g niphedipine (3:1),
 e. 14 μ g niphedipine (4:1), f. 35 μ g niphedipine (10:1).
 (Molar ratios = niphedipine:alamethicin).

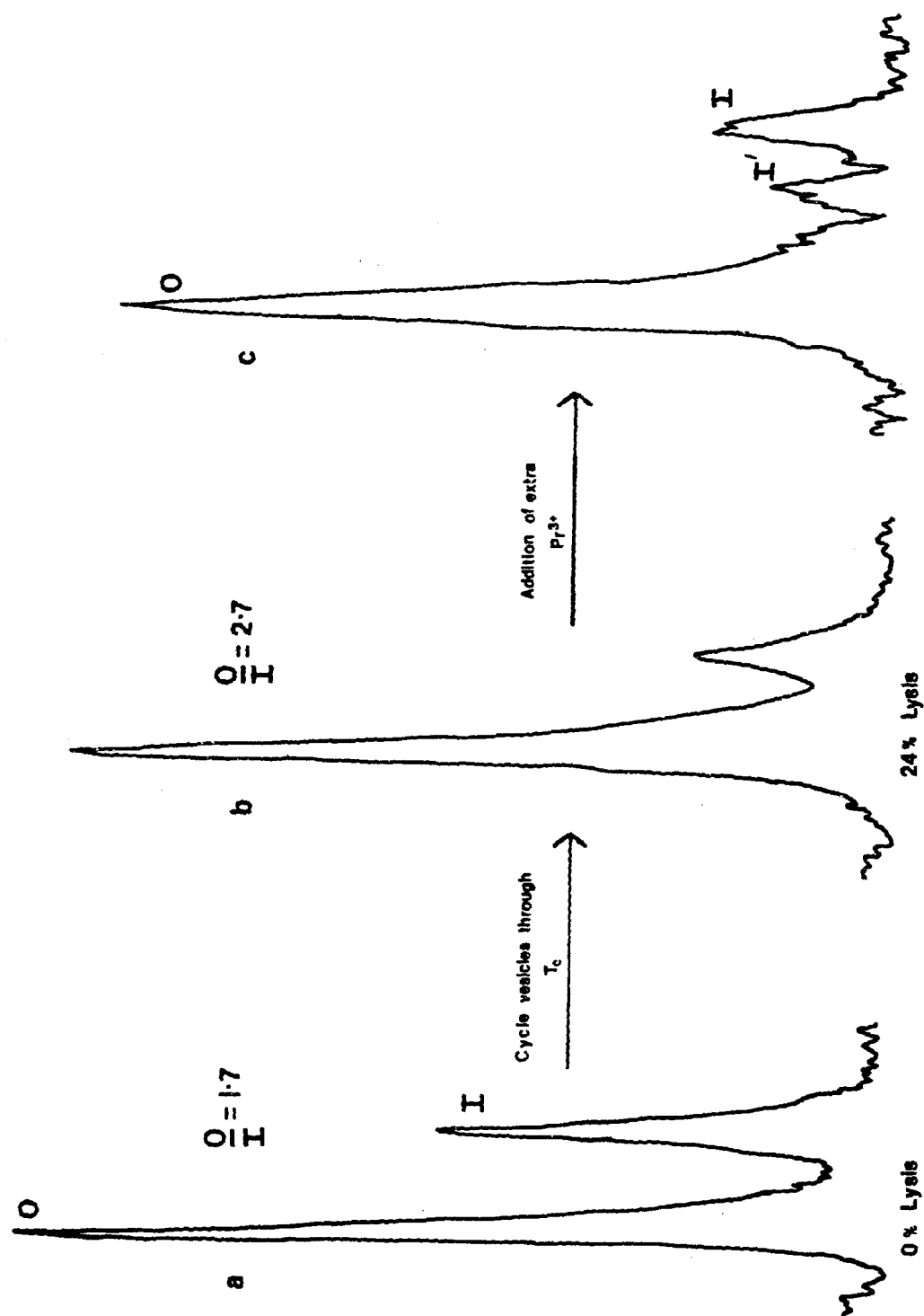


Fig 3.18 Effect on the ^1H -NMR head-group signals from DPPC vesicles in the presence of 5 mM extravesicular Pr^{3+} , of cycling the vesicles through the phase transition.
 (a) Signals from the vesicles at 60°C before cycling, (b) signals from vesicles at 60°C after eighteen cycles through T_c (60°C - 30°C - 60°C), (c) signals from vesicles in (b) except that the extravesicular concentration of Pr^{3+} has been increased to 20 mM.

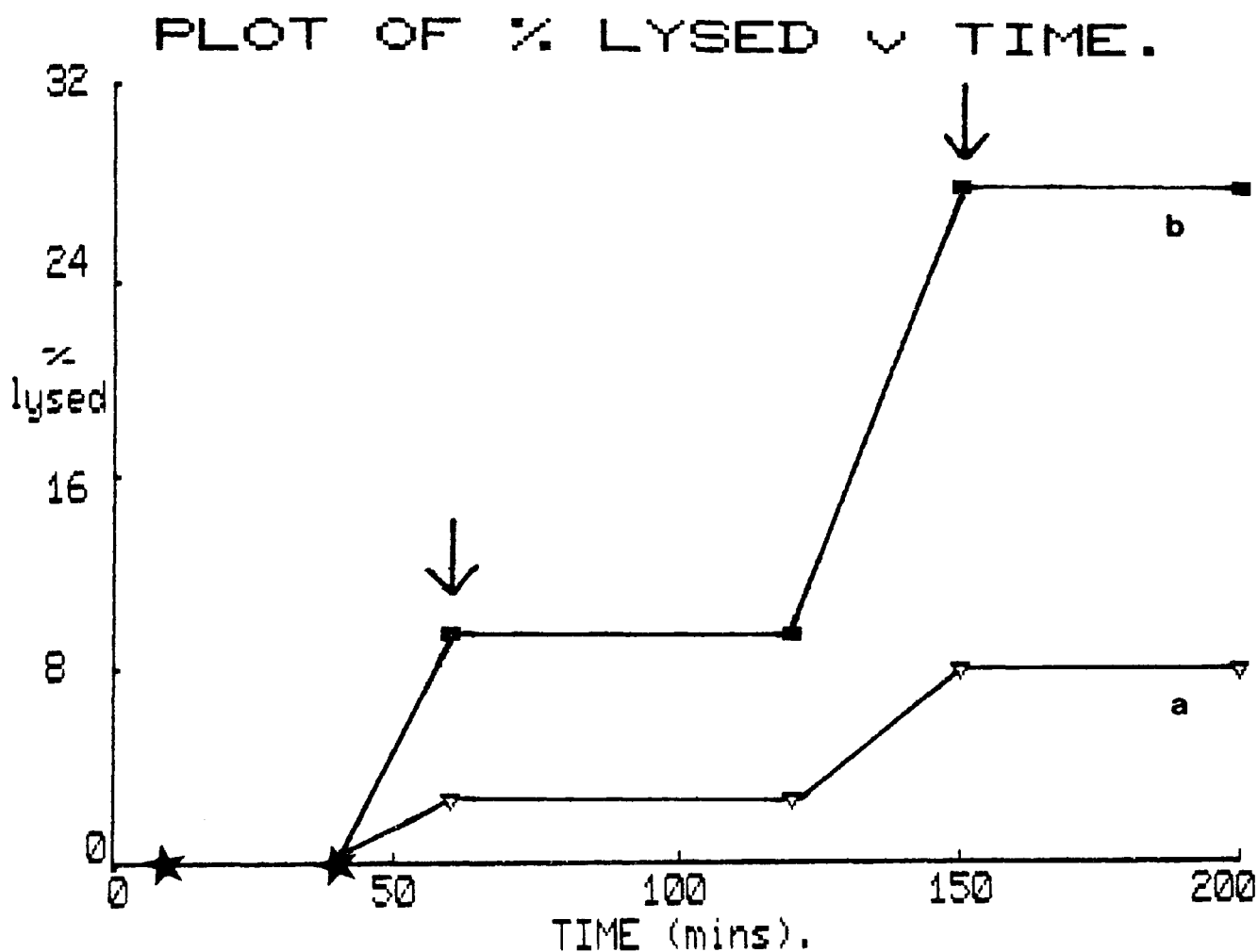


Fig 3.19 The effect of 0.1 mM Triton X100 on the lysis of DPPC vesicles caused by cycling the vesicles through the phase transition.

*indicates spectra taken during the initial incubation period. + indicates the times at which spectra were recorded after one cycle through the phase transition. Other points indicate the times at which spectra were recorded after incubation at 60°C.

a - control, b - vesicles in the presence of 0.1 mM Triton X100.

20 minutes) the % lysis increases. Fig 3.19 shows that the effect of 0.1 mM Triton X100 is to greatly increase the % of vesicles lysing at the phase transition. This is discussed with respect to the activation energy required for pore formation. The effect of the general anaesthetics, ethanol, diethyl ether and chloroform on this phenomenon is investigated in chapter 4.

3.3.3 The Effect of Bile Salts and Phospholipase A₂ on egg PC vesicles

The negative charge on the ionised bile salt (Fig 3.2) decreases the zeta-potential at the surface of the vesicle which results in a stronger interaction between the Pr^{3+} ion and the head group phosphate. This has the effect of shifting the outside signal downfield, with the degree of extra shift depending on the concentration of bile salt present.

The action of bile salts on egg PC vesicles in the presence of lanthanide is found to be two fold. Firstly at low concentrations of bile salts (0 to 1.5 mM) a transport type mechanism is observed in which signal I gradually shifts downfield in a similar manner to that described for alamethicin transport (see section 3.3.1). The second effect promoted by the bile salts is that of vesicular lysis. This is observed at higher concentrations of bile salts (> 1.5 mM) and is characterised by the appearance of a peak between the initial 0 and I signals, as shown in Fig 3.20. This peak I' corresponds to the inside signal of the lysed vesicles and its appearance in this region demonstrates that no bile salts are present in the intravesicular solution. Alternatively, but less likely, signal I' could correspond to semi-lysis with leakage of bile salt into the intravesicular solution. The signal ratio I' : I is therefore a representative of the proportion

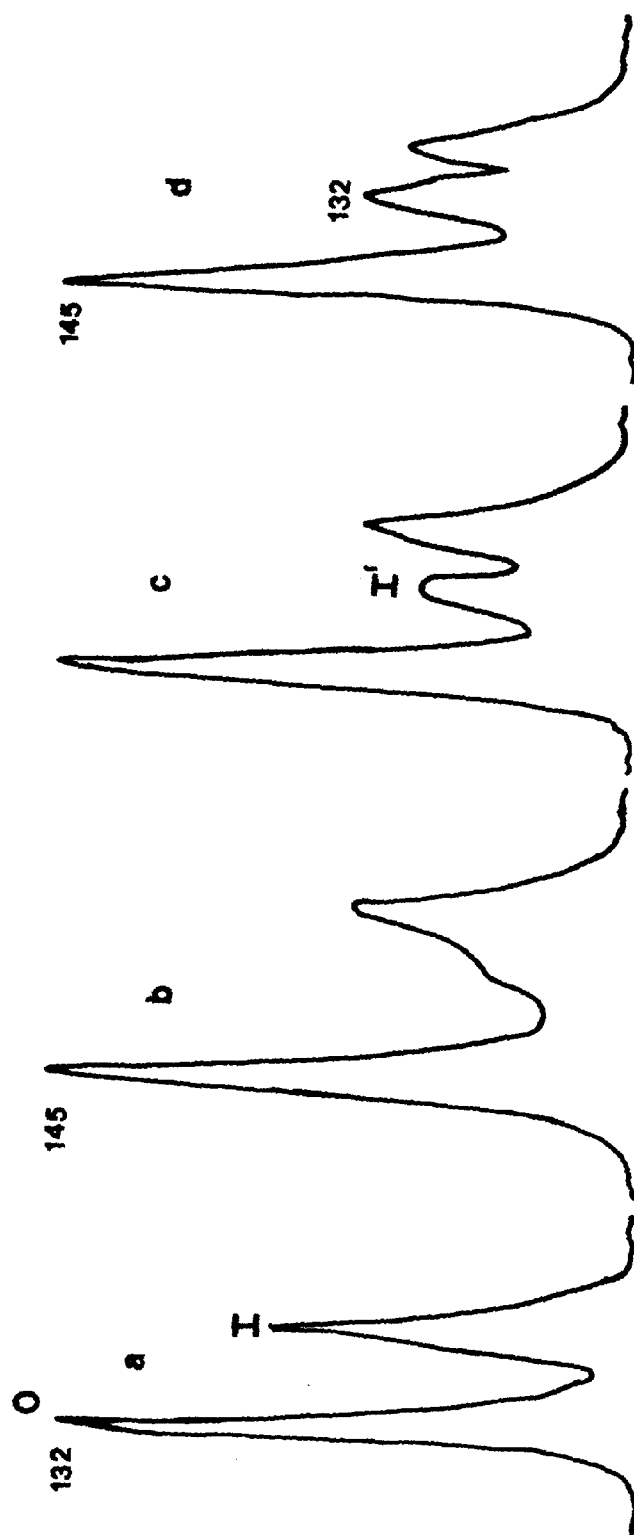


Fig 3.20 The time-dependent changes in the ^1H NMR signal (O and I) at 60 MHz, from egg PC vesicles (5 mM extravesicular Pr^{3+}) with 2 mM glycocholine at 37°C.
a. Before the addition of glycolate. b. 4 mins, c. 8 mins, d. 12 mins.
Signal I' arises from the inside signal of lysed vesicles (i.e. contain 5 mM Pr^{3+}).

of vesicles that have lysed.

Fig 3.21 shows the Pr^{3+} transport rates obtained by equimolar quantities of bile salts (1.5 mM) in egg PC vesicles at 37°C. The plot gives rates of transport of 0.0067, 0.0098, 0.0114 and 0.00875 mM/min for glycocholate, cholate, glycodeoxycholate and deoxycholate respectively. Only the initial rate of the glycodeoxycholate sample was measured since vesicular lysis began at around 50 minutes with a corresponding decrease in the transport rate.

Fig 3.22 shows the rates of lysis occurring in vesicles with equimolar quantities of bile salt (2 mM). The plot shows that the rate of lysis induced by the bile salts are in the order:

Deoxycholate > glycodeoxycholate > glycocholate > cholate.

These properties are discussed below with respect to their membrane damaging properties.

The nature of the lytic channels formed by the bile salts was investigated by a stoichiometry experiment in which rates of lysis were obtained at various concentrations of glycocholate (3.0 to 1.5 mM) at 37°C. Fig 3.23 is the result of plotting log rates of lysis against the log of glycocholate concentration used. The slope of the plot is 5.72 suggesting that six glycocholate molecules are involved in channel formation.

The action of PLA_2 (Naja naja) on egg PC vesicles (5 mM extravesicular Pr^{3+}) was investigated by varying the PLA_2 (10 units to 50 units/ml) and Ca^{2+} (2 to 20 mM) concentrations. These initial studies revealed very little activity and was attributed to the relatively high Pr^{3+} concentration which competes for the calcium binding sites on the enzyme (Slotboom et al 1982). However activity was obtained when Pr^{3+}

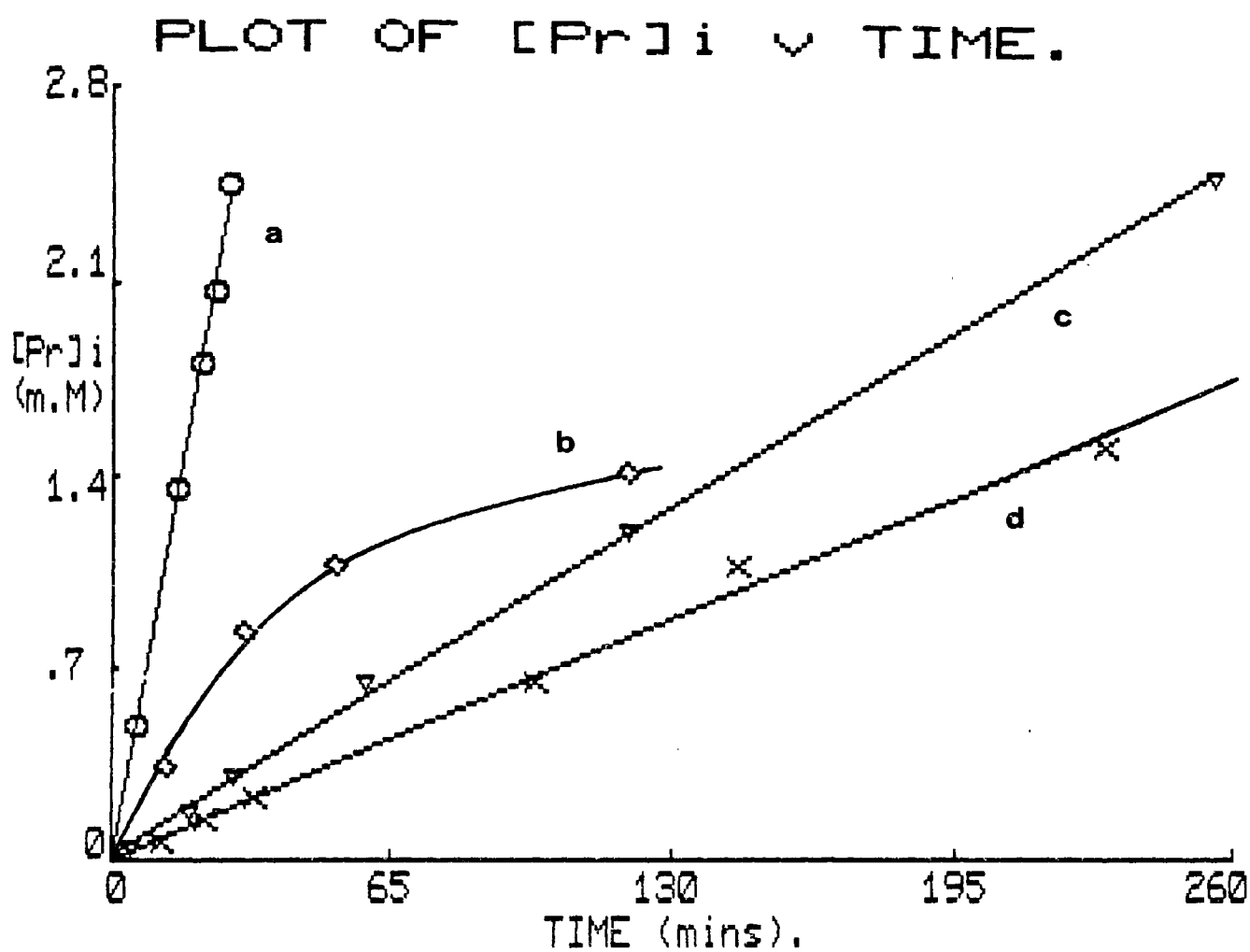


Fig 3.21 shows the carrier mediated transport activity of equimolar (1.5 mM) bile salt in egg PC vesicles at 37°C.
a. deoxycholate, b. glycodeoxycholate,
c. cholate, d. glycocholate.

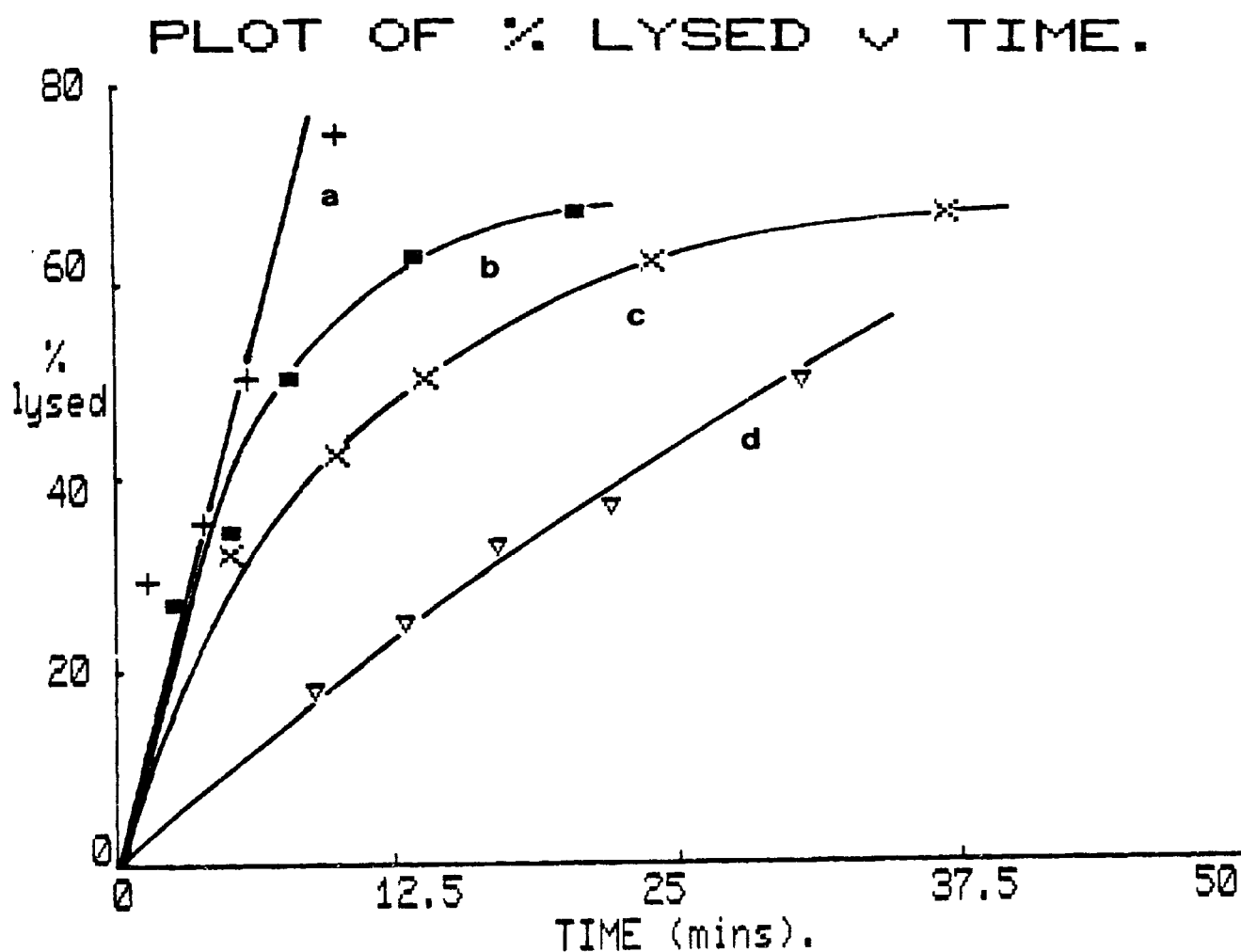


Fig 3.22 shows the rate of lysis in egg PC vesicles at 37°C obtained with equimolar (2.0 mM) bile salt.
a. deoxycholate, b. glycodeoxycholate,
c. glycocholate, d. cholate.

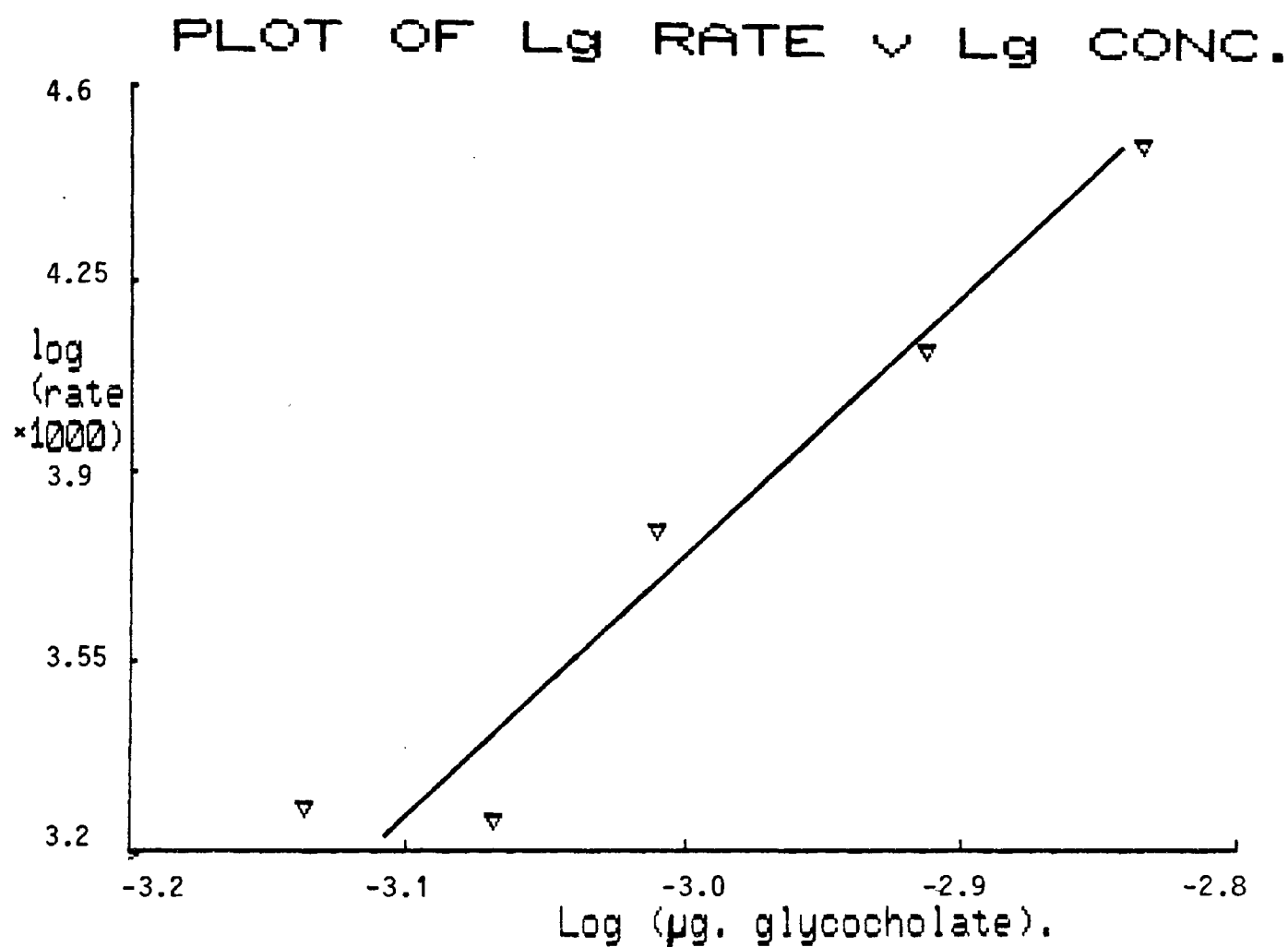


Fig 3.23 Stoichiometry plot for lytic channels produced by glycocholate in egg PC vesicles. The slope (5.72) indicates that six molecules of glycocholate are involved in each channel.

was substituted by 0.15 mM Dy^{3+} .

Fig 3.24 show the time-dependent changes in the ^1H -NMR spectrum for the inner and outer head groups of egg PC vesicles during an experiment using 28 units of pancreatic PLA_2 . Spectra a-d show that initially a gradual increase in the O/I ratio occurs which continues until a ratio of about 2.1 is obtained. During this period signal I remains unshifted showing that no Dy^{3+} ions have penetrated the intravesicular solution. However subsequent spectra (e-h) indicate that signal I is shifting downfield towards signal O corresponding to a increase in the intravesicular Dy^{3+} ion concentration, $[\text{Dy}]_i$.

A separate sample with identical conditions was set up to investigate whether the increase in the O/I ratio was due to vesicular lysis. In this case extra Dy^{3+} is added to a sample having an O/I ratio of 2.1 (Fig3.24d). No peak corresponding to the inside signal of lysed vesicles was revealed (see 3.3.2) thus indicating that no vesicular lysis has occurred.

Fig 3.25 shows that the variation in $[\text{Dy}]_i$ with time for three PLA_2 concentrations. The initial lack of transport corresponds to the period which the O : I ratio is changing. The rate of change in the O/I ratio and the consequent rate of transport are both seen to increase with higher PLA_2 concentrations. A molecular mechanism based on the changes occurring in the ^1H -NMR in combination with ^{31}P -NMR data (Hunt et al. in preparation) is proposed in the discussion section.

Similar time-dependent spectra to those shown in Fig 3.24 were also obtained for the combined action of PLA_2 and bile salts on egg PC vesicles. The results obtained from these experiments are shown in Figs 3.26, 3.27a and 3.27b. During each of these experiments the peak width of the acyl chain signal was monitored. Variation of only a few Hz were

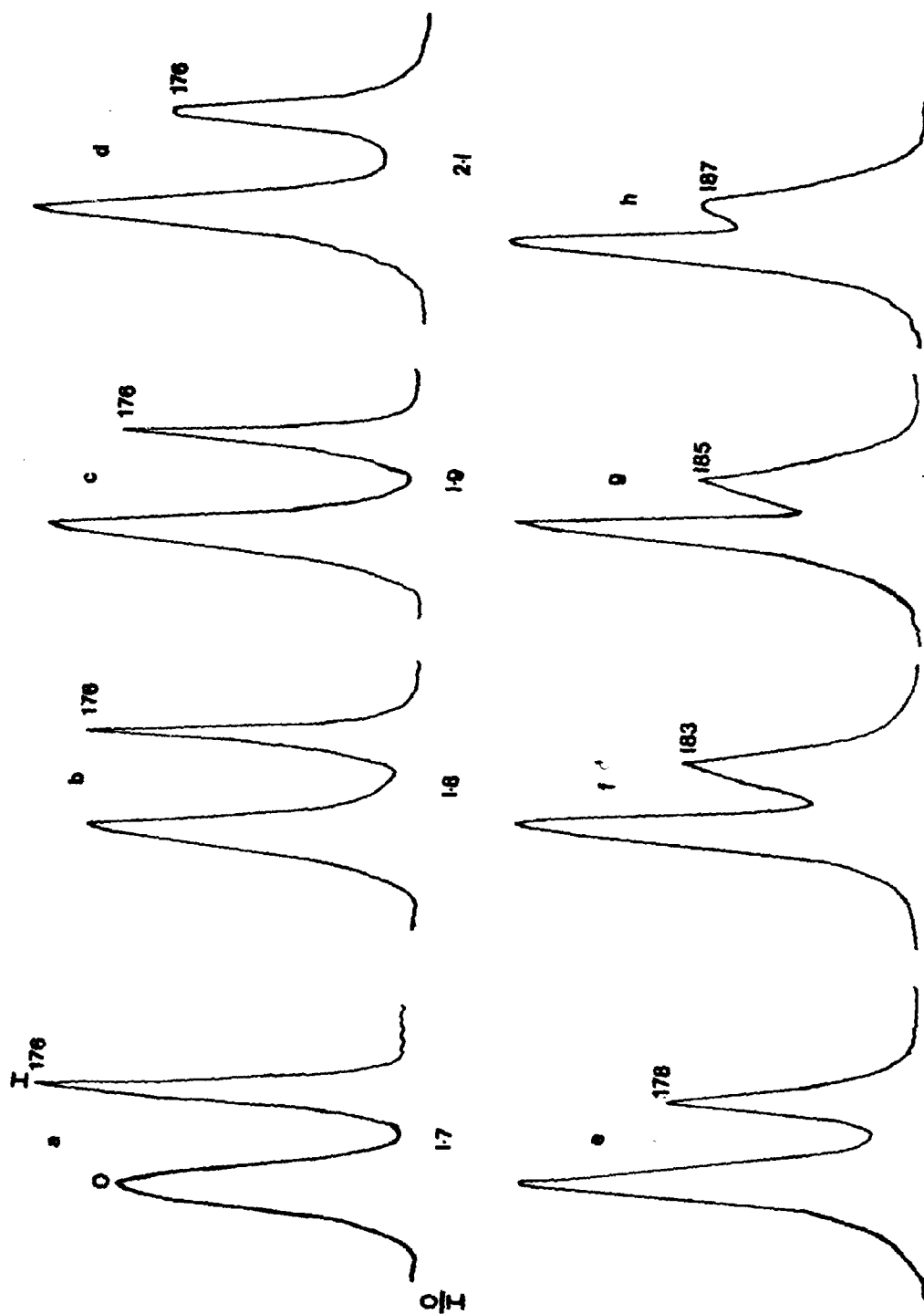


Fig 3.24 a-h show the time-dependent changes in the ^1H -NMR signal (0 and 1) at 90 MHz from egg PC vesicles in the presence of 28 units of pancreatic PLA_2 at 37°C . The chemical shift of signal 1 is measured with reference to signal H and are shown after (a) 7 min, (b) 90 min, (c) 120 min, (d) 180 min, (e) 240 min, (f) 480 min, (g) 550 min, (h) 680 min. a-d show a change in O/I ratio from 1.7—2.1, whilst e-h show a shift in signal 1 due to transport of Dy^{3+} into the intravesicular solution.

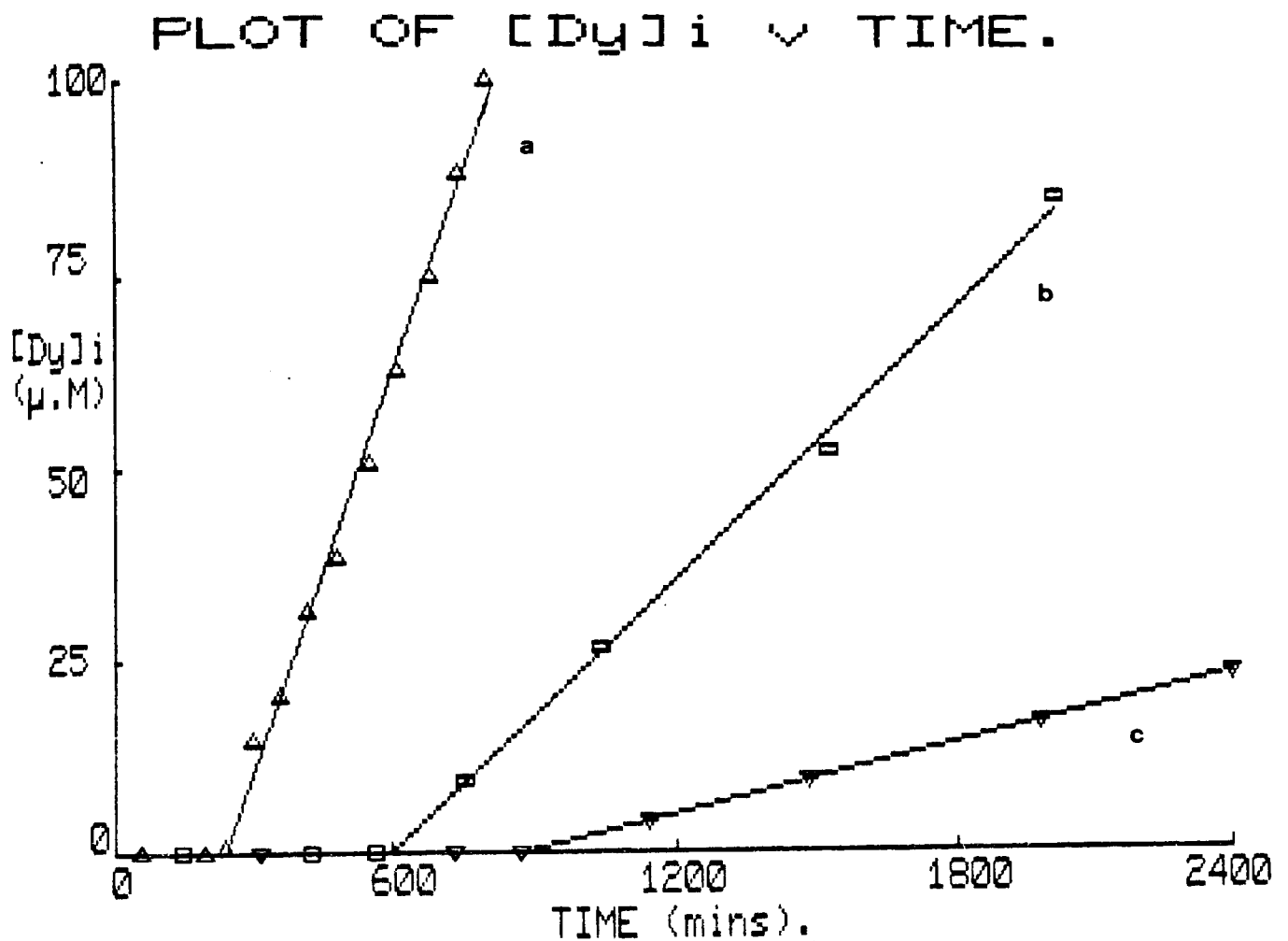


Fig 3.25 The increase in the intravesicular concentration of Dy^{3+} ions, $[Dy^{3+}]_i$ with time at $37^\circ C$ using 28 units (a), 7 units (b) and 2 units (c) of pancreatic PLA_2 . The initial stages where no increase in $[Dy^{3+}]_i$ is observed correspond to the period when the O/I ratio is increasing.

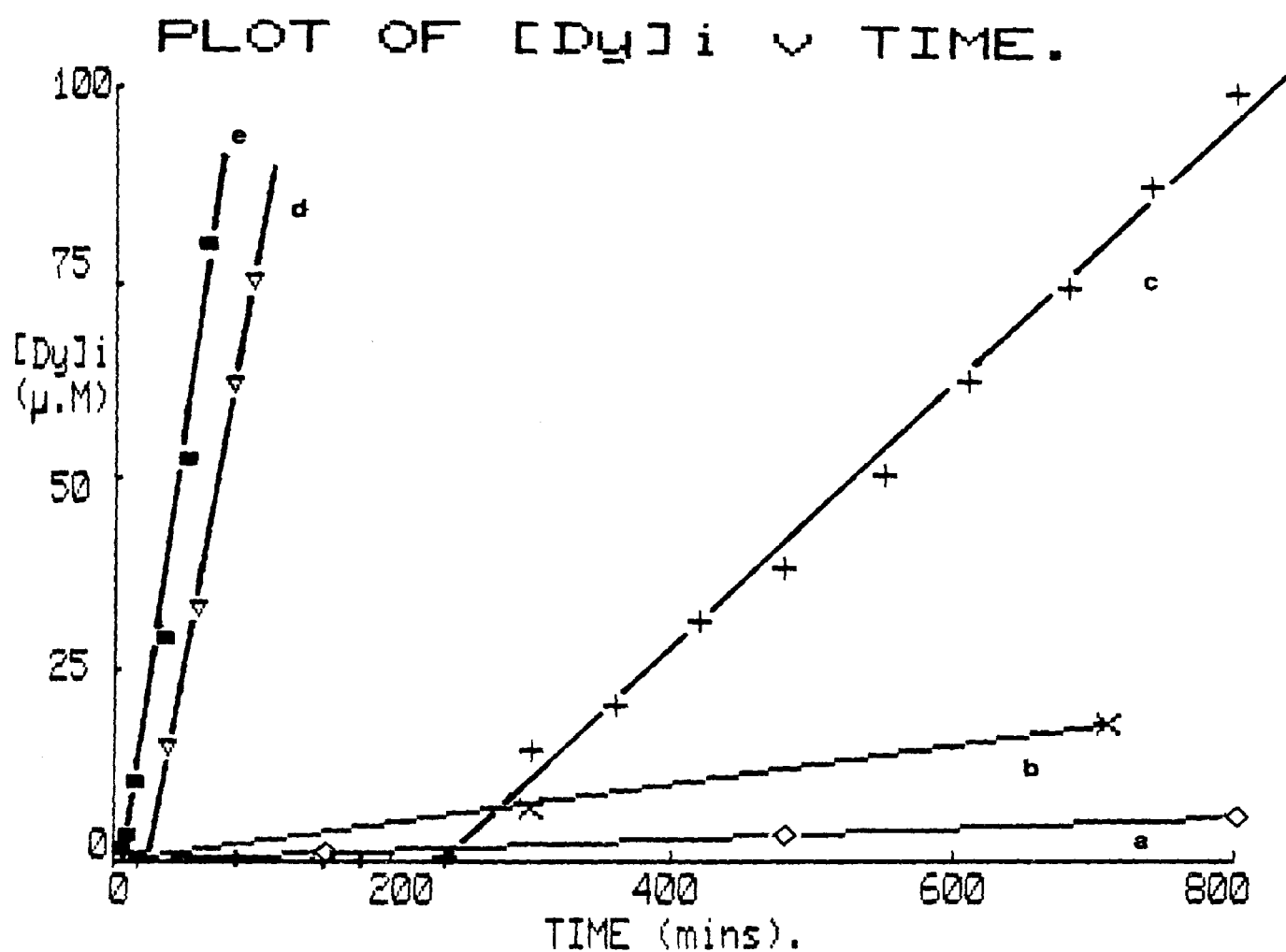


Fig 3.26 The synergistic action of 28 units of pancreatic PLA_2 with 0.5 mM bile salts in egg PC vesicles.
 a. 0.5 mM glycocholate, b. 0.5 mM glycodeoxycholate,
 c. 28 units pancreatic PLA_2 , d. 28 units PLA_2 + 0.5 mM glycocholate,
 e. 28 units PLA_2 + 0.5 mM glycodeoxycholate.

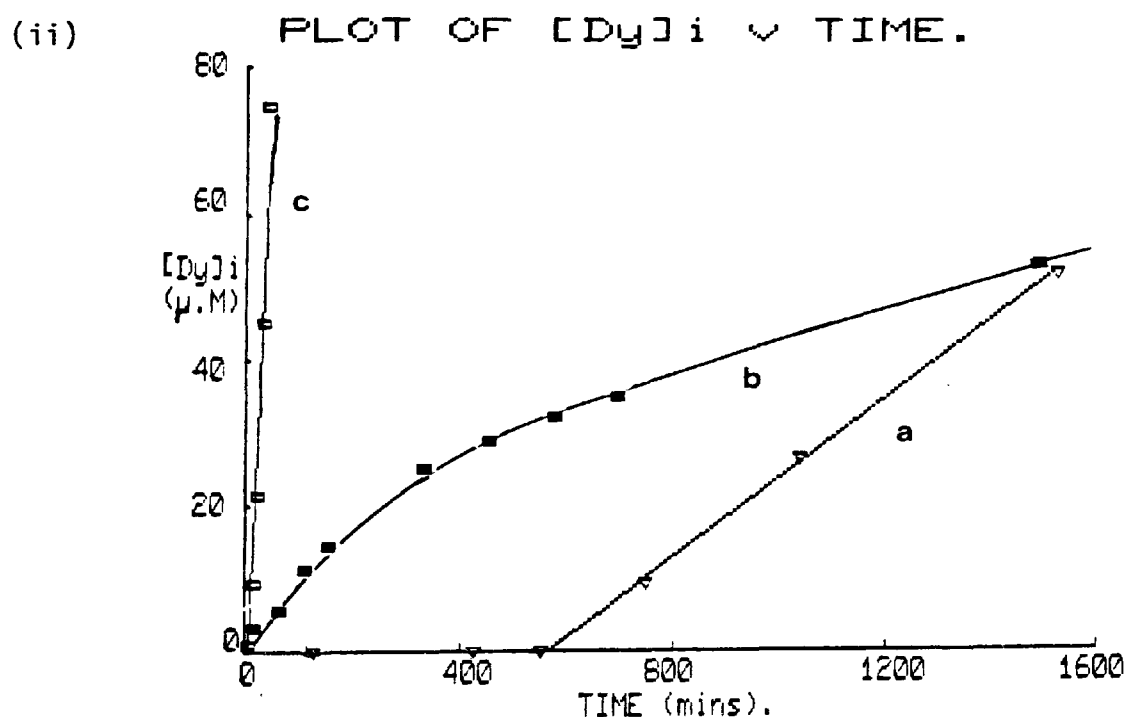
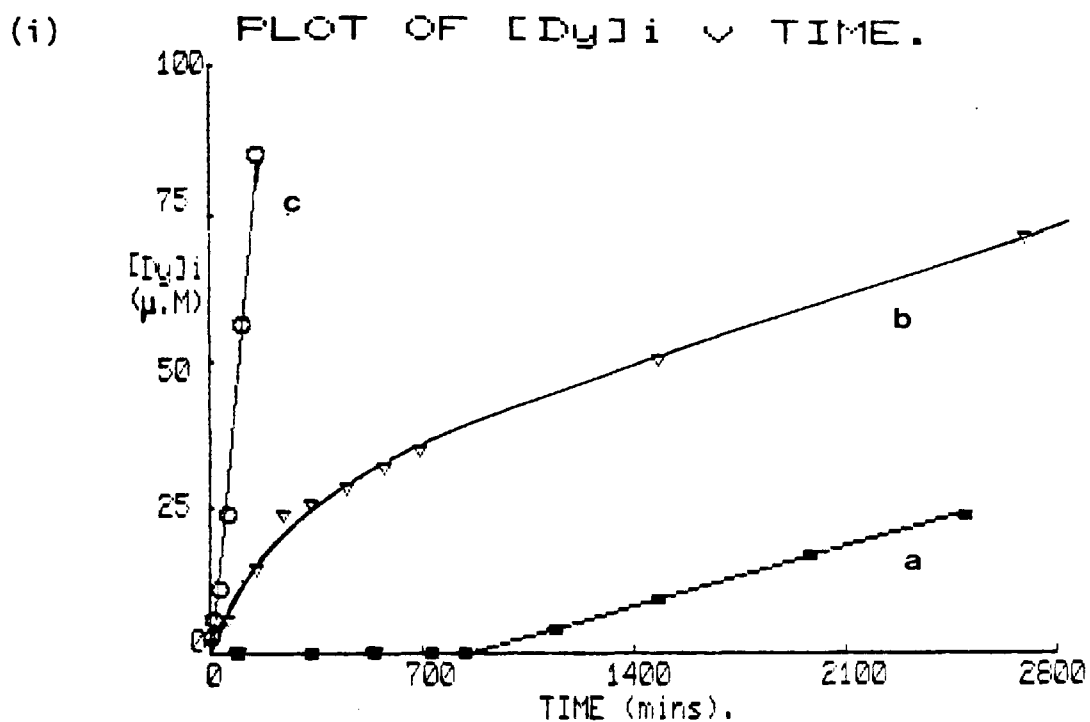


Fig 3.27 The increase in the intravesicular concentration of Dy^{3+} ions $[Dy]_i$ with time in egg PC vesicles ($37^{\circ}C$) incubated with:

- (i) a, 2 units PLA_2 , b. 1 mM glycocholate
c. 2 units PLA_2 and 1 mM glycocholate.
- (ii) a. 7 units PLA_2 , b. 1 mM glycocholate,
c. 7 units PLA_2 + 1 mM glycocholate.

observed indicating that no appreciable fusion occurs in these samples.

Table 3.2 shows a summary of the rates obtained from Figs 3.26, and 3.27. From this table it is seen that the rates obtained in the presence of both bile salt and PLA_2 are substantially greater than the sum of the rates obtained by their individual action. The synergistic activity and its consequences on liposome oral route drug targeting is discussed below.

Table 3.2

Rates of transport of Dy^{3+} ($\mu M/min$) produced by various concentrations of pancreatic phospholipase A_2 and bile salts in egg PC vesicles at $37^\circ C$

	UNITS OF PLA_2 per ml	CONCENTRATION OF BILE SALT		
		0	1.0 mM Glyco cholate	0.5 mM Glyco cholate 0.5 mM Glyco deoxycholate
0	-		0.03	0.07 0.025
2	0.015		0.543 (12.1) ^a (18.1) ^b	- -
7	0.059		1.667 (18.2) ^a (55.6) ^b	- -
28	0.172		-	0.923 (5.2) ^a (131.8) ^b 1.17 (5.9) ^a (46.8) ^b

(a,b) Figures in brackets represent the factors by which the rates obtained from the joint action of PLA_2 and bile salt exceed the rates obtained from the sum of the individual rates. (a) These factors were calculated using the PLA_2 rates shown in the table. (b) In calculating these factors, values of zero were used for all PLA_2 control rates since no transport is observed during the initial 200 minutes in these samples.

3.4 Discussion

3.4.1 Alamethicin mediated transport in DPPC and egg PC vesicles

The experimental results presented in section 3.3.1 show the first reports in which alamethicin mediated cation transport is demonstrated in DPPC and egg PC vesicles (Hunt and Jones 1982). Fig 3.5 indicates that Pr^{3+} ion transport by alamethicin is taking place in all the vesicles at approximately the same rate, since signal I moves downfield as a whole with very little broadening.

The observed stoichiometry of 4 alamethicin molecules per channel in either DPPC or egg PC vesicles (see 3.3.1.1) is lower than those reported for planar bilayer conductivity studies, which vary between 6 and 12 molecules for the various conductivity levels (Lattore 1981). The difference between the stoichiometry results for alamethicin in the two systems can be accounted for by factors such as :

- a. Curvature of the vesicular bilayer.
- b. Presence of hydrocarbon solvent in BLMs (see section 1.1.5.1).
- c. Absence of unstirred layer effects in the rapidly tumbling small vesicles.
- d. Transmembrane potential effects.

Transmembrane potential effects require further elaboration since BLM conductivity by alamethicin is usually only observed when a transmembrane potential is applied and when the ionophore is added to the aqueous phase of the positive side of the bilayer (Cherry et al 1972). However evidence for alamethicin conducting channels in the absence of a transmembrane potential has been obtained by many studies (Chapman et al 1969, Hauser et al 1970, Eisenberg et al 1973, Fringeli and Fringeli 1979, Fringeli 1980, Gogolein et al 1981, Latorre et al

1981, McIntosh et al 1982), thus suggesting that alamethicin channels can be formed in the absence of an applied transmembrane potential and therefore forms potential dependent and potential independent channels. The results in section 3.3.1 seem to be due to the latter type but the possibility exists that whilst the diffusion rate is negligible (0.1 mM Pr / 3 days) compared to the alamethicin rates, it could be sufficient to give the initial transmembrane potential (positive inside) required to open the channel once sufficient alamethicin has spanned the bilayer.

All the results obtained from alamethicin show no signs of vesicular fusion, as monitored by the peak width of the hydrocarbon signal (Liao and Prestegard 1980). This is in contrast to the results obtained by Lau and Chan (1974, 1975, 1976) where the results were dominated by alamethicin induced vesicular fusion. They proposed that alamethicin molecules acted as nuclei for the inverted micelle intermediates of vesicle-vesicle fusion, with the process allowing the entry of ions into the resultant fused vesicle. If the process they proposed is correct then after three to four vesicle-vesicle fusions (equivalent to intravesicular solution containing 3-4 ions) the relatively large vesicles produced would result in the loss of the high resolution ^1H -NMR signals due to broadening.

The results that Lau and Chan obtained are probably due to the relatively high concentrations of alamethicin they used (0.5 - 2.0 mg alamethicin with 50 mg/ml vesicles). This is consistent with the observation that widespread fusion occurs when higher concentrations of alamethicin 30 (70 $\mu\text{g/ml}$) are incubated with DPPC vesicles (results not shown). Lau and Chan (1976) also attempted to set up a transmembrane potential using K^+ /valinomycin but the observed transmembrane movement

of Eu^{3+} was then so fast that the kinetics could not be followed. Their experimental method was however complicated by the fact that fusion of vesicles was induced by the ionophore and dialysis of the vesicles made it difficult to know the final disposition of alamethicin.

A concentration of 20 μg of alamethicin per 1 ml of vesicular solution is equivalent to 6 alamethicin molecules per vesicle (based on an O/I ratio of 1.6, see chapter 2). The transport rate obtained from DPPC vesicles at this concentration (Fig 3.5) indicates that about 20 Pr^{3+} ions (2.5 mM intravesicular Pr^{3+}) are transported into each vesicle in 60 minutes, or at a rate of one Pr^{3+} ion per three minutes. Incubating a lower concentration of alamethicin (5 $\mu\text{g}/\text{ml}$) with DPPC vesicles gives spectra similar to those in Fig 3.5 but over a longer time scale. The resulting transport rate (Fig 3.7) corresponds to the transport of one Pr^{3+} ion / vesicle / 100 minutes.

The lower concentration of alamethicin (5 $\mu\text{g}/\text{ml}$) gives an average of between 2 and 3 alamethicin molecules per vesicle, which is below the vesicular concentration required to form transporting channels. Exchange of alamethicin molecules between vesicles must therefore take place for transport to occur in all the vesicles. Further studies employing ^1H -NMR to monitor transport, reveal that transfer of alamethicin molecules between DPPC vesicles does occur (Hunt, Jones and Veiro in prep) irrespective of whether alamethicin is incubated extravesicularly (as described in section 3.2.3) or sonicated in the bilayer (as described in 3.2.4b).

An equilibrium must therefore exist between alamethicin situated at the surface of the vesicle with alamethicin molecules which are spanning the bilayer. Alamethicin molecules in the α -helical

configuration (3.5 - 4.0 nm long) are just long enough to span the bilayer (Fox and Richards 1982). The α -amino isobutyric acid (AIB) residues give rise to a hydrophobic backbone down one side of the alamethicin molecule, whilst hydrophilic groups are situated along the length of the opposite side (Gln 7, Gln 19, Phe 20, Glu 18, AcAib 1, Aib 3 and Aib 13 - see Fig 3.1, Fox and Richards 1982, Jung et al 1979, 1982, Marshall and Balasubramanian 1979). The hydrophilic groups present in the central region of the molecule would make it energetically unfavourable for alamethicin monomers to span the bilayer. However alamethicin dimers (having limited life times) may form at the surface of the vesicle by H-bonding between their hydrophilic surfaces. This would result in an exterior hydrophobic shell, with exception of the two ends of the dimer, which have projecting hydrophilic groups (AcAIB 1, Gln 19, Phe 20). This interaction may therefore induce such dimers into spanning the lipid bilayer, such that the hydrophobic groups interact with the fatty acyl chains and the hydrophilic groups to interact with the polar head group region. Lateral diffusion of the dimers in the plane of the bilayer (the rate of which is dependent on lipid fluidity) would allow these dimers to function as nuclei for oligomeric channel formation by interaction with other monomers, dimers or trimers. The equilibrium between alamethicin at the surface of the vesicles with those spanning the bilayer will therefore depend on the life time of each oligomer.

The channel life time can be calculated by assuming that hydrated ions pass through the channels at a rate of 10^8 ions / second / channel (Hall 1978). On this assumption the transport rate of one ion / 3 minutes / vesicle obtained by 20 μ g of alamethicin (Fig 3.6) results in a channel lifetime of 10 nanoseconds (ns) with channels being formed at

a rate of approximately one per 3 minutes. Therefore the rate of formation and lifetimes of the alamethicin channels in lipid vesicles is low. This suggests that the alamethicin monomers are located at the vesicle surface for a majority of the time, an observation that is consistent with the BLM studies of Gordon and Haydon (1975). Alternatively dimers in the transmembrane position may not meet very often in the bilayer.

From the results in Fig 3.6 and 3.7 it can be concluded that :

- a. An incubation time allows more alamethicin to partition into and span the bilayer than when no incubation time is used.
- b. Sonicating alamethicin in the bilayer increases the rate of channel formation with respect to the incubation method. This may be a result of a higher alamethicin concentration spanning the bilayer.
- c. Sonicating alamethicin intra and extravesicularly results in the preferential partition of the intravesicular alamethicin oligomers (of relatively long lifetime) into the bilayer thus giving a large increase in the rate of channel formation.

It is also possible, in b and c above, that the channel life time could be changed due to conformational changes in the alamethicin molecules induced by the method of vesicle preparation.

In Fig 3.8 the difference in rates obtained by equal concentrations of alamethicin (20 $\mu\text{g/ml}$) in DPPC vesicles (1 ion / 3 minutes / vesicle) and egg PC vesicles (1 ion / 300 minutes / vesicle) may arise from the difference in order and fluidity in the two systems. The greater fluidity and disorder in the egg PC bilayer may be lowering the rate of conducting oligomer formation in the bilayer and/or

inhibiting the partition of the alamethicin into the bilayer, thus resulting in a greater activation energy value (72 KJ/mol) than in DPPC vesicles (59 KJ/mol) as shown in Fig 3.10 and 3.11.

3.4.1.1 The effect of mixed lipids on alamethicin 30 transport

The rate obtained from egg PC / 50 mole % DPPC (0.7×10^{-2} mM/min in Fig 3.12) is slower than the average rate of 1.215×10^{-2} mM/min obtained from the two control rates. This result suggests that the formation of lipid domains (separate regions of egg PC and DPPC) could be possible, where the rate reflects alamethicin (of reduced effective concentration) transport through DPPC domains. Alternatively the slower rate may be due to the fluidity of the mixed lipid bilayer resembling the egg PC bilayer than that of DPPC bilayer.

Figures 3.13, 3.14 and Table 3.1 indicate that all the lipid mixtures used (except for egg PC / 5 mole % PA with Pr^{3+}) potentiate the rate of cation transport by alamethicin. The difference in the result obtained with 5 mM Pr^{3+} to that obtained with Dy^{3+} may be due to the difference in the ionic concentrations. Signal I' (in Fig 3.15) originating from partially lysed vesicles, suggests that the lifetime of the alamethicin channels has been increased from 10 ns to around 160 ns, thus allowing a pulse of Pr^{3+} ions to get across the membrane. However this process can only occur once in any single vesicle (since no reduction in the intensity of signal I'), which may be a consequence of the altered ionic concentration gradient. Alternatively, the semilysis occurring could be a consequence of the formation of larger channels composed of a greater number of alamethicin monomers.

The net decrease in the the rate of Pr^{3+} transport by alamethicin

may be a consequence of the distribution of PA in the bilayer. PA preferentially occupies the inner monolayer (see section 1.1.6) and therefore gives a higher charge density than the outer monolayer. This negative charge may therefore give rise to repulsion of the negative charge on alamethicin (C terminal) and thus reducing the probability of the bilayer spanning conformation (for further discussion refer to Hunt et al. 1984).

The formation of H_{II} phase (in PC/CL and PC/PA) is a possible mechanism for the increased alamethicin transport rates of Dy^{3+} . For the PC/PA mixture the ratio of PC/PA rate : control rate is 2.58 : 1. However when calcium is present the ratio changes to 3 : 1. Calcium is known to induce H_{II} phase with PC/PA bilayers (Cullis and De Kruijff 1979, Mirghani 1982), but no transport by non bilayer phases occurs in this system. Therefore the increased rate observed in the presence of calcium may result from the H_{II} phase (induced by the calcium) stabilizing the alamethicin channels. A similar type of mechanism may also occur in the PC/CL and PC/PE systems, but in these cases non bilayer phase transport must be accounted for.

It is also possible that the interaction of a non bilayer phase with alamethicin may induce conformational changes in the ionophore molecule or in the oligomer channels. A similar proposal has been suggested for the lipid - gramicidin system (Wallace et al 1982) where it is thought that the peptide-lipid interaction is important in maintaining channel conformation. In the alamethicin system the lipid interaction may increase either the lifetime of the channel or the rate of channel formation or even both. Studies using higher alamethicin and lipid concentrations with large vesicles and ^{31}P -NMR would allow further investigation of this system.

The ratio of the PC/PE rate : control rate (from Table 3.1) for Pr^{3+} transport (4 : 1), Dy^{3+} transport (2.3 : 1) and $\text{Dy}^{3+}\text{-Ca}^{2+}$ transport (2.4 : 1) indicate that the presence of PE potentiates the Pr^{3+} transport rate more than Dy^{3+} transport rate. This may be due to the ionic concentration affecting the PE distribution (Koynova and Tenchov 1983) since it is found that at high ionic concentrations PE is symmetrically distributed but a decrease in ionic strength results in a preferential localization of PE in the inner monolayer.

The transport properties of alamethicin therefore depend on the nature of the lipid environment, a property which has also been observed in BLM studies with alamethicin (Latorre and Donovan 1980). The possibility that alamethicin induces non bilayer phases in a similar fashion to that seen with gramicidin (Van Echteld et al 1981, 1982) is further emphasised by its promotion of vesicular fusion at high concentrations (70 μg alamethicin / ml of vesicular solution).

3.4.1.2 Effect of the calcium antagonists on alamethicin transport

Low concentrations of verapamil (up to 50 μg , i.e 10 : 1 verapamil : alamethicin) inhibits the Pr^{3+} transport rate mediated by alamethicin, with maximum inhibition occurring at the molar ratios of 2:1 and 10 : 1. At the higher verapamil concentrations, 20 : 1, 30 : 1, and 50 : 1 a potentiation in the alamethicin transport rate is observed. However much lower concentrations of nifedipine are required to show similar effects (1:1, 2:1 and 3:1 all inhibit, whilst 4:1 and 10:1 potentiate), a factor which may be due to its greater hydrophobicity (see Fig 3.2).

The inhibition shown at the lower antagonist concentrations is more likely to be due to metal ion - antagonist interaction at the

vesicle surface, rather than the antagonist reducing the rate of channel formation (Mirghani 1982). However this type of interaction does not explain the potentiation observed at the higher antagonist concentrations. Such interactions of antagonists at high concentrations have previously been observed in various tissues (Middleton et al 1981, Weiss 1978, Putney 1978, Foreman et al 1973) but no explanation has been given. The results reported here indicate that the potentiated rates are greater than the sum of the control rates (20 μ g of alamethicin and 250 μ g of verapamil) thus suggesting that a type of synergistic action must be taking place at these concentrations. Here the mechanism must involve a net increase in the channel life time. Possible explanations may involve:

- a. Surface antagonist inducing alamethicin into a bilayer spanning conformation and thus increasing the rate of channel formation.
- b. The antagonist having a stabilizing effect on a channel.
- c. The antagonists could form a part of a channel which has a longer lifetime, and/or a more frequent rate of formation.

The latter polyionophore concept has been suggested to explain the synergistic effects between various carrier ionophores (Grandjean and Laszlo 1982) and between calcium antagonists and carrier ionophores (Mirghani 1982).

3.4.2 Membrane permeability induced at the phase transition

The vesicular lysis obtained as a result of cycling DPPC vesicles through the phase transition (Figs 3.18 and 3.19) is consistent with the formation of pores which are capable of equilibrating the extravesicular and intravesicular solutions. However, the observation that this only occurs in a proportion of the vesicles (per any one

cycle) suggests that a relatively high activation energy is required for the formation of such pores and/or the passage of ions through them. A similar concept has been considered by Kanehisa and Tsong (1978), where an increase in the activation energy to water permeability in lipid bilayers is attributed to a reduction in pore size caused by a tighter packing of lipid molecules.

The results obtained using Triton X100 indicate that the degree of lysis has increased by approximately four orders of magnitude. This suggests a lowering of the activation energy required for the lytic process. Triton X100 is an amphiphile consisting of a highly branched hydrophobic portion (octyl phenyl) and a longer hydrophilic portion composed of 10 oxyethylene units. This property allows Triton X100 to partition into the bilayer (Inoue and Kitagawa 1976), to act as a carrier at low concentrations and channel ionophore at higher concentrations (Hunt 1980b, Schlieper and De Robertis 1977). Thus Triton X100 molecules in the bilayer may reduce the activation energy for vesicular lysis by functioning as nuclei for pore formation. Folded Triton X100 molecules could then line these channels. This may make pore formation at the phase transition more favorable and it may also give rise to wider pores thus allowing easier passage of ions. The effect of the general anaesthetics on these systems, including fusion induced by Triton X100, has been investigated and is described in chapter 4.

3.4.3 Effect of bile salts and PLA₂ on egg PC vesicles

The results in Fig 3.21 and 3.22 show that faster rates of ion transport and vesicular lysis are obtained with the dihydroxy bile salts, deoxycholate and glycodeoxycholate than with the trihydroxy bile salts, cholate and glycocholate. This may be explained by considering their membrane solubility. The dihydroxy bile salts have greater

solubility in the hydrophobic region of the bilayer and have been shown to partition into the hydrocarbon region much more efficiently than trihydroxy bile salts (Strange 1981). These observations are in agreement with the erythrocyte membrane damaging properties of these bile salts (Billington and Coleman 1978, Vyvoda et al 1977, Coleman et al 1978), in which the trihydroxy bile salts are able to remove a portion of the outer monolayer components without causing sufficient membrane damage to result in lysis.

The results in Fig 3.23 suggests that 6 bile salt molecules are involved in forming channels that cause vesicular lysis. A model for such a channel may involve H-bonding between two trimers (one in each monolayer) of bile salt. The hydroxyl and carboxylic groups line the channel and also interact with the head group region, whilst the hydrophobic groups form backbones for the interaction with the fatty acyl chains.

The effects of the general anaesthetics and cholesterol on the transport and lytic properties of these bile salts are described in chapters 4 and 5 respectively.

The results obtained from the action of PLA_2 on egg PC vesicles indicates that a redistribution of molecules occurs between the inner and outer monolayers. The O : I ratio change from 1.7 to 2.1 (Fig 3.24) indicates that about 20% of the inner monolayer choline-containing molecules have been transferred into the outer monolayer. To maintain vesicular stability these molecules must be replaced by non-choline containing molecules. To suggest a mechanism by which this occurs, the action of pancreatic PLA_2 on egg PC vesicles as monitored by ^{31}P -NMR (Hunt, Jones and Evans in prep) must also be considered.

PLA₂ catalyses the specific hydrolysis of the fatty acid ester bonds at the 2 position in 1,2 diacyl phospholipids such as PC, to give equimolar quantities of 1-acyl, lyso phosphatidylcholine (lyso PC) and fatty acid (Van den Bosch 1982, Slotboom et al 1982). Hydrolysis of PC molecules in PC vesicles can be monitored by ³¹P-NMR since the signals obtained by lyso PC appear 0.5 ppm downfield to the signal from PC (Brasure et al 1978, Roberts et al 1979). Four signals corresponding to PC and lyso PC from both inner and outer monolayers can be resolved when extravesicular Pr³⁺ ions are present. Monitoring these signals indicate an initial lack of hydrolysis (lag phase), which may be attributed to the tight packing of the lipid molecules above the phase transition and thus inhibiting the enzyme from penetrating the bilayer (Rowland and Woodley 1980). However once penetrated the defects caused by the hydrolysis product, lyso PC, gives the enzyme greater manoeuvrability and thus speeding up its effective rate of hydrolysis (Jain et al 1982). This role of lyso PC is also shown when the lag phase is abolished by preincubating lyso PC with bilayers (Jain and De Haas 1983).

When the ¹H-NMR O:I ratio is 2.1, about 40 % of the outer monolayer PC molecules have been hydrolyzed (from ³¹P-NMR). No inside lyso PC signal is observed by this time. This indicates that fatty acid from the outer monolayer is exchanging with inner monolayer PC molecules, a process that could be verified by monitoring the ¹³C-NMR signal from the acidic carbonyl in ¹³C enriched phospholipid.

The mechanism by which lipid redistribution takes place in membranes has gained much attention (see sections 1.1.6 and 1.4). Transbilayer movement of phospholipids is usually slow under equilibrium conditions (Kornberg and McConnell 1971) except at the phase transition (De Kruijff and Van Zoelen 1978) or when the equilibrium distribution of

component phospholipids is disturbed (De Kruijff and Wirtz 1977, De Kruijff and Baken 1978). It is also considered that the presence of proteins may play an important role in the transbilayer movement, by producing discontinuities in the bilayer structure (Van Zoelen et al 1978, Van der Steen et al 1981, De Kruijff et al 1978).

A likely mechanism for such redistributions involves the formation of inverted micelles (De Kruijff et al 1979a, Cullis and De Kruijff 1979). Thus in the present study the initial redistribution (during the O/I change) may be brought about by inverted micelles (mediating the transfer of $2n$ moles of fatty acid and n moles of PC from the outer monolayer and $2n$ moles of PC from the inner monolayer) in which the central aqueous pore is too small to accommodate a metal ion and hence the lack of transport at this stage. The process may be driven by the preference of the fatty acid for the highly curved inner monolayer (Cullis and De Kruijff 1979), and ends when a further increase in the proportion of fatty acid in the inner monolayer would destabilize the bilayer.

At this stage lyso PC in the outer monolayer exchanges with PC in the inner monolayer (from ^{31}P -NMR). This may be brought about by inverted micelles mediating the transfer of n moles of lyso PC and n moles of fatty acid from the outer monolayer and n moles of PC from the inner monolayer. No transport occurs during this time and therefore the central aqueous pores of these inverted micelles cannot accommodate metal ions.

Further spectra show that the vesicles become permeable to Ln^{3+} (Fig 3.24 e-h) when all the inner monolayer PC molecules have been replaced by lyso PC and fatty acid (from ^{31}P -NMR). Since no further

change in the O:I ratio occurs, this suggests that ion transport is mediated by inverted micelles composed of equimolar amounts of fatty acid and lyso PC from both monolayers. This process may be propagated by the preference of the fatty acid for the high degree of curvature present in the inverted micelle. The rate of transport therefore depends on the availability of lyso PC and fatty acid in the outer monolayer. Higher concentrations of PLA₂ give more hydrolysis product and hence result in the faster transport rates (Fig 3.25 and Table 3.2).

²H-NMR, ³¹P-NMR and DSC studies show that bilayers composed of high concentrations of lyso PC and fatty acid are stable even though the individual components form micelles when dispersed in an aqueous phase (Jain et al 1980, Jain and De Haas 1981, Allegrini et al 1983). The stability of such bilayers has been attributed to dimer formation between lyso PC and fatty acid, which gives a similar packing to the parent diacyl lipid molecule (Jain and De Haas 1981) but with the head group experiencing a greater motional freedom (Allegrini 1983). This stability was verified (results not shown) by making vesicles composed of equimolar amounts of oleic acid and lyso PC. ¹H-NMR experiments then showed that these vesicles were stable but were highly permeable to lanthanide ions in the absence of PLA₂ and Ca²⁺, thus giving further evidence for transport via inverted micelles.

It is observed that a large reduction in the time before transport commences and an increase in the rates of transport occurs when a relatively low concentration of bile salt (0.5 mM glycocholate or glycodeoxycholate) is present with 28 units PLA₂ / ml (Fig 3.26 and Table 3.2). It has been shown that in such mixtures no lag phase is apparent and the rate of hydrolysis is greatly increased (Van den Bosch et al 1974). This effect is verified by ³¹P-NMR (results not shown) and

may be explained by the bile salt causing slight perturbations or disorders in the outer monolayer thus providing PLA₂ with a more readily available substrate (Jain et al 1982). Similar increases in activity have been observed at the phase transition where perturbations are caused by domains of liquid crystal and gel phases (Okimara 1982).

The increased rate of hydrolysis leads to much quicker lipid redistribution followed by a faster rate of transport (Fig 3.26). However there is the possibility that bile salt molecules could form part of the inverted micelle and thus contribute to the rate of transport. This possibility is more likely at higher bile salt concentration (1.0 mM glycocholate) with smaller quantities of PLA₂ (Fig 3.27). In these samples transport was immediately apparent, thus suggesting that once the fatty acid and/or lyso PC is available in the outer monolayer they can form mixed inverted micelles with bile salt.

The permeability induced indicates that these inverted micelles have central aqueous pores large enough to accomodate metal ions. The rates obtained in these results (as summarized in Table 3.2) thus show convincing evidence that a synergistic action occurs between PLA₂ and bile salts in lipid bilayers. Such an interaction must be considered if liposomes are to be used in drug delivery via the oral route (Hunt and Jones 1984). The development of bilayers with resistance to this activity would be very beneficial to such studies.

The above results suggest that bile salts are providing some disruption for PLA₂ action and therefore from this respect bilayers resistant to bile salt (at duodenal concentration of 10 mM) are prime candidates. The results obtained with the bile salts (section 3.3.3, Richards and Gardener 1978) indicate that fluid bilayers are more prone

to the disrupting properties of bile salts, but membranes containing SM / cholesterol (Coleman et al 1980) or DSPC/cholesterol (Rowland and Woodley 1980) show resistance to this action. Such bilayers may therefore prove useful in future studies.

CHAPTER 4

GENERAL ANAESTHETICS

4.1 Introduction

The effect of ethanol and other general anaesthetics on the central nervous system are not understood at the molecular level (see section 1.5). However their physiological effect seem likely to be centred on the process involved in synaptic transmission (Richards 1980, Barker 1975). This includes fusion of synaptic vesicles with the presynaptic membrane to release neurotransmitter, the passage of neurotransmitter to the receptors on the postsynaptic membrane and the opening of ion channels in the postsynaptic membrane.

The understanding of such processes as transmembrane ion transport and membrane fusion has benefited from the simplification of the systems involved by using model lipid membranes in a large number of studies. However investigations into the effects of ethanol and the general anaesthetics on transmembrane channels using lipid bilayer membranes are surprisingly limited (Hendry et al 1978, Dluzewski and Halsey 1980, 1981, Pope et al 1982) and their effects on membrane fusion do not seem to have been significantly studied at all in model systems.

This study therefore set out to investigate the action of ethanol, diethyl ether and chloroform on a variety of mechanisms involved in membrane permeability and membrane fusion (Hunt and Jones 1982). The choice of these three compounds seemed suitable since they are all uncharged molecules and have a wide range of partition coefficients from aqueous to membrane phase (Vanderkooi et al 1977, Hill 1975).

Small unilamellar lipid vesicles in conjunction with ^1H -NMR and lanthanide shift ions such as Pr^{3+} and Dy^{3+} can be used to study a

number of different mechanisms of membrane permeability. These include :

- a. Channel formation at the bilayer phase transition, which causes vesicular lysis (see chapter 3).
- b. Carrier mediated transport by ionophores such as A23187, ionomycin and the bile salts (Hunt 1975, Hunt and Tipping 1978, Hunt and Jawaharlal 1980, Mirghani 1982).
- c. Channel mediated transport by ionophores such as alamethicin 30 and the bile salts (see chapter 3).
- d. Non bilayer phase mediated transport, for example in vesicles composed of a mixture of egg PC and CL in the presence of calcium ions (see chapter 3).

In the present study the effect of ethanol, diethyl ether and chloroform on such membrane events is investigated.

Experiments using Triton X100 have been included to extend the experimental conditions to study the effects of the three compounds on Triton-stabilized channels at the phase transition (see chapter 3) and also on vesicular fusion (Hunt 1980b, Alonso et al 1981). Polyethelene glycol (PEG) at high aqueous concentrations is known to promote cell fusion (Lucy 1978). Therefore, its fusion properties in lipid vesicles and the effect of the three anaesthetic compounds on this property is investigated. The effects of the anaesthetics on fusion induced by non bilayer phases (Mirghani 1982) in mixed lipid vesicles is also investigated. The investigation of such fusion processes by NMR has now been well established and in this study use is made of the line broadening methods developed by Prestegard and coworkers (Gent and Prestegard 1974, Liao and Prestegard 1980).

Until recently the trend has been to explain general anaesthesia in terms of hydrophobic effects such as bilayer fluidity or expansion

(see section 1.5). These lipid based theories have now been effectively criticised (Richards 1980, Franks and Leib 1982) and a number of studies reported in which hydrophilic effects such as H-bonding are implicated (Fink 1980). Such implications are further discussed later in this chapter.

Diazepam is a tranquilizing, psychotropic benzodiazepine which is mainly used as a antianxiety or sedative drug. It has also been used as a centrally acting muscle relaxant (Bowman and Rand 1980, chapter 8). Concern has arisen from the wide use of the benzodiazepines, especially since some experimental evidence suggests that the effects of the benzodiazepines are potentiated by ethanol (Gray 1978, MacLeod et al 1977, Seiax 1978) and may have cancer promoting properties (Horrobin 1979). Further a recent report states that brain damage, similar to that found in alcoholics, has been found in people who have taken diazepam for prolonged periods (Doyle 1982).

Diazepam action is thought to be synaptic with its action centred on synaptic receptor sites on the postsynaptic membrane (Bowman and Rand 1980). However the possible action on synapse-associated fusion and transmembrane channels can not be dismissed. To probe possible synergistic actions the joint effect of ethanol and diazepam on transmembrane channels produced at the phase transition and by alamethicin 30, is investigated.

4.2 Materials and Methods

4.2.1 Chemicals

Absolute ethanol (spectroscopic grade), AnalaR diethyl ether (sodium dried to remove water) and polyethylene glycol (M wt 400) were obtained from BDH chemicals, Poole, Dorset. The AnalaR chloroform used was purified by passing over alumina, to remove ethanol and water, distilled and restabilized by addition of 1 % AnalaR methanol. A23187 was a gift from the Lilly Research Centre, Windlesham, Surrey. A stock solution was prepared in chloroform (1 mg/ml) and stored in the dark at room temperature. The calcium ionophore, ionomycin, was obtained as the calcium salt from The Squibb Institute, Princeton, New Jersey. The free acid was obtained by extracting the calcium salt three times with a 2:1 (v/v) spectroscopic hexane / 4N HCl mixture. The stock solution was made up in hexane (10 mg / 25 ml) and was stored at -5°C. Diazepam was obtained from Hoffman La Roche. A stock solution was prepared in chloroform (1 mg/ml) and stored at -5°C.

4.2.2 Incubations with phospholipid vesicles

A23187 was introduced by pipetting a known volume of chloroform stock solution into an empty NMR tube and the solvent removed using a jet of nitrogen, followed by evacuation for 20 minutes at 2 mm Hg. 1 ml of vesicular solution was then added to the NMR tube & incubated at 50°C with occasional shaking using a vortex mixer. Ionomycin from the hexane stock was introduced in a similar manner. Alamethicin was introduced and incubated as previously described in chapter 3 (see section 3.2.3).

For the samples containing ethanol or the anaesthetics, a known volume was added to the vesicular solution and coincubated with the ionophore in capped NMR tubes for 1 hr at 50°C before the addition of

Pr³⁺ stock solution.

For the phase transition - lysis samples (including those used for the T₂ measurements) the general anaesthetics were incubated with either vesicles and Pr³⁺ or vesicles, Triton X100 and Pr³⁺ for 1 hr before performing the experiment. Fusion studies with Triton X100 and PEG were performed at 60°C. Experiments were initiated by adding a known volume of stock Triton X100 solution or neat PEG to a vesicular solution containing Pr³⁺. For samples containing the general anaesthetics, they were incubated with the vesicles for 1 hr before performing the experiment.

Diazepam was introduced to the vesicles in a similar fashion as described above for A23187. For the phase transition - lysis studies diazepam was incubated with the vesicles and Pr³⁺ at 50°C for one hour. For the effects of diazepam on alamethicin, it was incubated with the vesicles and alamethicin for one hr at 50°C. In both these sets of experiments, the general anaesthetics were coincubated with the diazepam or with alamethicin and diazepam for one hour at 50°C before the addition of Pr³⁺.

In the bile salt studies the vesicles were incubated with Pr³⁺ and general anaesthetic for one hour at 50°C before the addition of bile salt. For the mixed lipid studies the vesicles were incubated with general anaesthetic for one hour before the addition of Dy³⁺ or Dy³⁺ and Ca²⁺.

4.2.3 Analysis of vesicular fusion

Fusion of vesicles is followed by monitoring the increase of the line width of the acyl chain hydrocarbon signal, H. Increase in this signal width results from the decrease in the tumbling rate of the

larger vesicles produced by fusion, with a consequent loss of averaging of the dipolar relaxation which contributes to the line width. Prestegard and coworkers have shown that the line width increases linearly with vesicle radius and that for 1:1 vesicle fusion (during which the radius of all the vesicles will increase by a factor of $2^{1/2}$) the line width of the hydrocarbon signal, H, increases by a factor of 1.57 (Liao and Prestegard 1980, Gent and Prestegard 1974). Hence from the peak width values the proportion of the vesicles which have undergone 1:1 fusion can be calculated (see appendix A).

4.3 Experimental Results

4.3.1 The effect of the general anaesthetics on the ^1H -NMR spectrum and phase transition of DPPC vesicles

Up to concentrations of 100 mM, ethanol and diethyl ether have negligible effects on the chemical shifts of the ^1H -NMR signals obtained from DPPC vesicles. Chloroform, however causes a marked upfield shift of the outer head group signal O towards signal I (Table 4.1a). The change is approximately linear with concentration and is 30 % at 100 mM chloroform. All three compounds decrease the line width of the head groups and the acyl chain signals and also affects the T_1 values of these signals. A summary of the results for chloroform and ethanol are shown in Table 4.1b. Again chloroform has the most marked effect.

The widths at half height ($\nu_{1/2}$) of the hydrocarbon signal, H, were measured in Hz over a range of temperatures spanning T_c in the absence (control) and presence of anaesthetic. $\nu_{1/2}$ values were converted to spin-spin relaxation times, T_2^* , using the relationship $T_2^* = 1/\pi\nu_{1/2}$. Fig 4.1 shows the effect of anaesthetics on T_2^* and on T_c . In each case the T_2^* are increased by the presence of all three compounds at temperatures above the phase transition (also shown by the $\nu_{1/2}$ values in Table 4.1b). For pure DPPC vesicles (control) the phase transition can be seen to extend from approximately 41°C to 35°C. The onset of the gel to liquid crystal phase transition (indicated by dotted lines in Fig 4.1) is significantly lowered by all three anaesthetics, with chloroform having the greatest effect on a molar basis. It was important to determine the extent of the range of the phase transition in the presence of anaesthetic, so as to ensure that the temperature ranges used in the subsequent lysis experiments were sufficient to span

Table 4.1

a. Effects of various chloroform concentrations on the chemical shift of the outside choline signals of DPPC vesicles (with 5mM Pr³⁺) at 50°C

Chloroform Concentration mM	Chemical Shift (I as reference) Hz
0	16.0
25	14.0
61	12.0
86	11.4
123	10.5

b. Effects of various chloroform and ethanol concentrations on the peak widths and spin lattice relaxation times of signals I, O and H

Chloroform concentration mM	$\nu_{1/2}$ Hz			T_1 seconds		
	O	I	H	O	I	H
0	4.0	4.5	13.0	0.43	0.34	0.30
25	3.7	4.2	13.0	0.45	0.35	0.31
61	3.2	4.1	12.5	0.48	0.38	0.35
86	3.0	3.9	12.3	0.51	0.41	0.39
123	2.8	3.7	12.0	0.53	0.46	0.43

Ethanol concentration
mM

0	4.0	4.5	13.0	0.43	0.34	0.30
43	4.0	4.5	13.0	0.44	0.33	0.31
86	3.9	4.5	12.8	0.45	0.31	0.32
172	3.9	4.5	12.7	0.46	0.34	0.32
430	3.6	4.3	12.6	0.49	0.32	0.34
860	3.5	4.3	12.4	0.48	0.34	0.35

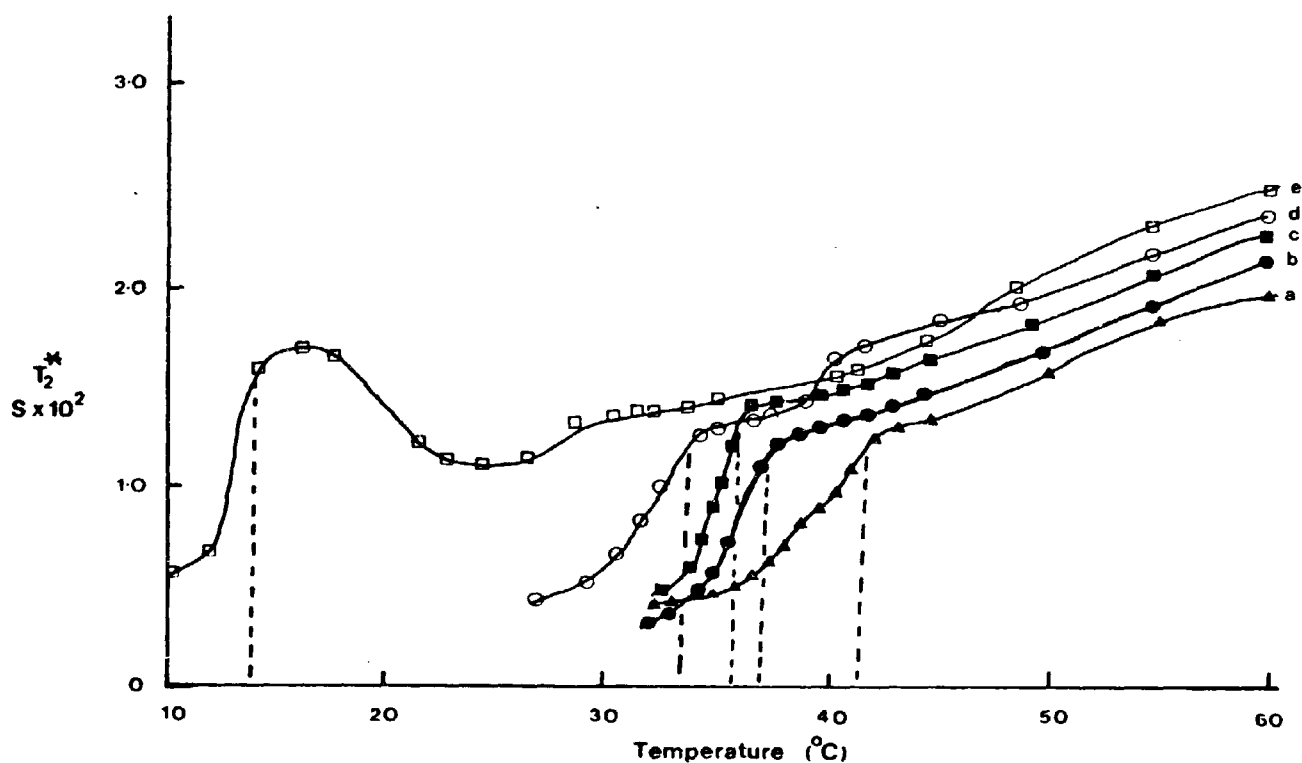


Fig 4.1 The temperature dependence of the spin spin relaxation time (T_2^*) for the acyl chain signal from DPPC vesicles.
a. Control vesicles in the presence of: b. 86 mM ethanol,
c. 86 mM diethyl ether, d. 25 mM chloroform,
e. 86 mM chloroform.
Dotted lines indicate the onset of the liquid-crystal to gel phase transition.

this phase change.

4.3.2 Effects of the general anaesthetics on vesicular lysis induced at the phase transition

Fig 4.2 shows a plot of the % lysis against time, when a series of cycles through the phase transition are used, separated by incubation periods at 60°C (see section 3.3.2). In each case the vesicles are seen to be impermeable to Pr^{3+} ions during the incubation periods at 60°C but on passing through the phase transition (three cycles in one hour) the % of lysed vesicles has increased. Fig 4.2 plainly shows that the effect of ethanol and diethyl ether is to increase the lysis, whilst that of chloroform is to decrease the % of vesicles that lyse during each cycle. The temperature range used for the cycles through the phase transition was such as to ensure passage into the gel and liquid crystal phases as judged by the effects of the anaesthetics on the range of the phase transition as shown in Fig 4.1. During the lytic processes the peak width of the hydrocarbon signal was monitored. Variations of only a few Hz were observed, indicating no appreciable fusion of vesicles occurs during the duration of the experiment.

Fig 4.3 shows the effect of anaesthetic on lysis produced by cycling vesicles, in the presence of Triton X100, through the phase transition. The results are similar to those shown in Fig 4.2 with chloroform strongly inhibiting the lysis even in the presence of Triton X100.

The spectra recorded for these experiments with Triton X100 showed a broadening of the hydrocarbon signal and the signal width was measured in order to estimate the degree of vesicle fusion (see appendix A). Increase values of $\nu_{1/2}$ at the end of the experiment shown in Fig

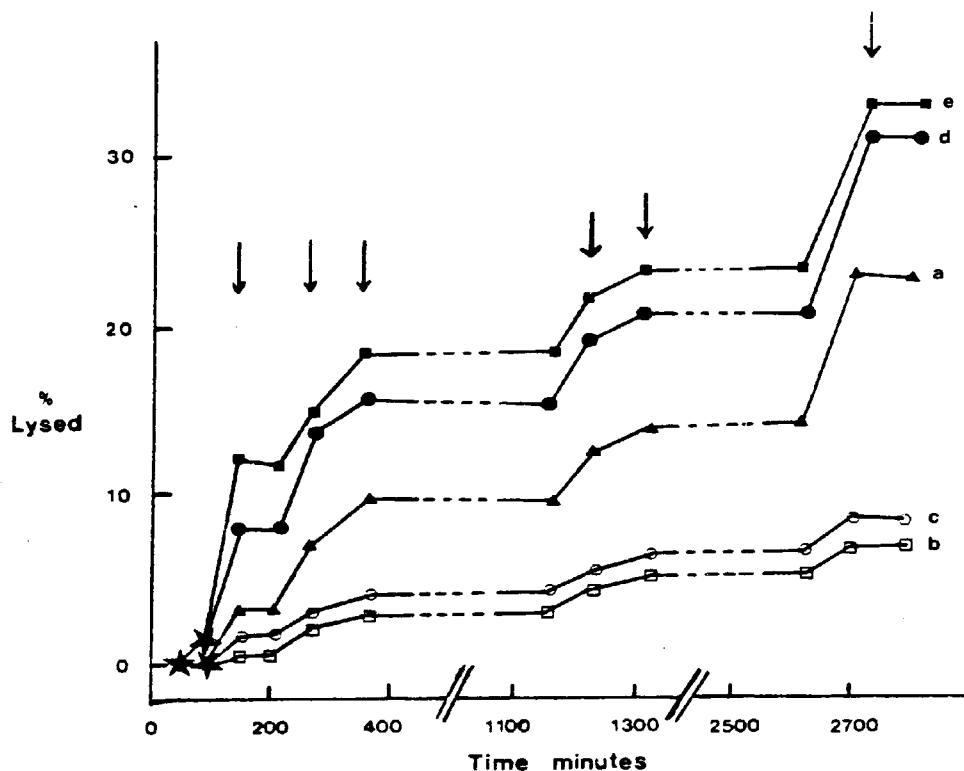


Fig 4.2

The effects of ethanol, diethyl ether and chloroform on lysis of DPPC vesicles caused by cycling the vesicles through the phase transition. * indicates spectra taken during the initial incubation period. Arrows + indicate the times at which spectra were recorded at 60°C after three cycles through the phase transition. Other points indicate the times at which spectra were recorded at 60°C after an incubation period at 60°C.

a. Control vesicles in the presence of: b. 86 mM chloroform, c. 25 mM chloroform, d. 86 mM ethanol, e. 86 mM diethyl ether.

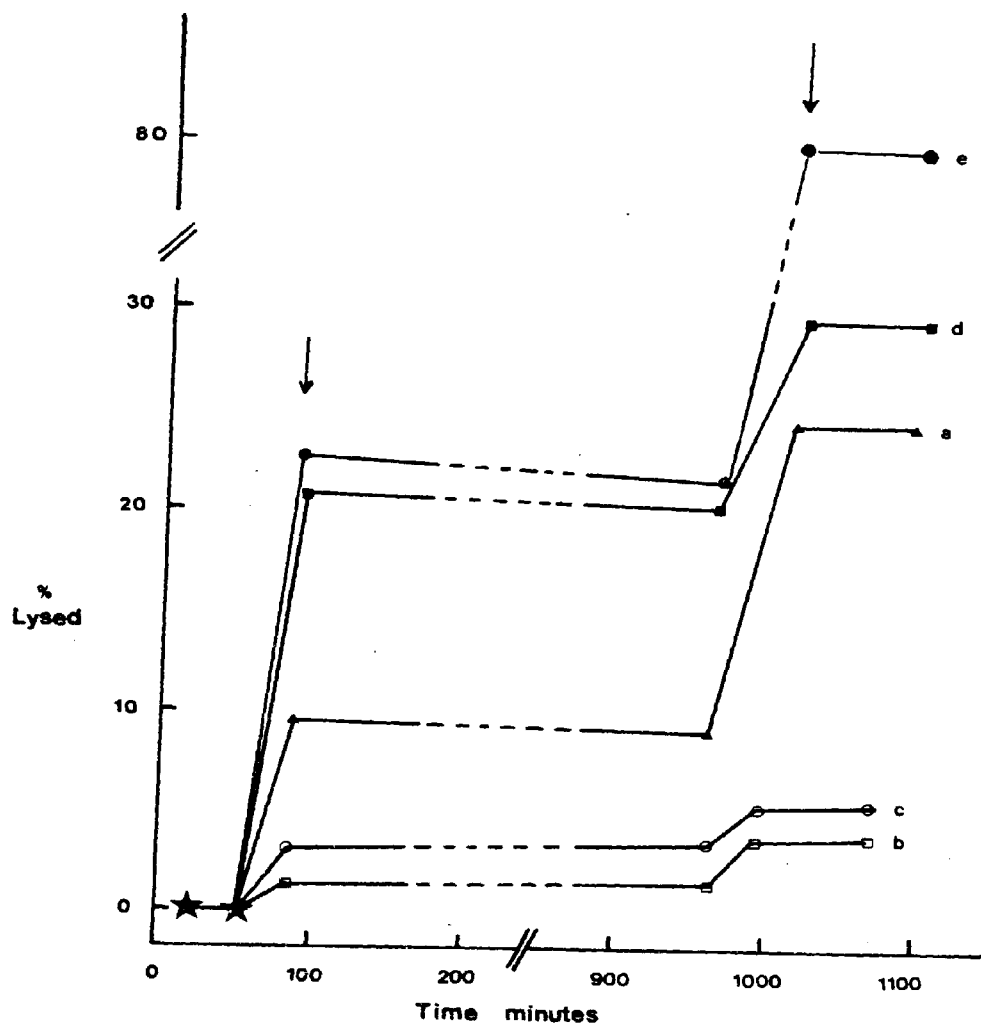


Fig 4.3 The effects of ethanol, diethyl ether and chloroform on lysis of DPPC vesicles in the presence of 0.1 mM Triton X100, through the phase transition. Conditions are identical to those used in Fig 3.19 (Triton X100 sample).
a. Control. Vesicles in the presence of: b. 86 mM chloroform,
c. 25 mM chloroform, d. 86 mM diethyl ether, e. 86 mM ethanol.

4.3 were: Control, 17 to 24 Hz; diethyl ether, 15 to 25 Hz; ethanol 18 to 28 Hz; chloroform (86mM), 14.4 to 17.4 Hz, corresponding to % fusion values of 75%, 100%, 100% and 35% respectively. Thus chloroform has the effect of inhibiting both lysis and fusion promoted by the presence of Triton X100. The effects of the anaesthetics on fusion induced by Triton X100, PEG and mixed lipids are described later in this chapter (section 4.3.5).

It should be noted that the fusion process is limited to a 1:1 vesicle fusion since no loss of the ^1H -NMR signal results. Also the 1:1 fusion has only a small effect on the O:I ratio. It can readily be calculated that when vesicles having a bilayer thickness of 4 nm increase in radius from 14 nm to $14 \times 2^{1/2}$ nm the O : I signal ratio will decrease from 1.7 to 1.57. Thus the 75 % fusion produced in the control sample of vesicles would cause a decrease in the O:I ratio from 1.7 to about 1.6. In contrast a 75 % lysis of vesicles would increase the O:I ratio from 1.7 to 9.8. The changes in the O:I ratio used to calculate the % lysis in Fig 4.3 are then almost entirely due to the lytic effect of Triton X100 at the phase transition and hardly effected by the limited fusion occurring.

4.3.3 The effect of the general anaesthetics on channel mediated transport by alamethicin 30 and on carrier-mediated transport by A23187 and ionomycin

Fig 4.4 shows the effects of various concentrations of ethanol, diethyl ether and chloroform on the rate of transport mediated by alamethicin in DPPC vesicles at 50°C. Chloroform strongly inhibits the rate of transport, the effect being marked down to the lowest concentration studied (5 mM). The action of ethanol and diethyl ether

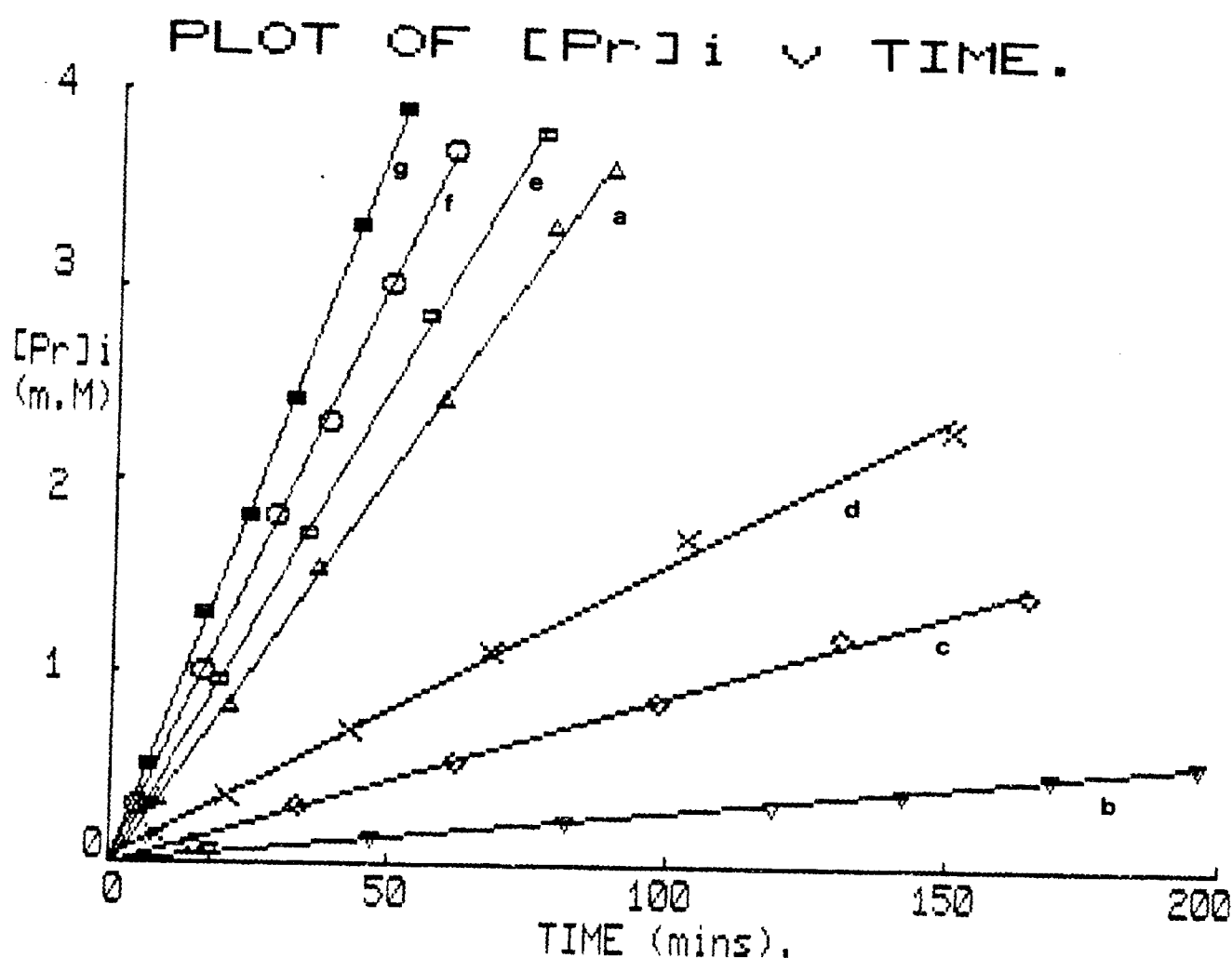


Fig 4.4 Effect of various concentrations of general anaesthetics on the alamethicin (20 $\mu\text{g/ml}$) transport rate in DPPC vesicles at 50°C.

a. Control. Vesicles in the presence of: b. 86 mM chloroform, c. 25 mM chloroform, d. 5 mM chloroform, e. 86 mM diethyl ether, f. 86 mM ethanol, g. 172 mM ethanol.

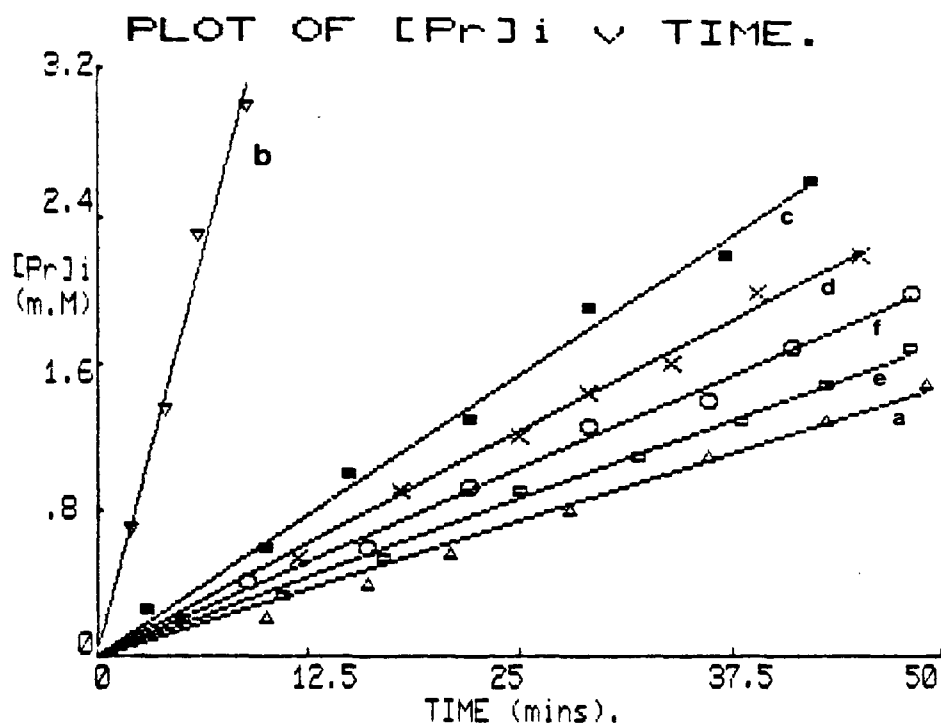
are seen to be similar to their effects on vesicle lysis in that channels are again stabilized to allow an increase in the transport rate of Pr^{3+} . Similar effects of the general anaesthetics on alamethicin transport were also obtained when alamethicin was presented to both surfaces of the bilayer or sonicated in the bilayer (results not shown). The effect on alamethicin transport in egg PC vesicles also follow the same trend (results not shown).

Fig 4.5 (i) and (ii) show the effects of various concentrations of the general anaesthetics on carrier transport mediated by the ionophores A23187 (10 $\mu\text{g/ml}$) and ionomycin (10 $\mu\text{g/ml}$) in DPPC vesicles at 50°C. A similar trend is seen in both results, in that all three general anaesthetics potentiate the transport rate, with chloroform having the greatest effect on a molar basis. In these results it is significant that chloroform increases the transport rate in contrast to its effect on the channel mediated mechanism.

4.3.4 The effect of ethanol and chloroform on the activity of bile salts in egg PC vesicles

The effect of various concentrations of chloroform and ethanol on the transport and lytic rates obtained with glycocholate (1.25 and 1.5 mM) at 50°C are shown in Fig 4.6. Similar effects were observed with the transport and lytic rates induced by glycodeoxycholate (results not shown). For both bile salts the effect of ethanol is to potentiate both the transport and lytic rates, whilst chloroform inhibits both these processes. It is apparent that the effect of chloroform on the bile salt transport rate conflict with the results obtained with A23187 and ionomycin. However the molecular mechanism involved in transport via the bile salts (inverted micelles) differ from that proposed for A23187 and

(i)



(ii)

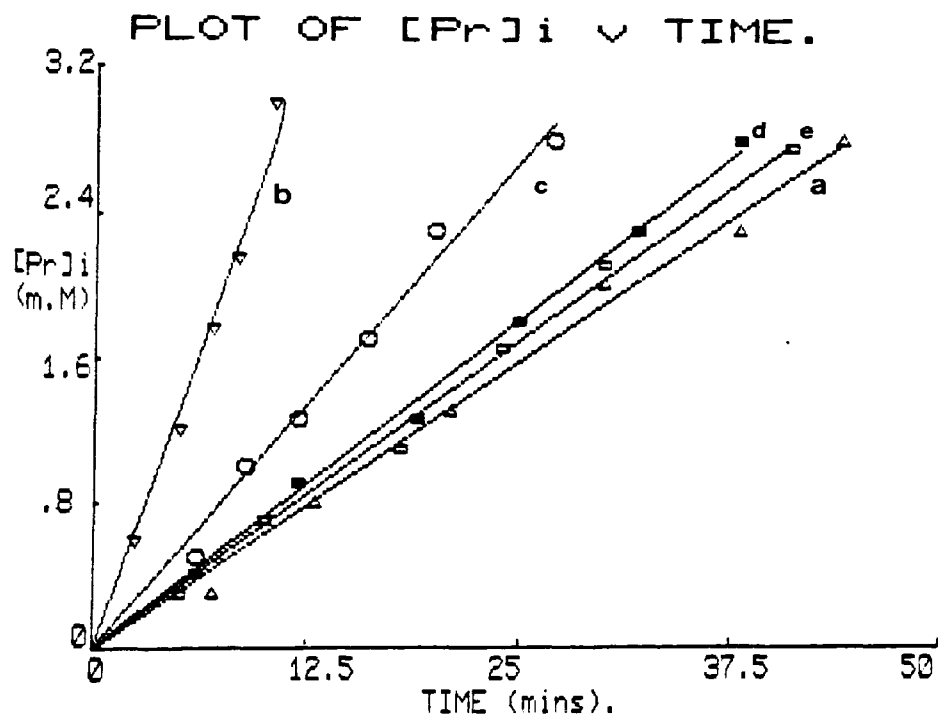


Fig 4.5 Effect of various concentrations of the general anaesthetics on carrier mediated Pr^{3+} transport in DPPC vesicles at $50^\circ C$.

(i) A23187, (ii) Ionomycin

a. Control. Vesicles in the presence of: b. 86 mM chloroform, c. 25 mM chloroform, d. 86 mM diethyl ether, e. 86 mM ethanol, f. 172 mM ethanol.

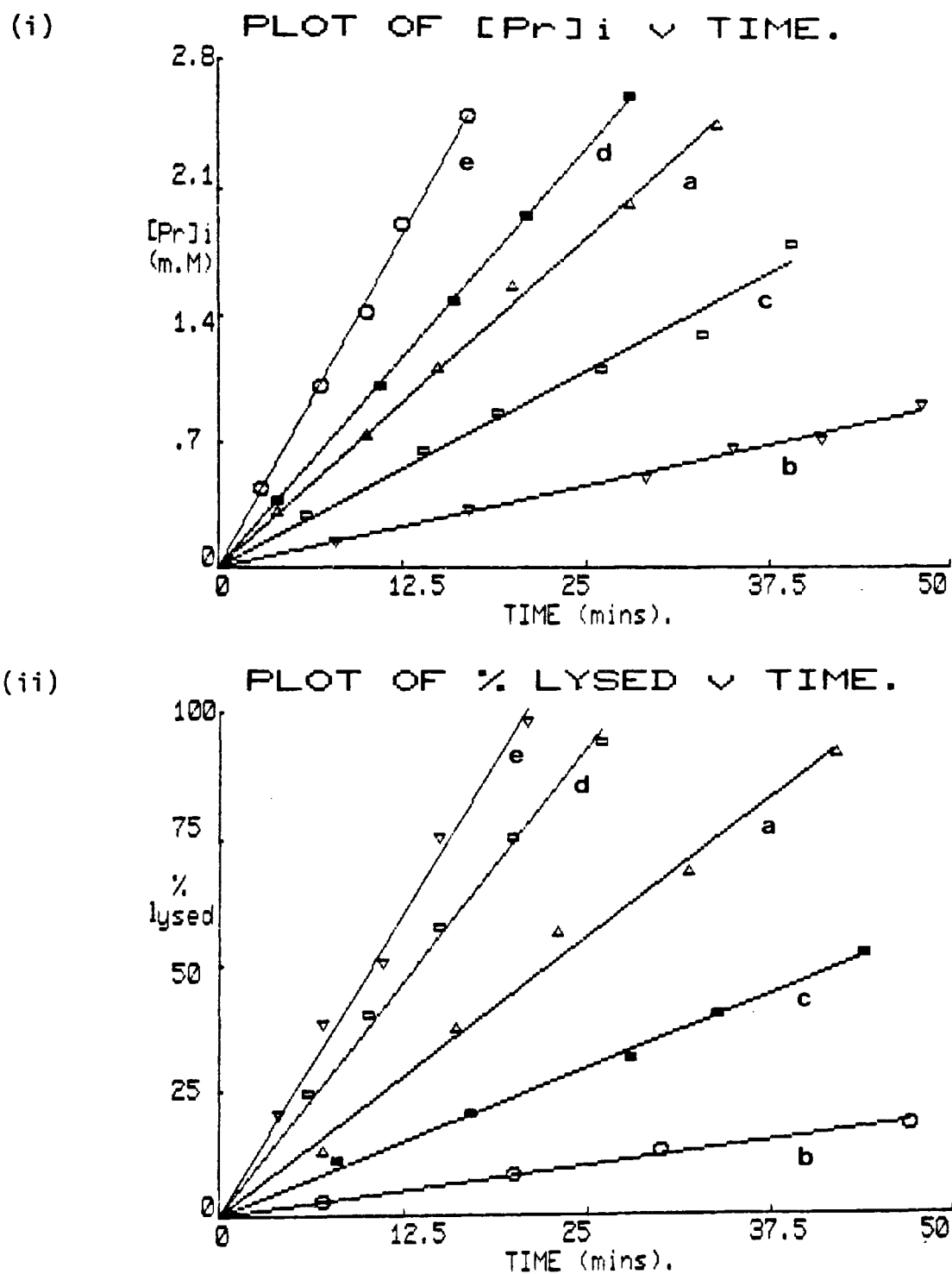


Fig 4.6 Effects of various concentrations of the ethanol and chloroform on: (i) glycocholate (1.25 mM) mediated transport of Pr^{3+} in DPPC vesicles at $50^{\circ}C$; (ii) rate of lysis by glococholate (1.5 mM) in DPPC vesicles at $50^{\circ}C$.

a. Control. Vesicles in the presence of: b. 86 mM chloroform,
c. 61 mM chloroform, d. 86 mM ethanol, e. 172 mM ethanol.

ionomycin (see section 1.3.1). It is with respect to these factors that the above results with the bile salts will be discussed below.

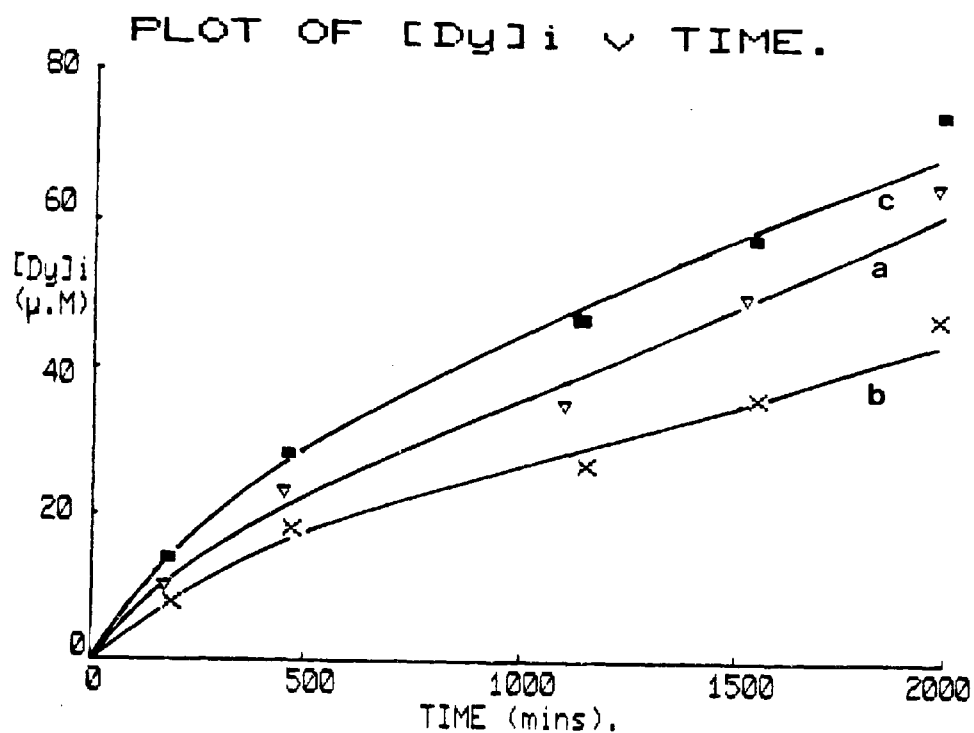
4.3.5 The effects of the general anaesthetics on transport and fusion in mixed lipid vesicles and on chemically induced fusion of DPPC vesicles

Fig 4.7(i) shows the effects of ethanol (86 mM) and chloroform (25 mM) on the non bilayer phase transport (as previously described in sections 1.6 and 3.3.1.3) of Dy^{3+} into egg PC / 40 mole % PE vesicles at 50°C. It can be seen that ethanol slightly potentiates the rate whilst chloroform has an inhibitory effect. Broadening of the hydrocarbon signal occurred during the transport process, indicating that vesicular fusion was taking place. Fig 4.7(ii) shows the effects of ethanol and chloroform on the rate of fusion. The rate is potentiated by ethanol and inhibited by chloroform, and therefore are similar to their effects on Dy^{3+} transport.

Fig 4.8 shows that the same effects of ethanol and chloroform are obtained with transport and fusion in egg PC / 10 mole % CL at 50°C. However in this case Ca^{2+} (2 mM) was required to induce the non bilayer phase involved in mediating the fusion and transport processes (see section 1.4).

Fig 4.9(i) shows the effect of equimolar (86 mM) ethanol, diethyl ether and chloroform on the rate of DPPC vesicle fusion (at 60°C) induced by Triton X100 (0.9 mM). Ethanol and diethyl ether here again are seen to potentiate the formation of inverted micelles involved in mediating the fusion process. Similar results are obtained with PEG although 650 mM was required to induce significant fusion (Fig 4.9 ii).

(i)



(ii)

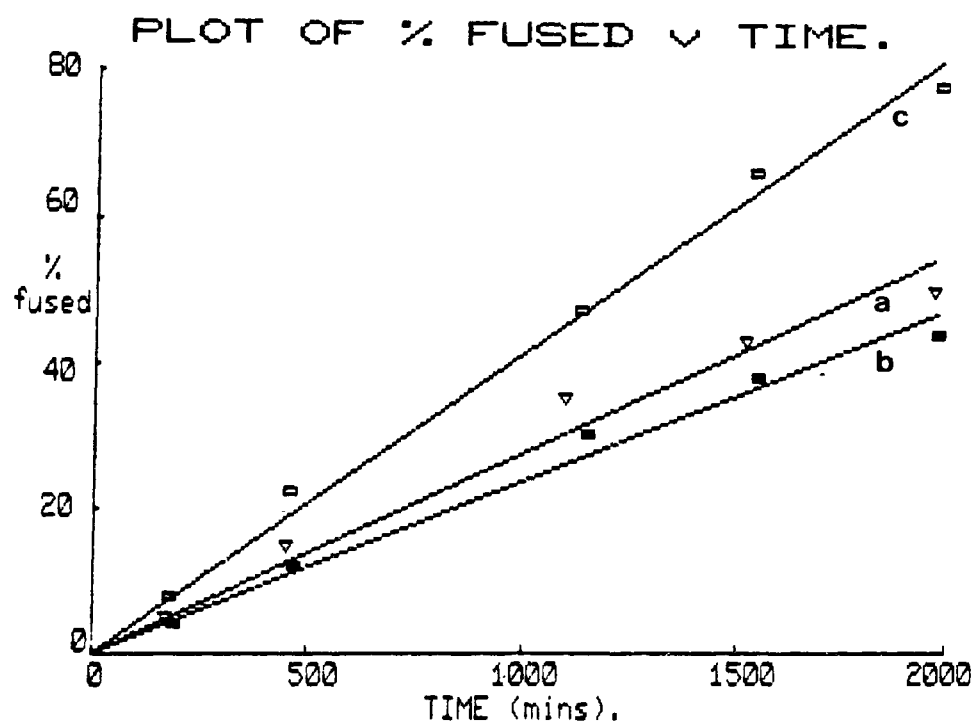


Fig 4.7 Effect of ethanol and chloroform on:
(i) non-bilayer phase mediated transport of Dy^{3+} in egg PC/40 mole % PE vesicles at $50^\circ C$;
(ii) fusion of egg PC/40 mole % PE vesicles at $50^\circ C$.
a. Control. Vesicles in the presence of: b. 25 mM chloroform, c. 86 mM ethanol.

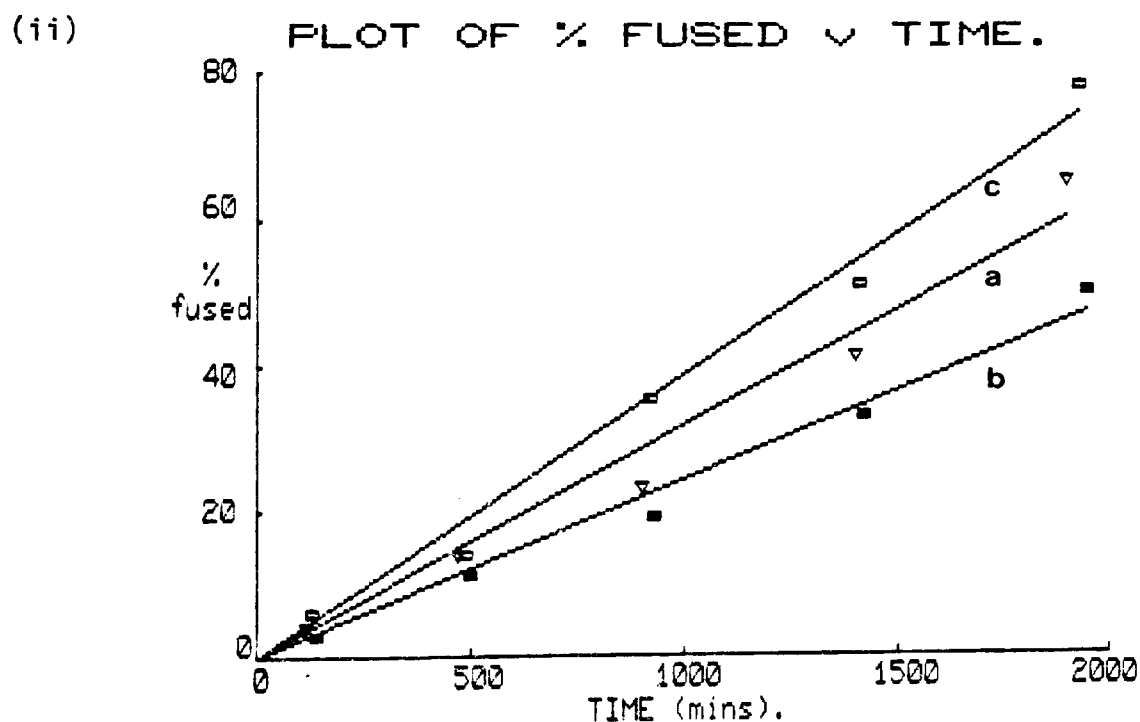
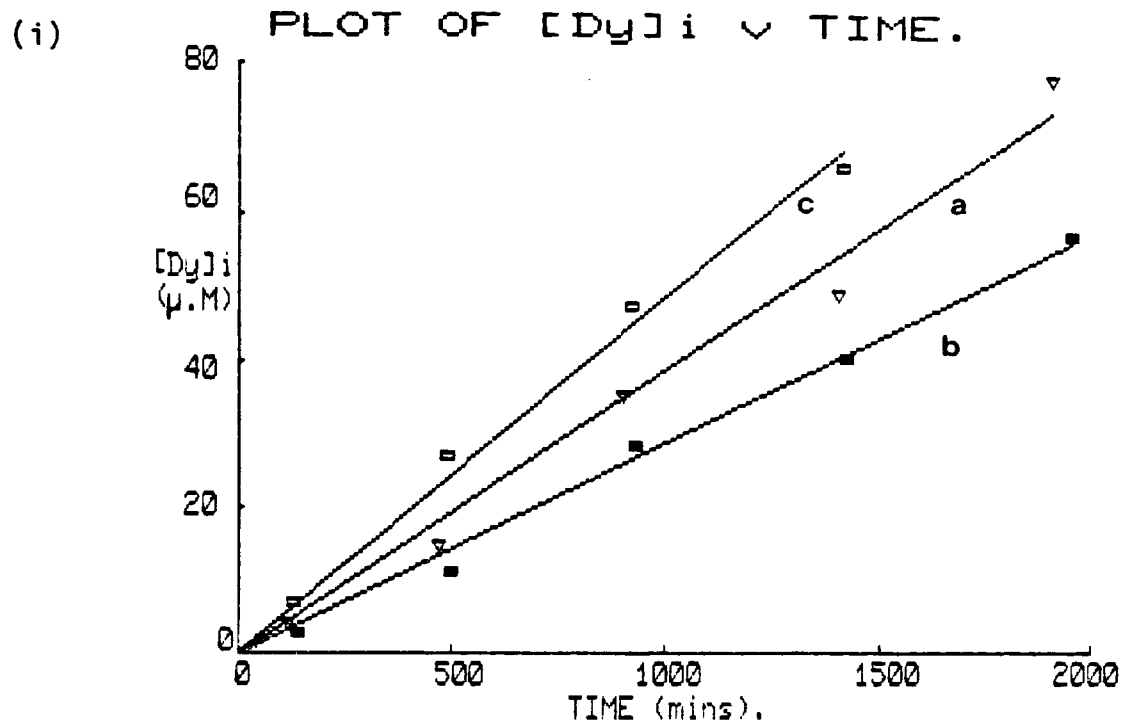
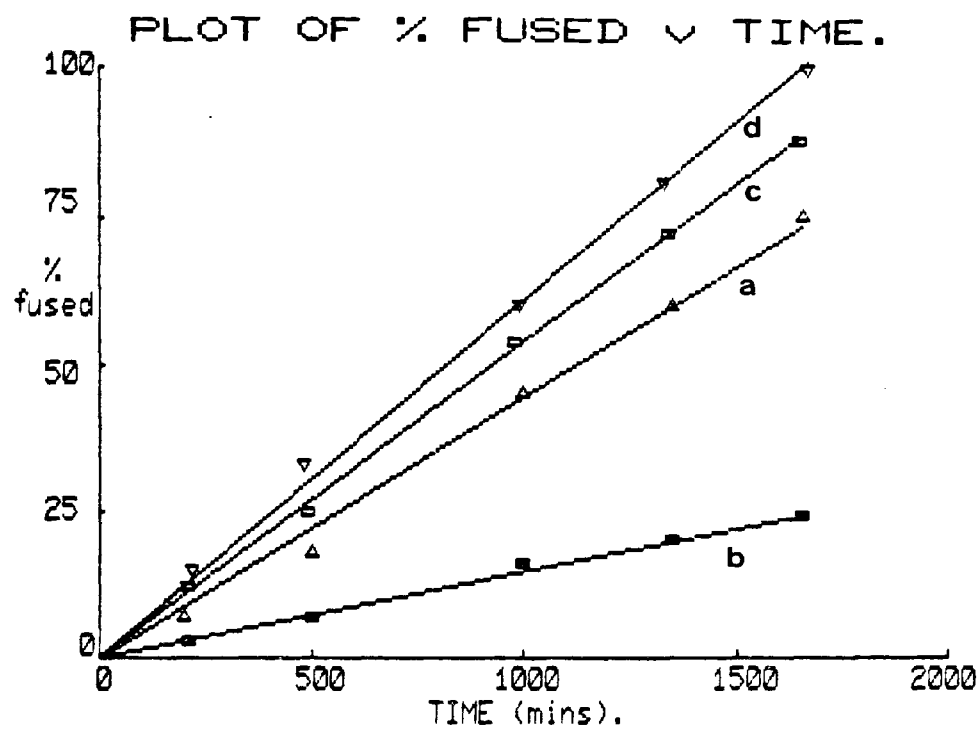


Fig 4.8 Effect of ethanol and chloroform on: (i) non-bilayer phase mediated transport of Dy^{3+} in egg PC/10 mole % CL vesicles with 2 mM Ca^{2+} at $50^\circ C$; (ii) fusion of egg PC/10 mole % CL vesicles with 2 mM Ca^{2+} at $50^\circ C$.
a. Control. Vesicles in the presence of: b. 25 mM chloroform, c. 86 mM ethanol.

(i)



(ii)

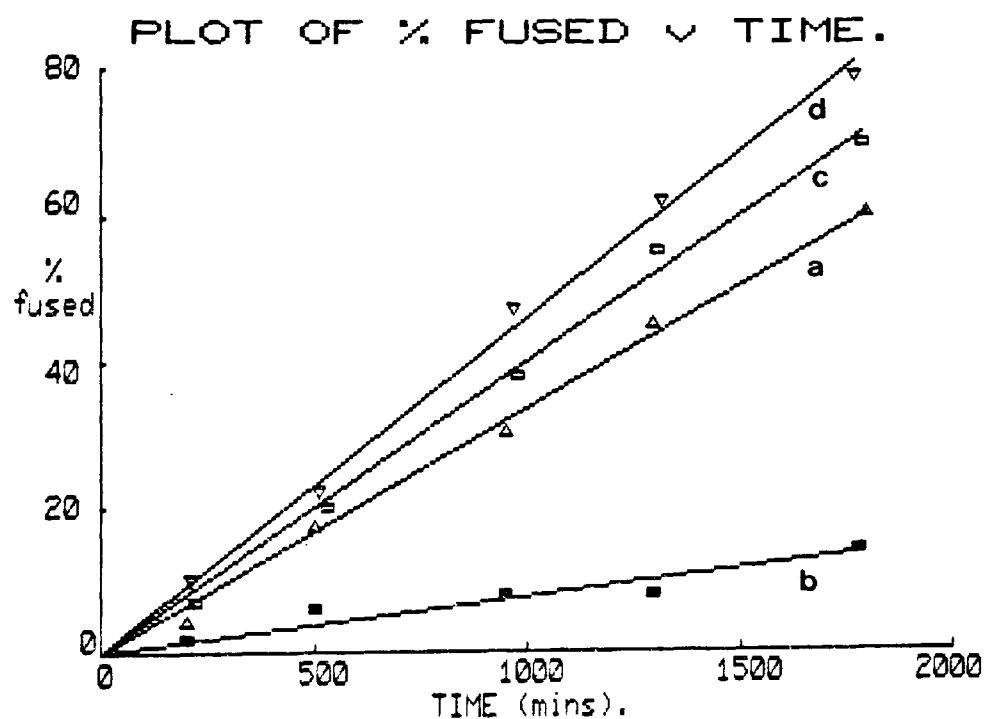


Fig 4.9 Effect of the general anaesthetics on fusion in DPPC vesicles at 60°C. Fusion induced by: (i) 0.9 mM Triton X100; (ii) 650 mM PEG (400).
a. Control. Vesicles in the presenece of: b. 86 mM chloroform, c. 86 mM diethyl ether, d. 86 mM ethanol.

4.3.6 Effects of diazepam on alamethicin 30 channels and on permeability induced at the phase transition in DPPC vesicles

Cycling DPPC vesicles through the phase transition in the presence of Pr^{3+} and 0.35 or 0.875 mM diazepam (100 or 250 $\mu\text{g/ml}$) shows no extra effect on the degree of lysis than that obtained by the control (DPPC vesicles with no diazepam in Fig 4.10). However in the presence of 86 mM ethanol and varying concentrations of diazepam, potentiation in the degree of lysis is seen. Fig 4.10 shows that the degree of lysis potentiation is dependent on the diazepam concentration.

Incubating diazepam (up to 0.875 mM) with DPPC vesicles and Pr^{3+} , shows that it possesses no ionophoric properties of its own (results not shown). However Fig 4.11(i) shows that diazepam has a profound effect on the alamethicin transport rate. In the presence of 0.35 mM or 0.875 mM diazepam the alamethicin control rate, 0.033 mM/min, is increased to 0.055 mM/min and 0.086 mM/min respectively (Table 4.2), suggesting that diazepam is stabilizing the alamethicin channels. When 86 mM ethanol is also present further potentiation is also observed with the resulting rates (0.111 and 0.193 mM/min) being greater than the sum of the respective control rates (Table 4.2).

Fig 4.11(ii) shows the effect of varying the ethanol concentration on the rate obtained from alamethicin (20 $\mu\text{g/ml}$) and diazepam (100 $\mu\text{g/ml}$). In contrast to the effect of 86 mM ethanol (as above), at lower ethanol concentrations (34 and 17mM) the resulting rates (0.064 and 0.077 mM/min) are not greater than the sum of the respective control rates.

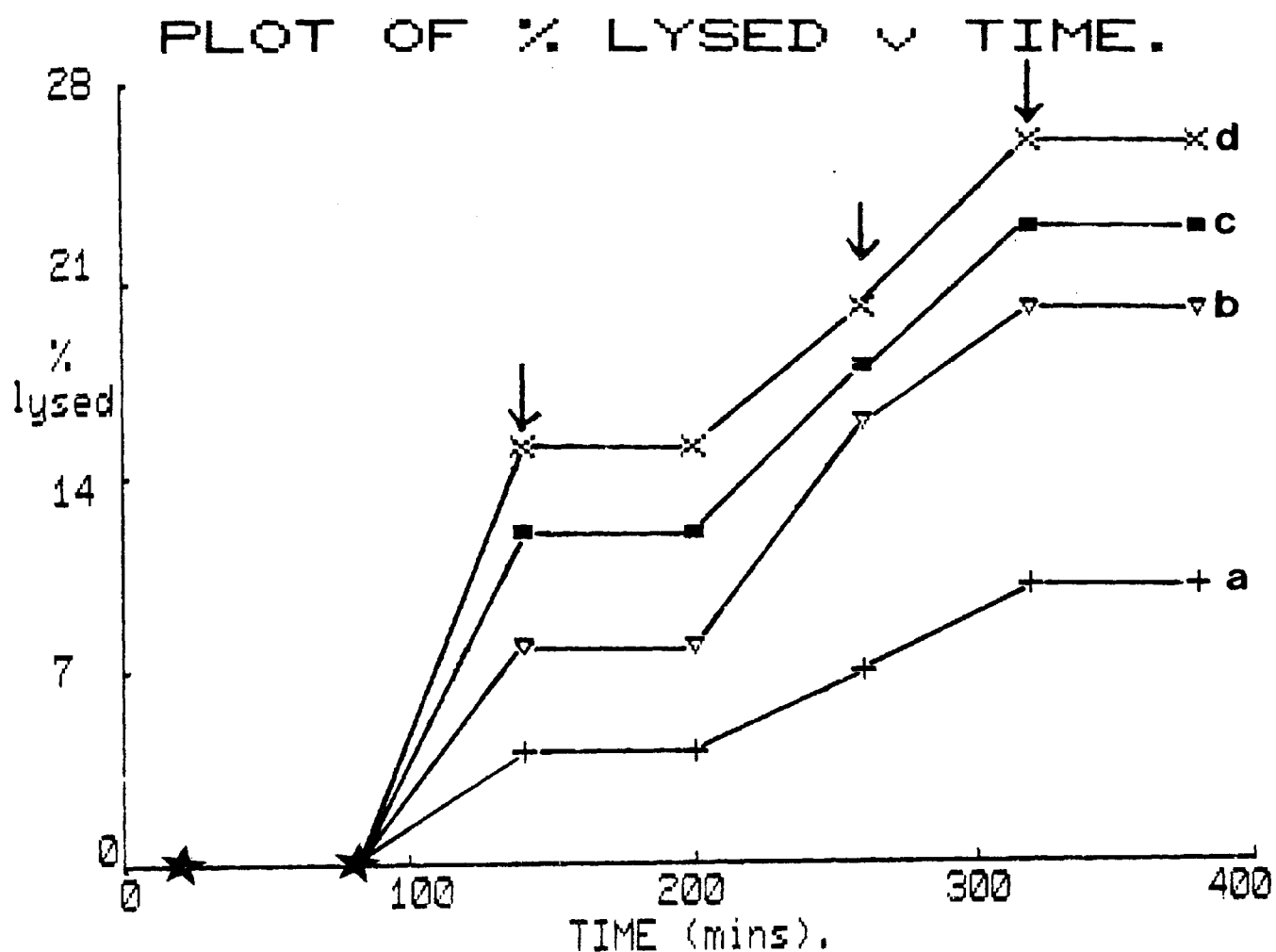
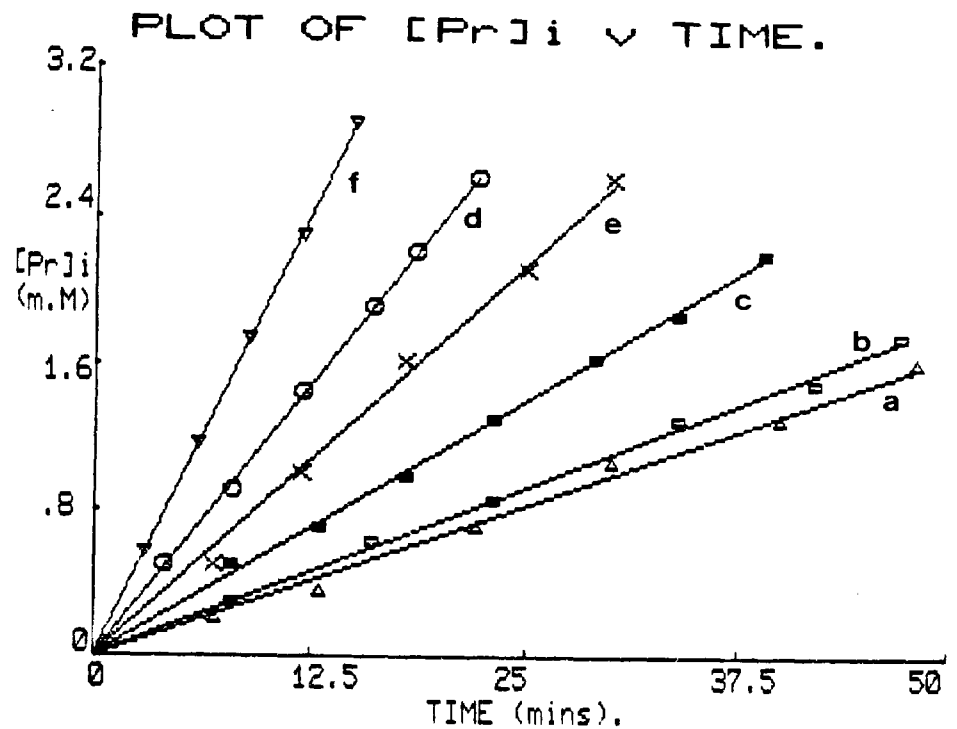


Fig 4.10 Effects of diazepam and ethanol on lysis of DPPC vesicles caused by cycling the vesicles through the phase transition. * and + see Fig 4.2.

a. Control and also vesicles in the presence of 0.35 mM and 0.875 mM diazepam. Vesicles in the presence of: b. 86 mM ethanol, c. 86 mM ethanol and 0.35 mM diazepam, d. 86 mM ethanol and 0.875 mM diazepam.

(i)



(ii)

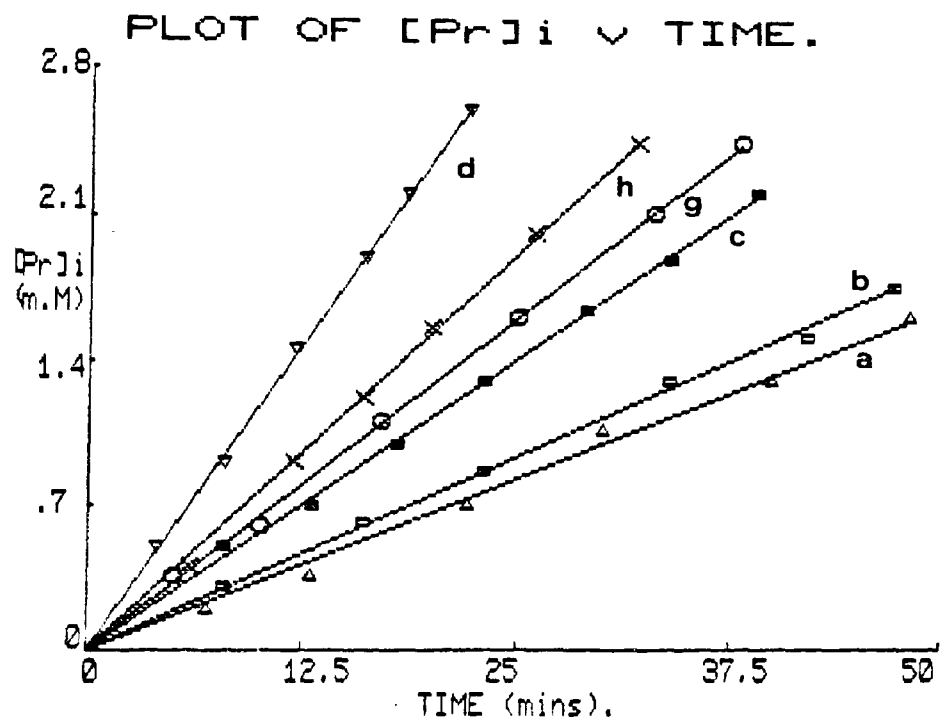


Fig 4.11 Effect of various concentrations of ethanol and diazepam on the rate of Pr^{3+} transport by alamethicin in DPPC vesicles at $50^{\circ}C$.

(i) Varying concentrations of diazepam with a constant ethanol concentration.

(ii) Varying concentrations of ethanol with a constant diazepam concentration.

a. Control. Vesicles in the presence of: b. 86 mM ethanol,
c. 0.35 mM diazepam, d. 86 mM ethanol and 0.35 mM diazepam,
e. 0.875 mM diazepam, f. 86 mM ethanol and 0.875 mM diazepam,
g. 17 mM ethanol and 0.35 mM diazepam, h. 34 mM ethanol and
0.35 mM diazepam.

Table 4.2

The effect of various concentrations of ethanol and diazepam on the
alamethicin transport rate in DPPC vesicles at 50°C

DIAZEPAM CONCENTRATION mM	ETHANOL CONCENTRATION mM			
	0	17	34	86
0.0	0.033	0.034	0.035	0.037
0.35	0.055	0.064 (0.72)	0.077 (0.86)	0.119 (1.30)
0.875	0.086	-	-	0.193 (1.60)

Figures in brackets represent the factors by which the rate obtained by the joint effect of ethanol and diazepam is greater than the rate obtained by the sum of their individual action.

4.4 Discussion

The observation that chloroform decreases the line width of the lipid signals (Table 4.1b) agrees with previous studies by Shieh and coworkers (1975, 1976) (Yakono et al 1981) and Vanderkooi and coworkers (1977), and the implication is that the anaesthetic fluidises the bilayer. Both ethanol and chloroform are seen to induce a greater decrease in the line width in the outer choline groups than in the line width of the hydrocarbon signal. This is in agreement with the results obtained by Yokono et al (1981) who found that a two fold greater concentration of anaesthetic was required to induce the phase transition when partitioned preferentially into the hydrocarbon region than when partitioned preferentially into the head group region. These results suggest that the action of these anaesthetics is primarily in the interfacial (head group) region.

The lowering of the phase transition temperature has previously been observed for all three anaesthetics as well as for other fluorinated ether anaesthetics, with the effect being ascribed to the disordering of the acyl chains (Vanderkooi et al 1977, Koehler et al 1978, Rosenberg 1980, Rowe 1982, 1983). The phase transition width is not increased by the presence of the three anaesthetic compounds (Fig 4.1) indicating that the cooperativity of the transition (see chapter 2) is not decreased. This observation is consistent with the results of Rowe (1981, 1982) but disagrees with Mountcastle and coworkers (1978) who proposed that anaesthetic action causes a reduction in transition cooperativity which has an effect on protein function.

The observed upfield shift in the outer head group signal 0 (Table 4.1a) implies that there is sufficient chloroform in the bilayer - water boundary region to influence the binding of Pr^{3+} ions to the

phosphate sites on the outer head groups of the vesicles. A similar deduction was made by Koehler et al (1977) who observed that Gd^{3+} caused changes in the line width of the ^{19}F -NMR signal from halothane only in the presence of PC liposomes. These experiments indicate that anaesthetic and lanthanide ion coexist at the membrane surface.

The observation that ethanol and diethyl ether both increase the extent of lysis at the phase transition, whilst chloroform decreases the lysis (Fig 4.2), may result from a change in the activation energy for the opening of the channels, thus resulting in more or less channels being opened per phase transition cycle. A number of authors have implicated the modification of the energy barrier to ionic permeability with water penetration and interaction with lipid bilayers (Kenehisa and Tsong 1978, Griffith et al 1974, Israelachvili et al 1980). Also in the case of gel areas being dispersed in the fluid phase, the boundary effect (see chapter 3) will induce increased water penetration into the hydrocarbon region of the bilayer (Fettiplace and Haydon 1980). A reasonable hypothesis consistent with the above observations would be that the effect of the three anaesthetic compounds on vesicular lysis is mediated by their action on the structure or properties of water associated with channels or with the polar head groups (water of hydration).

The effects of the anaesthetics are even more marked for Triton stabilized channels (Fig 4.3) than for Triton free channels (Fig 4.2). Again the striking feature is increased lysis by the oxygen containing compounds and decreased lysis by chloroform. Triton X100 is strongly hydrated in solution and therefore the channels at T_c will be lined by this amphipathic molecule so introducing an additional water content to

the channel. The strong effect of ethanol, diethyl ether and chloroform on these channels again implies that their interaction with the channel water is significant in determining their action on lytic channels. Similar effects to the anaesthetics are observed by their action on vesicular lysis caused by bile salt channels (Fig 4.6 ii). In this case the channel interior is lined by bile salt hydroxyl groups which are therefore available for H-bonding with the channel water. The effects of the anaesthetics on these interactions may therefore be significant in determining their action.

Studies with alamethicin (Latorre et al 1981, Fox and Richards 1982), including those described in chapter 3, indicate that in the oligomeric channel, H-bonding is extensive especially at the annulus formed at Gln 7 residues (see Fig 3.1). The Gln 7 side chain amide protons will donate a hydrogen bond to water forming a ring of hydrogen bonded water, the structure of which effectively controls the size of the channel. Changes in this hydrogen bonded water provide an explanation for the observations that the higher conductance states of the alamethicin channels are only moderately sensitive to cation radius (Eisenberg et al 1977) which implies that the current increases are due to changes in channel cross section rather than increases in the number of parallel open channels. Given that halogenated hydrocarbon anaesthetics, such as chloroform, have been shown by infra red methods (Sandorfy 1980) to perturb H-bonds in membranes, the H-bonded water content of the alamethicin channels must be regarded as a likely target for the observed effects of ethanol and the two general anaesthetics as indicated in Fig 4.4.

In contrast to the channel mediated transport, when the carrier ionophores A23187 or ionomycin are used, all three compounds, ethanol,

diethyl ether and chloroform increase the rate of transport (Fig 4.5 i and ii). The carrier mechanism involves the metal ions losing their water of hydration before coordinating with the ionophore molecules. The exterior of the complex formed is hydrophobic, making it soluble in the hydrocarbon region of the bilayer. The increase in transport rate is likely to be controlled by the increase in fluidity of the bilayer by the anaesthetics, and involves relatively little water interaction, which further demonstrates the possible significance of anaesthetics having an effect on the H-bonds of water.

The result that chloroform inhibits the bile salt transport rate (Fig 4.6i) is not consistent with its effects on A23187 and ionomycin. However bile salt transport is thought to be mediated by inverted micelles (Hunt 1980b) which contain water in their central aqueous pores. Thus the action of the anaesthetics could be centred on the water contents of the inverted micelle or on the interaction between water and the phospholipid head groups and/or bile salt polar groups. The results obtained from the effects of chloroform and ethanol on the inverted micelle mediated ion transport in PC/PE (Fig 4.7i) and PC/CL (Fig 4.8i) are consistent with their effects on bile salt transport. This further emphasises that their action is centred on the water associated with the inverted micelle.

The effects of the anaesthetics on membrane fusion follows the same pattern as seen for their effects on transport mediated by inverted micelles. The same pattern is seen irrespective of whether the fusion is chemically induced by Triton X100 and PEG (Fig 4.9) or promoted by the presence of non bilayer phase inducing lipids PE and CL (Fig 4.7ii and Fig 4.8ii). Fusion in such systems is thought to be mediated by the

formation of an inverted micelle between two adjacent bilayers (see section 1.4). The effects of the anaesthetics on the fusion and transport processes involving inverted micelles are therefore similar. These observations do not seem to be in agreement with those of Cullis and coworkers (Cullis et al 1980c, Hornby and Cullis 1981) who found that in soya PE/PC liposomes, ethanol stabilizes the bilayer phase and chloroform stabilizes the H_{II} phase. However the difference may be a consequence of the different compositions of the membranes and the concentration of the anaesthetics used. The importance of the lipid-water and water-water interaction in the formation of inverted micelles have been discussed by Sen et al (1982) with particular emphasis being made to the stability of H-bonds between lipid head groups and water. Again these results indicate that these H-bonds are primary sites for anaesthetic action.

For such systems to be investigated further it is clear that the action of clinical levels of anaesthetics needs to be explored. These concentrations are some what more difficult to obtain, but quoted values are of the order of about 50 mM ethanol, 15 mM diethyl ether and 1 mM chloroform (Franks and Lieb 1982, Seeman 1972). Seeman indicates that the concentration required for local anaesthesia are ten times these values and therefore for ethanol physiological concentrations have been used. The lowest value of chloroform studied was 5 mM for alamethicin transport. The large effect on the transport rate (Fig 4.4) indicates that inhibition will be expected down to physiological concentrations for this type of anaesthetic.

Taken together the similarities in the effects of ethanol, diethyl ether and chloroform on each channel system imply a common element in the mechanism. Since for each mechanism of channel formation

studied the importance of water structure and function in the channels is strongly indicated, it is difficult to avoid the implications that the effects of these compounds on channel water is the unifying feature of the results. Such an unifying feature can also be applied to the effect of the anaesthetics on lipid-water or water-water interactions involved in the processes of transport and fusion, mediated by inverted micelles.

It would clearly be premature to claim to have demonstrated a possible novel mechanism for general anaesthesia on the small range of compounds and model system. However the lipid based theories of general anaesthesia (see section 1.5) have recently been strongly and effectively criticised (Richards 1980, Franks and Lieb 1982) and direct protein - anaesthetic action is seen to be unlikely on structural grounds (Franks and Lieb 1982). The results therefore suggest a modification of the protein hypothesis, in that an important locus of action of the general anaesthetics could be their effect on water structure and function in the ion channel and/or on the fusion mechanism of the synaptic vesicles with the presynaptic membrane, at synapses in the nervous system.

The proposed interaction with water differ from those of Pauling (1961) and Miller (1961) in that they involve more general interaction of the type proposed by Brockerhoff (1982) and Kamaya et al (1982,1980) which include a variable effect of H-bonding depending on the chemical nature of the anaesthetic. A recent theoretical model of ionic channels which accounts well for the electrical properties of Na^+ and K^+ channels is based on a H-bonded ordered water channel at a protein site spanning the membrane (Edmonds 1980,1981). Experiments such as those described in

this model begin to provide specific tests for this anaesthetic theory.

Richards (1980) has pointed out that it is very unlikely that all general anaesthetics act at a single type of site. Clearly other studies on a range of anaesthetics, systems of membrane channels and fusion sites will be required to reinforce the hypothesis that effects on water structure and properties are important in the mechanism of general anaesthesia.

The observation that diazepam in the absence of ethanol has no effect on the degree of lysis and that it potentiates the degree of lysis when in the presence of ethanol (Fig 4.10) suggests that diazepam and ethanol have a synergistic action on the formation of lytic channels at the phase transition. Diazepam possesses no ionophoric properties of its own but has the effect of potentiating the rate of transport by alamethicin. This suggests that diazepam is stabilizing the alamethicin channels. The result obtained by the action of both diazepam and ethanol (86 mM) indicate that they have a synergistic effect on alamethicin transport (Fig 4.11(i), Table 4.2). However this synergistic behaviour seems to be dependent on the ethanol concentration (Fig 4.11(ii), Table 4.2).

These results are in agreement with other studies which find a similar synergistic effect between diazepam and ethanol (MacLeod et al 1977, Seiax 1978) and emphasize the possibility that a similar type of synergistic action could take place in ion channels of postsynaptic membranes. However, Ciofalo (1980) reported that chronic effects of ethanol alter the properties of the benzodiazepine receptors in rat synaptic membranes. This suggests that a role for ethanol could be to modify the interaction of diazepam with its receptors on the postsynaptic membrane.

CHAPTER 5

CHOLESTEROL AND MEMBRANES

5.1 Introduction

Information regarding the physical and functional properties of cholesterol and membranes has been obtained from studies employing a range of physical techniques (NMR, ESR, DSC, X-ray diffraction) and artificial lipid bilayers (Demel and De Kruijff 1976). The evidence from such studies suggests that the primary role for cholesterol in membranes is to produce a state of intermediate membrane fluidity. That is, an ordering of the bilayer in the liquid crystal phase and a disordering of the bilayer in the gel phase. This concept explains the increase in cholesterol content of membranes (microsomes, mitochondria, synaptosomes, erythrocytes and neurones) obtained from ethanol treated animals (Chin and Goldstein 1977, 1981, Goldstein and Chin 1981, Johnson et al 1979). The increased fluidity induced by ethanol (see chapter 4) is therefore neutralized by an increase in the cholesterol : phospholipid ratio and to a lesser extent by a reduction in the unsaturated fatty acid content.

The condensing effect of cholesterol in fluid bilayers is found to reduce the passive diffusion of water and small molecules. However in gel state bilayers the passive permeability is enhanced in the presence of cholesterol (Bittman and Blau 1972). Studies using various sterols have shown that the requirements for such criteria are a planar sterol nucleus, a 3β hydroxy group and an aliphatic side chain. Another function for cholesterol may therefore be to seal membranes against the non specific passive diffusion of small molecules.

^{31}P and ^1H -NMR studies indicate that cholesterol (up to 30 mole %) is evenly distributed between the inner and outer monolayers

of phospholipid vesicles. Above 30 mole %, cholesterol is asymmetrically distributed in favour of the inner monolayer (De Kruijff et al 1976, Huang et al 1974). The asymmetric distribution of cholesterol in erythrocyte membranes, as analyzed by freeze fracture, revealed more cholesterol localized in the outer monolayer (Houslay and Stanley 1982). This is attributed to the higher sphingomyelin content of this monolayer and such effects are thought to contribute to the lateral organisation of lipids and proteins in membranes. Therefore, in addition to altering membrane fluidity, cholesterol also changes the composition of the fluid lipid pool in which proteins diffuse. Such a property allows cholesterol to control the activity of membrane proteins.

A direct influence of cholesterol is found in the calcium transport protein, ATPase, from the sarcoplasmic reticulum (Warren et al 1975). The ATPase requires an annulus of about thirty phospholipid molecules for its enzymatic activity. It is found that when molecules in the annulus lipid are replaced by cholesterol there is a reversible alteration of ATPase activity. It was suggested that the annulus lipid excludes cholesterol, leading to a lateral segregation of lipids. Such a situation may be promoted by the preference of cholesterol for the more fluid bulk lipid than for the more rigid annulus lipid (De Kruijff et al 1974). In addition the sphingomyelin content may promote cholesterol poor domains and thus give rise to an environment favorable for protein activity (Demel et al 1977).

However cholesterol is found to be a requirement for channel formation by the polyene antibiotics, filipin, nystatin and amphotericin B (Gomperts 1977). It is proposed that the hydrophobic side of the polyene lactone ring interacts with cholesterol via Van der Waals

interactions. Hydrogen bonding takes place through the 3 β hydroxy group of cholesterol and the keto group in the polyene to give a complex containing equimolar amounts of polyene and cholesterol. Such complexes give rise to 1 nm diameter pores which allow the passage of hydrated ions, thus resulting in broad specificity.

BLM studies with the polypeptide gramicidin, indicate that cholesterol reduces the mean channel life time (Pope et al 1982). Wu and coworkers (1977,1978) suggest that this could be due to cholesterol reducing the lateral diffusion rate of gramicidin in the plane of the bilayer. Latorre (1976) found that a greater voltage was required to induce conductance in planer bilayers containing alamethicin and cholesterol than in cholesterol-free bilayers. It is not clear whether cholesterol slows down channel kinetics by changing membrane fluidity, the membrane dipole potential or the alamethicin partition coefficient. In contradiction to these results, other studies have observed increased alamethicin pore-state lifetimes in bilayers containing cholesterol (Mueller and Rudin 1968, Latorre and Donavan 1980, Gordon and Haydon 1976). Sackmann and Boheim (1979) attribute the fast transition rates between the alamethicin conductance in sarcoplasmic reticulum membranes to the high cholesterol content of these membranes. In the present study the ^1H -NMR methods are used to investigate the effects of cholesterol on the alamethicin induced permeability in DPPC and egg PC vesicles. The action of ethanol and chloroform on these systems is also investigated.

Previous ^1H -NMR studies show that the presence of 10 mole % cholesterol in DPPC vesicles increases the bile salt transport rate of Pr^{3+} ions (Hunt and Jawaharlal 1980). 40 mole % cholesterol is found to completely inhibit transport induced by the bile salts but vesicular lysis is observed with the deoxy bile salts. Lysis in these systems

could be induced by bile salts only when cholesterol was present. However cholesterol is not a requirement for the bile salt induced lysis of egg PC vesicles (see chapter 3) and therefore in this chapter the effect of cholesterol on transport and lysis induced by bile salts in egg PC vesicles is investigated by ^1H -NMR methods.

5.2 Materials and Methods

5.2.1 Chemicals

Cholesterol (Puriss grade) was obtained from Koch-Light, Colnbrook, Bucks. A stock solution was prepared in chloroform (20 mg/ml) and was stored at -5°C.

5.2.2 Preparation of vesicles

DPPC / cholesterol and egg PC / cholesterol vesicles were prepared by pipetting the required volumes of the stock solutions into a sonicating tube. The contents of the tube were then mixed. This was followed by solvent removal and liposome sonication as previously described in sections 2.2 and 3.2.

5.2.3 Lysis and transport processes

The ^1H -NMR spectrum of DPPC / 25 mole % cholesterol vesicles in the presence of 5 mM Pr^{3+} at 50°C is shown in Fig 5.1. The broad hydrocarbon signal H, results primarily from the cholesterol reducing the bilayer fluidity above the thermotropic phase transition (see section 1.6). Changes in the head group signals (O and I) are used to monitor the processes of transport and lysis as described in sections 3.2.6 and 3.3.3.

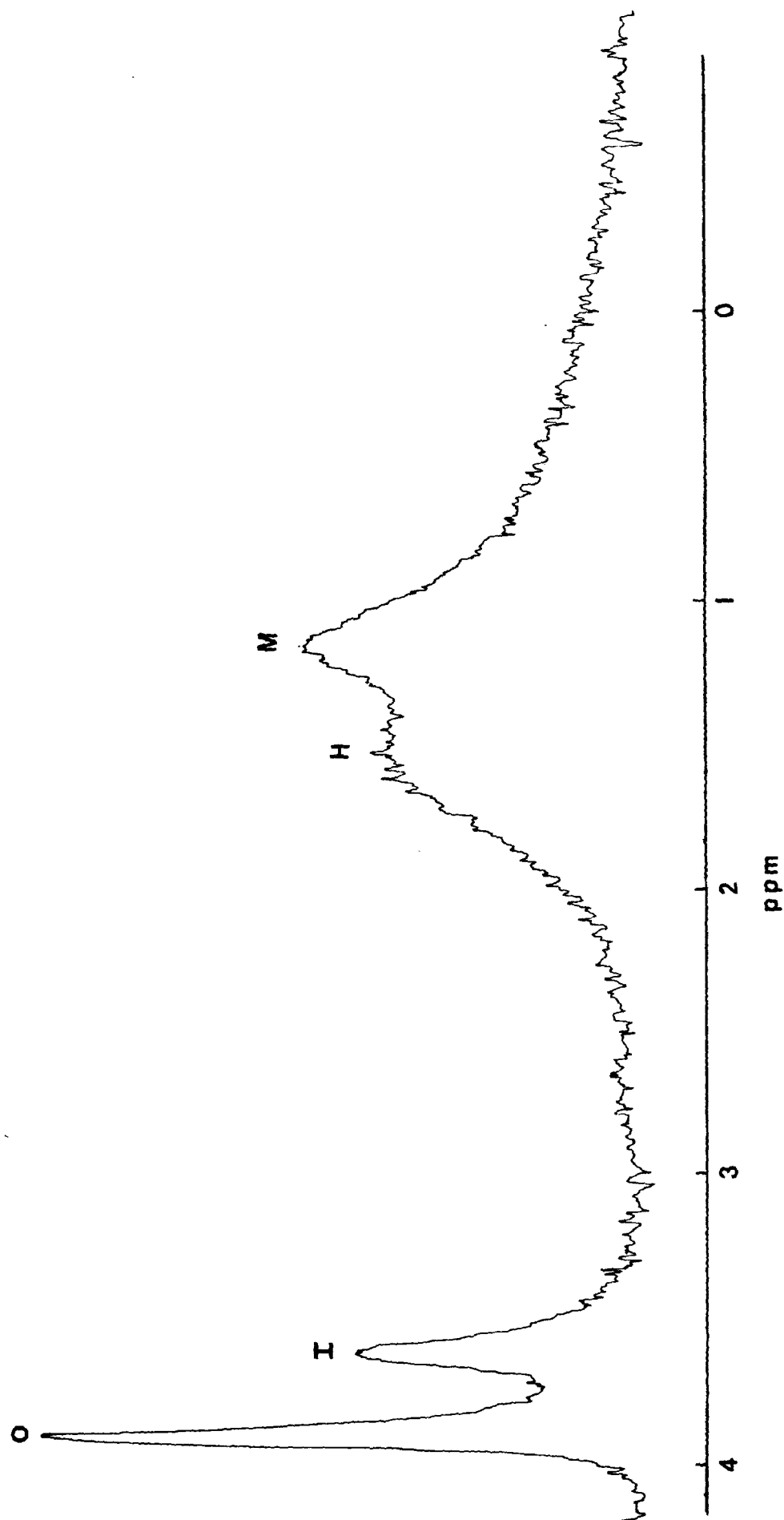


Fig 5.1 The 60 MHz ^1H -NMR spectrum of DPPC/25 mole % cholesterol vesicles at 50°C in the presence of 5 mM Pr^{3+} , showing signals from the extravesicular choline head-groups O, the intravesicular choline head-groups I, the lipid acyl chain methylenes, H and the lipid acyl chain methyl signals M. The chemical shifts are shown with reference to external TMS.

5.3 Experimental Results

5.3.1 The effect of cholesterol on alamethicin induced transport in DPPC and egg PC vesicles

Fig 5.2(i) shows the effect of 25 mole % and 40 mole % cholesterol on the Pr^{3+} transport rate obtained by alamethicin (5 $\mu\text{g/ml}$) incubated with DPPC vesicles. The plot gives rise to rates of 1.25×10^{-3} , 9.1×10^{-3} and 5.54×10^{-5} mM/min for 0 mole %, 25 mole % and 40 mole %, respectively. Fig 5.2(ii) shows the effect of cholesterol on the rates of transport obtained by alamethicin (5 $\mu\text{g/ml}$) which was introduced by cosonication with the lipid (see section 3.2.4b). The plot gives rise to rates of 1.45×10^{-3} , 0.163 and 3.8×10^{-4} mM/min for 0 mole %, 25 mole % and 40 mole % cholesterol respectively.

Fig 5.3(i) shows the plot obtained from a similar experiment (to those shown in Fig 5.2i) in which alamethicin (40 $\mu\text{g/ml}$) was incubated with egg PC vesicles containing various amounts of cholesterol. The presence of 40 mole % cholesterol gives a rate of 0.04×10^{-3} mM/min whilst the cholesterol deficient vesicles give a rate of 3.3×10^{-3} mM/min. The plot in Fig 5.3 is obtained from a similar experiment to those shown in Fig 5.3 (ii), where alamethicin (40 $\mu\text{g/ml}$) is used with egg PC vesicles. This plot gives rise to initial rates of 26.8×10^{-3} , 4.3×10^{-3} and 1.9×10^{-3} mM/min for 0 mole %, 25 mole % and 40 mole % cholesterol, respectively.

5.3.2 The effects of ethanol and chloroform on the alamethicin transport rates in DPPC / cholesterol and egg PC / cholesterol vesicles

Fig 5.4 (i) and (ii) show the effects of 25 mM chloroform and 86 mM ethanol on the rate of Pr^{3+} transport into DPPC / 25 mole %

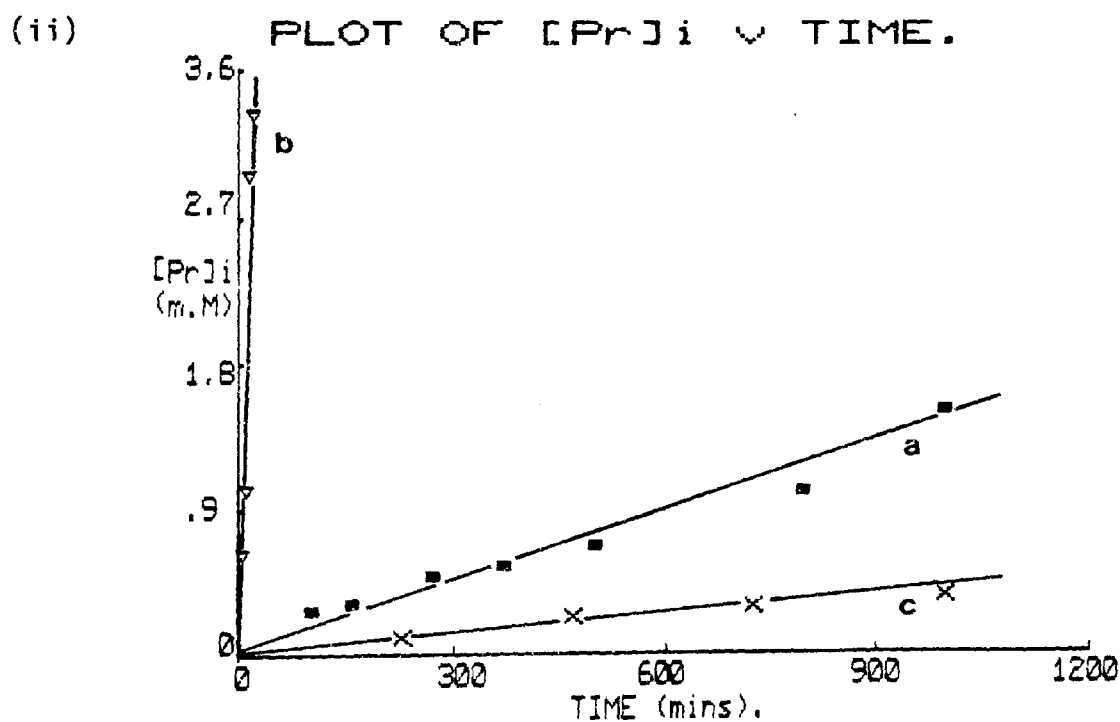
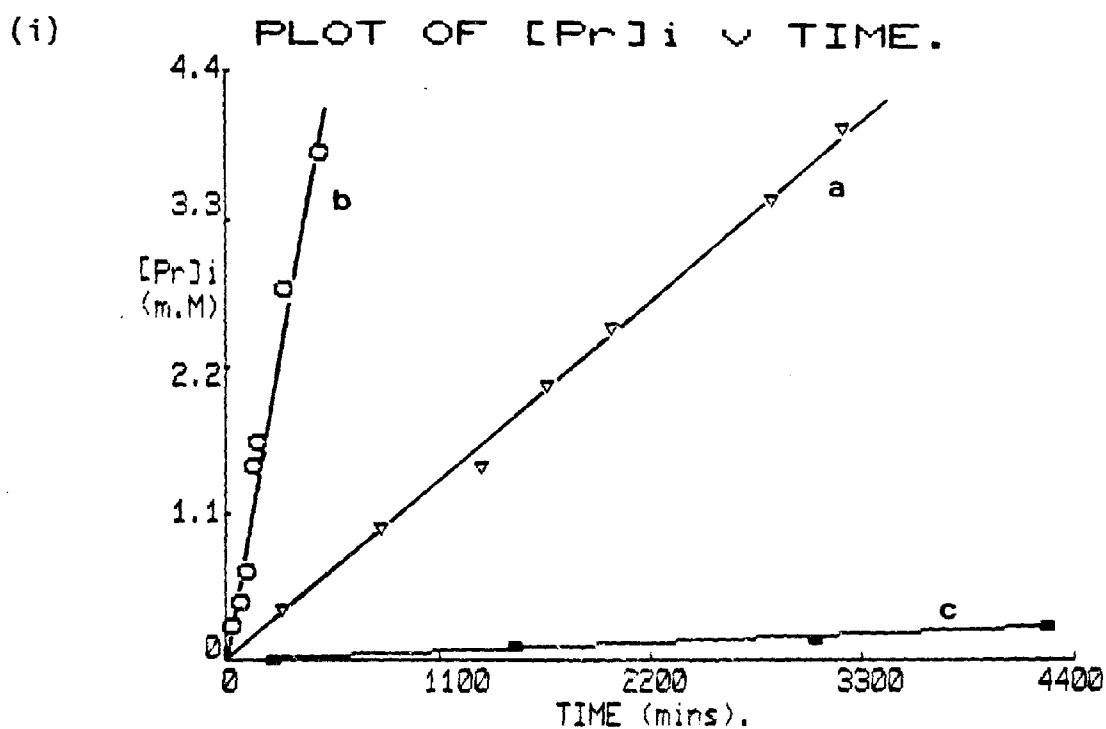


Fig 5.2 The effect of cholesterol on the Pr^{3+} transport rate by alamethicin in DPPC vesicles at $50^{\circ}C$.

(i) Alamethicin incubated with the vesicles, (ii) alamethicin introduced by cosonication with the lipid.

Cholesterol concentrations used were: a. 0 mole %, b. 25 mole %, c. 40 mole %.

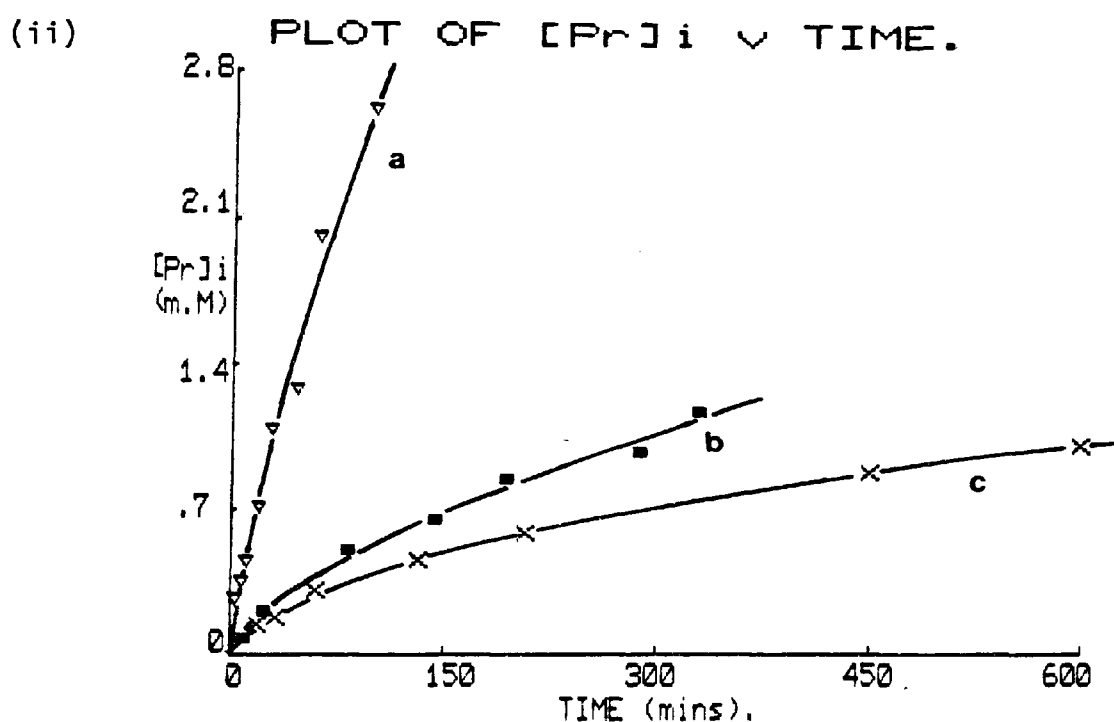
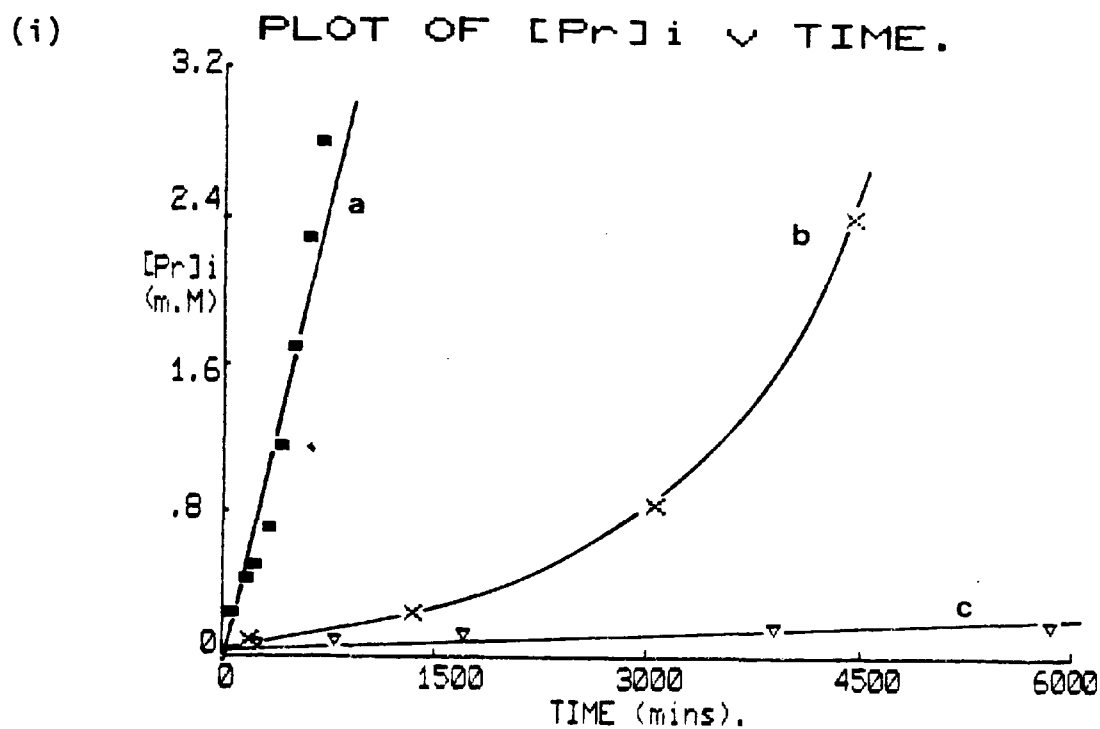


Fig 5.3 The effect of cholesterol on the Pr^{3+} transport rate by alamethicin in egg PC vesicles at $50^{\circ}C$.
 (i) Alamethicin incubated with the vesicles, (ii) alamethicin introduced by cosonication with the lipid.
 Cholesterol concentrations used were: a. 0 mole %, b. 25 mole %, c. 40 mole %.
 Note the difference in time scales between (i) and (ii).

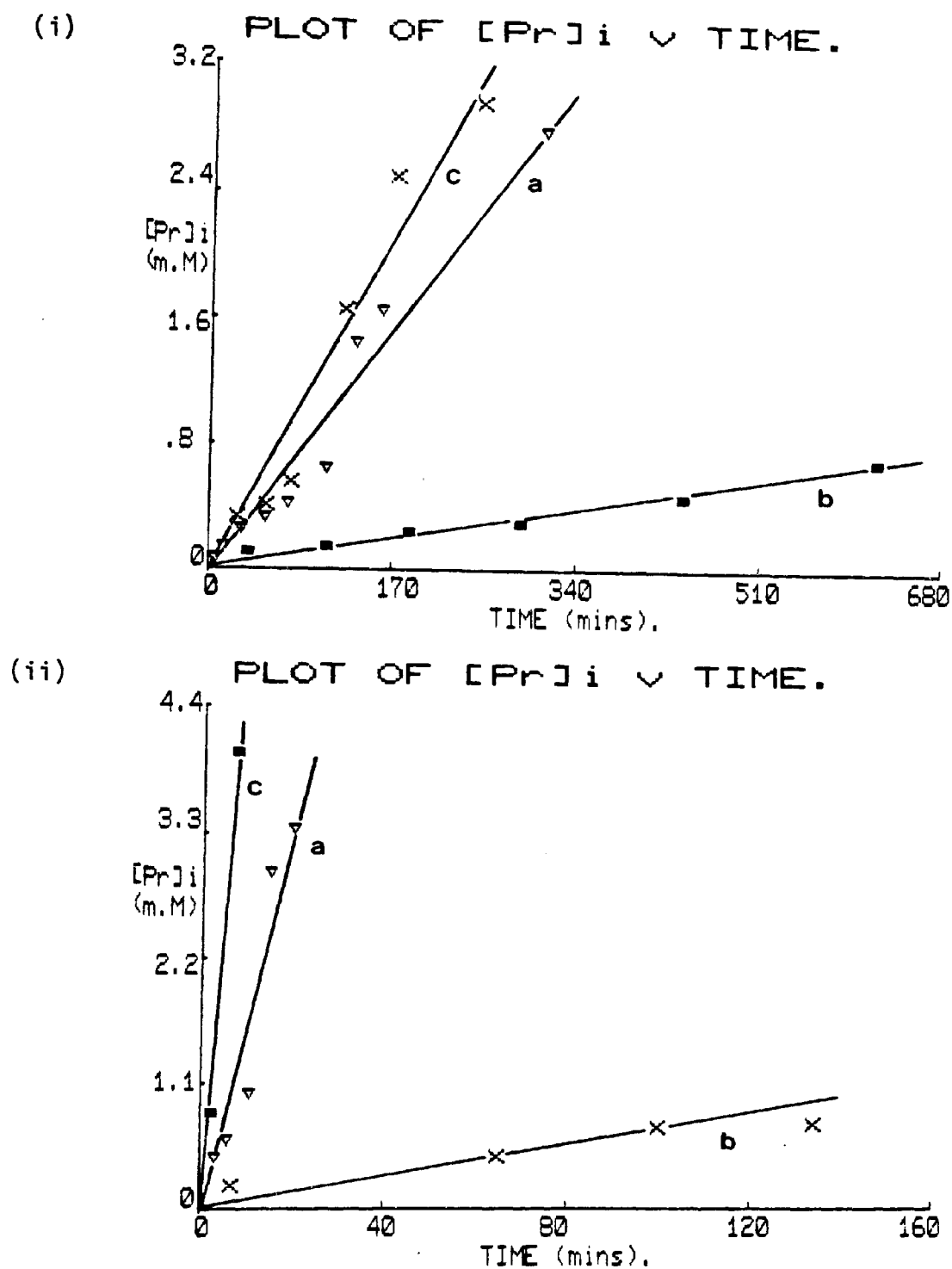


Fig 5.4 The effect of ethanol and chloroform on the Pr^{3+} transport rate by alamethicin in DPPC/25 mole % cholesterol vesicles at $50^{\circ}C$.

(i) Alamethicin incubated, (ii) alamethicin cosonicated with lipid.

a. Control. Vesicles in the presence of: b. 25 mM chloroform, c. 86 mM ethanol.

Note the difference in time scales between (i) and (ii).

cholesterol vesicles mediated by alamethicin (5 $\mu\text{g/ml}$) which is either incubated with the vesicles (Fig 5.4i) or introduced by cosonication with the lipid (Fig 5.4ii). The control, ethanol and chloroform samples in Fig 5.4(i) give rise to rates of 9.1×10^{-3} , 12.3×10^{-3} and 1.1×10^{-3} mM/min respectively, whilst rates of 0.16, 0.51 and 6.2×10^{-3} mM/min respectively are obtained from Fig 5.4(ii). Therefore in both plots the rate of transport is potentiated by ethanol and strongly inhibited by chloroform.

The plots in Fig 5.5 are obtained from similar experiments using vesicles composed of 40 mole % cholesterol. A similar trend is seen for the effects of ethanol and chloroform in Fig 5.5(i) and (ii), in that in both cases ethanol and chloroform potentiate the control rate, but the form of the plots is very different in (i) and (ii).

Fig 5.6 (i) and (ii) show that in egg PC / 25 mole % cholesterol vesicles, both ethanol and chloroform potentiate the rate of transport induced by alamethicin (40 $\mu\text{g/ml}$) when it is incubated with the vesicles (Fig 5.6i) or introduced by cosonication with the lipid (Fig 5.6ii). The effect of chloroform on the transport rate is seen to be much greater when alamethicin is incubated with the vesicles, whereas ethanol has a greater effect when alamethicin is introduced by cosonication with the lipid. Similar trends in the effects of ethanol and chloroform on alamethicin transport are also observed in vesicles composed of egg PC / 40 mole % cholesterol (Fig 5.7i and ii).

These results are discussed below in terms of the asymmetric cholesterol distribution and the formation of phospholipid - cholesterol complexes via H-bonding.

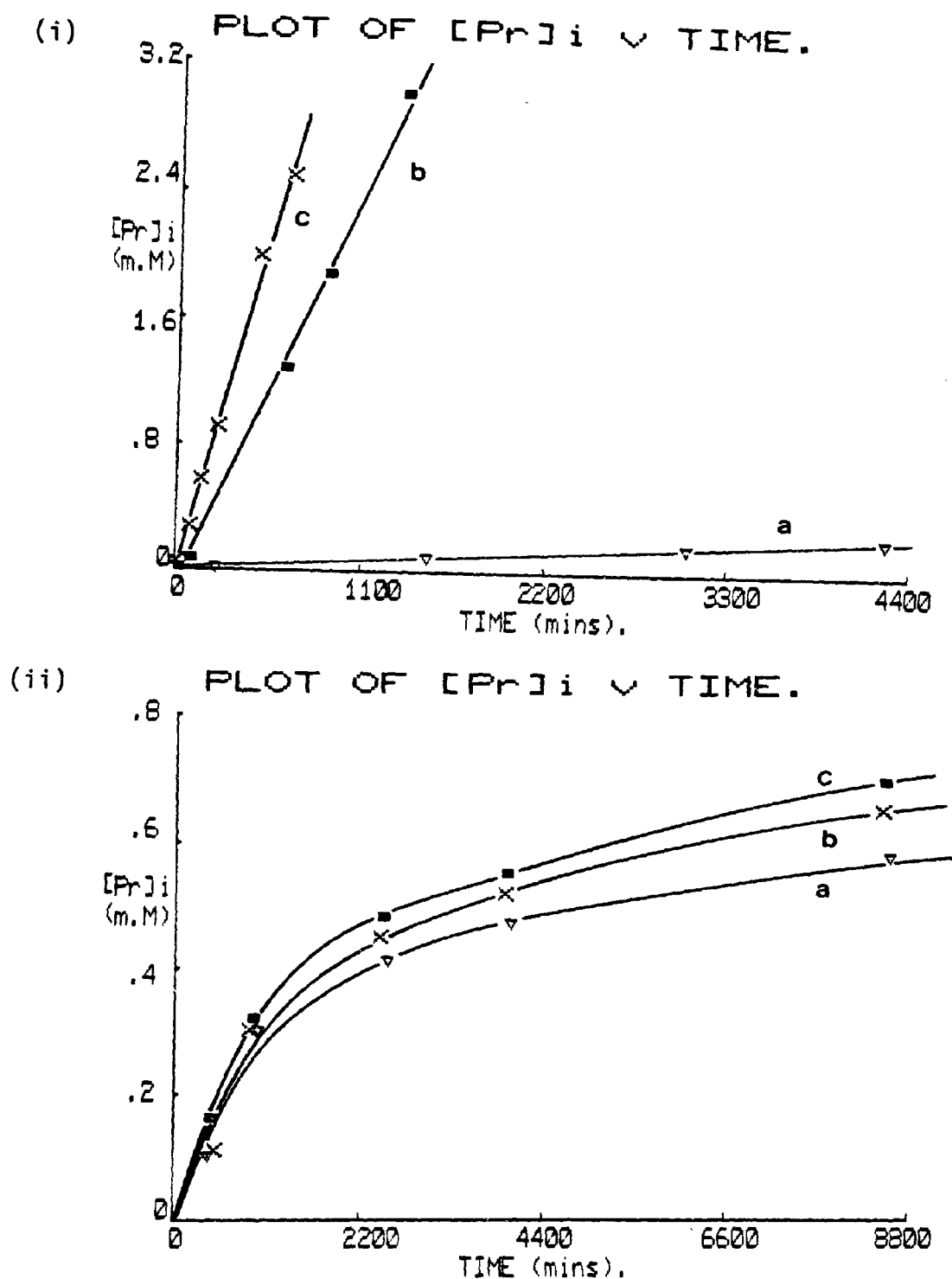
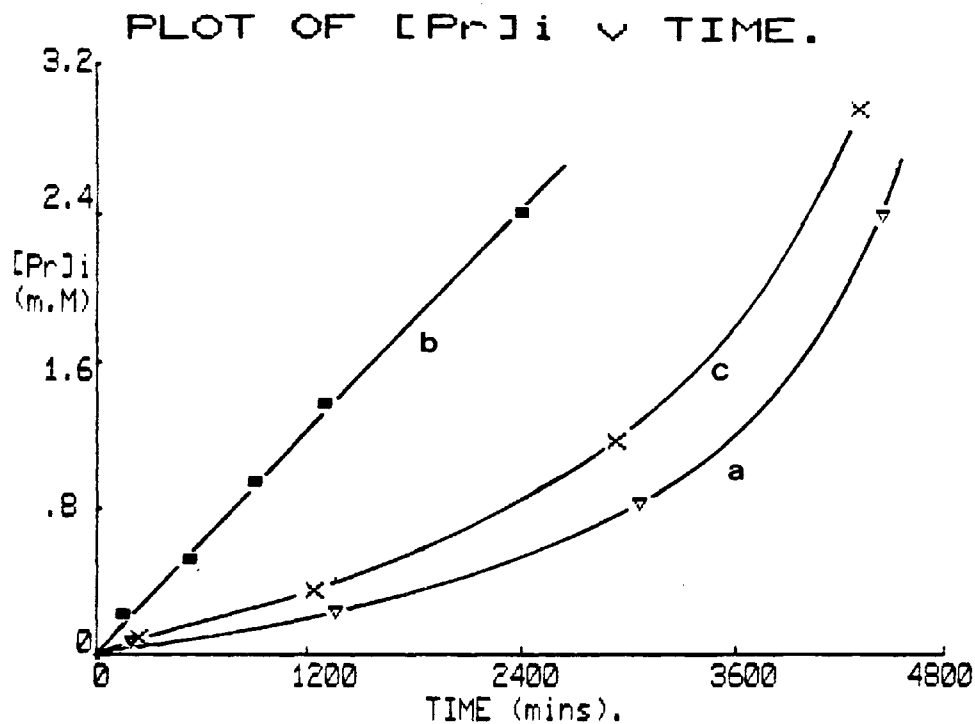


Fig 5.5 The effect of chloroform and ethanol on the Pr^{3+} transport rate by alamethicin in DPPC/40 mole % cholesterol vesicles at $50^{\circ}C$.

(i) Alamethicin incubated, (ii) alamethicin cosonicated with lipid.

a. Control. Vesicles in the presence of: b. 25 mM chloroform, c. 86 mM ethanol.

(i)



(ii)

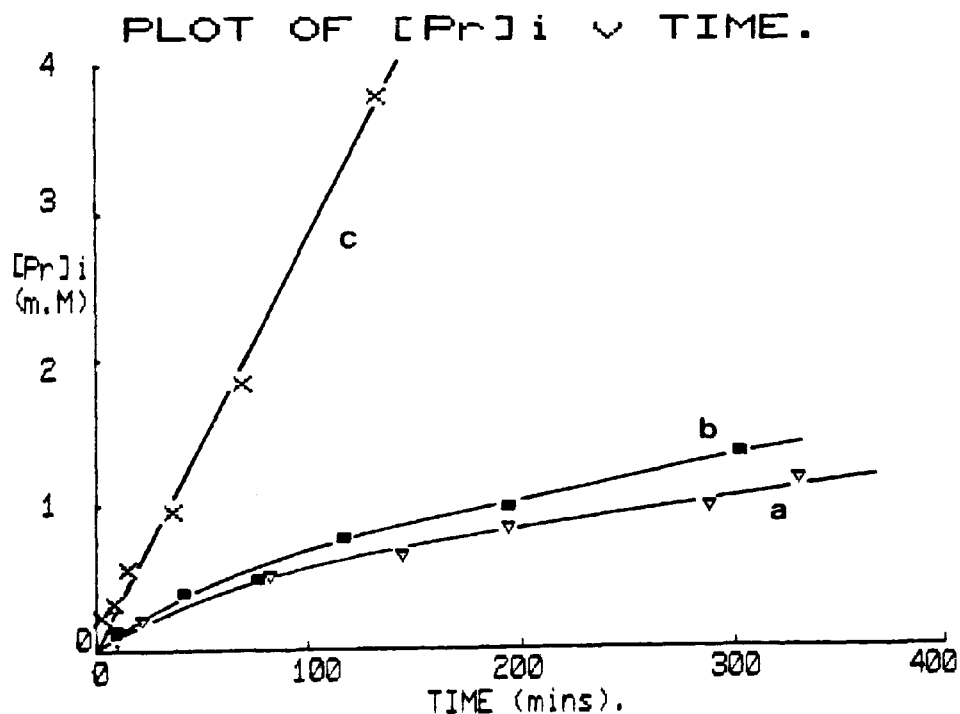


Fig 5.6 The effect of chloroform and ethanol on the Pr^{3+} transport rate by alamethicin in egg PC/25 mole % cholesterol vesicles at $50^{\circ}C$.
(i) Alamethicin incubated, (ii) alamethicin cosonicated with lipid.
a. Control. Vesicles in the presence of: b. 25 mM chloroform, c. 86 mM ethanol.
Note the difference in time scales between (i) and (ii).

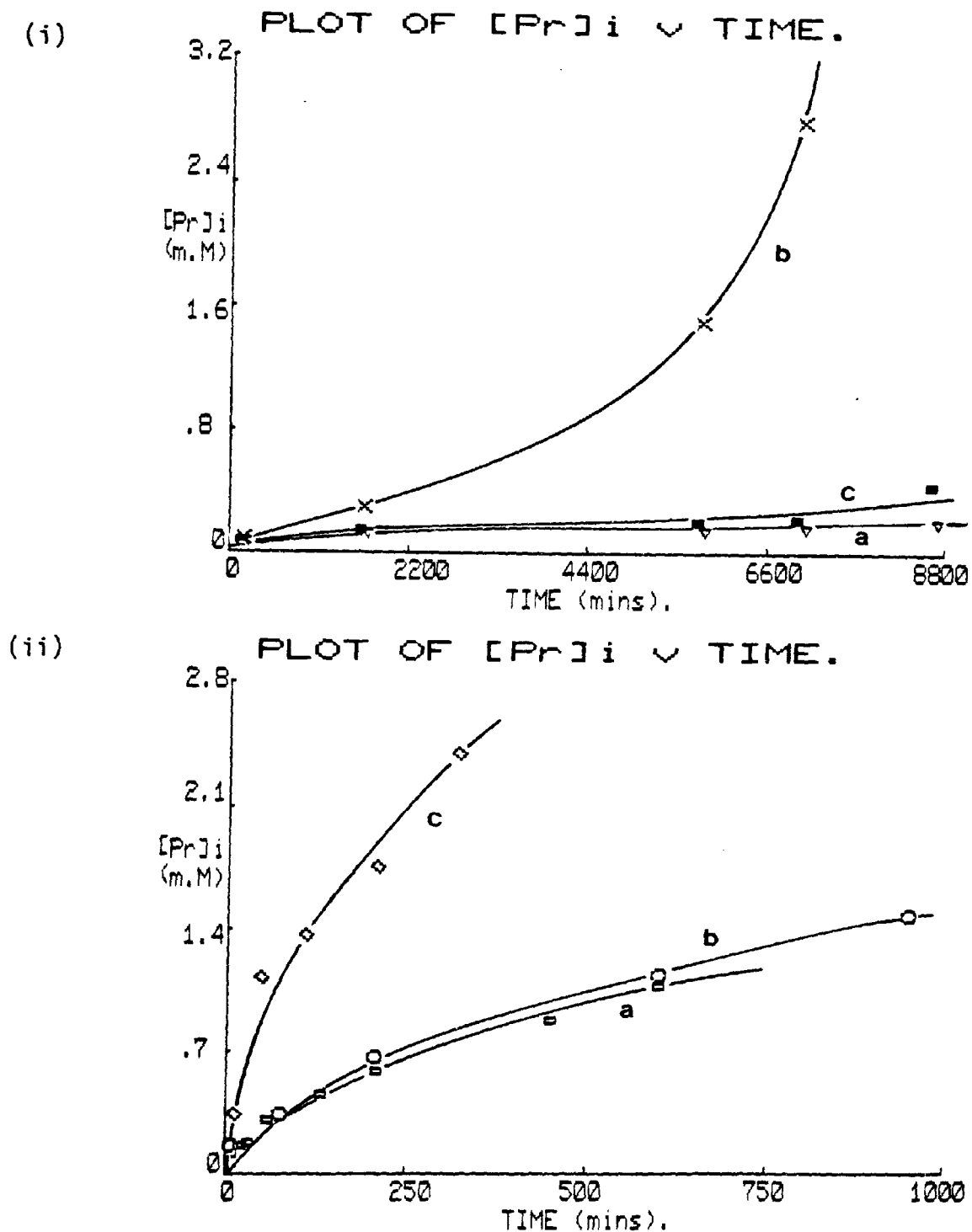


Fig 5.7 The effect of chloroform and ethanol on the Pr^{3+} transport rate by alamethicin in egg PC/40 mole % cholesterol vesicles at $50^{\circ}C$.
 (i) Alamethicin incubated, (ii) alamethicin cosonicated with lipid.
 a. Control. Vesicles in the presence of: b. 25 mM chloroform, c. 86 mM ethanol.
 Note the difference in time scales for (i) and (ii).

5.3.3 The effect of cholesterol on the transport and lytic rates induced by bile salts in egg PC vesicles

Fig 5.8 (i) shows the effect of 30 mole % cholesterol on the rate of Pr^{3+} transport by the bile salts, cholate and deoxycholate (1.5 mM) in egg PC vesicles at 37°C . The plot gives rise to rates of 0.98×10^{-2} and 8.75×10^{-2} mM/min for cholate and deoxycholate, respectively in the absence of cholesterol and to 0.47×10^{-2} and 18×10^{-2} mM/min for cholate and deoxycholate, respectively in vesicles containing 30 mole % cholesterol. During the course of these experiments no accompanying lysis is observed.

The effect of 30 mole % cholesterol on glycocholate and glycodeoxycholate transport in egg PC vesicles is shown in Fig 5.8(ii). In the absence of cholesterol rates of 0.67×10^{-2} and 1.14×10^{-2} mM/min are obtained for glycocholate and glycodeoxycholate, respectively whereas in the presence of 30 mole % cholesterol rates of 0.41×10^{-3} and 0.73×10^{-2} mM/min respectively, are obtained. However the transport rates for glycodeoxycholate are accompanied by vesicular lysis (plots not shown) having approximate rates of 0.4 % vesicles lysed / min (0 mole % cholesterol) and 0.65 % vesicles lysed / min (30 mole % cholesterol).

Fig 5.9 shows the effect of cholesterol on the rate of lysis obtained by incubating 2 mM glycocholate and glycodeoxycholate with egg PC vesicles at 37°C . In the presence of 30 mole % cholesterol, cholate and deoxycholate (2 mM) did not give rise to vesicular lysis, but resulted in the very rapid transport rates of 0.26 and 0.67 mM/min respectively (see Fig 3.22 for lytic rates for 0 mole % cholesterol). Therefore in egg PC vesicles cholesterol is seen to slightly potentiate the lytic properties of glycodeoxycholate whereas it inhibits the lytic

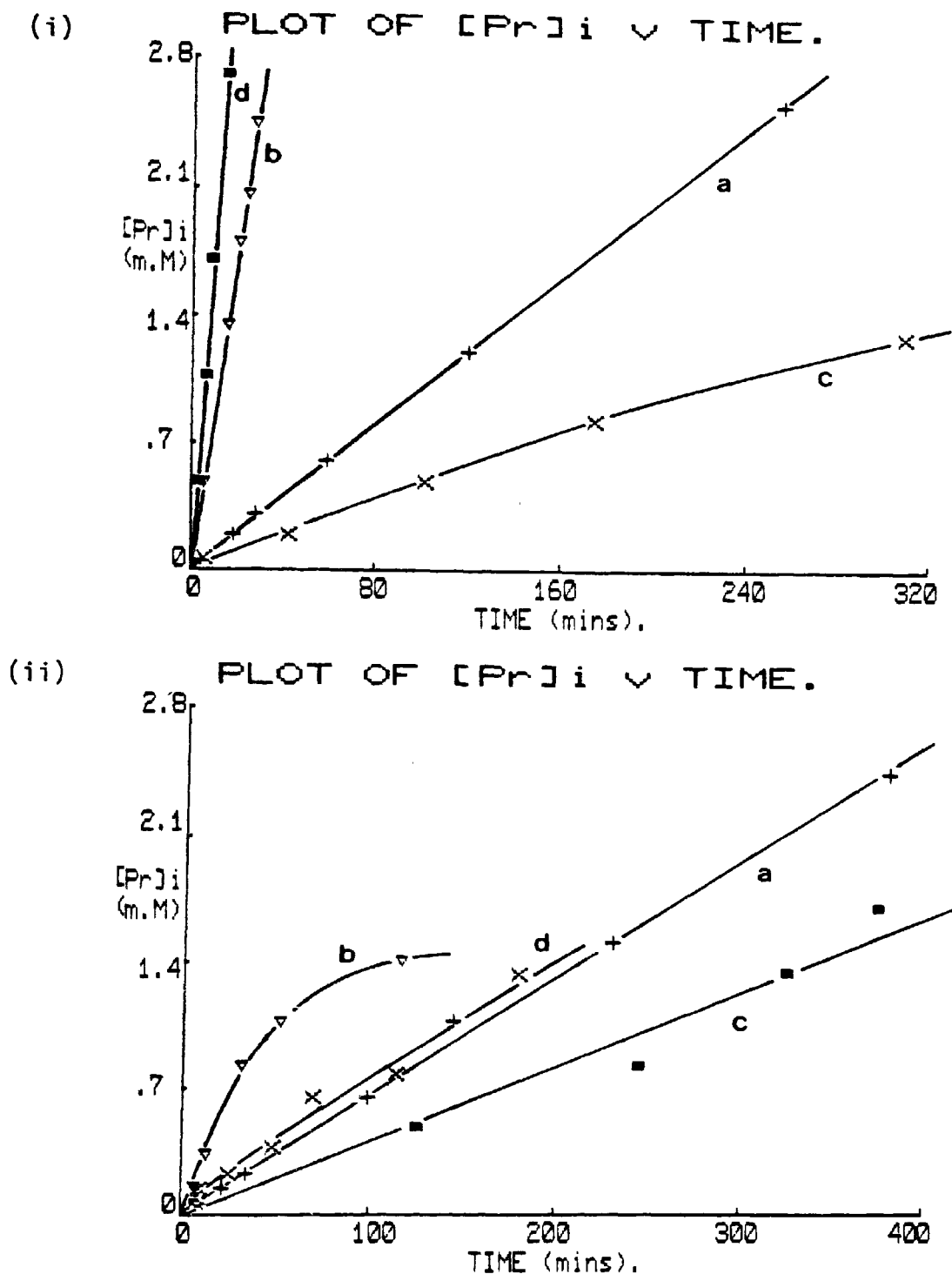


Fig 5.8 The effect of cholesterol on the Pr^{3+} transport rates induced by bile salts (1.5 mM) in egg PC vesicles at $37^{\circ}C$.

(i) Unconjugated bile salts with vesicles containing no cholesterol: a. cholate, b. deoxycholate. Vesicles containing 30 mole % cholesterol: c. cholate, d. deoxycholate.

(ii) Conjugated bile salts with vesicles containing no cholesterol: a. glycocholate, b. glycodeoxycholate. Vesicles containing 30 mole % cholesterol: c. glycocholate, d. glycodeoxycholate.

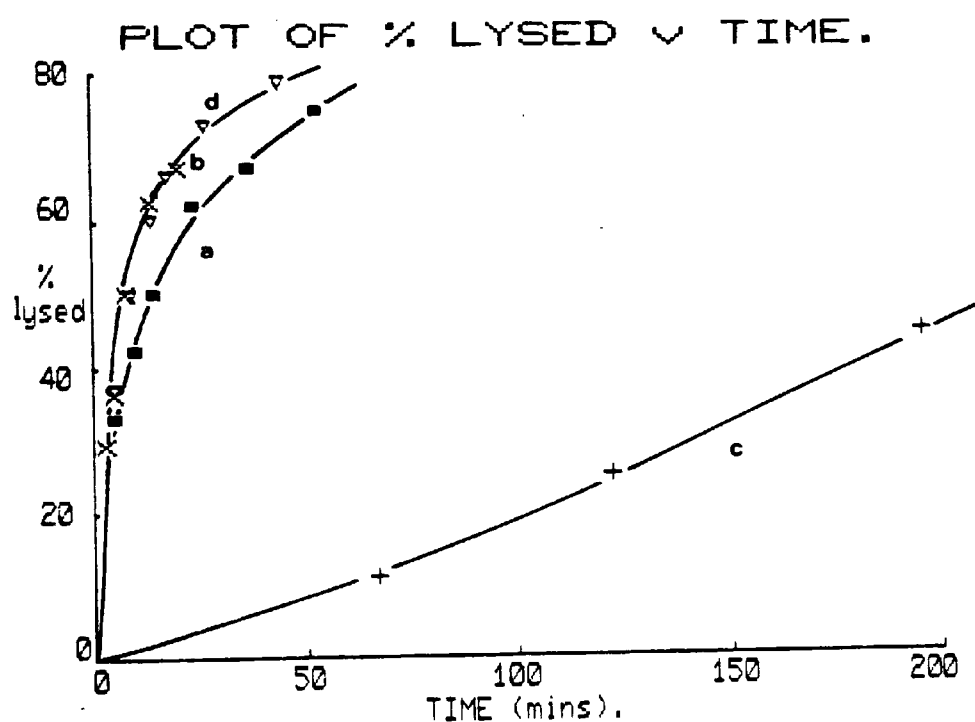


Fig 5.9 The effect of cholesterol (30 mole %) on the lytic rates induced by bile salts in egg PC vesicles at 37°C. For 0 mole % cholesterol: a. glycocholate, b. glycodeoxycholate. For 30 mole % cholesterol: c. glycocholate, d. glycodeoxycholate.

properties of cholate, deoxycholate and glycocholate.

5.4 Discussion

The ^1H -NMR data obtained from the vesicles containing cholesterol (Fig 5.1) show that the signal arising from the terminal methyl groups of the acyl chains is sharp relative to the broadened out hydrocarbon signal. This suggests that the degree of motional freedom experienced by the methyl groups is not greatly restricted in the presence of cholesterol. Such an observation is in agreement with ^2H -NMR and X-ray diffraction studies which show that the ring region of cholesterol only restricts the motional freedom of the first twelve methylenes, whilst the remaining methylenes interact with the more mobile alkyl side chain of cholesterol (McIntosh 1978, Taylor et al 1982).

For vesicles containing up to 30 mole % cholesterol a consistent O : I ratio of 1.6 was observed. However the presence of 40 mole % cholesterol reduces this ratio to 1.5 and indicates that the vesicular diameter has been increased from 38 nm to 45 nm. Such increases in vesicular dimensions have previously been observed by ^{31}P -NMR studies (De Kruijff et al 1976).

5.4.1 Effect of cholesterol on the alamethicin transport rate

The results demonstrate that cholesterol modulates, in a similar manner, the transport rate induced either by alamethicin incubated with the vesicles or by alamethicin co-sonicated with the lipid. The presence of 25 mole % cholesterol in DPPC vesicles enhances the alamethicin transport rate, whilst 40 mole % cholesterol inhibits this rate (Fig 5.2). In egg PC vesicles however, cholesterol inhibits the alamethicin transport rate with the degree of inhibition increasing with higher

cholesterol content (Fig 5.3). These results with egg PC / cholesterol vesicles are in agreement with the BLM studies of Latorre et al.(1976) who observed a progressive decrease in channel conductance with increasing cholesterol content.

Cholesterol reduces the lateral diffusion of lipid molecules in the plane of the bilayer (Wu et al 1977, 1978) and will therefore affect the lateral diffusion of alamethicin molecules that are spanning the bilayer. There is also the possibility of cholesterol inhibiting the partition of alamethicin from the surface of the membrane into the bilayer spanning conformation. Such factors would decrease the rate of channel formation, thus giving a slower rate of transport, which may explain the inhibition of the rate induced by cholesterol in DPPC / 40 mole % cholesterol, egg PC / 25 mole % cholesterol and egg PC / 40 mole % cholesterol and can also account for the much slower rates obtained when the alamethicin is incubated with the vesicles as opposed to being co-sonicated in the bilayer (see Fig 5.2 and 5.3).

The enhanced rate in DPPC / 25 mole % cholesterol suggests that either the channel lifetimes are increased or that channels containing a greater number of alamethicin monomers (increases the channel diameter) are produced. Similar increases due to cholesterol have been obtained with BLM studies, where the effect is attributed to an increase in pore state lifetime (Muller and Rudin 1968, Gordon and Haydon 1976).

A possible explanation for the different effects of 25 mole % cholesterol on the alamethicin transport rate in DPPC and egg PC vesicles, requires consideration of the physical properties of the constituent phospholipids. At 50°C the pure DPPC bilayers are at a temperature only marginally greater than the upper limit of the phase

transition (42°C). In the presence of 25 mole % the transition range is broadened so that the upper limit increases to approximately 47°C (Hunt and Tipping 1978). These bilayers will therefore be substantially more ordered than bilayers of egg PC / 25 mole % cholesterol which are approximately 50°C higher than the upper limit of their phase transition. Egg PC also possess a variety of saturated and unsaturated acyl chains, thus allowing the possibility of cholesterol preferentially associating with the more fluid molecules (De Kruijff et al 1974).

5.4.2 Effects of ethanol and chloroform on alamethicin transport in vesicles containing cholesterol

The results in Fig 5.4 demonstrates that chloroform and ethanol affect the transport rate (induced by alamethicin) in a similar manner to that obtained in the absence of cholesterol (see chapter 4). This suggests that the nature of the channels produced in DPPC 25 mole % cholesterol vesicles is similar to the channels produced in DPPC vesicles, and that any extra interaction induced by cholesterol do not interfere with the action of ethanol and chloroform.

However for DPPC 40 mole % cholesterol, egg PC / 25 mole % cholesterol and egg PC / 40 mole % cholesterol both ethanol and chloroform enhance the alamethicin transport rates to varying degrees. It is interesting to note that in the absence of ethanol or chloroform the effect of cholesterol in these samples is to reduce the rate of transport with respect to the rate obtained from cholesterol deficient vesicles.

The effect of chloroform is seen to be more pronounced in samples where alamethicin is incubated with the vesicles than when alamethicin in co-sonicated with the lipid (Fig 5.5, 5.6 and 5.7). The partitioning

of the alamethicin from the membrane surface into the bilayer may therefore be enhanced by the greater fluidising nature of chloroform. In addition chloroform may also be affecting H-bonding between the cholesterol hydroxyl group and the acyl chain carbonyl. This effect would reduce the order induced by cholesterol and may result in the rate of lateral diffusion being increased, thus giving rise to an increased frequency of alamethicin channel formation. Such effects may therefore be overshadowing the normal inhibition shown by chloroform on channel mediated transport (see chapter 4). It is clear from these results that the introduction of cholesterol gives rise to several extra interactions which give the relatively complex results with ethanol and chloroform.

5.4.3 The effect of cholesterol on bile salt activity

To interpret the effects of cholesterol on bile salt activity in egg PC vesicles, some properties of the bilayer in the absence of cholesterol are considered first. That bile salts can induce lysis in egg PC vesicles but cannot do so in DPPC vesicles (see section 5.1) suggests that physical properties within the two bilayers may be responsible for the different bile salt activity. Differences in order and fluidity within the two bilayers may therefore be significant factors in determining the mechanism of action.

The presence of unsaturated fatty acids in egg PC bilayers give rise to a lower molecular order and therefore to a greater phospholipid molecular volume, than for DPPC molecules. Reduced intermolecular interactions resulting in head groups which are more loosely packed, have previously been found to be important factors in determining the mode of detergent action (Zaslavsky et al 1981). The above properties may therefore allow bile salts to perturb egg PC bilayers more

efficiently than DPPC bilayers, thus allowing them to partition into regions favorable for channel formation.

The presence of cholesterol in these bilayers causes a further increase in the head group separation (Zaslavsky et al 1981). Such an effect is more pronounced in DPPC bilayers (hence the observed lysis) than in egg PC bilayers, since the condensing property of cholesterol would be greater in egg PC bilayers (Jain 1972). The result is a relatively small increase in the head group separation in egg PC bilayers.

The inclusion of 30 mole % cholesterol in egg PC vesicles inhibits the transport rate of each bile salt except deoxycholate (Fig 5.8). This inhibition is more likely a result of decreased bilayer fluidity, in conjunction with the possibility of cholesterol being involved in the inverted micelle complex (see chapter 3). The potentiation observed with deoxycholate may be due to its relatively hydrophobic nature and to its small molecular size giving rise to small inverted micelles with a low activation energy for transport.

The conjugated bile salts can induce lysis in egg PC/cholesterol vesicles whereas the unconjugated cannot, which stresses the significance of the bile salt glycine moiety in the formation of transmembrane channels. This gives an extra hydrophilic group to align the water filled channels and also to give the complex sufficient length to span the bilayer. However the unconjugated bile salts, cholate and deoxycholate induce transport rather than lysis when cholesterol is present. The reduced rate of lysis observed with glycocholate most likely results from cholesterol molecules inhibiting the formation of transmembrane channels (see Fig 5.9). These results indicate that 30 mole % cholesterol in egg PC bilayers reduce the membrane damaging

capabilities of the bile salts. Such a property is very useful in the design of liposomes as drug packaging material for delivery by the oral route (see chapter 3) and intravenous routes where in the latter case studies have shown that increasing the cholesterol content of liposomes abolishes the destructive action of serum high density lipoproteins (Gregoriadis and Davis 1979, Gregoriadis 1981, Kirby and Gregoriadis 1981).

CHAPTER 6

THE PREPARATION AND USE OF LARGE UNILAMELLAR VESICLES

6.1 Introduction

The most important attributes of small unilamellar vesicles (diameter < 100 nm) is that they can be prepared as a homogeneous population of vesicles that can be separated from contaminating multilamellar liposomes by simple techniques, are easily and simply prepared by sonication with good reproducibility, are stable over relatively long periods (weeks) and give rise to high resolution NMR signals thus allowing their characterization down to the molecular level. However there are some disadvantages the principals of which are:

- a. The low encapsulation efficiency of the aqueous space, usually in the range of 0.1 to 1.0 % depending on the lipid concentration.
- b. The low ratio of captured volume per ml. of lipid, due to the volume occupied by lipid in the bilayer being an appreciable fraction of the vesicle total volume.
- c. The high degree of bilayer curvature which may effect molecular packing (Sheetz and Chan 1972) and promotes an asymmetric distribution of lipid between the two monolayers (see section 1.1.6).

Biological membranes with some exceptions (the convoluted cristae of the mitochondrial inner membrane, the brush borders of intestinal epithelial cells, retinal rod outer segments and disks and the membranes of the small neurotransmitter storage vesicles) are thought to be better represented by larger vesicular structures.

Large unilamellar vesicles (LUV) with an average diameter of 300 nm, have an internal volume 10^3 times greater than that of sonicated

vesicles. Springer's group have employed this property to investigate the gramicidin mediated transport of Na^+ ions using ^{23}Na -NMR in conjunction with a lanthanide shift complex (Pike et al 1982). The greater capture volume of LUV allows sufficient internal Na^+ ions to give rise to an NMR signal.

Schieren and coworkers (1978) have demonstrated that LUVs prepared by the ether evaporation method (Szoka and Papahadjopoulos 1980) have a greater volume trapping capacity than multilamellar vesicles. High degrees of encapsulation have usefully been employed in drug targeting studies especially with respect to packaging of relatively large molecules ($> 40,000$ daltons) since they cannot be trapped inside small vesicles (Szoka and Papahadjopoulos 1980). This method has gained success in a number of targeting studies including enzyme replacement therapy and the delivery of nucleic acids to cells (Fraley and Papahadjopoulos 1981, Ryman and Tyrrell 1980, Poste 1980). The consequence of vesicle size variation in drug targeting efficiency has been discussed in two recent reviews (Ryman and Tyrrell 1980, Yatvin and Lelkes 1982). One study has demonstrated the preparation of cell size ($8\text{ }\mu\text{m}$ in diameter) unilamellar vesicles which can encapsulate cell organelles and virions (Kim and Martin 1981, Poste 1980).

The various anisotropic motions associated with LUVs make them very useful for study with ^{31}P -NMR (see section 1.4). Many studies have employed this method to detect phase changes in biomembranes (for a recent review see Cullis et al 1983). Burnell and coworkers (1980b) employed ^{31}P -NMR to develop a method for obtaining the average vesicular diameter. The method involved the preparation of a range of LUVs of defined size (by a modified ethanol injection technique) and comparing

their ^{31}P -NMR spectra with those predicted by the theories of Freed (Burnell et al 1980b).

Many techniques have been developed for the preparation of LUVs of various sizes. These include detergent removal, ethanol or ether infusion, french press extrusion, reverse phase evaporation and calcium induce fusion of small vesicles (Szoka and Papahadjopoulos 1980). The size and homogeneity of the vesicles produced have been analysed mainly by electron microscopy, although light scattering techniques, analytical centrifugation and NMR have been used for sizing homogeneous preparations (Szoka and Papahadjopoulos 1980). Techniques guided towards obtaining uniformly sized vesicles have not received a great deal of attention but the few methods developed involve, sepharose chromatography, centrifugation and polycarbonate millipore filters. The methods have recently been considered very useful and important in drug targeting where the vesicular size is critical in the efficiency of delivery (Szoka and Papahadjopoulos 1980, Hauser 1982).

LUVs have also been involved in protein reconstitution studies mainly using detergent removal methods (Razin 1972, Korenbrot 1977). In protein reconstitution studies a preference is indicated for the use of non-ionic detergents since they have been shown to retain the native characteristics of the proteins whereas the ionic detergents and the bile salts alter them (Stubbs et al 1976). The non-ionic detergent octyl glucoside has been successfully used in the preparation of protein containing and protein free LUVs. The rapid removal of this detergent from mixed micellar complexes are attributed to its high cmc (25 mM) and small molecular weight (Jackson et al 1982, Stubbs et al 1976).

In the present study LUV are prepared by the method of detergent (octyl glucoside) removal. Characterisation of the vesicular

preparations are made by electron microscopy and ^{31}P -NMR. LUVs are prepared as an extension to the work done on small vesicles in this study. Success in their preparation would allow the study of :

- a. ^{23}Na transport by gramicidin (monitored by ^{23}Na -NMR) and the effects of the general anaesthetics.
- b. Lipid phase changes by ^{31}P -NMR and the effects of the general anaesthetics.
- c. Drug packaging efficiency (by ^{13}C -NMR) and the interaction with pancreatic PLA_2 and bile salts by ^{31}P -NMR.
- D. Protein reconstitution (such as the acetylcholine receptor) and the effects of the general anaesthetics.

6.2 Materials and Methods

6.2.1 Chemicals

Tris buffer (Puris AnalR grade) was obtained from Koch-Light Laboratories (Colnbrooke, Bucks). Potassium nitrate (AnalaR grade) was purchased from BDH Chemicals (Poole, Dorset) and concentrated hydrochloric acid was obtained from May and Baker (Dagenham, England). Octyl- β -D-glucopyranoside (octyl glucoside) was purchased from Sigma (Poole, Dorset).

6.2.2 Experimental Procedure

Egg PC (30 mg) dried on the inner surface of a sonicating vessel (as described in 3.2.2) was solubilised in a solution of 585 mM octyl glucoside to give an egg PC concentration of 39 mM and an octyl glucoside : egg PC molar ratio of 15:1. The lipid-detergent solution was dialyzed against two 1.5 litre changes of buffer for 24 hrs each. The composition of the buffer in this step included 10 mM Tris and 1 mM KNO_3 with the pH adjusted to 7.5 with concentrated HCl. During the dialysis the lipid solution became turbid due to removal of octyl glucoside.

The dialyzed lipid solution was pipetted into a polycarbonate centrifugation tube (NO. 34411-119) and spun at 50,000g for 30 minutes at 4°C in a MSE Prep Spin 50 centrifuge fitted with a 10 x 10 ml aluminium angle rotor. The clear supernatant was removed and the lipid pellet resuspended in a solution of 10 mM Tris and 1 mM KNO_3 in D_2O to give a final volume of 1 ml.

^{31}P -NMR spectra were obtained using a Jeol FX90Q multinuclear FT NMR spectrometer operating at 36.23 MHz for ^{31}P . Spectra were accumulated at 37°C using continuous ^1H decoupling (at 89.55 MHz) and 4K data points in the transformed spectra. Typically 4000 scans were

required using a 16 μ s pulse (45°), a 0.2 second pulse delay and a sweep width of 10 KHz. To enhance the signal to noise ratio the free induction decay was multiplied by an exponential function resulting in 50 Hz line broadening (for ^{31}P -NMR of small vesicles no line broadening was used). Spin lattice relaxation times were obtained by the inversion recovery method (see chapter 2), using a 10 second pulse delay and pulse intervals in the range of 50 ms to 6 seconds.

Vesicular dimensions were determined from ^{31}P -NMR spectra by a similar method used for small unilamellar vesicles in chapter 2. However in this case 100 mM Pr^{3+} was required to give resolved inner and outer head group ^{31}P -NMR signals. Vesicular size and homogeneity were also determined by electron microscopy (with the assistance of Alun Davies and the Electron Microscopy Unit at the Welsh National School of Medicine). A drop of the vesicular solution was applied to a 200 mesh grid coated with parlodin sprayed with a thin film of carbon. After 30 seconds the excess liquid was blotted out and the grid washed successively with three drops of the staining solution (2% phosphotungstic acid at pH 7.4) and the grid tilted at an angle of 60° to the horizontal. With the grid held horizontal an additional drop of phosphotungstic acid solution was applied for 30 seconds. The excess liquid was blotted off by a piece of fine filter paper and the grid was allowed to air dry prior to observation under the electron microscope (Phillips EM 300).

6.3 Experimental Results

Fig 6.1 shows an electron micrograph obtained from the resuspended lipid pellet (see section 6.2.2). It shows that LUV with an average diameter of 250 nm have been prepared. It also demonstrates that vesicles of fairly uniform size has been produced. Fig 6.2a shows a ^{31}P -NMR spectrum obtained from a sample containing LUV. The signal is distinctly non-lorentzian and is composed of a high field peak and a low field shoulder, with a chemical shift anisotropy (see section 1.4) of approximately 40 ppm. A ^1H -NMR spectrum of this solution (not shown) was found to be featureless but for a water signal.

Fig 6.2b shows the ^{31}P -NMR spectrum obtained from sonicated egg PC vesicles (30 mg/ml) under the same conditions as above. This shows a relatively narrow and isotropic signal which is situated approximately 15 ppm downfield to the peak in Fig 6.2a. ^{31}P -NMR T_1 values of 1.7 seconds and 1.2 seconds were obtained by the inversion recovery method for the peaks in Figs 6.2a and b respectively.

The addition of 100 mM Pr^{3+} to the LUV solution gives rise to the spectrum shown in Fig 6.3. This spectrum shows separate signals arising from the ^{31}P in the inner (upfield peak) and outer (downfield peak) head groups of the LUV. By integrating these signals an O : I ratio of 1.1 is obtained, thus confirming that the vesicles prepared are predominantly large and unilamellar with an average diameter of about 250 - 300 nm.

However further ^{31}P spectra taken a few hours after the addition of Pr^{3+} ions revealed a downfield shift of signal I towards signal O. This indicates that the vesicles produced are permeable to Pr^{3+} ions, but the degree of permeability was seen to vary among different preparations. These factors eliminated the possibilities of T_1 measurements on the separate signals and the study of transbilayer ion

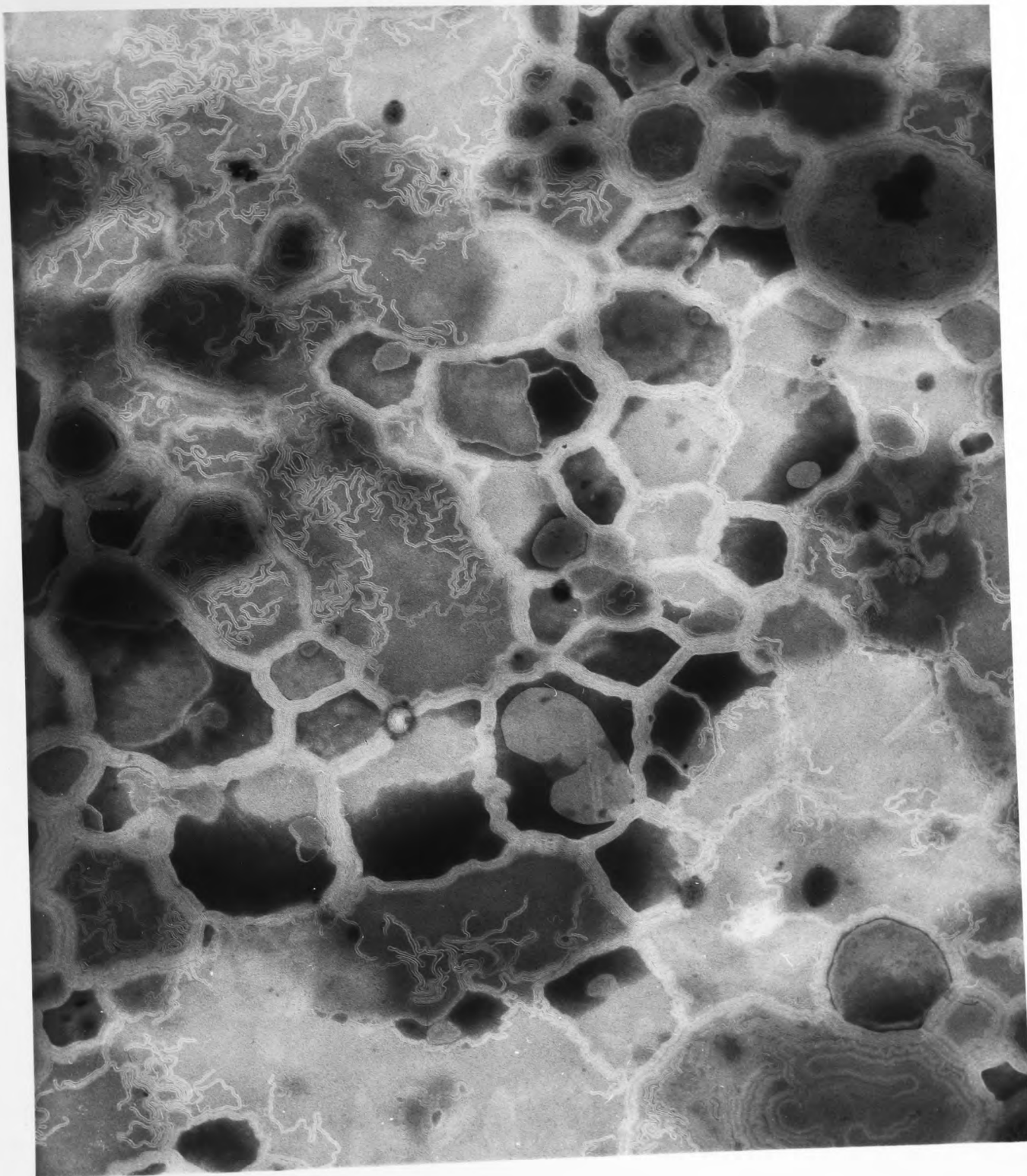
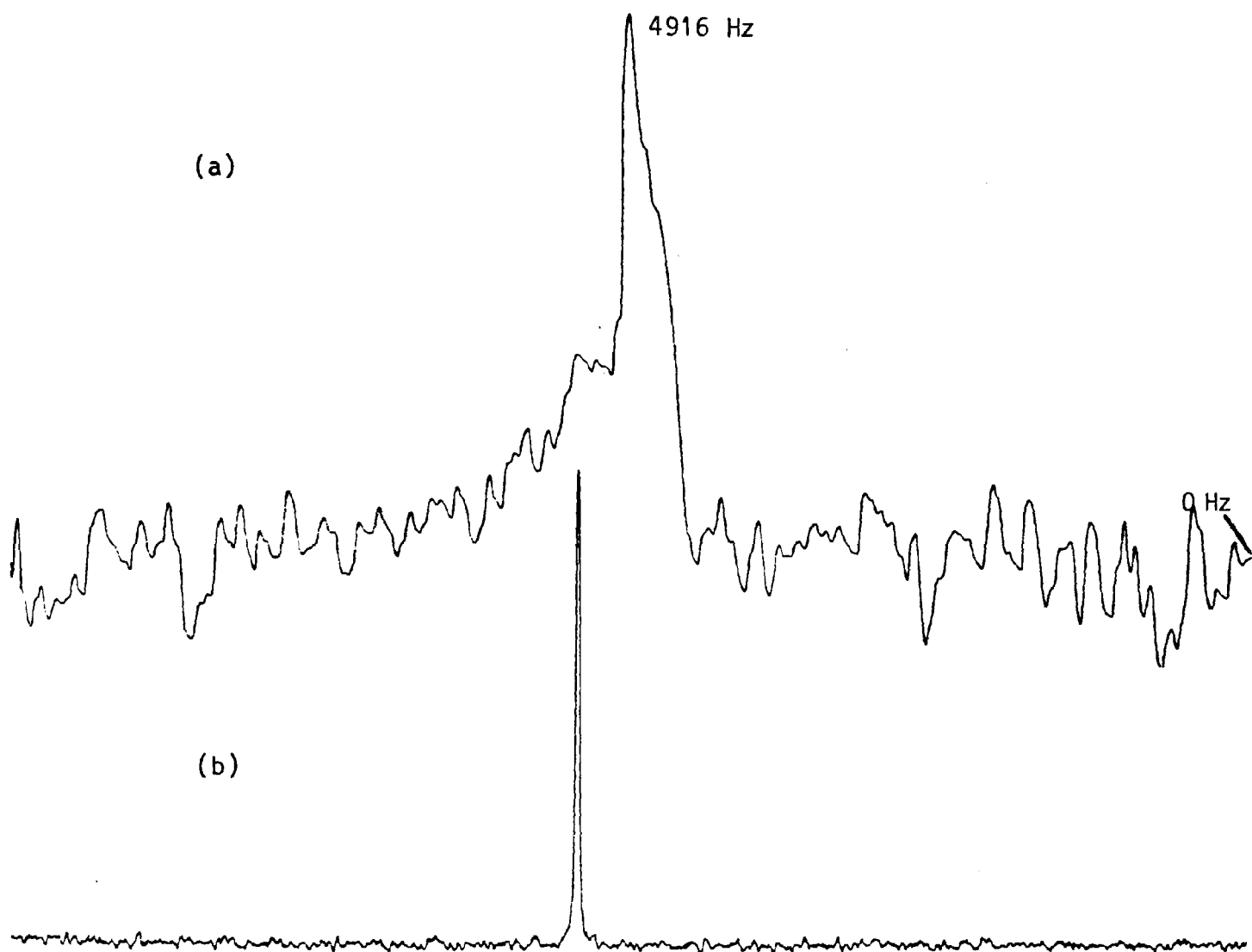


Fig 6.1 Electron micrograph of negatively stained large unilamellar egg PC vesicles taken with a magnification of 100,000. The vesicles are fairly uniform in size and free from multilamellar structures. The average diameter of the vesicles is 250 nm.



^{31}P Fig 6.2 ^{31}P -NMR spectra of: a. large unilamellar egg PC vesicles, b. sonicated egg PC vesicles.

The spectral width and offset in both cases is 10 KHz and 42 KHz respectively. See text for further NMR details.

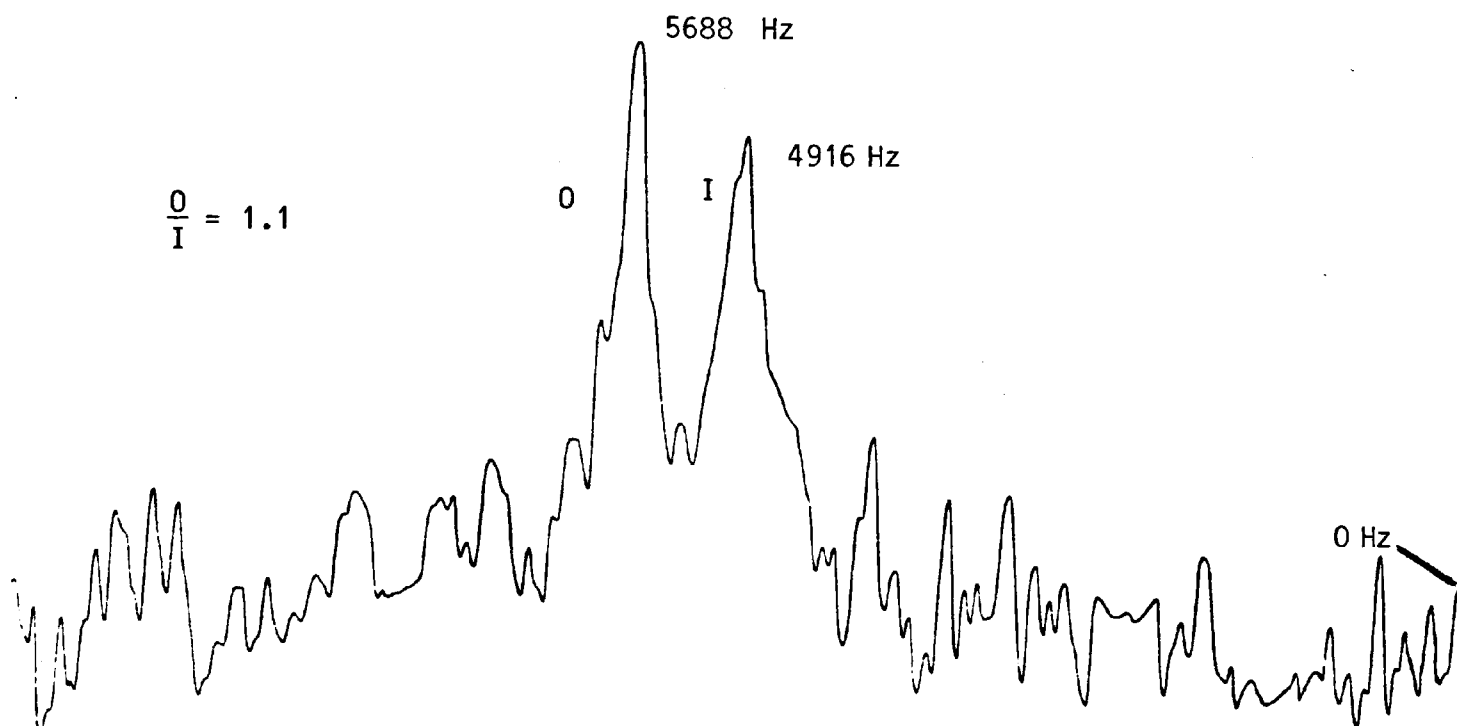


FIG 6.3 ^{31}P -NMR of large unilamellar egg PC vesicles with an extravesicular concentration of 100 mM Pr^{3+} . Refer to Fig 6.2 and text for details.

transport by various ionophores.

6.4 Discussion

The detergent removal method employed here has been successful in the preparation of LUV, as is shown in the electron micrograph in Fig 6.1. The ^{31}P -NMR spectrum showing a chemical shift anisotropy of about 40 ppm indicates that the vesicles in the preparation have an average diameter in excess of 200 nm (Burnell et al 1980b). Altering the egg PC concentration in the initial phospholipid - detergent solution or altering the volume of buffer, resulted in the formation of smaller vesicles contaminated with a small quantity of multilamellar structures (results not shown). These observations indicate that the rate of detergent removal and possibly the initial solubilisation of the lipid are critical factors in determining the type of vesicles produced. Previous studies have also concluded that such factors are critical in the formation of LUV (Mimms et al 1981, Jackson et al 1982).

The preparation of LUV by detergent (octyl glucoside) removal is considered to be dictated by kinetic events during the octyl glucoside removal from the mixed micelles (Mimms et al 1981). ^{31}P -NMR studies on such a system showed that three distinct stages are involved. In the first stage the ratio of detergent to lipid in the mixed micelles decreases, with a corresponding increase in the size of the micelles. The next stage involves the conversion of the mixed micelles into a mixed bilayer phase, which proceeds until all the micellar phase has disappeared. The final stage involves removal of detergent molecules which are associated with the lipid bilayer phase. The final stage is considered to be much slower than the first two stages and is reflected

in the long period required for dialysis (see materials and methods).

The permeability of LUV to Pr^{3+} ions is more likely a consequence of residual octyl glucoside associated with the lipid in the bilayer. This residual detergent may possibly be removed by dialyzing for a longer period or possibly by passing the LUV down a sepharose column. The latter method has previously been employed in which impermeable LUV were obtained (Mimms et al 1981). However in another study a similar method gave rise to LUV which were permeable to Mn^{2+} , which was also attributed to residual detergent (Jackson et al 1982).

The longer T_1 value (1.7 seconds) obtained from the LUV indicate that the phosphate groups in these bilayers are experiencing a greater degree of motional freedom than the phosphate groups in the bilayers of small vesicles, which have a shorter relaxation time (1.2 seconds). The increased mobility in LUV suggests that the bilayer curvature gives packing restrictions which are much less apparent in LUV than in the bilayers of small vesicles. Alternatively these values may result from a difference in correlation time. The correlation time in LUV is expected to be longer than in small vesicles. This may place the LUV in a range where the T_1 is increasing (see Fig 2.2).

The results obtained here and from a recent publication stress the importance of improving existing methods for preparing vesicles as well as introducing new ones so that it would be possible in the future to optimize the vesicle preparation so that a specific clinical objective can be met (Hauser 1982). New methods (including recently available commercial equipment such as: a. Lipoprep, Roth Scientific, Alpha House, Alexandra road, Farnborough, Hants. b. LUVETS, Sciema Technical Services, 9500 Cambie Road, Richmond, B.C. Canada and also refer to Hope et al 1984) are expected to increase the number of

successful applications of lipid vesicles as drug carriers and as models for studying transport kinetics.

CHAPTER 7

GENERAL CONCLUSION

In conclusion, the studies presented in this thesis have demonstrated quite clearly the potential of the NMR technique in the study of model membranes. The functional significance of non bilayer phases in membrane events and the role of hydrogen-bonds in the proposed action of the general anaesthetics give a large scope for further studies to be carried out by NMR methods.

Further studies in relation to those carried out in this thesis may include:

- a. The preparation of large unilamellar vesicles of a variety of sizes (by use of Lipoprep and/or LUVETS as explained in chapter 6) and the reconstitution of membrane proteins such as acetyl choline receptors and Na^+/K^+ ATPase.
- b. The use of other magnetic nuclei to monitor transport by channels and carriers, for example ^{23}Na -NMR for monitoring ^{23}Na transport into large unilamellar vesicles by gramicidin.
- c. The use of NMR pulse sequences such as saturation transfer (De Kruijff et al 1980) which may be employed to quantify the various phases present in bilayers.
- d. The extension of the work on general anaesthetics to a greater range of general anaesthetics (such as halothane and methoxy fluorane) and local anaesthetics, and the study of their effects on a variety of lipid mixtures (for phase properties), ionophores and reconstituted protein.
- e. Further investigation on small and large unilamellar vesicles with PLA_2 and bile salts using a variety of lipid compositions (for

example, cholesterol, stearylamine, dicetyl phosphate, sphingomyelin and phosphatidic acid) for the developement of resistive bilayers. The size of the pores in inverted micelles may be measured by the use of ions with various ionic radii. Futher extension to the work on drug targeting may also include the interaction of vesicles (of various composition) with lipoproteins for targeting by the intravenous route.

REFERENCES

- Akitt J W (1973). NMR and Chemistry. John Wiley.
- Allegrini P.R, Van Scharrenburg G, De Haas G H and Seelig J (1983).
Biochim. Biophys. Acta. 731, 448-455.
- Alonso A, Villena A and Goni F M (1981). FEBS Lett. 123, 200-204.
- Antanov V F, Petrov V, Molnar A A, Predvoditelev D A and Ivanov A S
(1980). Nature, 283, 585-586.
- Balaasubramanian T M, Kendrick N C E, Taylor M, Marshall G R, Hall J E,
Vodyanoy I and Reusser F (1981). J. Am. Chem. Soc. 103, 6127.
- Bangham A D, Standish M M and Watkins J C (1965). J. Mol. Biol. 13, 238.
- Bangham A D (1968). Progress in Biophysics and Molecular Biology.
(Editors: Butler J A V and Noble D); Pergamon , 29-95.
- Bangham A D, Hill M W and Miller N G A (1974). Methods in Membrane
Biology. (Editor: Korn E); Plenum Press, 1-68.
- Bar R S, Deamer D W and Cornwell D G (1966). Science, 153, 1010-1012.
- Baumann G and Mueller P (1974). J of Supramol. Struct. 2, 538-557.
- Bayer M E and Remsen C C (1970). J. Bacteriol. 101, 303.
- Berden J A, Barker R W and Radda G K (1975a). Biochim. Biophys. Acta.
375, 186-208.
- Berden J A, Barker R W and Radda G K (1975b). Biochim. Biophys. Acta.
436, 729.
- Bergelson L D, Barsukov L I, Dubrovnia N I and Bystrov V F (1970). Dokl.
Akad. Nauk. SSSR. 194, 708.
- Bergelson L D (1977). Methods in Membrane Biology, Vol.9 (Editor:
Korn E). Plenum Press, 275-335.
- Bergelson L D and Barsukov L I (1977). Science, 224-30.
- Bett N J and Wells M S (1980). J. of Colon and Rectum, 23(6), 408-410.
- Barker J L (1975). Brain Res. 92, 35-55.

- Billington D and Coleman R (1978). *Biochim. Biophys. Acta.* 509, 33-47.
- Bittman R and Blau L (1972). *Biochemistry*, 11(25), 4831-4839.
- Blackberg L, Hernell O and Olivecona T (1981). *J. Clin. Invest.* 67(6), 1748-1752.
- Blok M C, Vander Neutkok E C M, Van Deenen L L M and De Gier J (1975). *Biochim. Biophys. Acta.* 406, 187-196.
- Boggs J M (1980). *Can. J. of Biochem.* 58(10), 755-770.
- Boheim G and Kolb H A (1978). *J. Memb. Biol.* 38, 99-150.
- Bowman W C and Rand M R (1980). *Textbook of Pharmacology* (second edition). Blackwell Scientific Publications, Oxford.
- Brasure E B, Henderson T O, Glonek T, Pattniak N M and Stanu A M (1978). *Biochemistry*, 17(19), 3934-3938.
- Bretsher M S (1973). *Science*, 181, 622-629.
- Brockerhoff H (1974). *Lipids*, 9, 645-650.
- Brockerhoff H (1982). *Lipids*, 17, 1001-1003.
- Browning J L (1981). *Liposomes: From Physical Structure to therapeutic application.* (Editor: Knight C G). Elsevier, chapter 7.
- Built G, Galley H U, Seelig A, Seelig J and Zacai G (1978). *Nature*, 271, 182-184.
- Burnell E, Van Alphen, Verkleij A J and De Kruijff B (1980a). *Biochim. Biophys. Acta.* 597, 492-501.
- Burnell E, Cullis P R and De Kruijff B (1980b). *Biochim. Biophys. Acta.* 603, 63-69.
- Burns R A and Roberts M F (1980). *Biochemistry*, 19, 3100-3106.
- Bystrov V F, Dubronivia N I, Barsukov L I and Bergelson L D (1972). *FEBS Lett.* 25, 337.
- Chaney M O, Jones M D and Debono M (1976). *J. Antibiotics*, 29, 422.

- Chapman D, Williams R M and Ladbroke B D (1967). *Chem. Phys. Lipids*, 1, 445-475.
- Chapman D, Kamat V B, De Gier J and Penkett S A (1968). *J. Mol. Biol.* 31, 101.
- Chapman D, Cherry R J, Finer E G, Hauser H, Phillips M C, Shipley G G and McMullen A I (1969). *Nature*, 224, 692.
- Chapman D and Chen S (1972). *Chem. Phys. Lipids*, 8, 318.
- Chapman D and Urbina J (1974). *J. Biol Chem.* 249(8), 2512-2521.
- Chapman D (1975). *Quart. Rev. Biophys.* 8(2), 185-235.
- Chapman D (1982). *Biological Membranes Vol 4*. (Editor: Chapman D). Academic Press. Chapter 4.
- Chen S T (1978). Ph.D Dissertation, State University of New York, Stony Brook, New York.
- Cherry R J, Chapman D and Graham D E (1972). *J. Memb Biol.* 7, 325-344.
- Chin J H and Goldstein D B (1977a). *Science*, 197, 684-685.
- Chin J H and Goldstein D B (1977b). *Mol. Pharmacol.* 13, 435-441.
- Chruszczuk A, Wishnia A and Springer C S Jr (1977). *Biochim. Biophys. Acta.* 470, 161-169.
- Chruszczuk A, Wishnia A and Springer C S Jr (1981). *Biochim. Biophys. Acta.* 648, 28-48.
- Church J and Zsoter T T (1980). *Can. J. Physiol. Pharmacol.* 58, 254.
- Ciofalo F R (1980). *Proc West Pharmacol. Soc.* 23, 441-448.
- Clement N R and Gould J M (1981). *Biochemistry*, 20, 1544.
- Coleman R, Holdsworth G and Vyvoda O S (1978). *Membrane alteration as basis of liver injury*, 143-156.
- Coleman R, Lowe P J and Billington D (1980). *Biochim. Biophys. Acta.* 559, 294-300.
- Conrad M J and Singer S J (1981). *Biochemistry*, 20, 808-818.

- Copeland B R and McConnell H M (1980). *Biochim. Biophys. Acta.* 599, 95-109.
- Cornell B A, Middlehurst J and Separvic F (1980). *Biochim. Biophys. Acta.* 598, 405-410.
- Cotman C, Blank M C, Moehl A and Snyder F (1969). *Biochemistry*, 8, 4606.
- Cullis P R and De Kruijff B (1976). *Biochim. Biophys. Acta.* 436, 523-540.
- Cullis P R, De Kruijff B and Richards R E (1976). *Biochim. Biophys. Acta.* 426, 433-446.
- Cullis P R (1976). *FEBS Lett.* 70(1), 223-228.
- Cullis P R and McLaughlin S (1977). *Trends Biochem. Soc.* 196-199.
- Cullis P R, Verkleij A and Ververgaert P H J Th (1978a). *Biochim. Biophys. Acta.* 513, 11-20.
- Cullis P R, Van Dijck P W M, De Kruijff B and De Gier J (1978b). *Biochim. Biophys. Acta.* 513, 21-30.
- Cullis P R and De Kruijff B (1978a). *Biochim. Biophys. Acta.* 513, 31-42.
- Cullis P R and De Kruijff B (1978b). *Biochim. Biophys. Acta.* 507, 207-218.
- Cullis P R and Hope M J (1978). *Nature*, 271, 672-674.
- Cullis P R and De Kruijff (1979). *Biochim. Biophys. Acta.* 559, 399-420.
- Cullis P R, De Kruijff B, Hope M J, Nayar R and Schmid S L (1980a). *Can. J. Biochem.* 58(10), 1091-1100.
- Cullis P R, De Kruijff B, Hope M J, Nayar R, Rietveld A and Verkleij A J (1980b). *Biochim. Biophys. Acta.* 600, 625-635.
- Cullis P R, Hornby and Hope M J (1980c). *Progress in Anaesthesiology* Vol.2. (Editor: Fink B). Raven Press, 397-403.
- Cullis P R and Hope M J (1980). *Biochim. Biophys. Acta.* 597, 533-542.

- Cullis P R, De Kruijff B, Hope M J, Verkleij A J, Nayar R, Farren S B, Tilcock C, Madden T D and Bally M B (1983). Membrane Fluidity in Biology - Concepts of Membrane Structure. Academic Press, chapter 2
- Darke A, Finer E G, Flook A G and Phillips M C (1972). J. Mol Biol. 63, 265-279.
- Dawson R M C, Hemington N C and Irvine R F (1983). Biochem. Biophys. Res. Commun. 117, 196-201.
- Deedwana P C (1982). Western J. of Medicine, 137, 24-31.
- Degani H (1978). Biochim. Biophys. Acta. 509, 357.
- Degani H and Lenkinski R E (1980). Biochemistry, 19, 3430.
- Degani H, Simon S and McLaughlin A C (1981). Biochim. Biophys. Acta. 646, 320.
- De Grip W J, Drenthe E H S, Van Echteld C J A, De Kruijff B and Verkleij A (1979). Biochim. Biophys. Acta. 558, 330-337.
- De Kruijff B, Van Dijck P W M, Demel R A, Schuijff A, Branes F and Van Deenen L L M (1974). Biochim. Biophys. Acta. 356, 1-7.
- De Kruijff B, Cullis P R and Radda C K (1975). Biochim. Biophys. Acta. 406, 6-20.
- De Kruijff B, Cullis P R and Radda C K (1976). Biochim. Biophys. Acta. 436, 729-740.
- De Kruijff B and Wirtz K W A (1977). Biochim. Biophys. Acta. 468, 318-326.
- De Kruijff B and Baken P (1978). Biochim. Biophys. Acta. 507, 38-47.
- De Kruijff B, Van Zoelen E J J and Van Deenen L L M (1978). Biochim. Biophys. Acta. 509, 537-542.
- De Kruijff B and Van Zoelen E J J (1978). Biochim. Biophys. Acta. 511, 105-115.
- De Kruijff B (1978). Biochim. Biophys. Acta. 506, 173-182.

- De Kruijff B, Verkleij A, Van Echteld C J A, Gerritsen W T, Mombers C, Noordam P C and De Gier J (1979a). *Biochim. Biophys. Acta.* 555, 200-209.
- De Kruijff B, Van Den Besselaar A M H D, Van den Bosch and Van Deenen L L M (1979b) *Biochim. Biophys. Acta.* 555, 181-192.
- De Kruijff B and Cullis P R (1980). *Biochim. Biophys. Acta.* 602, 477-490
- DeKruijff B, Morris G A and Cullis P R (1980). *Biochim. Biophys. Acta.* 598, 206-211.
- De Kruijff B, Verkleij A, Leanissen-Bijvelt, Van Echteld C J A, Hille J and Rijnbout H (1982). *Biochim. Biophys. Acta.* 693, 1-12.
- Demel R and De Kruijff B (1976). *Biochim. Biophys. Acta.* 457, 109-132.
- Demel R, Jansen J W C M, Van Dijck P W M and Van Deenen L L M (1977). *Biochim. Biophys. Acta.* 465, 1-10.
- Dluzewiski A R and Halsey M J (1980). *Progress in Anaesthesiology*, Vol 2. Molecular mechanisms of general anaesthesia (Editor: Fink B). Raven Press, 405-409.
- Dluzewiski A R and Halsey M J (1981). *Br. J. Anaesth.* 53, 184P.
- Donis J, Grandjean J, Grosjean H and Laszlo P (1981). *Biochem. Biophys. Res. Commun.* 102, 690-696.
- Dos Remedios C G (1981). *Cell Calcium*, 2, 29-51.
- Doyle C (1982). *Observer* April 18, 1.
- Duzgunes N, Wilschut J, Fraley R and Papahadjopoulos D (1981). *Biochim. Biophys. Acta.* 642, 182-185.
- Edmonds D T (1980). *Proc. Royal Soc. London*, B211, 51-62.
- Edmonds D T (1981). *Trends Biochem. Sci.* 6, 92-94.
- Eisenberg M, Hall J E and Mead C A (1973). *J. Memb. Biol.* 14, 143-176.

- Eisenberg M, Kleinberg M E and Shaper J H (1977). J. Ann. N.Y. Acad. Sci. 303, 281-291.
- Engelman D M and Rothman J E (1972). Nature, 247, 3694-3697.
- Fettiplace R and Haydon H (1980). Physiol. Rev. 60, 510-550.
- Finer G, Flook A G and Hauser H (1972). Biochim. Biophys. Acta. 260, 49-58.
- Fink B (1980). Progress in Anaesthesiology Vol 2 (Molecular Mechanisms of Anaesthesia). Raven Press.
- Flechenstein A (1977). Ann. Rev. Pharmacol. Toxicol. 17, 149-166.
- Foot M, Cruz T and Llandinin N (1982). Biochem. J. 208, 631-640.
- Forman J C, Monger J L and Gomperts B D (1973). Nature, 245, 249.
- Forsen S and Lindman B (1981). Methods in Biochemical Analysis, Vol 27. (Editor: Glick D). John Wiley, 289-486.
- Forsyth P A, Marcelja S, Mitchell D J and Ninham B W (1977). Biochim. Biophys. Acta. 469, 335-344.
- Fox R O and Richards F M (1982). Nature, 300, 325-30.
- Fraley R and Papahadjopoulos D (1981). Trends Biochem. Sci. 77-81.
- Franks N P and Lieb W R (1982). Nature, 300, 487-493.
- Fringeli U P and Fringeli M (1979). Proc. Nat. Acad. Sci. 76(8), 3852-3856.
- Fringeli U P (1980). J. Mol. Biol. 54, 203-212.
- Gadian D G (1982). Nuclear Magnetic Resonance and its application to living systems. Clarendon Press.
- Gally H-U, Niederberger W and Seelig J (1975). Biochemistry, 14(16), 3647.
- Gent M P N and Prestegard J H (1974). Biochemistry, 13, 4027-4033.
- Gerritsen W J, Van Zoelen E J J, Verkleij A, De Kruijff B and Van Deenen L L M (1979). Biochim. Biophys. Acta. 551, 248-259.

- Gerritsen W J, De Kruijff B, Verkleij A, De Gier J and Van Deenen L L M (1980). *Biochim. Biophys. Acta.* 598, 554-560.
- Gisin B F, Kobayashi S and Hall J E (1977a). *Proc. Nat. Acad. Sci.* 74(1), 115-119.
- Gisin B F, Kobayashi S, Davies D G and Hall J E (1977b). *Peptides. Proc. of the fifth peptide symp. (Editors: Goodman and Meienhofer). John Wiley and Sons.*
- Gisin B F, Davis, Borowaska, Hall J E and Kobayashi S (1981). *J. Am. Chem. Soc.* 103, 6373-6377.
- Gogelein H, De Smedt H, Van Driessche W and Borghgraef R (1981), 640, 185-194.
- Gomez-Poyou A and Gomez-Lojero C (1977). *Current Topics in Bioenergetics*, 6, 222-257.
- Goldstein D B and Chin J H (1981). *Fed. Proc.* 40(7), 2073-2076.
- Gomperts B D (1977). *The Plasmamembrane. Academic Press.*
- Gomperts B D, Bennett J P and Allan D (1981). *Eur. J. Biochem.* 117, 559.
- Gordon L G M and Haydon D A (1972). *Biochim. Biophys. Acta.* 255, 1014-1018.
- Gordon L G M and Haydon D A (1975). *Phil Trans. Royal Soc. London*, B.270(908), 433.
- Gordon L G M and Haydon D A (1976). *Biochim. Biophys. Acta.* 436, 541-456
- Grandjean J and Laszlo P (1982). *Biochem. Biophys. Res. Commun.* 104(4), 1293-97.
- Gray J A (1978). *Br. J. Psychol.* 69, 417-434.
- Gregoriadis G and Davis L (1979). *Biochem. Biophys. Res. Commun.* 89, 1287-1293.

- Gregoriadis G and Allison A C (1980). *Liposomes in Biological Systems*. John Wiley.
- Gregoriadis G (1981). *Lancet*, 241-246.
- Griffith O H, Dehinger P J and Van S P (1974). *J. Memb. Biol.* 15, 159-192.
- Hall J E (1975). *Biophys. J.* 15, 934.
- Hall J E (1978). *Membrane Transport in Biology Vol.1 Concepts and Models*. (Editor: Tosteson). Springer Verlag, chapter 13.
- Hall J E (1981). *Membrane Transport*. (Editors Bonting and De Pont). Elsevier, chapter 4.
- Hashimoto A and Kawada J (1979). *Endocrinology (Japan)*, 26(3), 337-344.
- Hauser H and Dawson R M C (1967). *Eur. J. Biochem.* 1, 61-69.
- Hauser H, Finer E G and Chapman D (1970). *J. Mol. Biol.* 53, 419-433.
- Hauser H, Phillips M C, Levine B A and Williams R J P (1975). *Eur. J. Biochem.* 58, 133-144.
- Hauser H, Phillips M C, Levine B A and Williams R J P (1976). *Nature*, 261, 390-395.
- Hauser H, Levine B A and Williams R J P (1976b). *Trends in Biochem. Sci.* December, 278-282.
- Hauser H, Hinckely C L, Krebs J, Levine B A, Phillips M C and Williams R J P (1977). *Biochim. Biophys. Acta.* 468, 364-377.
- Hauser H (1982). *Trends Biochem. Sci.* 3(7), 274-277.
- Haydon D A and Hladky S B (1972). *Quart. Rev. Biophys.* 5(2), 187.
- Haydon D A, Hendry B M, Levinson S R and Requena J (1977). *Biochim. Biophys. Acta.* 470, 17-34.
- Hendler R W (1971). *Physiol Rev.* 51(1), 66-97.
- Hendry B M, Urban B W and Haydon D A (1978). *Biochim. Biophys. Acta.* 513, 106-116.

- Hill M W (1975). *Biochem. Soc. Trans.* 3, 149-152.
- Hill M J (1977). *Origins of Human Cancer*, 1027-39.
- Hinckley C L (1969). *J. Am. Chem. Soc.* 91, 5160.
- Hitchcock P B, Mason R, Thomas K M and Shipley G (1974). *Proc. Nat. Acad. Sci.* 71, 3036-3040.
- Hokin L E (1981). *J. Memb. Biol.* 60, 77-93.
- Hope M J, Bally M B, Webb G and Cullis P R (1984). *Biochemistry* (in press)
- Hornby A P and Cullis P R (1981). *Biochim. Biophys. Acta.* 647, 285-292.
- Horrobin D (1979). *Lancet*, 5th May.
- Horwitz A F, Michaelson D and Klein M P (1973). *Biochim. Biophys. Acta.* 298, 1.
- Houslay M D and Stanley K K (1982). *Dynamics of Biological Membranes.* John Wiley.
- Huang C (1969). *Biochemistry*, 8(1), 344.
- Huang C, Sipe J P, Chow S T and Martin R B (1974). *Proc. Nat. Acad. Sci.* 71(2), 359-362.
- Hubbel W C and McConnell (1971). *J. Am. Chem. Soc.* 93, 314-326.
- Hui S W and Stewart T P (1981). *Nature*, 290, 427.
- Hui S W, Stewart T P, Yeagle P L and Albert A D (1981). *Arch. of Biochem Biophys.* 207(2), 227-240.
- Hui S W and He N (1983). *Biochemistry*, 22, 1159-1164.
- Hunt G R A (1975). *FEBS. Let.* 58, 194-196.
- Hunt G R A and Tipping L R H and Belmont M R (1978). *Biophys. Chem.* 8, 341-355.
- Hunt G R A and Tipping L R H (1978). *Biochim. Biophys. Acta.* 507, 242-261.

- Hunt G R A (1980a). *Chem. Phys. Lipids*, 27, 353-364.
- Hunt G R A (1980b). *FEBS. Let.* 119, 132-136.
- Hunt G R A and Jawaharlal K (1980). *Biochim. Biophys. Acta.* 601, 678-684
- Hunt G R A and Jones I C (1982). *Biosci. Rep.* 2, 921-928.
- Hunt G R A and Jones I C (1983). *Biochim. Biophys. Acta.* 736, 1-10.
- Hunt G R A and Jones I C (1984). *J. of Microencapsulation*, in press.
- Hunt G R A, Jones I C and Veirol J (1984). *Biosci. Rep.* 4, 403-413.
- Hutton W C, Yeagle P L and Martin R B (1977). *Chem. Phys. Lipids*, 9, 255-265.
- Inagaki F and Migazawa T (1981). *Prog. in NMR. Spec.* 14, 67-111.
- Inoue K and Kitagawa T (1976). *Biochim. Biophys. Acta.* 426, 1-16.
- Israelachvili J N, Mitchell J and Ninham B W (1977). *Biochim. Biophys. Acta.* 470, 185-201.
- Israelachvili J N, Marcelja S and Horn D G (1980). *Quart. Rev. Biophys.* 13, 121-200.
- Jackson D A, Schmidt C F, Lichtenberg D, Litman B J and Albert A D (1982). *Biochemistry*, 21, 4576-4582.
- Jacobs R E and Oldfield E (1981). *Prog. in NMR. Spec.* 14(3), 113-136.
- Jain M K (1972). *The Bimolecular Lipid Membrane*. Van Nostrand.
- Jain M K and Wu N Y M (1977). *J. Memb. Biol.* 34, 157-201.
- Jain M K, Van Echteld C J A, Ramez F, De Gier J, De Haas G and Van Deenen L L M (1980). *Nature*, 284, 486-487.
- Jain M K and De Haas G (1981). *Biochim. Biophys. Acta.* 642, 203-211.
- Jain M K and De Haas G (1983). *Biochim. Biophys. Acta.* 736, 157-162.
- Jain M K, Egmond M R, Verkleij A, Apitz-Castro R, Dijkman R and De Haas G (1982). *Biochim. Biophys. Acta.* 688, 341-348.

- Janiak M J, Small D M and Shipley G G (1976). *Biochemistry*, 15(21), 4575-4580.
- Janoff A S and Miller K W (1982). *Biological Membranes Vol.4*. (Editor: Chapman D). Academic Press, 417-476.
- Johnson D A, Lee N M, Cooke R and Loh H H (1979). *Mol. Pharmacol.* 15, 739-746.
- Jung G, Bruckner H and Oekonomopulos R (1979). *Proc. Am. Peptide Symp.* 647-657.
- Jung G, Katz E, Schmitt H, Voges K, Manistrina G and Boheim G (1982). *Studies in Physical and Theoretical Chemistry Vol.24*. The Physical Chemistry of Transmembrane Ion Motion. (Editor: Spach G). Elsevier, 647-658.
- Kamaya H, Ueda I and Eyring H (1980). *Progress in Anaesthesiology Vol 2*. (Editor: Fink B). Raven Press, 429-432.
- Kamaya H, Kaneshina S and Ueda I (1980). *Biochim. Biophys. Acta.* 646, 135-142.
- Kanehisa M I and Tsong T Y (1978). *J. Am. Chem. Soc.* 100(2), 424-432.
- Kates R E (1983). *Drugs*, 25, 113-124.
- Katsikas H and Quinn P J (1981). *FEBS Let.* 133(2), 230-234.
- Katz A M and Messinero F C (1981). *Am. Heart J.* 102(32), 491.
- Kim S and Martin G M (1981). *Biochim. Biophys. Acta.* 646, 1-9.
- Kirby C and Gregoriadis G (1981). *Biochem. J.* 199, 251-254.
- Knight C G (1981). *Liposomes: From Physical Structure to Therapeutic Applications*. Elsevier N.Holland Biomedical Press.
- Knowles P E, Marsh D and Rattle H W E (1976). *Magnetic Resonance of Biomolecules*. John Wiley.
- Koehler L S, Fossel E T and Koehler K A (1977). *Biochemistry*, 16, 3700-3707.

- Koehler K A, Jain M K, Stone E E, Fossel E T and Koehler L S (1978).
Biochim. Biophys. Acta. 510, 177-185.
- Korenbrodt J I (1977). Ann. Rev. Physiol. 39, 19-49.
- Kornberg R D and McConnell H M (1971). Biochemistry, 10, 111.
- Koynova R D and Tenchov B G (1983). Biochim. Biophys. Acta. 727, 351-356
- Ladbrooke B D, Williams R M and Chapman D (1968). Biochim. Biophys.
Acta. 150, 333.
- Ladbrooke B D and Chapman D (1969). Chem. Phys. Lipids. 3, 304-357.
- Latorre R, Alvarez O and Hall J E (1976). Biophys. J. 16, 80a.
- Latorre R and Donovan J J (1980). Acta. Physiol. Scand. Suppl. 481,37.
- Latorre R, Miller C G and Quay S (1981). Biophys J. 36(3), 803-809.
- Latorre R and Alvarez O (1981). Physiol. Rev. 61(1), 77-150.
- Lau A L Y and Chan S I (1974). Biochemistry, 13(24), 4942.
- Lau A L Y and Chan S I (1975). Proc. Nat. Acad. Sci. 72(6), 2170-2174.
- Lau A L Y and Chan S I (1976). Biochemistry, 15(12), 2551.
- Lauger P (1972). Science, 178, 24-30.
- Lawaczeck R, Kainoshio M and Girardet J (1975). Nature, 256, 584.
- Lawaczeck R, Kainoshio M and Chan S I (1976). Biochim. Biophys. Acta.
443, 313-330.
- Lee A G, Birdsall N J M and Metcalfe J C (1973). Biochemistry, 12, 1650.
- Lee A G (1975). Prog. Biophys. Mol. Biol. 29(1), 3-56.
- Lee A G, Birdsall N J M and Metcalfe J C (1974). Methods in Membrane
Biology Vol 2. (Editor: Korn B). Plenum Press, 1-156.
- Lee A G (1976). Nature, 262, 545-548.
- Lentz B R, Barrow D A and Hoechli M (1980). Biochemistry, 19, 1943-1954.
- Levine Y K, Birdsall N J M, Lee A G and Metcalfe J C (1972).
Biochemistry, 11, 1416.

- Levine Y K (1973). Progress in Surface Science Vol.3. (Editor: Davison), Pergamon, 279-352.
- Levine Y K, Birdsall N J M, Metcalfe J C and Robinson J D (1973). Biochim. Biophys. Acta. 291, 392.
- Liao M J and Prestegard J H (1980). Biochim. Biophys. Acta. 559, 81-94.
- Lippert J C and Peticolas W L (1971). Proc. Nat. Acad. Sci. 68, 1572-1576.
- Lis L J, Lis W T, Parsegian V A and Rand R P (1981). Biochemistry, 20, 1771-1777.
- Litman B J (1975). Biochim. Biophys. Acta. 413, 157.
- Lucy J A (1978). Cell Surface Reviews Vol.5. (Editors: Poste G and Nicolson G L). Elsevier, 267-304.
- Luzzati V, Reiss-Husson F, Rivas E and Gullick-Krzywcki R (1966). Ann N.Y. Acad. Sci. 137, 409-413.
- Luzzati V (1968). Biological Membranes. Physical Fact and Function. (Editor: Chapman D). Academic Press.
- Luzzati V and Tardieu A (1974). Ann. Rev. Phys. Chem. 25, 79-94.
- MacDonald R C, Simon S A and Baer E (1976). Biochemistry, 15, 885-891.
- Machy P and Leserman L D (1983). Biochim. Biophys. Acta. 730, 313-320.
- MacLeod S M, Giles H G, Patzalek G, Thiessen J I and Sellers E M (1977). Europ. J. Clin. Pharmacol. 11, 345-349.
- Mandersloot J G, Gerritsen W J, Leunissen-Bijvelt J, Van Echteld C J A, Noordam P C and De Gier J (1981). Biochim. Biophys. Acta. 640, 106-113.
- Marcelja S (1979). Biochim. Biophys. Acta. 555, 362-367.
- Marcelja S and Wolfe J (1979). Biochim. Biophys. Acta. 557, 24-31.
- Marsh D (1975). Essays in Biochemistry Vol 11. (Editors: Campbell P N and Marshall RA) Academic Press, 139-180.

- Marshall G R and Balasubramanian T M (1979). Proc. Am. Peptide Symp. 639-646.
- Martin D R and Williams R J P (1976). Biochem. J. 153, 181-190.
- Martin G P and Martin J (1981). J. Mol. Pharmacol. 31, 754-759.
- Mas-Oliva J and Nayar W G (1980). Br. J. Pharmacol. 70, 617-624.
- Mathew M K and Balaram P (1983). Mol. and Cellular Biochem. 50, 47-64.
- Mayo B C (1973). Chem. Soc. Rev. 2, 49-74.
- McLaughlin A C, Herbette L, Blaise J, Wang C, Hymel L and Fleisher L (1981). Biochim. Biophys. Acta. 643, 1-16.
- McLaughlin A C, Herbette L, Blaise J, Wang C, Hymel L and Fleisher L (1982). Biophys. J. 37, 49-50.
- McIntosh T J (1978). Biochim. Biophys. Acta. 513, 43-58.
- McIntosh T J, Ting-Beall R and Zampighi G (1982). Biochim. Biophys. Acta. 685, 51.
- Melling J and McMullen A I (1975). ISC-IAMS. Proc. Sci. Japan, 5 446-452.
- McNamee P and McConnell H M (1973). Biochemistry, 12, 2951.
- Michaelson D M, Horwitz A F and Klein M P (1973). Biochemistry, 12, 2637.
- Michell R H (1975). Biochim. Biophys. Acta. 415, 81-147.
- Michell R H (1979). Trends in Biochem. 4, 128-131.
- Michell R H and Kirk C J (1981). Trends in Pharmacol. Sci. 2, 86-89.
- Middleton E, Drzewiecki G and Triggle R (1981). Biochem. Pharmacol. 30, 2867-2869.
- Miller S C (1961). Proc. Nat. Acad. Sci. 47, 1515-1524.
- Miller R G (1980). Nature, 287, 166-167.
- Mirghani Z E M (1982). Ph.D. Dissertation, Polytechnic of Wales.

- Mimms L T, Zampighi G, Nozaki Y, Tanford C and Raynolds T A (1981). *Biochemistry*, 20, 833-840.
- Montal M and Miller P (1972). *Proc. Nat. Acad. Sci.* 69, 3561.
- Mountcastle D B, Biltonen R L, and Halsey M J (1978). *Proc. Nat. Acad. Sci.* 75(10), 4906-4910.
- Mueller P, Rudin D O, Tien H T and Westcott W C (1962). *Circulation*, 26, 1167.
- Mueller P and Rudin D O (1968). *Nature*, 217, 713.
- Mullins L J (1954). *Chem. Rev.* 54, 289-323.
- Nalbone G, Lairon D, Charbonnier-Augeire M, Vigne J L, Leonardi J, Chabert C, Hauton J L and Verger R (1980). *Biochim. Biophys. Acta.* 620(3), 612-626.
- Nayar R, Hope M J and Cullis P R (1982). *Biochemistry*, 21, 4583-4589.
- Nishizuka Y (1983). *Phil. Trans. R. Soc. London*, B202, 101-112.
- Noordam P C, Van Echteld C T A, De Kruijff B, Verkleij A and De Gier J (1980). *Chem. Phys. Lipids*, 27, 221-232.
- Okimara E, Uibuyashi, Marinoto, Migahara and Utsumi (1982). *FEBS Lett.* 145(1), 82-86.
- Oldfield E and Chapman D (1971). *Biochem. Biophys. Res. Commun.* 43, 610-616.
- Op den Kamp J A F, Kauerz M T and Van Deenen L L M (1975). *Biochim. Biophys. Acta.* 406, 169-177.
- Opella S J, Yesinowski J P and Waugh J S (1976). *Proc. Nat. Acad. Sci.* 73, 3812-3815.
- Ovchinnikov Y A, Kiryushkin A A and Kozhevnikova I V (1971). *J. Gen Chem USSR.* 41, 2105-2116.
- Ovchinnikov Y A, Ivanov V T and Shkpob A M (1974). *Membrane Active Complexones.* Elsevier.

- Papahadjopoulos D and Miller N (1967). *Biochim. Biophys. Acta.* 135, 625-638.
- Papahadjopoulos D (1972). *Biochim. Biophys. Acta.* 265, 69.
- Papahadjopoulos D, Jacobson K, Nir S and Isac T (1973). *Biochim. Biophys. Acta.* 311, 330-348.
- Patel H M and Ryman B E (1977). *Biochem. Soc. Trans.* 5, 1139-1141.
- Patel H M, Harding H G L, Logue F, Kessor C, MacCuish A C, MacKenzie J C, Ryman B E and Scobie I (1978). *Biochem. Soc. Trans.* 6, 784-785
- Pauling L (1961). *Science*, 134, 15-21.
- Payne J W, Jakes R and Hartley B S (1970). *Biochem. J.* 117, 757-766.
- Phillips M, Williams R M and Chapman D (1969). *Chem. Phys. Lipids*, 3, 234-244.
- Phillips M, Chapman D and Finer E G (1972a). *Chem. Phys. Lipids*, 8, 127.
- Phillips M, Finer E G and Hauser H (1972b). *Biochim. Biophys. Acta.* 193, 35-44.
- Phillips M and Finer E G (1974). *Biochim. Biophys. Acta.* 356, 199-206.
- Pike M M, Simon S R, Balschi J A and Springer C S Jr (1982). *Proc. Nat. Acad. Sci.* 79, 810-814.
- Podo F (1975). *Biochimie.* 57, 461.
- Pope C G, Urban B W and Haydon D A (1982). *Biochim. Biophys. Acta.* 688, 279-283.
- Poste G (1980). *Liposomes in Biological Systems.* (Editors: Gregoriadis G and Allison A C). John Wiley, chapter 4.
- Pressman (1968). *Fed. Proc.* 27(6), 1283-1288.
- Presti F T and Chan S I (1982). *Biochemistry*, 21, 3821-3830.
- Putney J W (1978). *Pharmacol Rev.* 30, 209.
- Quay S C and Latorre R (1982). *Biophys. J.* 37, 154-156.

- Quinn P J (1976). *Molecular Biology of Cell Membranes*. MacMillan Press.
- Racker E (1972). *J. Biol. Chem.* 247, 8198-8200.
- Rand R P and Sengupta S (1972). *Biochim. Biophys. Acta.* 255, 484-492.
- Rand R P, Chapman D and Larsson K (1975). *Biophys. J.* 15, 1117.
- Razin S (1972). *Biochim. Biophys. Acta.* 265, 241-296.
- Reeves J P and Dowben R M (1969). *J. Cell. Physiol.* 73, 49.
- Rice D M, Meadows M D, Scheinman A O, Goni F M, Gomez-Fernandez J C, Moscarello M A, Chapman D and Oldfield E (1979). *Biochemistry*, 26, 5893-5903.
- Richards C D (1980). *Topical Reviews in Anaesthesia Vol 1*. (Editors: Norman J and Whitman J G). Wright and Sons, 1-84.
- Richards M H and Gardner C R (1978). *Biochim. Biophys. Acta.* 543, 508-522.
- Ringler M W and Patton J S (1983). *Biochim. Biophys. Acta.* 751, 444-454.
- Rinehart K C, Cook J C, Meng H, Olson K C and Padney R C (1977). *Nature*, 269, 832-833.
- Roberts F M, Adamish M, Robson R J and Dennis E A (1979). *Biochemistry*, 18(15), 3301-3308.
- Robertson D (1981). *J. Cell. Biol.* 91, 189-204.
- Roelofs B and Schatzmann H J (1977). *Biochim. Biophys. Acta.* 464, 17-36.
- Rojas E and Tobias J M (1965). *Biochim. Biophys. Acta.* 94, 394-404.
- Rosenberg P H (1980). *Progress in Anaesthesiology Vol.2*. (Editor: Fink B). Raven Press, 325-335.
- Rothman J E and Lenard J (1977). *Science*, 195, 743-753.
- Rouser G, Nelson G L, Fleicher S and Simon G (1968). *Biological Membranes. Physical Fact and Function*. (Editor: Chapman D). Academic Press, 5-69.

- Rowe E S (1982). *Mol. Pharmacol.* 22, 133-139.
- Rowe E S (1983). *Biochemistry*, 22(14), 3299-3305.
- Rowland M H and Woodley J E (1980). *Biochim. Biophys. Acta.* 620, 400-409
- Ryman B E and Tyrrell D A (1980). *Essays in Biochemistry Vol.16.*
(Editors: Campbell P N and Marshall R). Academic Press, 49-98.
- Sackmann E, Trauble H, Galla H J and Overath P (1973). *Biochemistry*,
12(26), 5360-5369.
- Sandermann H (1978). *Biochim. Biophys. Acta.* 515, 209-237.
- Sandorfy C (1980). *Progress in Anaesthesiology Vol.2.* (Editor: Fink).
Raven Press, 353-359.
- Saunders L, Perrin J and Gammack D B (1962). *J. Pharm. Pharmacol.* 14,
567.
- Schieren H, Rudolph S, Finkelstein M, Cole P and Weissmann G (1978).
Biochim. Biophys. Acta. 542, 137-153.
- Schlieper P and De Robertis E (1977). *Arch. Biochem. Biophys.* 184,
204-208.
- Seelig J (1970). *J. Am. Chem. Soc.* 92, 3881-3887.
- Seelig J and Niederberger W (1974). *Biochemistry*, 13(8), 1585-1588.
- Seelig J (1977). *Quart. Rev. Biophys.* 10(3), 35-39.
- Seelig J and Seelig A (1977). *Biochemistry*, 16(1), 45.
- Seeman P (1972). *Pharmacol. Rev.* 24, 583-655.
- Seelig J, Seelig A and Tamm L (1982). *Lipid-Protein Interactions, Vol 2.*
(Editors: Jost P C and Griffith O H). John Wiley, 127-148.
- Seixas F A (1978). *Currents in Alcoholism Vol.3.* Grimen and Statton,
407-417.
- Sen A, Brain A P R, Quinn P J and Williams W P (1982). *Biochim.*
Biophys. Acta. 686, 215-224.

- Serhan C N, Fridovich J, Goetzl E J, Dunham P B and Neissmann G (1982).
J. Biol. Chem. 257, 4746-4752.
- Shamoo A E and Murphy T J (1979). Current Topics in Bioenergetics Vol.9.
147-177.
- Shapiro Y E, Viktrov A V, Voikova V I, Barsukov L I, Bystrov V F and
Bergelson L S (1975). Chem. Phys. Lipids, 14, 227.
- Sheetz M P and Chan S J (1972). Biochemistry, 11, 4573.
- Shieh D D, Ueda I and Eyring H (1975). Progress in Anaesthesiology
Vol.1. (Editor: Fink B). Raven Press.
- Shieh D D, Ueda I, Lin H L and Eyring H (1976). Proc. Nat. Acad. Sci.
73, 3999-4042.
- Shimshick E J and McConnell H M (1973a). Biochemistry, 12(12),
3251-3260.
- Shimshick E J and McConnell H M (1973b). Biophys. Res. Commun. 53,
446-451.
- Singer S J and Nicolson G L (1972). Science, 175, 720-731.
- Singer S J (1973). Hospital Practice, May, 81-96.
- Slotboom A J, Verheij H M and De Haas G H (1982). Phospholipids.
(Editors: Howthorn J N and Ansell G B). Elsevier Biomedical Press,
359-434.
- Smith I C P (1977). Aldrichimica Acta. 10(3), 35-39.
- Smith I C P, Tallock A P, Stockton G W, Schrier S, Joyce A, Butler K W,
Boulanger Y, Blackwell B and Bennett L G (1978). Ann. N.Y. Acad.
Sci. 308, 8-28.
- Smith I C P (1979). Can. J. Biochem. 57(1), 1-14.
- Stark G and Benz R (1971). J. Memb. Biol. 5, 133.
- Steger L D and Desnick R J (1977). Biochim. Biophys. Acta. 464, 530-546.
- Stockton G W and Smith I C P (1976). Chem. Phys. Lipids, 17, 251-263.

- Strange R C (1981). *Biochem. Soc. Trans.* 170.
- Stubbs G W, Smith H G and Litman B J (1976). *Biochim. Biophys. Acta.* 425, 46-56.
- Taylor M G, Akiyama T, Saito H and Smith I C P (1982). *Chem Phys Lipids*, 31, 359-379.
- Thayer A M and Kohler S J (1981). *Biochemistry*, 20, 6831-6834.
- Tilcock C P S and Cullis P R (1981). *Biochim. Biophys. Acta.* 641, 189-201.
- Tilcock C P S and Cullis P R (1982). *Biochim. Biophys. Acta.* 684, 212-218.
- Tilcock C P S, Bally M B, Ferren S B and Cullis P R (1982). *Biochemistry*, 21, 4596-4601.
- Ting T Z, Hayan P S, Chan S I, Poll J O and Springer C S Jr (1981). *Biophys. J.* 34, 189-216.
- Trauble H and Sackmann E (1972). *J. Am. Chem. Soc.* 94, 4499.
- Trauble H and Eibl H (1974). *Proc. Nat. Acad. Sci.* 71(1), 214-219.
- Tyson C A, Van de Zande H and Green D E (1976). *J. Biol. Chem.* 251, 1326-1332.
- Van den Besselaar A M H P, De Kruijff B, Van den Bosch H and Van Deenen L L M (1979). *Biochim. Biophys. Acta.* 555, 193-199.
- Van den Bosch H (1982). *Phospholipids*. (Editors: Hawthorne J N and Ansell G B). Elsevier Biomedical Press, Chapter 9.
- Van den Bosch H, Aarsman A J and Van Deenen (1974). *Biochim. Biophys. Acta.* 348, 197-207.
- Vanderkooi J M, Landberg R, Selick H and McDonald G C (1977). *Biochim. Biophys. Acta.* 464, 1-16.
- Van der Steen A T M, De Jong W A L, De Kruijff B and Van Deenen (1981). *Biochim. Biophys. Acta.* 647, 63-72.

- Van Echteld C J A, Van Stigt R, De Kruijff B, Leunissen-Bijvelt J, Verkjeij A and De Gier J (1981). *Biochim. Biophys. Acta.* 648, 287-291.
- Van Echteld C J A, De Kruijff B, Verkleij A, Leunissen-Bijvelt J and De Gier J (1982). *Biochim. Biophys. Acta.* 692, 126-138.
- Van Ventie R V and Verkleij A J (1981). *Biochim. Biophys. Acta.* 645, 262-269.
- Van Zoelen E J J, De Kruijff B and Van Deenen L L M (1978). *Biochim. Biophys. Acta.* 508, 97-108.
- Verkjeij A, Mombers C, Gerritsen W J, Leunissen-Bijvelt J and Cullis P R (1979). *Biochim. Biophys. Acta.* 555, 358-361.
- Verkleij A J, Van Echteld C J A, Gerritsen W J, Cullis P R and De Kruijff B (1980). *Biochim. Biophys. Acta.* 600, 620-624.
- Verkleij A J, De Maayd R, Leunissen-Bijvelt J and De Kruijff B (1982). *Biochim. Biophys. Acta.* 684, 255-262.
- Vyvoda O S, Coleman R and Holdsworth G (1977). *Biochim. Biophys. Acta.* 465, 68-76.
- Wallace B A, Veatch W R and Boulton E R (1982). *Biophys. J.* 37, 197-199.
- Warren G B, Houslay M D, Metcalfe J C and Birdsall W J M (1975). *Nature*, 255, 684.
- Wekrell F W and Wirthlin T (1978). *Interpretation of Carbon-13 NMR Spectra.* Heyden.
- Westman J and Eriksson L E G (1979). *Biochim. Biophys. Acta.* 557, 62-78.
- White S H (1974). *Biochim Biophys Acta.* 356, 8-16.
- White S H, Peterson D C, Simon S and Yafuso M (1976). *Biophys. J.* 16, 481-489.
- Williams R J P (1970). *Quart. Rev.* 24, 331-356.

- Worcester D C and Franks N P (1976). J. Mol. Biol. 100, 359.
- Wu E S, Jacobson K and Papahadjopoulos D (1977). Biochemistry, 16, 3936.
- Wu E S, Jacobson K, Szoka F and Portis A (1978). Biochemistry, 17, 5543.
- Yatvin M B and Lelkes P I (1982). Med. Phys. 9(2), 149-175.
- Yeagle P C, Hutton W C, Martin R B, Sears B and Huang C (1976). J. Biol. Chem. 251(7), 2110-2112.
- Yellin N and Levin I W (1977). Biochim. Biophys. Acta. 468, 490-494.
- Yokono S, Shieh D D and Ueda I (1981). Biochim. Biophys. Acta. 645, 237-242.
- Young S P and Gomperts B D (1977). Biochim. Biophys. Acta. 469, 281-291.
- Zaslavsky B Y, Borovskaya A A, Davidovich Y A and Rogozhin S V (1981). Chem. Phys. Lipids, 28, 181-187.
- Zsoter T T (1980). Am. Heart J. 99, 805-810.
- Zsoter T T and Church J G (1983). 25, 93-112.

APPENDIX A

CALCULATION OF THE % LYSIS FROM THE O:I RATIO AND CALCULATION OF THE % FUSION FROM THE PEAK WIDTH OF THE HYDROCARBON SIGNAL

1. Calculation of the % lysis from the O:I ratio

Example

For O:I ratio increase from 1.7 to 3.1 :

$$\frac{O_i}{I_i} = \frac{1.7}{1} \quad \text{and therefore} \quad \frac{O_i + I_i}{I_i} = 2.7$$

$$\frac{O_i + I_L}{I_u} = \frac{3.1}{1} \quad \text{hence} \quad \frac{O_t + I_i}{I_i} = 4.1$$

We also have $O_t = O_i + I_L$ and $I_i = I_L + I_u$

where O_i = outside signal, initial intensity
 I_i = inside signal, initial intensity
 O_t = outside signal total intensity
 I_L = inside signal intensity for lysed vesicles
 I_u = inside signal intensity for unlysed vesicles

Substituting in the above equation we have :

$$\frac{O_i + I_L + I_u}{I_u} = 4.1$$

Let K represent the total area constant. Then :

$$\begin{aligned} K &= O_i + I_i = 2.7 I_i \\ &= O_i + I_L + I_u = 4.1 I_u \\ &= 4.1 I_u \end{aligned}$$

therefore:

$$4.1 I_u = 2.7 I_i$$

$$I_u = \frac{2.7}{4.1} I_i$$

$$\text{Fraction lysed} = 1 - \frac{2.7}{4.1} = \frac{1.4}{4.1} = 0.34$$

$$\text{Therefore \% of lysed vesicles} = 0.34 \times 100 = \underline{34 \%}$$

2. Calculation of the \% 1:1 fusion from the peak width at half height of the hydrocarbon signal

Based on the observations of Liao and Prestegard (1980)

100 \% fusion of each vesicle corresponds to the ratio:

$$\frac{55}{35} = 1.57 \quad \text{indicating that the hydrocarbon peak width has increased from 35 Hz to 55Hz}$$

Example

Initial peak width = 14.4 Hz

Final peak width = 17.4 Hz

$$\text{Ratio} = \frac{17.4}{14.4} = 1.2$$

Therefore:

$$\% \text{ of vesicles fused} = \frac{(1.2 - 1)}{(1.57 - 1)} \times 100 = \underline{35 \%}$$

APPENDIX B

POSTER PAPERS AND ORAL COMMUNICATIONS PRESENTED AT MEETINGS

Poster papers presented at:

1. RSC Symposium on Recent Advances in the Chemistry of Lipids,
Cambridge, September 1982.

HYDROPHILIC/HYDROPHOBIC INTERACTIONS of GENERAL ANAESTHETICS
with ION CHANNELS in LIPID MEMBRANES
G.R.A. Hunt & I.C. Jones
The Polytechnic of Wales,
Pontypridd, Cardiff,
Wales.

Channel-mediated transport of the lanthanide ion Pr^{3+} has been studied using an ^1H -NMR method. Channels are formed in dipalmitoyl phosphatidylcholine vesicular bilayers by (a) the gel to liquid crystal phase transition, (b) Triton X-100, (c) the polypeptide alamethicin 30. Transport is inhibited by chloroform but increased by ethanol and diethyl ether, independently of the method of channel formation (a), (b) or (c). All three compounds depress the phase transition temperature and fluidise the membrane. These results are therefore in favour of a hydrophilic model of anaesthetic action in which they affect the water structure of the ion channel, rather than a hydrophobic alteration in lipid structure or fluidity.

2. Symposium on the Use of Liposomes in Medicine,
Charing Cross Hospital Medical School, September 1983.
Liposomes by the oral route. NMR studies using small unilamellar vesicles reveal a synergistic attack by the bile salts and phospholipase A_2 . G R A Hunt and I C Jones.

3. Second SCI-RSC Medicinal Chemistry Symposium,

Cambridge, September 1983.

USE OF LANTHANIDE IONS, NMR SPECTROSCOPY AND PHOSPHOLIPID VESICLES
AS A SYSTEM FOR EVALUATING THE BEHAVIOUR OF CALCIUM IONOPHORES
AND THE CALCIUM ANTAGONISTS

G.R.A. Hunt, I. C. Jones and Z-E. M. Mirghani
Department of Science
The Polytechnic of Wales
Pontypridd CF37 1DL U.K.

Lanthanide ions such as Pr^{3+} have been used as calcium probes in many studies of calcium ionophores and calcium-binding proteins. We will describe their use in conjunction with ^1H and ^{13}C -NMR spectroscopy to investigate the metal-ion binding sites on the calcium antagonists such as verapamil, nifedipine and D600, and the effects of these antagonists on carrier and channel-mediated transport across phospholipid vesicular membranes.

It will be shown that on the addition of shift reagents such as $\text{Pr}(\text{fod})_3$ to chloroform solutions of the calcium antagonists, changes in the ^1H -NMR spectrum enable the binding-sites to be located. Further, on addition of Pr^{3+} to phospholipid vesicles in the presence of calcium antagonist and calcium ionophore, the effect of the antagonist on transmembrane transport of Pr^{3+} can be evaluated from the time-dependent changes in the ^1H -NMR spectra of the phospholipid membranes. Comparative results will be reported using natural ionophores such as A23187, ionomycin and alamethicin, together with synthetic ionophores such as NaFod. In agreement with clinical studies on the antagonists, concentration factors will be shown to be critical in their effectiveness.

The system described will be shown to be useful for the assessment of synthetic compounds such as calcium ionophores and calcium antagonists, as well as throwing light on the mechanism of their action.

Oral Communication presented at:

FEBS Advanced Course on "Structure and Dynamics of Membrane Lipids"

Utrecht, April 1984.

A ^1H and ^{31}P -NMR study into the effects of phospholipase A_2 action on sonicated egg PC vesicles.

APPENDIX C

Published Papers

**Lanthanide-ion transport across phospholipid vesicular membranes:
a comparison of alamethicin 30 and A23187
using ^1H -NMR spectroscopy**

G. R. A. HUNT and I. C. JONES

*The Department of Science, The Polytechnic of Wales,
Pontypridd CF37 1DL, U.K.*

(Received 25 September 1982)

The kinetics of Pr^{3+} transport by the ionophores alamethicin 30 and A23187 across unilamellar phospholipid vesicular membranes has been compared by following the time-dependent changes in the ^1H -NMR spectrum of the vesicles. The measured rates of transport allow stoichiometries of the transporting species to be deduced which are consistent with channel- and carrier-mediated mechanisms respectively. The method provides a useful complement to planar bilayer conductivity studies of these systems.

It has recently been emphasized that in order to investigate transmembrane transport mechanisms the development of a range of physical methods is required which can probe the membrane systems at a molecular level (1). Several groups have already begun to explore the application of NMR techniques to the problem, initially using model systems (2-5). By employing unilamellar vesicular membranes we have demonstrated that a number of mechanisms can be distinguished for the transport of lanthanide ions by membrane-active substances including surfactants (6,7) and carrier-type ionophores (8). Recently it has been confirmed that the pore-forming polypeptide, alamethicin 30, can transport lanthanide ions across planar lipid bilayers in a manner which differs in its voltage dependence than for univalent ions (9). We have therefore examined by NMR the transport of the ion Pr^{3+} by alamethicin 30 in a vesicular system and report here a comparison of the results with those using the carrier-type ionophore A23187. In contrast to previous work (10-12) we see no sign of vesicle fusion at the concentration of alamethicin used and are able to follow the kinetics of transport, which leads to a value for the stoichiometry consistent with a channel mechanism. Our initial results with alamethicin 30 also indicate that it provides a system well-suited to the investigation of the effects of a range of substances such as drugs and anaesthetics on channel-mediated transport.

©1982 The Biochemical Society

Materials and Methods

DL- α -dipalmitoyl phosphatidylcholine (DPPC) was obtained from Lipid Products, Redhill, Surrey; alamethicin 30 from the PHLS Centre for Applied Microbiology and Research, Porton Down, Salisbury; and praseodymium chloride ($\text{PrCl}_3 \cdot 6\text{H}_2\text{O}$, 99.99%) from Lancaster Syntheses, Eastgate, Morecombe. A23187 was a gift from the Lilly Research Centre, and gramicidin A (Dubos, 85% gramicidin A) was obtained from Sigma. Deuterium oxide ($^2\text{H}_2\text{O}$) was purchased from Aldrich and was 99.8% ^2H , Gold Label.

The vesicular membranes were prepared by sonication of lipid in $^2\text{H}_2\text{O}$ as described previously (13) to give concentrations of DPPC equal to 10 mg/ml or 25 mg/ml. The technique produces a uniform population of small unilamellar vesicles of average diameter 26 to 30 nm. The former more dilute solutions were used for the experiments with alamethicin 30, when the ^1H -NMR spectra were obtained using a Jeol FX60Q FT NMR and 10-mm NMR tubes containing 1 ml of vesicle solutions. Usually 8 or 16 pulse sequences were used (π - τ - $\pi/2$) with pulse interval τ of about 3 s to minimize the $^1\text{H}_2\text{O}$ signal. The more concentrated vesicle solutions were used for the experiments with A23187 or gramicidin, when the ^1H -NMR spectra were obtained using a Jeol C60HL continuous-wave spectrometer and 0.5-ml sample in 5-mm NMR tubes. Both spectrometers operated at 60 MHz and were fitted with calibrated temperature control. Alamethicin 30 was introduced into the vesicle solution by adding a known volume of $^2\text{H}_2\text{O}$ stock solution of the polypeptide (1 mg/ml) to 1 ml of vesicle solution in the NMR tube, followed by incubation at 50°C for 30 min. Known volumes of stock chloroform solutions of the ionophores A23187 or gramicidin were added to the empty 5-mm NMR tubes followed by evaporation under a stream of N_2 gas and then evacuation. The dry ionophores were then incubated with 0.5 ml of vesicle solution for 60 min at 60°C.

Transport was initiated by pipetting a known volume ($\approx 10 \mu\text{l}$) of stock PrCl_3 solution in $^2\text{H}_2\text{O}$ into the NMR tubes such that the extravesicular concentration was 5 mM Pr^{3+} . The transport of Pr^{3+} from the extravesicular solution into the intravesicular cavity was monitored by observing the changes in ^1H -NMR spectrum as follows. Fig. 1a shows the spectrum of the DPPC vesicles immediately after the addition of the Pr^{3+} . The temperatures used are above the gel-to-liquid-crystal phase transition for this lipid (13) so their high-resolution signals are seen: signal O from the extravesicular choline head groups and signal I from the intravesicular head groups, while the broad signal H is from the lipid acyl chains. The separation of the signals O and I is due to a pseudocontact, dipolar interaction of the paramagnetic Pr^{3+}aq (which is in rapid exchange between the $^2\text{H}_2\text{O}$ and the phosphate sites on the head groups of the outer monolayer) with the nearby outer choline protons. The separation of head-group signals thus results principally from a downfield shift of signal O and such shifts are now well documented (14). When Pr^{3+} ions are transported across the lipid unilayer into the intravesicular solution the rise in intravesicular concentration of Pr^{3+} causes signal I to move downfield towards signal O. By measuring the change in chemical shift (Hz) of signal I with time the rate of transport can be

obtained. In order to convert the experimentally observed shifts into an intravesicular concentration of Pr³⁺ a calibration graph is necessary. This calibration is obtained by sonicating known concentrations of Pr³⁺ into the vesicles (during their preparation) and then adjusting the extravesicular concentration to 5 mM. At each different intravesicular concentration of Pr³⁺ the shift of signal I is measured. The form of this calibration graph has been shown previously (5).

This method is based on that described previously (4,5) but more recent experiments (8) have shown that the stability of the vesicular preparations in the presence of lanthanide ions is such that considerably slower rates of transport can be measured over at least 10⁴ min. This allows a much greater range of concentration of ionophore to be used with a corresponding increase in accuracy of the determined stoichiometry of transporting species (8).

Results

Fig. 1a-f shows the time-dependent changes in the spectrum of the inner and outer head groups (signals I and O) during the course of an experiment using 20 µg of alamethicin 30 per ml of vesicle solution (10 mg of DPPC) at 50°C. Similar time-dependent spectra were

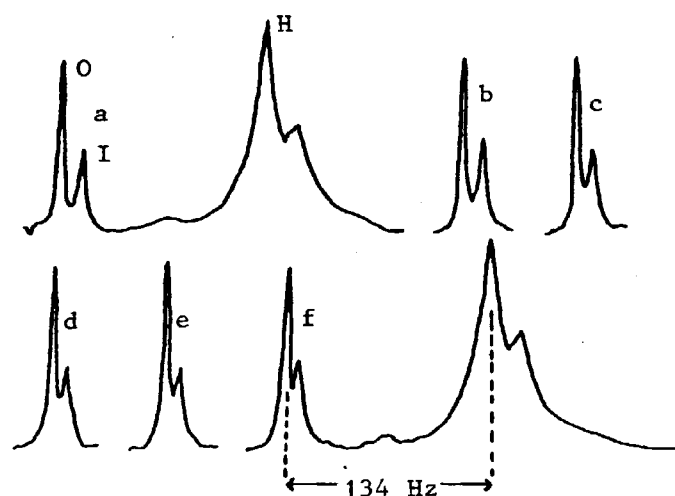


Fig. 1. The ¹H-NMR spectrum of dipalmitoyl phosphatidylcholine vesicles at 50°C in the presence of 5mM extravesicular Pr³⁺. Signals O, I, and H originate from the outer lipid head groups, the inner head groups, and the acyl chains, respectively. (b-f) Downfield movement of signal I during the transport of Pr³⁺ from the extravesicular to the intravesicular region, mediated by alamethicin 30 (20 µg/10 mg of DPPC). Shifts in signal O are measured with respect to signal H and are shown after (b) 4.5 min, (c) 10 min, (d) 16 min, (e) 24 min, (f) 35 min. The full spectrum is given in (f) to indicate the lack of broadening of the acyl-chain signal H during the transport of Pr³⁺.

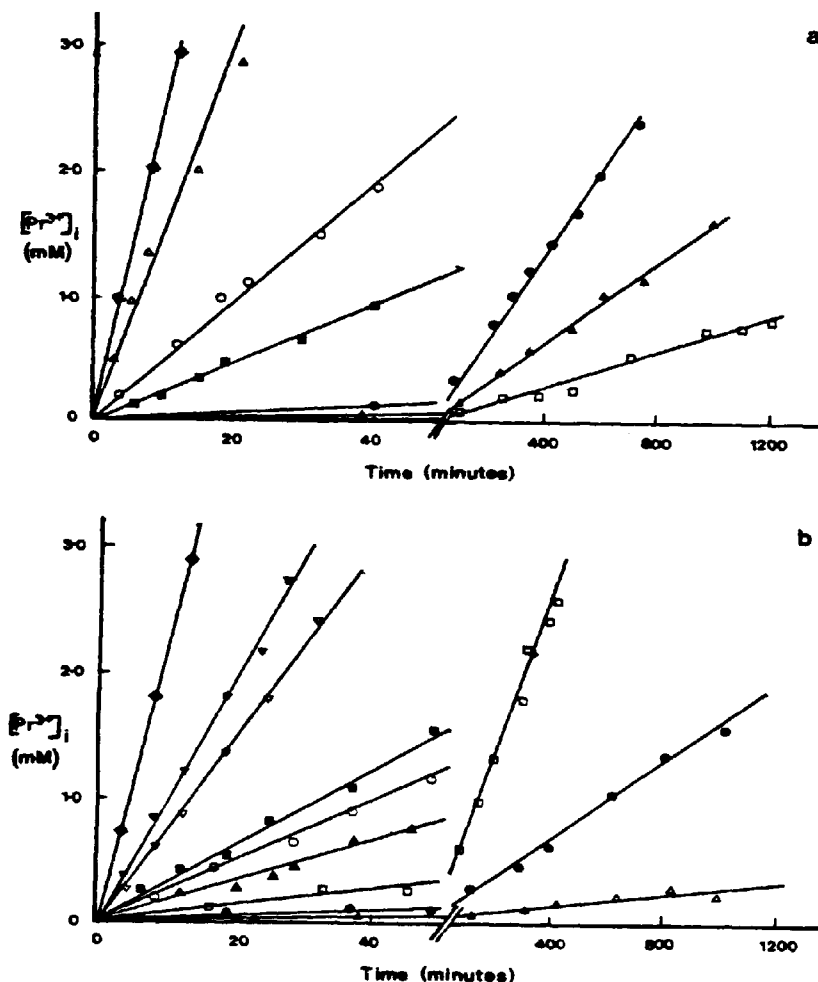


Fig. 2. Changes in concentration of Pr^{3+} as a function of time in the intravesicular region, $[\text{Pr}^{3+}]_i$, due to varying concentrations of ionophores.

(a) alamethicin 30 per 10 mg of DPPC at 50°C : \blacklozenge 30 μg , \triangle 25 μg , \circ 20 μg , \blacksquare 15 μg , \bullet 10 μg , \blacktriangle 7.5 μg , \square 5 μg .
 (b) A23187 per 25 mg of DPPC at 60°C : \blacklozenge 8 μg , ∇ 4 μg , \blacksquare 3.5 μg , \bullet 2.5 μg , \circ 2.0 μg , \blacktriangle 1.5 μg , \square 1.0 μg , \bullet 0.5 μg , \triangle 0.25 μg .

obtained using the range of concentrations of alamethicin shown in Fig. 2a. On conversion of the measured shift of signal I in Hz into intravesicular concentration of praseodymium ion $[\text{Pr}^{3+}]_i$, using a calibration graph (see 'Materials and Methods') the corresponding plots of $[\text{Pr}^{3+}]_i$ against time are shown in Fig. 2a for each concentration of alamethicin used.

The results of similar experiments with A23187 are shown in Fig. 2b, and a linear dependence of $[\text{Pr}^{3+}]_i$ with time is observed for both ionophores. The slopes of the plots in Fig. 2 give the rates at which Pr^{3+} crosses the vesicular membrane. No appreciable transport of

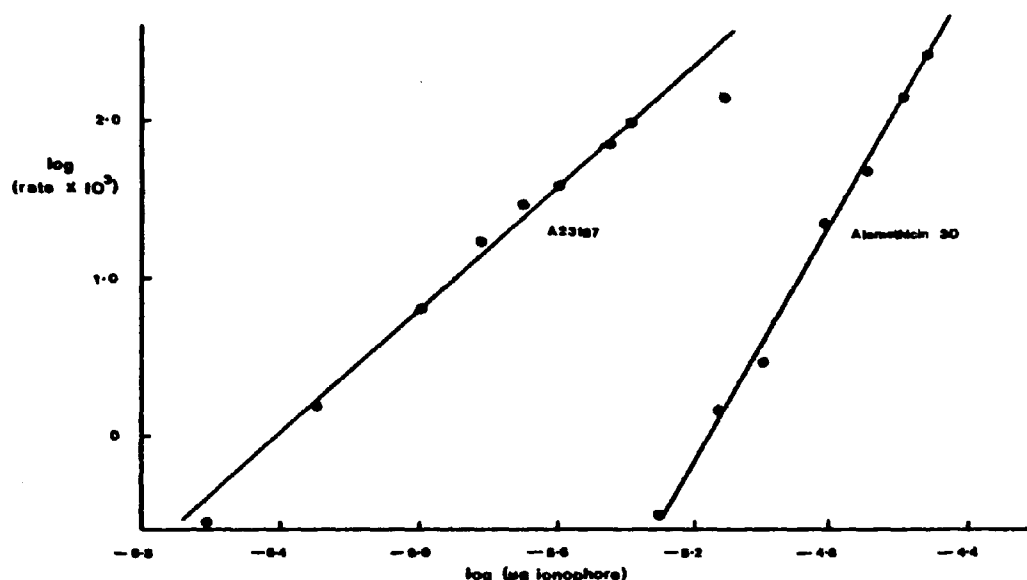


Fig. 3. The effect of increasing concentration of the ionophores alamethicin 30 and A23187 on the rate of transport of Pr³⁺ into dipalmitoyl phosphatidyl choline vesicles. The rates are expressed in Hz/min as measured from the slopes of the lines shown in Fig. 2 a and b.

Pr³⁺ was observed using a similar range of concentrations of gramicidin A even though the time scale was extended by several days.

Fig. 3 is a result of plotting the logarithm of rates of transport (as obtained from Fig. 2) against the logarithm of the concentration of ionophore used. The slopes of these plots are 1.9 and 4.05 for A23187 and alamethicin 30, respectively.

By observing the rates of transport over a range of temperatures for a given concentration of ionophore, Arrhenius plots can be constructed and the activation energy calculated. The value of 58 kJ mol⁻¹ was obtained for alamethicin 30, which compares with a previously published result of 116 kJ mol⁻¹ for A23187 (5).

It is important to note that using this method of investigating transport of paramagnetic ions, the spectrum of the vesicles can be monitored at all times. In the above experiments using alamethicin and A23187, the integrated signal areas of peaks O and I remain constant during the transport, as can be seen for alamethicin 30 in Fig. 1. The ratio of the signal areas can be shown (15) to be a reliable indication of the vesicle size; in our case the ratio of areas O:I was 1.6 ± 0.1 , indicating a vesicle diameter of about 30 nm. As is discussed below it was also important to measure the signal width of the acyl chain peak H during transport since this is a sensitive measure of vesicle fusion in the system (16). It can be seen from Fig. 1a and f that no appreciable line broadening of signal H occurs during the observed transport using alamethicin 30.

Discussion

The reliability of this method for the determination of stoichiometries of transported species has been previously established using Pr^{3+} complexes of known structure (8). The slope of 1.9 obtained in Fig. 3 indicates that the species $\text{Pr}(\text{A23187})_2^+$ is involved in the rate-determining step, which is likely to be the diffusion of this hydrophobic complex across the bilayer and over the image-potential barrier generated by the charge on the complex (5,8). This result represents an improvement on the previously determined stoichiometry (5), which was $\text{Pr}(\text{A23187})_2^{2+}$, and undoubtedly results from the larger range of concentrations and rates studied here. The revised value is also more consistent with the $\text{Ca}(\text{A23187})_2$ complex determined by X-ray analysis (17), since Pr^{3+} and other lanthanide ions are known to have similar co-ordination properties to Ca^{2+} and thus give rise to suitable probe species for this ion (18,19). Indeed, the use of the ionophores A23187 and ionomycin (G.R.A. Hunt and Z.E.M. Mirghani, unpublished results) as carrier ionophores for lanthanides is a good example of this latter point.

The failure of gramicidin A to act as an ionophore for multivalent ions was suggested by earlier work where the Na^+ -conduction channels were shown to be blocked by Ca^{2+} (20). A similar result for Dy^{3+} was recently reported by Springer and colleagues (3) and is likely to result from the narrow channel formed by the gramicidin helices (21). However, the development of the gramicidin/vesicle system when studied by ^{23}Na -NMR should provide a useful method of studying the gating of Na^+ or K^+ ionic channels by polyvalent ions such as Ca^{2+} and Ln^{3+} (lanthanide ion).

In contrast, we find that alamethicin 30 does transport Pr^{3+} in vesicular membranes. The observed stoichiometry of 4 is lower than that reported for the planar bilayer (BLM; black lipid membrane) conductivity studies (22), though in the latter system the polypeptide melittin also required only four monomers to form a channel (23). The difference between the stoichiometry results for alamethicin 30 in the two systems could be accounted for by such factors as (a) curvature of the vesicular bilayers, (b) presence of hydrocarbon solvent in the BLM, (c) absence of unstirred layer effects in the rapidly tumbling small vesicles, (d) transmembrane potential effects. The latter factor needs more careful comment since in the BLM, conductivity of M^+ by alamethicin is usually seen only when a transmembrane voltage is applied and when the ionophore is added to the aqueous phase on the positive side of the bilayer (22). There are several differences in the case of Ln^{3+} transport by alamethicin 30 in BLM, when a smaller voltage dependence is seen and the lower conductivity levels are preferentially adopted (9). Further, while early workers proposed that alamethicin monomers were absorbed on the surface of the bilayer and migrated to form the channel on application of the voltage (24,25), later results indicate that the polypeptide partitions into the membrane even in the absence of a potential (26,27). In fact a recent report suggests that alamethicin can be applied to the negative (non-conducting) side of the BLM, when it diffuses across the bilayer and gives rise to channels (28). The diffusion time required in these later studies (27,28) indicates

that the incubation time of 30 min we allow is sufficient for equilibration of the alamethicin 30 across the vesicular membrane. There is a very slow diffusion of Pr³⁺ across DPPC bilayer at temperatures above the phase transition even in the absence of ionophores (6,8). While this diffusion rate is negligible compared with the alamethicin-mediated rates obtained as above, it could be sufficient to give the initial transmembrane potential (intravesicular positive) required to open the channels once sufficient alamethicin had diffused across the bilayer.

The previous papers on alamethicin interaction with vesicles by Lau and Chan (10-12) were dominated by the observation of alamethicin-induced vesicle fusion. This may have been due to their use of unseparated fractions of alamethicin 30 and 50, which are known to have different membrane effects (29). We also find that fusion can be induced at high concentrations of alamethicin 30 (70 µg/10 mg of DPPC), but as shown above very little fusion is evident at 20 µg/10 mg of DPPC. Lau and Chan also attempted to set up a transmembrane potential using K⁺/valinomycin (12), but the observed transmembrane movement of Eu³⁺ was then so fast that the kinetics could not be followed. Their experimental method was, however, complicated by the fact that fusion of vesicles preceded the ionophore-mediated transport, both Eu³⁺ and La³⁺ were present, and incubation and dialysis of vesicles made it difficult to know the final disposition of the alamethicin.

By analogy with the single-channel behaviour in BLM it would be expected that with alamethicin 30, bursts of ions would cross the vesicular bilayer. We do observe such a rapid equilibration of Pr³⁺ when DPPC vesicles are near the phase-transition temperature and the channels then formed are stabilized by Triton X-100 (7). Evidently in our vesicle system as used above, the rate of formation and life-time of the alamethicin-30 channels is low, and similar slow transport rates were found by Pierce and co-workers (30) using the polyene ionophore nystatin. The channels can be stabilized by preparing the vesicles with the alamethicin incorporated in the bilayer or by including cholesterol, since we observe greatly increased transport rates under these conditions (results not shown). The simpler system employed here should also be amenable to study the effect of setting up a transmembrane potential via K⁺ and valinomycin as used by Lau and Chan.

Besides the contrast in stoichiometry, further confirmation of the difference in mechanism for the transport of Pr³⁺ by A23187 and alamethicin 30 comes from preliminary observations on the effect of ethanol and general anaesthetics on these systems (G.R.A. Hunt and I.C. Jones, in preparation). Thus, for example, CHCl₃ promotes transport by A23187, but strongly inhibits in the case of alamethicin 30. These initial observations using alamethicin 30 in vesicular membranes suggest that it can be a valuable adjunct to its study by BLM methods and will allow further investigation of a range of experimental conditions on channel-mediated transport.

Acknowledgement

The support of part of this work by the Sir Halley Stewart Trust is gratefully acknowledged.

References

1. Hokin LE (1981) *J. Membrane Biol.* **60**, 77-93.
2. Ting TZ, Hagan PS, Chan SI, Doll JO & Springer CS Jr (1981) *Biophys. J.* **34**, 189-216.
3. Pike MM, Simon SR, Balschi JA & Springer CS Jr (1982) *Proc. Natl. Acad. Sci. U.S.A.* **79**, 810-814.
4. Hunt GRA (1975) *FEBS Lett.* **58**, 194-196.
5. Hunt GRA & Tipping LRH (1978) *Biophysical Chem.* **8**, 341-355.
6. Hunt GRA & Jawaharlal K (1980) *Biochim. Biophys. Acta* **601**, 678-684.
7. Hunt GRA (1980) *FEBS Lett.* **119**, 132-136.
8. Hunt GRA (1980) *Phys. Chem. Lipids*, **27**, 353-364.
9. Gögelein H, de Smedt, H, Van Driessche, W & Borghgraef R (1981) *Biochim. Biophys. Acta* **640**, 185-194.
10. Lau ALY & Chan SI (1974) *Biochemistry* **13**, 4942-4948.
11. Lau ALY & Chan SI (1975) *Proc. Natl. Acad. Sci. U.S.A.* **72**, 2170-2174.
12. Lau ALY & Chan SI (1976) *Biochemistry* **15**, 2551-2555.
13. Hunt GRA & Tipping LRH (1978) *Biochim. Biophys. Acta* **507**, 242-261.
14. Bergelson LD (1978) in *Methods in Membrane Biology* (Korn E, ed), vol. 9, pp 275-335.
15. Hutton WC, Yeagle PL & Martin RB (1977) *Chem. Phys. Lipids* **19**, 255-265.
16. Liao MJ & Prestegard JH (1979) *Biochim. Biophys. Acta* **550**, 157-173.
17. Chaney MO, Jones ND & Debono M (1976) *J. Antibiotics* **29**, 422.
18. Hughes MN (1981) *The Inorganic Chemistry of Biological Processes* (2nd ed), p 273, Wiley.
19. dos Remedios CG (1981) *Cell Calcium* **2**, 29-51.
20. Bamberg E & Lauger P (1977) *J. Memb. Biol.* **35**, 351-375.
21. Haydon DA & Hladky SB (1972) *Quart. Rev. Biophys.* **5**, 187-282.
22. Cherry RJ, Chapman D & Graham DE (1972) *J. Membrane Biol.* **7**, 325-344.
23. Tosteson MT & Tosteson DC (1981) *Biophys. J.* **36**, 109-116.
24. Baumann G & Mueller P (1974) *J. Supramolec. Struct.* **2**, 583-557.
25. Boheim G & Kolb H-A (1978) *J. Membrane Biol.* **38**, 99-150.
26. Fringeli UP & Fringeli M (1979) *Proc. Natl. Acad. Sci. U.S.A.* **76**, 3852-3856.
27. Fringeli UP (1980) *J. Membrane Biol.* **54**, 203-212.
28. Schindler H (1979) *FEBS Lett.* **104**, 157.
29. Melling J & McMullen AI (1975) *ISC-IAMS Proceedings, Science Council of Japan* **5**, 446-452.
30. Pierce HD Jr, Unran AM & Oehlschlager AC (1978) *Can. J. Biochem.* **56**, 801-807.

BBA 71893

A ^1H -NMR INVESTIGATION OF THE EFFECTS OF ETHANOL AND GENERAL ANAESTHETICS ON ION CHANNELS AND MEMBRANE FUSION USING UNILAMELLAR PHOSPHOLIPID MEMBRANES

G.R.A. HUNT and I.C. JONES

Department of Science, The Polytechnic of Wales, Pontypridd CF37 1DL, Mid Glamorgan (U.K.)

(Received May 3rd, 1983)

Key words: *Lanthanide ion; Anesthetic-membrane interaction; Membrane permeability; Ion channel; Phase transition; Membrane fusion; ^1H -NMR; (Phospholipid membrane)*

Using ^1H -NMR of small unilamellar vesicles in the presence of the lanthanide probe ion Pr^{3+} , the effects of ethanol, diethyl ether and chloroform on various mechanisms of channel-mediated transport were studied. The mechanisms include channel formation by the polypeptide Alamethicin 30 and vesicular lysis at the gel to liquid-crystal phase transition of the lipid. Channel stabilisation and membrane fusion induced by sub-critical micelle concentrations of Triton X-100 were also investigated. The observation that ethanol and diethyl ether increase membrane permeability and fusion while chloroform inhibits them suggests a common locus of action on the properties and structure of channel-associated water. This conclusion is discussed in terms of current theories of general anaesthesia.

Introduction

The effects of ethanol and other general anaesthetics on the central nervous system are not understood at the molecular level [1,2]. However, their physiological action seems likely to be centred on the processes involved in synaptic transmission [2,3] which include the opening of calcium channels and fusion of synaptic vesicles with the plasma membrane. Our understanding of these processes of transmembrane transport and membrane fusion has benefitted from the simplification of the systems involved by using model lipid membranes in a very large number of studies. However, investigations into the effects of ethanol or general anaesthetics on transmembrane channels using lipid bilayer membranes are surprisingly limited [4-6] and their effects on membrane fusion do not seem to have been significantly studied at all in model systems.

We have therefore investigated the action of

ethanol, diethyl ether and chloroform on a variety of mechanisms of membrane permeability using unilamellar phospholipid vesicles and on their fusion stimulated by Triton X-100. The choice of these three compounds seemed suitable for an initial study since they are all small uncharged molecules and have a wide range of partition coefficient from aqueous to membrane phase [7,8].

Our previous work with small phosphatidylcholine vesicles has shown that ^1H -NMR in conjunction with paramagnetic probe ions such as the lanthanide ion Pr^{3+} , can be used to study a number of different mechanisms of membrane permeability. These include (a) channel formation at or near the bilayer gel to liquid-crystal phase transition temperature (T_c) which causes vesicular lysis [9,10]; (b) carrier-mediated transport by ionophores such as A23187 [11-13]; and (c) pore-mediated transport by ionophores such as the polypeptide Alamethicin 30 [13]. We here report the application of these methods to investigate the

effects of ethanol, diethyl ether and chloroform on channel formation in phosphatidylcholine vesicular membranes. Experiments using Triton X-100 have been included in order to extend the experimental conditions to study the effect of the three compounds on Triton-stabilised channels at T_c [10,14] and on vesicular fusion [10,15]. The investigation of such fusion processes by NMR has now been well established and we have made use of the line-broadening methods developed by Prestegard and co-workers [16,17].

Until recently the trend has been to explain general anaesthesia in terms of hydrophobic effects such as bilayer fluidity or expansion [18]. These lipid-based theories have now been effectively criticised [2,19] and a number of studies reported in which hydrophilic effects such as hydrogen bonding are implicated [20]. Our results support these indications of anaesthetic action at aqueous interfaces and in particular suggest that the effects of ethanol and the general anaesthetics studied on the structure and properties of the water in the channels could account for their stimulation or inhibition of the observed channel-mediated transport of Pr^{3+} . Our observations are also in keeping with recent studies which indicate the probable importance of water in both the ionic permeability of the lipid bilayer at the phase transition [21–23] and in the structure of ion channels formed by Alamethicin [24].

Materials and Methods

Chemicals

Dipalmitoylphosphatidylcholine (DPPC) was obtained from Lipid Products, South Nutfield, Redhill, and Triton X-100 (Scintillation grade) was purchased from BDH, and an average molecular weight of 624 (9.5 oxyethylene units) was used to calculate molarities. A23187 was a gift from the Lilly Research Centre, Windlesham, Surrey. Alamethicin 30 was obtained from PHLS Centre for Applied Microbiology and Research Porton Down, Salisbury, and praseodymium chloride ($\text{PrCl}_3 \cdot 6\text{H}_2\text{O}$) from Lancaster Synthesis. Deuterium oxide ($^2\text{H}_2\text{O}$ - 99.8% Gold Label) was purchased from Aldrich, Gillingham, Dorset. The AnalaR chloroform used was purified by passing over alumina to remove ethanol and water, distilled and restabilised by addition of 1% AnalaR

methanol. Absolute ethanol (spectroscopic grade) and AnalaR diethyl ether (sodium dried to remove water) were obtained from BDH Chemicals, Poole, Dorset.

Experimental procedures

The vesicular membranes were prepared by sonication of lipid in $^2\text{H}_2\text{O}$ as described previously [9] to give a DPPC concentration of 10 mg/ml. The ^1H -NMR spectra of the vesicular solutions were obtained at 60°C, or 50°C in the case of the experiments using the ionophores, i.e. above the phase transition temperature of the DPPC vesicles. A JEOL FX60Q FT NMR spectrometer operating at 60 MHz and fitted with a calibrated temperature control was used to record the spectra. The 10-mm NMR tubes contained 1 ml of vesicle solution confined by a vortex plug and capped. Typically, 15 pulse sequences were used (π - τ - $\pi/2$) with a pulse interval, τ of about 3.0 s to minimise ^2HHO , ethanol and ether peaks. The desired concentration of Pr^{3+} in the extravascular solution was obtained by adding a known volume of a stock solution of PrCl_3 in $^2\text{H}_2\text{O}$ to the vesicle solutions in the NMR tube. In experiments on phase transitions and lysis of the vesicular membranes using ethanol, ether and chloroform, appropriate volumes of these were pipetted into the NMR tubes containing the vesicles and Pr^{3+} , and incubated for 1 h before performing the experiment.

The ^1H -NMR spectrum of DPPC vesicles at 60°C includes high resolution signals from the lipid acyl chains (H) and choline headgroups. On adjusting the extravascular concentration to 5 mM Pr^{3+} , the spectrum shown in Fig. 1 is obtained. Separate signals are now seen originating from the extravascular headgroups 'O' and intravesicular headgroups 'I'. The resulting separation is mainly due to the downfield shift of signal 'O', this being concentration dependent [25]. Such shifts are now well documented [26] and are caused by pseudo-contact, dipolar interaction of Pr^{3+} in rapid exchange between $^2\text{H}_2\text{O}$ and the phosphate sites on the extravascular headgroups. The ratio of the areas $O:I$ is approx. 1.7 ± 0.05 obtained by integrating the two peaks and indicates that vesicles of average diameter of 28 nm have been formed [27].

Observation of the phase transition temperature T_c , of the vesicular membranes and the effects on it of ethanol, diethyl ether and chloroform was made by monitoring the temperature dependence of the line widths in the ^1H -NMR spectrum as described previously [9] except that here the linewidths at half-height ($\nu_{1/2}$) of the acyl chain signal (H) was measured from temperatures above the phase transition down to the lowest temperature before the linewidth was too great to be separated from the base-line noise.

Using the changes in the spectrum shown in Fig. 1 which occur when the vesicles interact with membrane active substances we can distinguish between the following types of event: (I) Transmembrane transport or diffusion of the probe ion Pr^{3+} into all vesicles simultaneously. (II) Lysis of the membranes in which 'holes' or channels are formed in some of the vesicles so that equilibration of the 5 mM Pr^{3+} takes place across the bilayer but without the loss of vesicular integrity. (III) Fusion of the vesicles. These events have been distinguished in our previous studies [9–13] and are illustrated in the results below.

Lysed vesicles were obtained by cycling the vesicular solution from 60°C to below T_c and back to 60°C three times over 60 min in the NMR tube, spectra being taken before and after each series of cycles. Triton X-100 was introduced (to a final concentration of 0.1 mM) by pipetting a stock solution of Triton X-100 in $^2\text{H}_2\text{O}$ into the vesicular solution which was already equilibrated with Pr^{3+} and anaesthetic for 1 h. This was further equilibrated at 60°C for 30 min before a single cycle through T_c over a 20-min period.

The ionophores were introduced into dry NMR tubes by pipetting a known volume of a chloroform stock solution. The solvent was carefully removed under a stream of nitrogen followed by evacuation. One ml of vesicular solution was then added and incubated at 50°C for 1 h. In some experiments Alamethicin 30 was introduced into the vesicular solution by adding a known volume of $^2\text{H}_2\text{O}$ stock solution of the polypeptide (1 mg/ml) to 1 ml of the vesicle solution in the NMR tube, followed by incubation at 50°C for 60 min. Transport was initiated by the addition of the stock Pr^{3+} solution to give an extravesicular concentration of 5 mM and followed at 50°C by

observation of the NMR spectrum at suitable time intervals. In the case of samples containing ethanol or anaesthetic these were added to the vesicular solution and co-equilibrated with the ionophore for 1 h at 50°C before the addition of Pr^{3+} .

Experimental Results

1. The effects of ethanol, diethyl ether and chloroform on the ^1H -NMR spectrum and phase transition of DPPC vesicles

Up to concentrations of 0.1 M, ethanol and diethyl ether have negligible effects on the chemical shifts of the ^1H -NMR signals obtained from the vesicles as shown in Fig. 1. Chloroform, however, causes a marked upfield shift of the outer headgroup signal 'O' towards signal 'I'. The change is approximately linear with concentration and is 3% at 100 mM CHCl_3 .

All three compounds decrease the line width of the headgroup and acyl chain signals. Again chloroform has the most marked effect. The widths at half-height ($\nu_{1/2}$) of the acyl chain signal (H) were measured in Hz over a range of temperatures spanning the phase transition temperature T_c , in the absence (control) and in the presence of the three compounds under study. The measurements of $\nu_{1/2}$ were converted to spin-spin relaxation

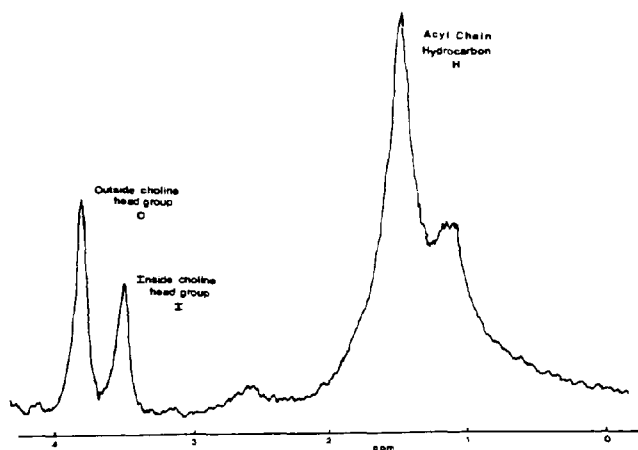


Fig. 1. The 60-MHz ^1H -NMR spectrum of dipalmitoylphosphatidylcholine vesicles at 60°C in the presence of 5 mM Pr^{3+} , showing signals from the extravesicular choline headgroups (O), the intravesicular choline headgroups (I) and the lipid acyl chain signals (H). The chemical shifts are shown with reference to external TMS.

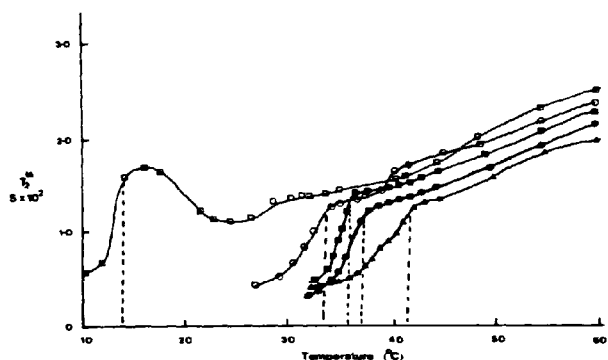


Fig. 2. The temperature dependence of the spin-spin relaxation time (T_2^*) for the acyl chain signal (H in Fig. 1) from dipalmitoylphosphatidylcholine vesicles, \blacktriangle — \blacktriangle , Control. Vesicles in the presence of: \bullet — \bullet , 86 mM ethanol; \blacksquare — \blacksquare , 86 mM diethyl ether; \circ — \circ , 25 mM chloroform; \square — \square , 86 mM chloroform. Dotted lines indicate the onset of the liquid-crystal to gel phase transition.

times, T_2^* using the relationship $T_2^* = 1/\pi\nu_{1/2}$. The effect of the compounds on T_2^* and on the phase transition temperature can be seen in Fig. 2. In each case the T_2^* values are increased by the presence of all three compounds at temperatures above the phase transition. The temperature range over which liquid-crystalline and gel phases co-exist is known to be greater for small unilamellar vesicles than larger bilayer structures [28]. For the pure DPPC vesicles T_c can be seen to extend from about 41°C to 35°C. The onset of the liquid-crystal to gel phase transition (indicated by the dotted lines in Fig. 2) is significantly lowered by all three compounds, with chloroform having the greatest effect on a molar basis. It was important to determine the extent of the range of T_c in the presence of various concentrations of the compounds studied since we wished to ensure that the temperature range used in subsequent lysis experiments were sufficient to span the gel to liquid-crystal phase change even in the presence of the added ethanol or anaesthetics.

2. Effects on vesicular lysis

On cycling through the phase transition, channels are formed in the vesicles which allow rapid equilibration of the Pr^{3+} ions across the bilayer. However, only a fraction of the vesicles lyse during each cycle. This process is demonstrated in Fig. 3 where a sample of DPPC vesicles (5 mM extraves-

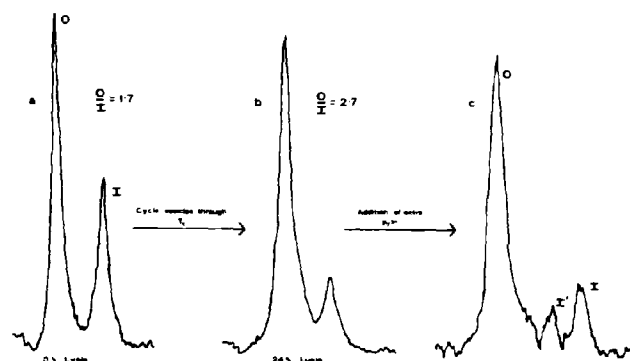


Fig. 3. Effect on the ^1H -NMR headgroup signals from dipalmitoylphosphatidylcholine vesicles in the presence of 5 mM extravesicular Pr^{3+} (O extravesicular headgroup signal, I intravesicular headgroup signal) of cycling the vesicles through the phase transition. (a) signals from the vesicles at 60°C before cycling; (b) signals from vesicles at 60°C after six sets of three cycles through T_c (60°C-30°C-60°C) with time intervals as shown in Fig. 4 (control); (c) signals from the vesicles as in (b) except that the extravesicular concentration of Pr^{3+} has been increased to 20 mM.

icular Pr^{3+}) has been cycled three times through T_c (60°C-30°C-60°C) over 60 min and the process repeated at the time intervals shown in Fig. 4. The effect on the ratio of the signals O/I is clearly seen (1.7 \rightarrow 2.7). Addition of extra Pr^{3+} (20 mM) to the sample after lysis reveals the signal I' from the inside headgroup signal of the lysed vesicles (as shown in Fig. 3) while the remaining signal I arises from the unlysed vesicles. This also demonstrates that vesicular integrity is maintained during the lysis procedure. Thus from the change in O/I ratio the % lysed vesicles is readily calculated.

Fig. 4 shows a plot of the % lysis against time, when a series of cycles through T_c are used separated by incubation periods at 60°C. In each case the vesicles are seen to be impermeable to Pr^{3+} ions during the incubation periods at 60°C but on passing through T_c (three cycles in one hour) the % lysis increases. Fig. 4 also plainly shows the effect of ethanol and diethyl ether is to increase the lysis, while that of chloroform is to decrease the % of the vesicles which lyse. The temperature range used for the cycles through T_c were such as to ensure passage into the gel and liquid-crystalline phases as judged by the effects of the three compounds on the range of T_c as shown in Fig. 2.

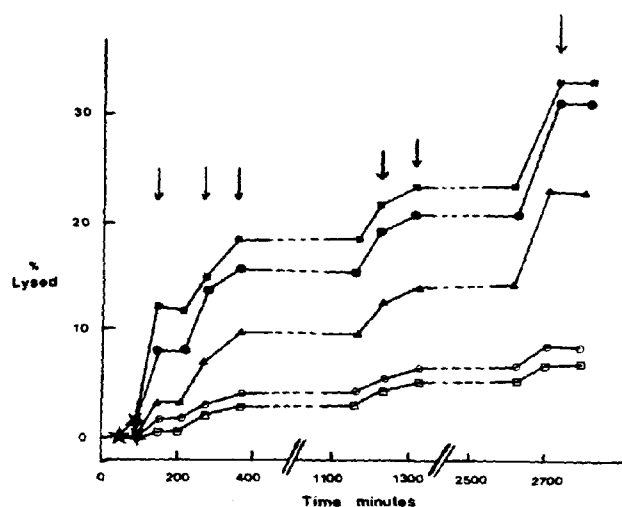


Fig. 4. The effect of ethanol, diethyl ether and chloroform on lysis of dipalmitoylphosphatidylcholine vesicles caused by cycling the vesicles through the phase transition temperature. ★ Indicates spectra taken during initial incubation period. Arrows ↓ indicate the times at which spectra were recorded at 60°C after three cycles through T_c . Other points indicate the times at which spectra were recorded at 60°C after an incubation period at 60°C, ▲——▲, control. Vesicles in the presence of: □——□, 86 mM chloroform; ○——○, 25 mM chloroform; ●——●, 86 mM ethanol; ■——■, 86 mM diethyl ether.

During the lytic processes the peak width of the acyl chain signal (H) was monitored. Variations of only a few Hz were observed, indicating that no appreciable fusion of vesicles occurred over the duration of the experiment.

3. Vesicular lysis and fusion in the presence of Triton X-100

Similar experiments were carried out using vesicles in the presence of 0.1 mM Triton X-100. At this concentration Triton does not increase the diffusion permeability of the vesicles to Pr^{3+} [10]. The effect of this concentration of Triton X-100, however, greatly increases the lysis of the vesicles at the phase transition. Thus only one cycle through T_c over 20 min was used between each measurement of the O/I ratio and incubation period at 60°C. Fig. 5 shows the % lysis obtained for the control (Triton X-100 only) and in the presence of ethanol, diethyl ether and chloroform. The results are similar to those in Fig. 4 with chloroform

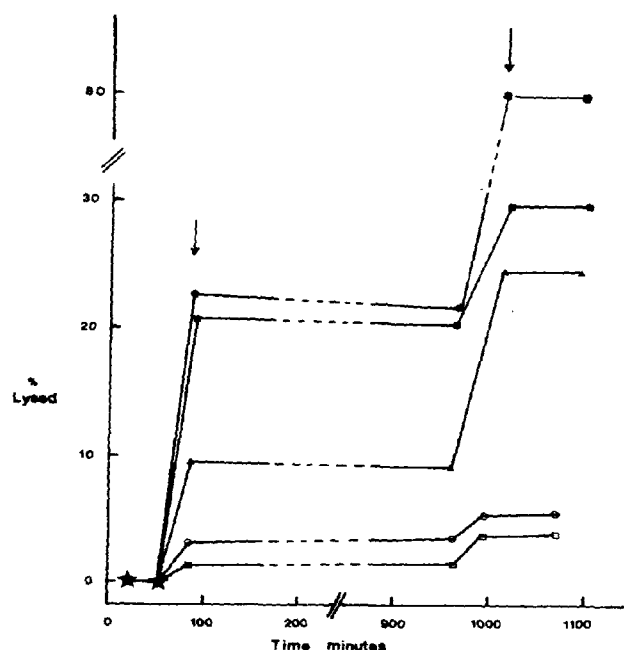


Fig. 5. The effect of ethanol, diethyl ether and chloroform on lysis of dipalmitoylphosphatidylcholine vesicles caused by cycling the vesicles, in the presence of 0.1 mM Triton X-100, through the phase transition. ★ Indicates spectra taken during initial incubation period. Arrows ↓ indicate the times at which spectra were recorded after one cycle through T_c . Other points indicate the times at which spectra were recorded after incubation at 60°C, ▲——▲, control. Vesicles in the presence of: □——□, 86 mM chloroform; ○——○, 25 mM chloroform; ■——■, 86 mM diethyl ether; ●——●, 86 mM ethanol.

strongly inhibiting the lysis even in the presence of Triton X-100.

The spectra recorded during these experiments showed a broadening of the acyl chain signal (H) and the signal width was measured in order to estimate the degree of fusion of the vesicles occurring. Increase in this signal width results from the decrease in tumbling rates of the larger vesicles produced by fusion, with a consequent loss of averaging of the dipolar relaxation which contributes to the linewidth. Prestegard and co-workers [16,17] have shown that the linewidth increases linearly with vesicle radius and that for complete 1:1 vesicle fusion (during which the radius of all the vesicles will increase by $\sqrt{2}$) the linewidth of the methylene acyl chain signal (H) increases by a factor 1.57. Our observed increases in the value of

$\nu_{1/2}$ for the acyl chain signals corresponding to the results shown at the end of the experiment in Fig. 5 were: control (17 to 24 Hz); diethyl ether (15 to 25 Hz); ethanol (18 to 28 Hz) and chloroform at 86 mM (14.4 to 17.4 Hz). The values of the % fusion calculated using Prestegard's factor 1.57 from the linewidth increases are, then: control 75%, diethyl ether 100%, ethanol 100%, chloroform 35%. Thus chloroform has the effect of inhibiting both the lysis and fusion promoted by the presence of Triton X-100.

It should be noted that this limited 1:1 fusion, in which the radius increases by $\sqrt{2}$, will have only a small effect on the O/I ratio. It can readily be calculated that when vesicles of membrane thickness 4 nm increase in radius from 14 nm to $14\sqrt{2}$ nm the O/I signal will decrease from 1.70 to 1.57. Thus the 75% fusion produced in the control sample of vesicles would cause a decrease in the O/I ratio from 1.7 to about 1.6. In contrast a 75% lysis of the vesicles would increase the O/I ratio from 1.7 to 9.8. The changes in O/I ratio used to calculate the % lysis in Fig. 5 are then almost entirely due to the lytic effect of Triton at T_c and are hardly affected by the limited fusion occurring.

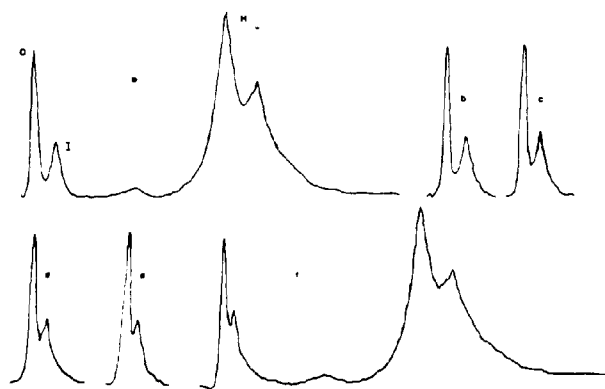


Fig. 6. Time-dependent downfield shifts of the intravesicular headgroup signal (I) from phosphatidylcholine vesicles at 50°C in the presence of 5 mM extravesicular Pr^{3+} , 5 mM chloroform and Alamethicin 30 (20 μg per 10 mg DPPC). The spectra show the result of transport of the Pr^{3+} from outside to inside the vesicles at the following intervals after the addition of the 5 mM Pr^{3+} : (a) 3.0 min; (b) 7.0 min; (c) 13.25 min; (d) 24.0 min; (e) 35.5 min; (f) 46.0 min. The full spectrum is given in (a) and (f) to indicate the lack of broadening of the acyl chain signal H during the transport of Pr^{3+} .

4. Effect of ethanol and general anaesthetics on channels formed by Alamethicin 30 and on carrier-mediated transport by A23187

As we have shown previously and outlined in Materials and Methods, the time-dependent changes in the headgroup signals of the vesicles can be used to monitor transmembrane transport of Pr^{3+} by carrier [11–13] and pore-forming ionophores [13]. Fig. 6 illustrates the observed downfield movement of the intravesicular headgroup signal I during the transport of Pr^{3+} ions from outside to inside the vesicles by Alamethicin 30 in the presence of 5 mM CHCl_3 . The uniform downfield movement of signal I indicates that equal amounts of Pr^{3+} are transported into all vesicles. These shifts of signal I are converted into intravesicular concentrations of Pr^{3+} using a calibration graph [12]. Data obtained as in Fig. 6 can then be converted into the time-dependence of the transport of Pr^{3+} into the vesicles.

Plots of the intravesicular concentration of Pr^{3+} against time are shown in Fig. 7 which illustrates the data obtained using 20 μg Alamethicin 30 per 1 ml of vesicular solution (10 mg DPPC) and shows the effect of various concentrations of

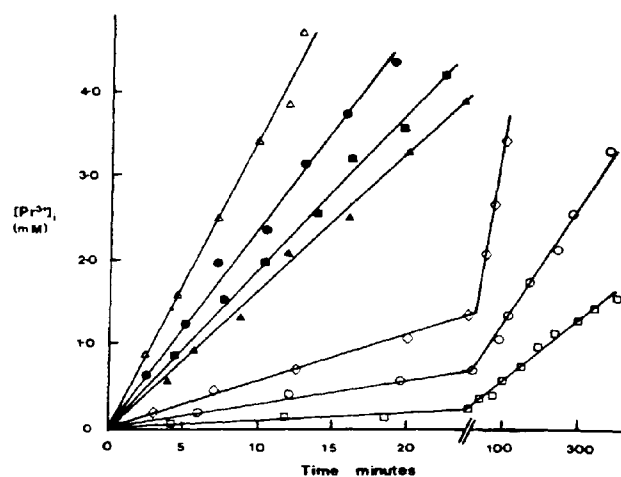


Fig. 7. Increase in the intravesicular concentration, $[\text{Pr}^{3+}]_i$, of Pr^{3+} as a function of time at 50°C using 20 μg Alamethicin 30 per 1 ml of vesicles (10 mg DPPC) and an extravesicular concentration of 5 mM Pr^{3+} . Δ — Δ , control. Vesicles in the presence of: \square — \square , 86 mM chloroform; \circ — \circ , 25 mM chloroform; \diamond — \diamond , 5 mM chloroform; \blacksquare — \blacksquare , 86 mM diethyl ether; \bullet — \bullet , 86 mM ethanol; \triangle — \triangle , 172 mM ethanol.

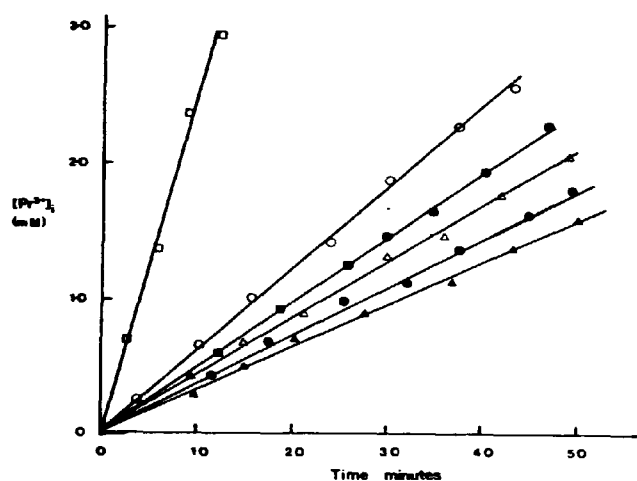


Fig. 8. Increase in the intravesicular concentration, $[\text{Pr}^{3+}]$, of Pr^{3+} as a function of time at 50°C using $10\ \mu\text{g}$ A23187 per 1 ml of vesicles (10 mg DPPC) and 5 mM extravesicular Pr^{3+} . \blacktriangle — \blacktriangle , control. Vesicles in the presence of: \bullet — \bullet , 86 mM ethanol; \triangle — \triangle , 172 mM ethanol; \blacksquare — \blacksquare , 86 mM diethyl ether; \circ — \circ , 25 mM chloroform; \square — \square , 86 mM chloroform.

ethanol, diethyl ether and chloroform on the channel-mediated transport. The plots are seen to be linear and the slopes therefore give the rates of transport of Pr^{3+} across the vesicular bilayer. Chloroform strongly inhibits the rate of transport, the effect being marked down to the lowest concentration studied, 5 mM. Also the action of ethanol and diethyl ether is similar to their effects on vesicle lysis in that channels are again stabilised to allow increase in transport of the Pr^{3+} .

As a comparative experiment using a carrier-type ionophore, the effects of these same compounds on A23187-mediated transport was measured. The results are shown in Fig. 8. It is significant that chloroform increases the transport rate, in contrast to the channel-mediated mechanisms. The effect of ethanol and diethyl ether is, however, again to stimulate transport rates. Similar experiments were also performed with the carrier ionophore ionomycin (results not shown) and again all three compounds increased the transport rate.

Discussion

Our observation that chloroform decreases the linewidth of the lipid signals agrees with previous

studies by Shieh et al. [29] and Vanderkooi and co-workers [7] and the implication is that the anaesthetic fluidises the bilayer. The lowering of the phase transition temperature has also been previously observed for all three compounds [7] and other fluorinated ether anaesthetics [30] and the effect is ascribed to a disordering of the acyl chains. The observed upfield shift of the outer headgroup signal *O* implies that there is sufficient chloroform in the bilayer-water boundary region to influence the binding of the Pr^{3+} to the phosphate sites on the outer headgroups of the vesicles. A similar deduction was made by Koehler et al. [31] who observed that Gd^{3+} caused changes in the linewidth of the ^{19}F -NMR signal from halothane only in the presence of phosphatidylcholine liposomes. These experiments indicate that anaesthetic and lanthanide ion coexist at the membrane surface.

The mechanism by which the permeability of lipid bilayers is increased at the phase transition is still unresolved. Permeable boundary layers between coexisting gel and fluid domains or an increase in the lateral compressibility of the bilayer have both been proposed and discussed [32]. Observations using planar lipid bilayers show large conductance changes via transient single channels indicating that a few defects of quite extended size occur at T_c [33,34]. Our previous observations [8,10] and the results reported here confirm this since in DPPC vesicles the channels which open at T_c are sufficiently large to allow equilibration of the 5 mM Pr^{3+} across the phospholipid bilayer. We have described this process as vesicular lysis, but it should be noted that as demonstrated in Fig. 3, the vesicular membrane integrity is not lost and impermeability is restored on raising the temperature above T_c .

Our observation that ethanol and diethyl ether both increase the extent of lysis at T_c , while chloroform decreases it, may result from a change in the activation energy for the opening of the channels (resulting in more or less channels being opened per passage through T_c) or from channels being stabilised or extended by the ethanol and diethyl ether and destabilised by chloroform. A number of authors have implicated the effect of water penetration and interaction into the lipid bilayer in modifying the energy barrier to ionic

permeability [22,23]. Also in the case of gel areas dispersed in fluid, the boundary effect will induce increased water penetration into the acyl chain region of the bilayer [35]. A reasonable hypothesis consistent with our observations would therefore be that the effects of the three compounds on vesicular lysis is mediated by their action on the structure or properties of the water which is associated with the channels.

Both our preliminary studies using vesicles [10] and work elsewhere with planar membranes [14] suggest that at low concentrations near its critical micelle concentration (approx. 0.25 mM), Triton X-100 stabilises channels formed in lipid bilayers. The results reported above confirms this (compare the control vesicle lysis in Figs. 4 and 5, noting the much smaller number of cycles through T_c used in the presence of Triton). The effect of the three compounds studied is even more marked for Triton-stabilised channels (Fig. 5) than for Triton-free channels (Fig. 4). Again the striking feature is increased lysis by the oxygen-containing compounds and decreased lysis by chloroform.

Triton X-100, like all molecules containing polyoxyethylene groups including poly(ethylene glycol), is strongly hydrated in solution. The channels which are stabilised by Triton will be lined by this amphipathic molecule, so introducing an additional water content to the channel. The strong effect of ethanol, diethyl ether and chloroform on these channels again implies that their interaction with the channel water is significant in determining their action on lytic channels. The fusogenic action of Triton X-100 [10,15] is probably mediated by inverted micelles of Triton and lipid being formed between the fusing bilayers, if the general mechanism of fusion suggested by Cullis and de Kruijff [36] is applicable in this case. The inverted micelles will contain water and our suggestion is that the observed effects of ethanol and diethyl ether in promoting fusion, and chloroform in inhibiting it, can be mediated by their effects on the inverted micelle water or the interaction of the water with the phospholipid headgroups.

The polypeptide, channel forming, ionophore Alamethicin 30 has been extensively studied by conductivity measurements using planar lipid bilayers, and the work recently reviewed [37]. Following the observation that this ionophore could

also transport lanthanide ions across planar membranes [38] we used the NMR method described above to examine Alamethicin 30 mediated transport of Pr^{3+} across vesicular membranes [13]. Detailed structural information based on X-ray analysis and model building of Alamethicin is now available [24]. These studies indicate that in the channel formed by the aggregation of four or more monomers hydrogen bonding is extensive, especially at the annulus formed by Gln 7 residues. The Gln 7 side-chain amide protons will donate a hydrogen bond to water forming a ring of hydrogen-bonded water, the structure of which effectively controls the size of ion channel. Changes in this hydrogen-bonded water provide an explanation of the observation that the higher conductance substates of the Alamethicin channels are only moderately sensitive to cation radius [39] which implies that the current increases are due to changes in channel cross-section rather than increase in the number of parallel open channels. Given that halogenated hydrocarbon anaesthetics such as chloroform have been shown by infra-red methods [40] to perturb hydrogen bonds in membranes, the hydrogen bonded water content of the Alamethicin channels must be regarded as a likely target for the observed effects of ethanol and the two general anaesthetics, as indicated in Fig. 7. In contrast to the channel-mediated transport, when A23187 or Ionomycin are used, all three compounds, alcohol, ether and chloroform, increase the rate of transport as seen in Fig. 8.

In these initial experiments we were not rigorously attempting to explore the action of these compounds at clinical levels of concentration for general anaesthesia. These latter concentrations are difficult to obtain experimentally but quoted values are of the order 50 mM ethanol, 15 mM diethyl ether and 1 mM chloroform [19,41]. Seeman indicates that concentrations required for nerve block (as in local anaesthesia) are ten times these values [41]. For ethanol we have therefore used physiological relevant concentrations. The lowest values of chloroform studied were 5 mM for Alamethicin transport. The large effect on the transport rate observed indicates that inhibition will be expected down to physiological concentrations for this type of anaesthetic.

Taken together the similarities in the effects of

the three compounds on each channel system imply a common element in the mechanism. Since for each mechanism of channel formation studied, the importance of water structure and function in the channels is strongly indicated, it is difficult to avoid the implication that the effect of the compounds on channel water is the unifying feature of the results.

It would clearly be premature to claim to have demonstrated a possible novel mechanism of general anaesthesia on the basis of a small range of compounds and model systems. However, the lipid-based theories of general anaesthesia [18] have recently been strongly and effectively criticised [2,19] and direct protein-anaesthetic action is seen to be unlikely on structural grounds [19]. Our results suggest a modification of the protein hypothesis which would be worthy of further investigation, namely that an important locus of action of the general anaesthetics could be their effect on water structure and function in the ion channels at synapses in the central nervous system. We are aware that water structure was previously proposed as a mechanism of anaesthesia by Pauling [42] and Miller [43], but these theories were based on a direct effect of the hydrophilic anaesthetic on Ice I clathrate structures. We are proposing a more general interaction of the type put forward by Eyring and co-workers [44] which would include a variable effect on hydrogen bonding depending on the chemical nature of the anaesthetic. A recent theoretical model of ion channels which accounts well for the electrical properties of Na^+ and K^+ channels, is based on a hydrogen-bonded ordered water channel at a protein site spanning the membrane [45,46]. Experiments such as those described here begin to provide specific tests for this theory.

Richards [2] has pointed out that it is very unlikely that all general anaesthetics act at a single type of site. Clearly, further experiments on a wide range of anaesthetics, systems of membrane channels and fusion sites will be required to reinforce the hypothesis that effects on water structure and properties are important in the mechanism of anaesthesia.

Acknowledgement

The support of the Sir Halley Stewart Trust in part of this work is gratefully acknowledged, as

also the efficiency of Mrs. M. Morris in preparing the manuscript.

References

- 1 Bowman, W.C. and Rand, M.J. (1980) Textbook of Pharmacology, 2nd Edn., Blackwell, Chapter 7
- 2 Richards, D.C. (1980) Mechanisms of General Anaesthesia, in Topical Reviews in Anaesthesia, Vol. 1 (Norman, J. and Whitwam, J.G., eds.), pp. 1–84, J. Wright and Sons, Bristol
- 3 Barker, J.L. (1975) Brain Res. 92, 35–55
- 4 Hendry, B.M., Urban, B.W. and Haydon, D.A. (1978) Biochim. Biophys. Acta 513, 106–116
- 5 Dluzewski, A.R. and Halsey, M.J. (1981) Br. J. Anaesth. 53, 184P
- 6 Pope, C.G., Urban, B.W. and Haydon, D.A. (1982) Biochim. Biophys. Acta 688, 279–283
- 7 Vanderkooi, J.M., Landberg, R., Selick, H. and McDonald, G.G. (1977) Biochim. Biophys. Acta 464, 1–16
- 8 Hill, M.W. (1975) Biochem. Soc. Trans. 3, 149–152
- 9 Hunt, G.R.A. and Tipping, L.R.H. (1978) Biochim. Biophys. Acta 507, 242–261
- 10 Hunt, G.R.A. (1980) FEBS Lett. 119, 132–136
- 11 Hunt, G.R.A. (1975) FEBS Lett. 58, 194–196
- 12 Hunt, G.R.A., Tipping, L.R.H. and Belmont, M.R. (1978) Biophys. Chem. 8, 341–355
- 13 Hunt, G.R.A. and Jones, I.C. (1982) Biosci. Rep. 2, 921–928
- 14 Schlieper, P. and De Robertis, E. (1977) Arch. Biochem. Biophys. 184, 204–208
- 15 Alonso, A., Villena, A. and Goni, F.M. (1981) FEBS Lett. 123, 200–204
- 16 Gent, M.P.N. and Prestegard, J.H. (1974) Biochemistry 13, 4027–4033
- 17 Liao, M.-J. and Prestegard, J.H. (1980) Biochim. Biophys. Acta 599, 81–94
- 18 Janoff, A.S. and Miller, K.W. (1982) A Critical Assessment of the Lipid Theories of General Anaesthesia in Biological Membranes, Vol. 4 (Chapman, D., ed.), pp. 417–476, Academic Press, New York
- 19 Franks, N.P. and Lieb, W.R. (1982) Nature 300, 487–493
- 20 Fink, B.R. (ed.) (1980) Molecular Mechanisms of Anaesthesia (Progress in Anaesthesiology, Vol. 2), Raven Press, New York
- 21 Kenehiş, M.I. and Tsong, T.Y. (1978) J. Am. Chem. Soc. 100, 424–432
- 22 Griffith, O.H., Dehlinger, P.J. and Van, S.P. (1974) J. Membrane Biol. 15, 159–192
- 23 Israelachvili, J.N., Marcelja, S. and Horn, R.G. (1980) Q. Rev. Biophys. 13, 121–200
- 24 Fox, R.O. and Richards, F.M. (1982) Nature 300, 325–330
- 25 Hunt, G.R.A. and Tipping, L.R.H. (1980) J. Inorg. Biochem. 12, 17–36
- 26 Bergelson, L.D. (1978) in Methods in Membrane Biology (Korn, E.D., ed.), Vol. 9, pp. 275–335, Plenum Press, New York
- 27 Hutton, W.C., Yeagle, P.L. and Martin, R.B. (1977) Chem. Phys. Lipids 19, 255–265
- 28 Lee, A.G. (1975) Prog. Biophys. Mol. Biol. 29, 3–56

- 29 Shieh, D.D., Ueda, I., Lim, H.-C. and Eyring, H. (1976) *Proc. Natl. Acad. Sci. U.S.A.* 73, 3999-4002
- 30 Koehler, K.A., Jain, M.K., Stone, E.E., Fossel, E.T. and Koehler, L.S. (1978) *Biochim. Biophys. Acta* 510, 177-185
- 31 Koehler, L.S., Fossel, E.T. and Koehler, K.A. (1977) *Biochemistry* 16, 3700-3707
- 32 Marcelja, S. and Wolfe, J. (1979) *Biochim. Biophys. Acta* 557, 24-31
- 33 Antonov, V.F., Petrov, V.V., Molnar, A.A., Prevoditelev, D.A. and Ivanov, A.S. (1980) *Nature* 283, 585-586
- 34 Boheim, G., Hanke, W. and Eibl, H. (1980) *Proc. Natl. Acad. Sci. U.S.A.* 77, 3402-3407
- 35 Fettiplace, R. and Haydon, H. (1980) *Physiol. Rev.* 60, 510-550
- 36 Cullis, P.R. and De Kruijff, B. (1979) *Biochim. Biophys. Acta* 559, 399-420
- 37 Lattore, R. and Alvarez, O. (1981) *Physiol. Rev.* 61, 77-150
- 38 Gögelein, H., De Smedt, H., Van Driessche, W. and Borghgraef, R. (1981) *Biochim. Biophys. Acta* 640, 185-194
- 39 Eisenberg, M., Kleinberg, M.E. and Shaper, J.H. (1977) *Ann. N.Y. Acad. Sci.* 303, 281-291
- 40 Sandorfy, C. (1980) in *Molecular Mechanisms of Anaesthesia, Progress in Anaesthesiology, Vol. 2* (Fink, B.R., ed.), pp. 353-359, Raven Press, New York
- 41 Seeman, P. (1972) *Pharmacol. Rev.* 24, 583-655
- 42 Pauling, L. (1961) *Science* 134, 15-21
- 43 Miller, S.L. (1961) *Proc. Natl. Acad. Sci. U.S.A.* 47, 1515-1524
- 44 Kamaya, H., Ueda, I. and Eyring, H. (1980) in *Molecular Mechanisms of Anaesthesia, Progress in Anaesthesiology, Vol. 2* (Fink, B.R., ed.), pp. 429-433, Raven Press, New York
- 45 Edmonds, D.T. (1980) *Proc. R. Soc. Lond. B211*, 51-62
- 46 Edmonds, D.T. (1981) *Trends Biochem. Sci.* 6, 92-94

APPLICATION OF ^1H -NMR TO THE DESIGN OF LIPOSOMES FOR ORAL USE.

SYNERGISTIC ACTIVITY OF BILE SALTS AND PANCREATIC PHOSPHOLIPASE A_2
IN THE INDUCED PERMEABILITY OF SMALL UNILAMELLAR PHOSPHOLIPID VESICLES

G. R. A. Hunt and I. C. Jones

Department of Science
The Polytechnic of Wales
PONTYPRIDD, CF37 1DL, Mid Glam. U.K.

Running Title: Liposomes for oral use

ABSTRACT

^1H -NMR spectroscopy of small unilamellar phospholipid vesicles in the presence of the lanthanide probe ion Dy^{3+} has been used to study the permeability of these liposomes induced by the bile salts (glycocholate and glycodeoxycholate) and pancreatic phospholipase A_2 . A marked synergism is demonstrated in the combined effects of these digestive agents in producing permeability of the vesicles to Dy^{3+} . Changes in the ^1H -NMR spectrum of the vesicular phospholipid head-groups before permeability is induced, indicate that the products of the enzymic hydrolysis (lyso lipids and fatty acids) and transmembrane lipid exchange are involved in the permeability mechanism. The results are discussed in terms of the advantages of the use of NMR techniques in the future design of liposomes for oral use.

INTRODUCTION

The use of liposomes (lipid membrane vesicles) as carriers of therapeutic drugs is now being widely explored (Ryman et al., 1980; Gregoriadis and Allison, 1980; Knight, 1981, Yatvin and Lelkes, 1982). In particular the prospect of a more convenient method of administering insulin has attracted much attention to liposomal packaging and delivery of this drug by the oral route (Patel et al., 1978; Hashimoto and Hawada, 1979). While in general the oral use of liposomes has been less explored than the intravenous route, the above reports indicate that liposomes protect the insulin from rapid degradation. However, only about 1% of the packaged insulin reaches the target site and this has been attributed to the lack of liposomal stability in the harsh environment of the gastrointestinal tract (Ryman et al., 1980).

In order to explore how the stability of vesicular lipid membranes could be improved, Rowland and Woodley (1980) examined the separate actions of lipases and bile salts on liposomes of a variety of compositions. However, recent work suggests that interaction between bile salts and digestive enzymes can occur in the hydrolysis of triglyceride by lipase in milk fat globules (Blackberg et al . 1981) and in the hydrolysis of phospholipid by phospholipase A₂ in bile salt/lipid mixed micelles (Nalbone et al., 1980).

The possibility that bile salt and phospholipase activity may be cooperative has clear implications for the design and use of liposomes by the oral route. We have therefore commenced a series of studies to determine (a) whether or not bile salts and phospholipase A₂ increase the permeability of small unilamellar

phospholipid vesicles in a cooperative or synergistic manner, (b) the mechanism of this cooperative interaction, and (c) the compositions of liposomes most likely to resist this destabilisation of the integrity of liposomal carrier species. We report here the initial results on part (a) of these studies.

Our previous work on the ionophore and lytic action of bile salts in phospholipid vesicles used the technique of NMR spectroscopy and the lanthanide paramagnetic probe ion Pr^{3+} (Hunt, 1980; Hunt and Jawaharlal, 1980). We here extend these techniques to allow observation of the action of phospholipase A_2 in producing permeability of the vesicles to lanthanide ions, and show that the method demonstrates a clear synergism between the enzyme and conjugated bile salts as well as suggesting a mechanism for their action.

MATERIALS AND METHODS

Egg phosphatidylcholine (Egg PC) was obtained from Lipid Products, Redhill, and conjugated bile acids, glycocholic and glycodeoxycholic acid, in the form of their sodium salts, from Calbiochem. Porcine pancreatic and snake venom (naja naja) phospholipase A_2 (PLA_2) was purchased from Sigma. Analar calcium chloride was obtained from BDH; praseodymium chloride (99.9%) from Lancaster Synthesis (Morecambe, Lancs) and dysprosium chloride (99.9%) from Koch-Light. Deuterium Oxide ($^2\text{H}_2\text{O}$, 99.8% Gold Label) was purchased from Aldrich.

The vesicular membranes (small unilamellar liposomes) were prepared as described previously (Hunt and Tipping, 1978) using a probe type sonicator (Soniprobe 7532A, Dawe Instruments) except that since egg PC contains unsaturated acyl chains, precautions were taken against oxidation by sonicating the egg PC and $^2\text{H}_2\text{O}$ under N_2 and at 4°C . The vesicular solutions used contained 10 mg egg PC

per ml and ^1H -NMR spectra of these were obtained at 37°C using a JEOL FX 90Q multinuclear FT-NMR spectrometer fitted with calibrated temperature control. The 10 mm NMR tubes contained 1 ml of vesicular solution confined by a vortex plug and capped. Typically 10 pulse sequences were used (π - τ - $\pi/2$) with a pulse interval τ of about two seconds in order to minimise the ^1H -O- ^2H signal.

Extravesicular ionic concentrations of $150\text{ }\mu\text{M Dy}^{3+}$, 5 mM Pr^{3+} and 2 mM Ca^{2+} were obtained by pipetting small volumes ($\sim 10\text{ }\mu\text{l}$) of $^2\text{H}_2\text{O}$ stock solutions into the NMR tubes. The required units (2, 7 or 28) of PLA_2 were introduced into the NMR tubes by pipetting small volumes of a $^2\text{H}_2\text{O}$ stock solution of PLA_2 into the vesicular solutions containing the required metal ions. Stock solutions of the bile salts in $^2\text{H}_2\text{O}$ (0.1 M) were pipetted into the vesicular solutions to give extravesicular concentrations of 0.5 or 1.0 mM .

The ^1H -NMR spectrum of Egg PC vesicles at 37°C includes high resolution signals from the lipid acyl chains (H) and choline head-groups. On adjusting the extravesicular concentration to $150\text{ }\mu\text{M Dy}^{3+}$ and 2 mM Ca^{2+} the spectrum in Fig 1 was obtained. This showed separate signals originating from the extravesicular head-groups O, and intravesicular head-groups I. Such vesicular signal separations are now well documented (Bergelson, 1978) and result from a concentration-dependent downfield shift of signal O due to the effect of the paramagnetic Dy^{3+} in rapid exchange between the phosphate sites on the extravesicular head-groups. The ratio of the signal areas O:I is equivalent to the ratio of the number of choline groups in the outer monolayer of the vesicles to that in the inner monolayer. The ratio is also a reliable indication of the vesicle size (Hutton et al, 1977). In our case the initial ratio of area O:I was approximately 1.7 indicating an average vesicle diameter of 32 nm .

When Dy^{3+} ions are transported across the lipid bilayer into the intravesicular solution the rise in intravesicular concentration of Dy^{3+} causes signal I to move downfield towards signal O. By measuring the change in chemical shift (Hz)

of signal I with time the rate of transport can be obtained. In order to convert experimentally observed shifts into an intravesicular concentration of Dy^{3+} a calibration graph is necessary. This calibration graph (not shown) is obtained by sonicating known concentrations of Dy^{3+} into separate vesicle preparations and then adjusting the extravesicular concentration to $150 \mu\text{M Dy}^{3+}$. At each different intravesicular concentration of Dy^{3+} ions the shift of signal I is measured. This method of monitoring the rates of transport is based on that described previously for Pr^{3+} ions (Hunt et al, 1978; Hunt and Jones, 1982).

RESULTS

Initial experiments were performed with varying amounts of Naja Naja PLA_2 and an extravesicular concentration of 5 mM Pr^{3+} . Although a range of Ca^{++} concentrations were used, very little enzyme activity was detected. This was attributed to the relatively high Pr^{3+} concentration and consequent competition for the Ca^{++} binding sites on the enzyme. The Pr^{3+} was therefore substituted by 0.15 mM Dy^{3+} which gives a similar downfield shift of the outside choline head-group signal O. Subsequent experiments showed that Naja Naja PLA_2 and pancreatic PLA_2 were both active under these conditions, although as expected from previous studies in the literature (Slotboom et al, 1982) the snake venom PLA_2 activity was higher.

Fig 2 (a-h) shows the time-dependent changes in the $^1\text{H-NMR}$ spectrum of the inner and outer head-groups of Egg PC vesicles during an experiment using 28 units of pancreatic PLA_2 . Fig 2 (a-d) shows that initially a gradual increase in the ratio of the signal areas O:I occurs, which continues until a ratio of 2.1 is obtained. During this period the signal I remains unshifted, indicating that no Dy^{3+} ions have permeated into the intravesicular space. However, the subsequent spectra, Fig 2 (e-h) show that signal I ,

from the intravesicular head-groups, is shifting downfield towards signal 0. This shift corresponds to an increase in intravesicular concentration of Dy^{3+} ions due to a permeability of the vesicular membrane. Similar time-dependent spectra were obtained using 7 and 2 units of PLA_2 but over increasing time scales.

On conversion of the measured shift of signal I (in Hz) into the intravesicular concentration of dysprosium ion $[\text{Dy}^{3+}]_i$, using a calibration graph (see Materials and Methods), the corresponding plots of $[\text{Dy}^{3+}]_i$ against time are shown in Fig 3, for the three concentrations of PLA_2 used. The initial lack of transport corresponds to the period during which the O:I ratio is changing. A separate sample of vesicles also containing 28 units of PLA_2 and 0.15 mM Dy^{3+} was set up in order to investigate whether the increase in the O:I ratio was due to vesicular lysis (Hunt and Jones, 1983). In this case a further quantity of extravesicular Dy^{3+} is added to the sample having reached an O:I ratio of 2.1 (as in Fig 2d). No peak corresponding to the inside signal of lysed vesicles was revealed, indicating that no vesicular lysis has occurred.

We have shown previously (Hunt and Jawaharlal, 1980; Hunt, 1980) that the bile salts can induce permeability in small unilamellar vesicles at bile salt concentrations below that required to disrupt the vesicles. In order to investigate possible synergism in the activity of pancreatic PLA_2 and the bile salts, similar time-dependent spectra to those in Fig 2 were obtained from Egg PC vesicles undergoing the combined action of PLA_2 and bile salts. Experimental protocols were employed which explored the effects of both low and high concentrations of each reagent. Thus in the experiments illustrated in Fig 4 the concentration of bile salts used (0.5 mM) is such that very little membrane permeability is produced by bile salt acting alone. However, a marked synergistic effect is observed with 28 units/ml of PLA_2 . Figs 5 and 6 show the effect of reducing the concentration of PLA_2 to 2 units/ml and 7 units/ml respectively, but at a concentration of bile salt (1.0 mM) which can itself

produce moderately rapid permeability of the vesicles. At these concentrations of PLA₂ much slower enzyme activity is observed, but again the synergism with the bile salts is very apparent. Table 1 gives a summary of the rates of transport of Dy³⁺ obtained from the slopes of the graphs in Figs 4, 5 and 6. In the case of the rates obtained using 1 mM bile salt (Figs 5 and 6) the initial slopes were used.

It should be noted that the NMR signals from the vesicles give a constant indication of the vesicular stability. In particular the width of the acyl chain hydrocarbon signal (H in Fig 1) is very sensitive to change in the average vesicular dimensions, e.g. as caused by fusion of the vesicles into larger structures. No significant change in signal H was observed during the above experiments, indicating that the transport was not accompanied by vesicular fusion (Liao and Prestegard, 1980).

DISCUSSION

Phospholipase A₂ (PLA₂) catalyses the specific hydrolysis of the ester bond at the 2-position in 1,2-diacylphospholipids such as egg-PC, to give equimolar quantities of 1-acyl lysophosphatidylcholine (lyso PC) and fatty acid (FA). Details at the molecular level of the mechanism by which the enzyme attacks a macromolecular aggregate of lipids (e.g. a monolayer or bilayer) are still controversial (Slotboom et al, 1982). However, our observation that the O/I ratio increases from 1.7 to 2.1 indicates that there is a net transfer of choline-containing lipid (PC or lyso PC) from the inner to the outer monolayer. We postulate therefore that following the build-up of the hydrolysis products (lyso PC plus FA) in the outer monolayer, transmembrane lipid exchange (flip-flop) takes place in which PC in the inner monolayer is replaced by FA (plus some lyso PC). We have recently confirmed this lipid exchange using ³¹P-NMR (to be reported elsewhere) in which the rate of hydrolysis and the signals from PC and lyso PC in each monolayer can be separately measured.

NMR studies by others have shown that transmembrane migration of lyso PC in small vesicles (van Zoelen et al, 1978) and large unilamellar vesicles (van der Steen et al, 1981) is catalysed by the presence of the red blood cell protein, glycophorin, in the bilayer. The thermodynamic drive for the migration of the hydrolysis products of PLA₂ across the membrane may therefore be due to the asymmetry of the vesicular membrane in its composition or in its curvature.

The most likely mechanism for such exchange of lipid is that proposed by Cullis and de Kruijff (1979) who produce considerable evidence for the existence of inverted micelles within a bilayer structure which allows a rapid 'flip-flop' movement across the membrane. The aqueous compartment within the inverted micelles also provides a mechanism of transmembrane transport (Cullis et al, 1980) but the permeability will depend on the composition of the micelles and the size of the aqueous compartment. Our ³¹P-NMR results (not shown) indicate that the change in ¹H-NMR O/I ratio of 1.7 to 2.1 corresponds to the substitution

of approximately 20% PC by FA in the inner monolayer. This is followed by the exchange of outer monolayer lyso PC with inner monolayer PC, until all inner PC is replaced. Only at this stage is permeability induced. This suggests that the bilayer permeability to Dy^{3+}_{aq} results when the inverted micelles contain only lyso PC and FA. It is of significance to note here that recent studies have shown that stable vesicular bilayer membranes can be formed when composed entirely of equimolar amounts of lyso PC and FA (Allegrini et al, 1983; Jain and De Haas, 1981). We have confirmed these experiments but also observe that the vesicles composed only of lyso PC and FA are very permeable to lanthanide ions, as would be expected from the transport mechanism proposed above.

Based on the observations described (Figs 4 - 6) which indicate a strong synergistic activity of the bile salts in the PLA_2 -egg PC system, we can propose two mechanisms for this bile salt activity depending on the concentration of these detergents. At the lower concentration (0.5 mM) - see Fig 4 - the time required to produce the O/I ratio change is very short and the resulting transport rate rapid. The reduced time for the O/I ratio change suggests that the bile salts cause perturbation in the outer monolayer surface so rendering it a more suitable substrate for enzyme binding and activity. This is in accord with the current view of this enzyme-substrate interaction (Jain et al, 1982). However, the increased rate of transport observed (Fig 4) also indicates a participation of the bile salt molecules in the permeability mechanism. Our earlier experiments (Hunt and Jawaharlal, 1980) indicated that the bile salt-induced transport is due to the formation of inverted bile salt micelles. So the likely mechanism for the synergistic permeability would be mixed micelles composed of lyso PC, FA and bile-salt molecules.

This proposal is further confirmed by the results illustrated in Figs 5 and 6. Here it is seen that at a bile salt concentration of 1.0 mM then the synergistic transport commences immediately. No O/I ratio change occurs, but the vesicles

become immediately permeable. This strongly suggests that the bile salt molecules are themselves taking part in the formation of inverted micelles together with the hydrolysis products FA and/or lyso PC, i.e. once the FA and lyso PC are available in the outer monolayer then transporting inverted micelle species are formed in conjunction with bile salt molecules. It should be noted that our previous studies have shown that the stoichiometry of the bile salt inverted micelles is at least four, so that a large dependence of transport rate on concentration is observed (Hunt and Jawaharlal, 1980). Thus a significant change in behaviour of the system is expected on increasing the bile salt concentration by a factor of two (0.5 to 1.0 mM).

These experiments therefore show a distinct synergism in the activity of PLA_2 and bile salt, so that this should be taken into account in the design of liposomes for oral drug delivery. Clearly further work will be necessary in order to investigate vesicular compositions and sizes which are resistant to this synergistic attack in the digestive tract. We have made a start on these studies using small unilamellar vesicles containing cholesterol and a range of lipids. While large unilamellar liposomes are likely to have different behaviours and therefore need comparative investigation, it is interesting to note that the superior properties of small liposomes have recently been demonstrated for drug transfer to target cells (MacK^hky and Leserman, 1983).

The insight given by the NMR techniques into the mechanisms of the permeability induced by bile salts and phospholipases can clearly be of decisive value in considering which liposomal compositions and structures to use in future encapsulation and oral delivery systems.

REFERENCES

- ALLEGRI, P.R., VAN SCHARRENBURG, G., DE HASS, G.H. and SEELIG, J., 1983, ^1H and ^{31}P -NMR studies of bilayers composed of 1-acyl lysophosphatidylcholine and fatty acids. Biochim. Biophys. Acta, **731**, 448-455.
- BLACKBERG, L., HERNELL, O. and OLIVECRONA, T., 1981, Hydrolysis of human milk fat globules by pancreatic lipase. Role of colipase, phospholipase A_2 and bile salts. J. Clin. Invest., **67**, 1748-1752.
- BERGELSON, L.D., 1978, Paramagnetic hydrophilic probes in NMR investigations of membrane systems, Methods in Membrane Biology, Vol.9, edited by Korn, E.D. (Plenum Press N.Y.) pp 275-335.
- CULLIS, P.R. and DE KRUIJFF, B., 1979, Lipid polymorphism and the functional roles of lipids in biological membranes, Biochim. Biophys. Acta, **559**, 399-420.
- CULLIS, P.R., DE KRUIJFF, HOPE, M.J., NAYAR, R. and SCHMID, S.L., 1980, Phospholipids and membrane transport, Can. J. Biochem, **58**, 1091-1100.
- GREGORIADIS, G. and ALLISON, A.C. (Editors), 1980, Liposomes in Biological Systems, John Wiley & Sons Ltd., Chichester.
- HASHIMOTO, A. and HAWADA, J., 1979, Effects of oral administration of positively charged insulin liposomes on alloxan diabetic rats: Preliminary study, Endocrinol Japan, **26**, 237-344.
- HUNT, G.R.A., TIPPING, L.R.H. and BELMONT, M.R., 1978, Rate-determining processes in the transport of Pr^{3+} ions by the ionophore A23187 across phospholipid vesicular membranes. A ^1H -NMR and theoretical study. Biophys. Chem. **8**, 341-355.
- HUNT, G.R.A., 1980, A comparison of Triton X-100 and the bile salt taurocholate as micellar ionophores or fusogens in phospholipid vesicular membranes, FEBS. LETT., **119**, 132-136.
- HUNT, G.R.A. and JAWAHARLAL, K., 1980, A ^1H -NMR investigation of the mechanism for the ionophore activity of the bile salts in phospholipid vesicular membranes and the effect of cholesterol. BIOCHIM. BIOPHYS. ACTA, **601**, 678-684.

HUNT, G.R.A. and JONES, I.C., 1982, Lanthanide ion transport across phospholipid vesicular membranes: a comparison of alamethicin 30 and A23187 using ^1H -NMR spectroscopy. Bioscience Rep., 2, 921-928.

HUNT, G.R.A. and JONES, I.C., 1983, A ^1H -NMR investigation of the effects of ethanol and the general anaesthetics on ion-channels and membrane fusion using unilamellar phospholipid membranes. Biochim. Biophys. Acta, 736, 1-10.

HUTTON, W.C., YEAGLE, P.L. and MARTIN, R.B., 1977, The interaction of lanthanide and Ca^{2+} salts with phospholipid bilayer vesicles: the validity of the NMR method for determination of vesicle bilayer phospholipid surface ratios. Chem. Phys. Lipids, 19, 255-265.

JAIN, M.K. and DE HAAS, G.H., 1981, Structure of 1-acyl lysophosphatidylcholine and fatty acid complex in bilayers. Biochim. Biophys. Acta, 642, 203-211.

JAIN, M. K., EGMOND, M.R., VERHEIJ, H.M., APITZ-CASTRO, R., DIJKMAN, R. and DE HAAS, G.H., 1982, Interaction of phospholipase A_2 and phospholipid bilayers. Biochim. Biophys. Acta, 688, 341-348.

KNIGHT, C.G. (editor), 1981, Liposomes: From Physical Structure to Therapeutic Applications. Elsevier - North Holland Biomedical Press, Amsterdam.

LIAO, M.J. and PRESTEGARD J.H., 1980, Fusion kinetics of phosphatidylcholine-phosphatidic acid mixed lipid vesicles. A ^1H -NMR study. Biochim. Biophys. Acta, 559, 81-94.

MACHY, P. and LESERMAN, L.D., 1983, Small liposomes are better than large liposomes for specific drug delivery in vitro. Biochim. Biophys. Acta, 730, 313-320.

NALBONE, G., LAIRON, D., CHARBONNIER-AUGEIRE, M., VIGNE, J-L., LEONARDI, J., CHABERT, C., HAUTON, J.C. and VERGER, R., 1980, Pancreatic phospholipase A_2 EC-3.1.1.4 hydrolysis of phosphatidylcholines in various physiochemical states. Biochim. Biophys. Acta, 620, 612-626.

PATEL, H.M., HARDING, N.G.L., LOGUE, F., KESSOR, C., MacCUISH, A.C., MACKENZIE, J.C., RYMAN, B.E. and SCOBIE, I., 1978, Intrajejunal absorption of liposomally entrapped insulin in normal man. Biochem. Soc. Trans., 6, 784-5.

ROWLAND, R.N. and WOODLEY, J.F., 1980, The stability of liposomes in vitro to pH, bile salts and pancreatic lipase. Biochim. Biophys. Acta, 620, 400-409.

RYMAN, B.E. and TYRRELL, D.A., 1980, Liposomes - bags of potential. Essays in Biochemistry, Vol.16. Edited by Campbell, P.N. and Marshall, R.D. (Academic Press) pp49-98

SLATBOOM, A.J., VERHEIJ, H.M. and DE HAAS, G.H., 1982, On the mechanism of phospholipase A₂. Phospholipids, edited by Hawthorne, J.N. and Ansell, G.B. (Elsevier Biomedical Press) pp 359-434.

VAN DER STEEN, A.T.M., DE JONG, W.A.L., DE KRUIJFF, B. and VAN DEENEN, L.L.M., 1981, Lipid dependence of glycophorin-induced transbilayer movement of lysophosphatidylcholine in large unilamellar vesicles. Biochim. Biophys. Acta., 647, 63-72.

VAN ZOELLEN, E.J.J., DE KRUIJFF, B. and VAN DEENEN, L.L.M., 1978, Protein-mediated transbilayer movement of lysophosphatidylcholine in glycophorin-containing vesicles. Biochim. Biophys Acta, 508, 97-108.

YATVIN, M.B. and LELKES, P.I., 1982, Clinical prospects for liposomes. Med. Phys., 9, 149-175.

TABLE 1

Rates of transport of Dy^{3+} ($\mu\text{M min}^{-1}$) produced by various concentrations of pancreatic phospholipase A_2 and bile salts in egg PC vesicles at 37°C

UNITS OF PLA_2 per ml	CONCENTRATION OF BILE SALTS			
	0	1 mM Glycocholate	0.5 mM Glycocholate	0.5 mM Glycodeoxycholate
0	-	0.03	0.007	0.025
2	0.015	0.543 (12.1) ^a (18.1) ^b	-	-
7	0.059	1.667 (18.2) ^a (55.6) ^b	-	-
28	0.172	—	0.923 (5.2) ^a (131.8) ^b	1.17 (5.9) ^a (46.8) ^b

(a,b) Figures in brackets represent the factors by which the rates obtained for the joint action of PLA_2 and bile salt exceed the rates obtained from the sum of the individual rates. (a) These factors were calculated using the PLA_2 rates shown in the table. (b) In calculating these factors, values of zero were used for all PLA_2 control rates since no transport is observed during the initial 200 minutes in these samples.

CAPTIONS FOR FIGURES

Fig 1 The 90 MHz ^1H -NMR spectrum of egg phosphatidylcholine vesicles at 37°C in the presence of extravesicular concentrations 0.15 mM Dy^{3+} and 2 mM Ca^{2+} . Signals shown originate from the extravesicular choline head-groups O, the intravesicular choline head-groups I, and the lipid acyl chains H. Shifts are shown in p p m with respect to external T M S.

Fig 2 Spectra a-h show the time dependent changes in the ^1H -NMR signals originating from the inner and outer choline head-groups of egg PC vesicles in the presence of initial extravesicular concentrations of 0.15 mM Dy^{3+} and 2 mM Ca^{2+} and 28 units per ml of pancreatic phospholipase A_2 at 37°C . The chemical shifts of signal I are measured in Hz with reference to signal H (see Fig 1) and are shown after (a) 7 mins, (b) 70 mins, (c) 120 mins, (d) 180 mins, (e) 240 mins, (f) 480 mins, (g) 550 mins, (h) 680 mins. Spectra e - f show no further increase in the O:I ratio but show a downfield movement of signal I during the transport of Dy^{3+} from the extravesicular to the intravesicular region.

Fig 3 Increase in the intravesicular concentration $[\text{Dy}^{3+}]_i$ with time at 37°C using 28 units (∇ - ∇), 7 units (x-x) and 2 units (\blacksquare - \blacksquare) of pancreatic phospholipase A_2 per ml of vesicles (10 mg/ml egg PC). The initial stages where no increase in $[\text{Dy}^{3+}]_i$ is observed corresponds to the period when the O:I ratio is increasing.

Fig 4 Increase in the intravesicular concentration $[\text{Dy}^{3+}]_i$ with time at 37°C using egg PC vesicles (10 mg/ml) incubated with : +-+ 28 units PLA_2 ; \diamond - \diamond 0.5 mM glycocholate; x-x 0.5 mM glycodeoxycholate; ∇ - ∇ 28 units PLA_2 and 0.5 mM glycocholate; \blacksquare - \blacksquare 28 units PLA_2 and 0.5 mM glycodeoxycholate.

Fig 5 Increase in the intravesicular concentration $[Dy^{3+}]_i$ with time at 37°C using egg PC vesicles (10 mg/ml) incubated with: ▽-▽ 2 units PLA_2 ; +-+ 1 mM glycocholate; ■-■ 2 units PLA_2 and 1 mM glycocholate.

Fig 6 Increase in the intravesicular concentration $[Dy^{3+}]_i$ with time at 37°C using egg PC vesicles (10 mg/ml) incubated with: +-+ 7 units PLA_2 ; ■-■ 1 mM glycocholate; ▽-▽ 7 units PLA_2 and 1.0 mM glycocholate.

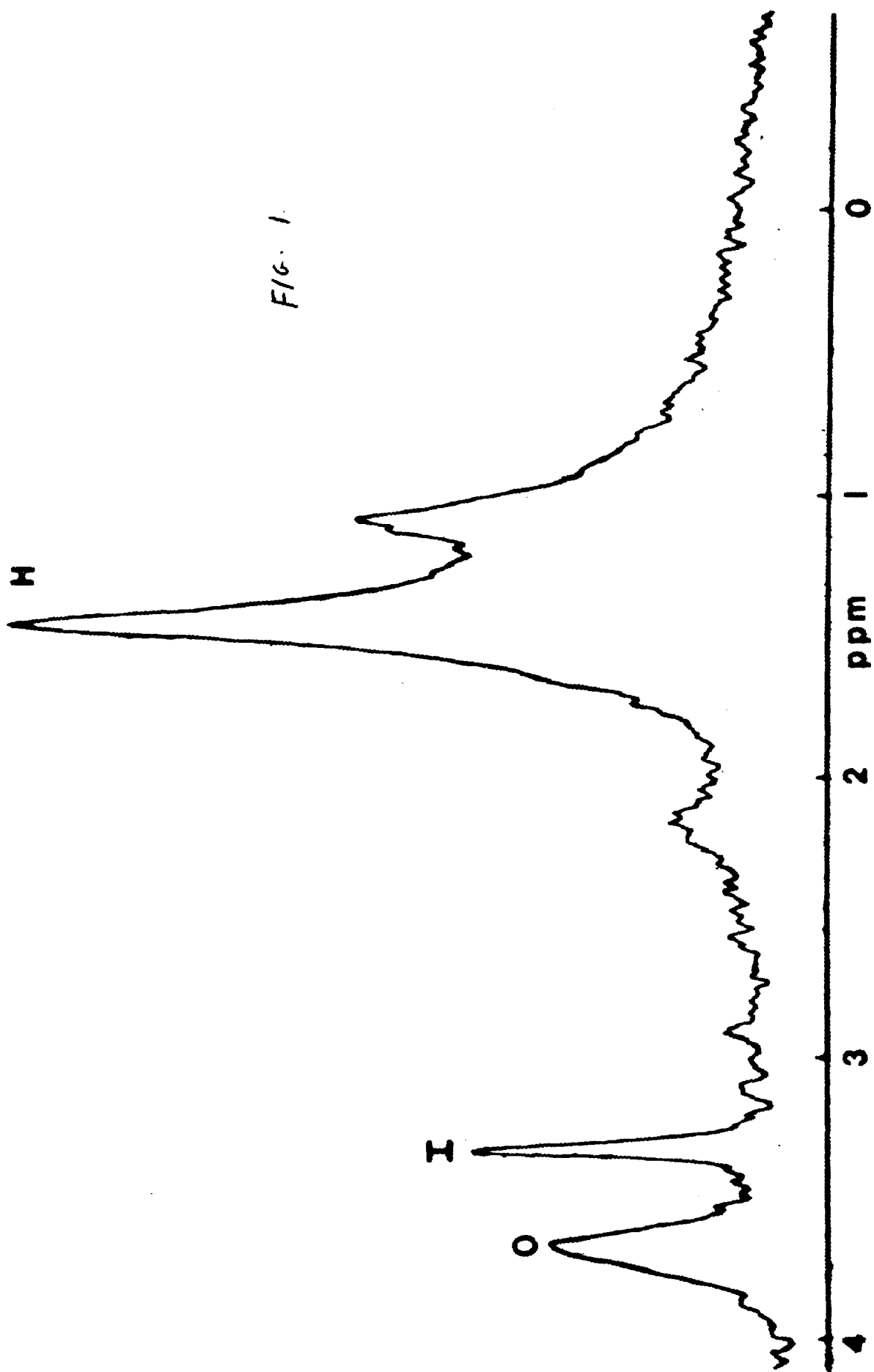
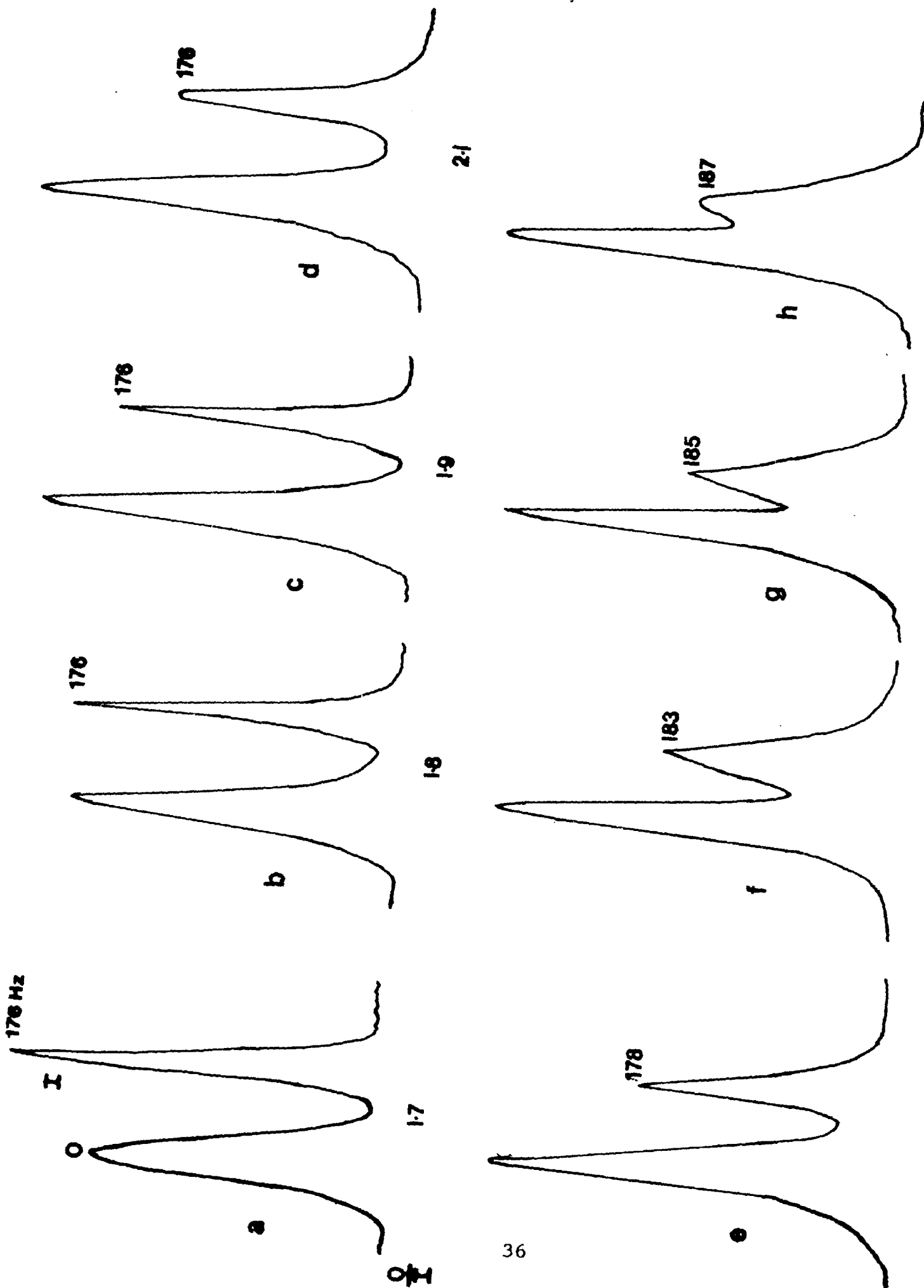


FIG. 2.



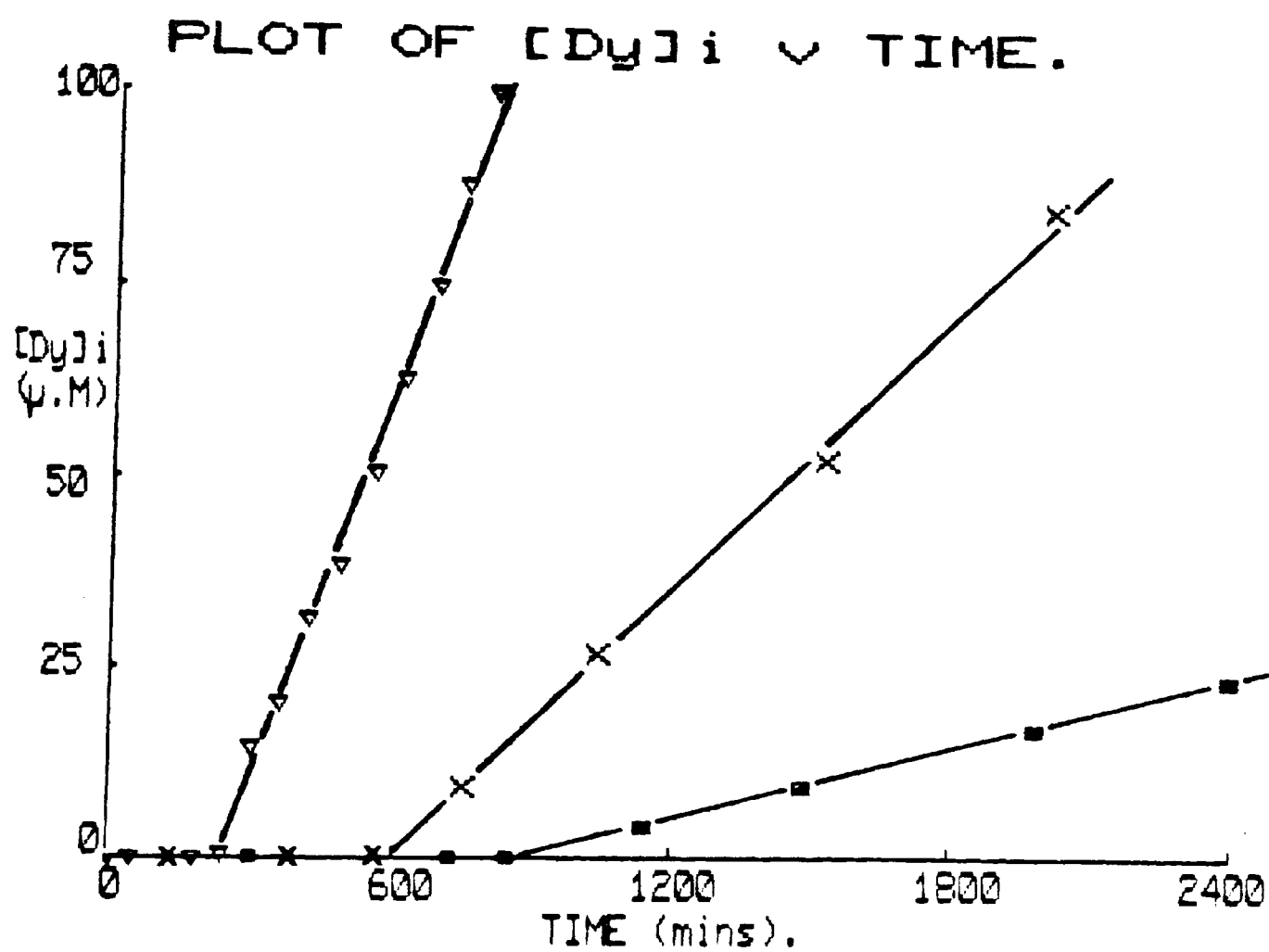


FIG 3

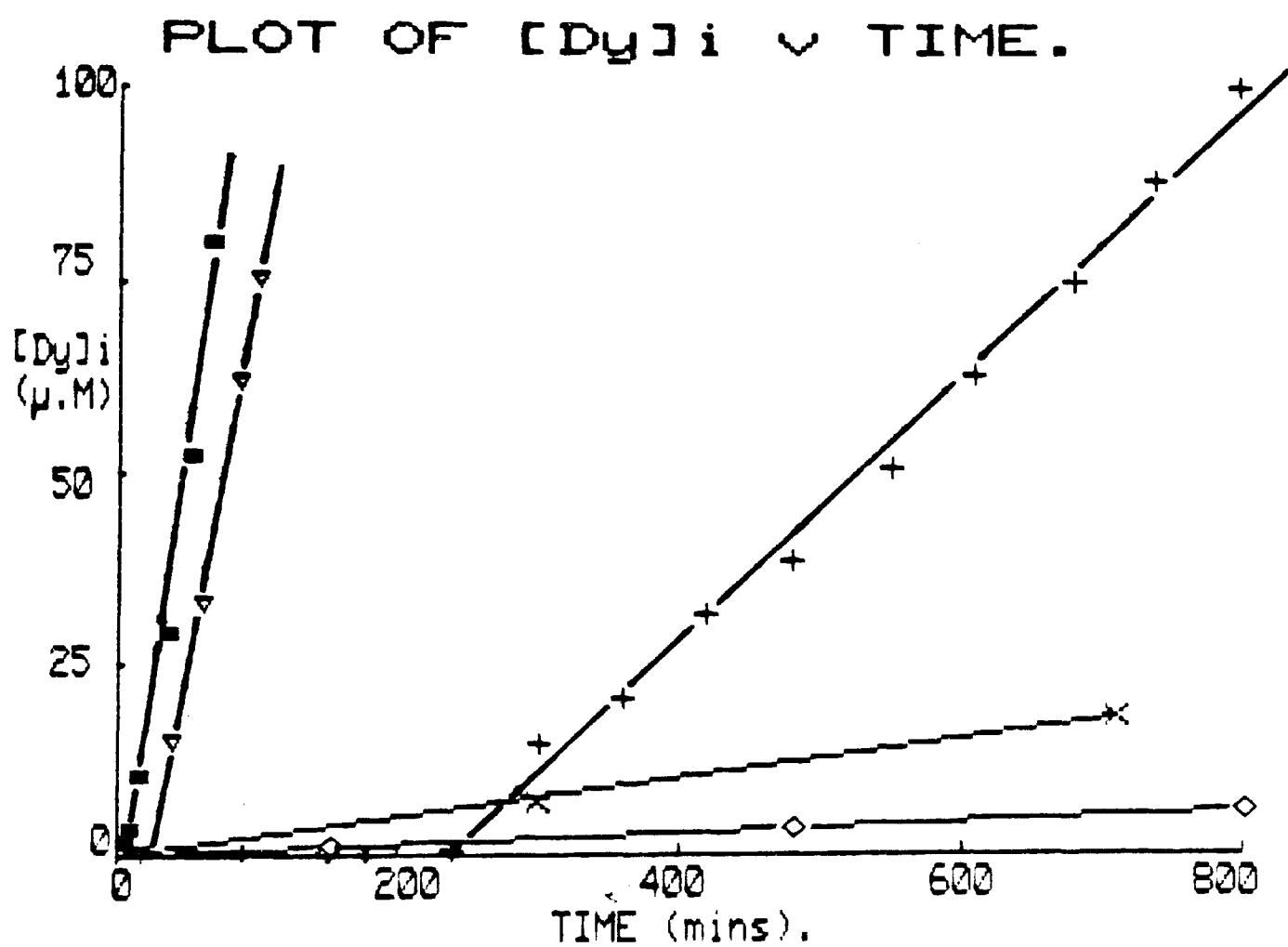


FIG. 4

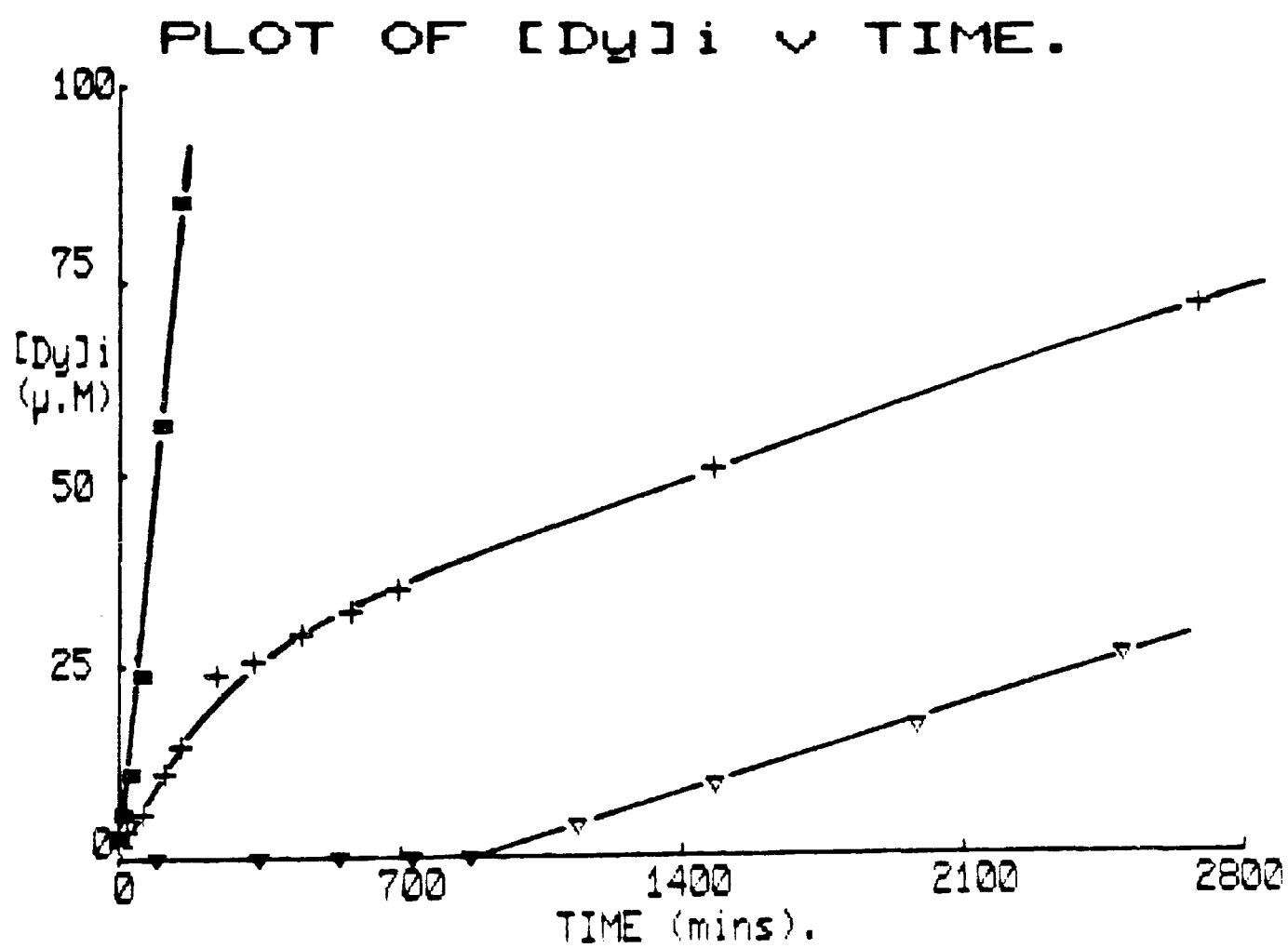


FIG 5

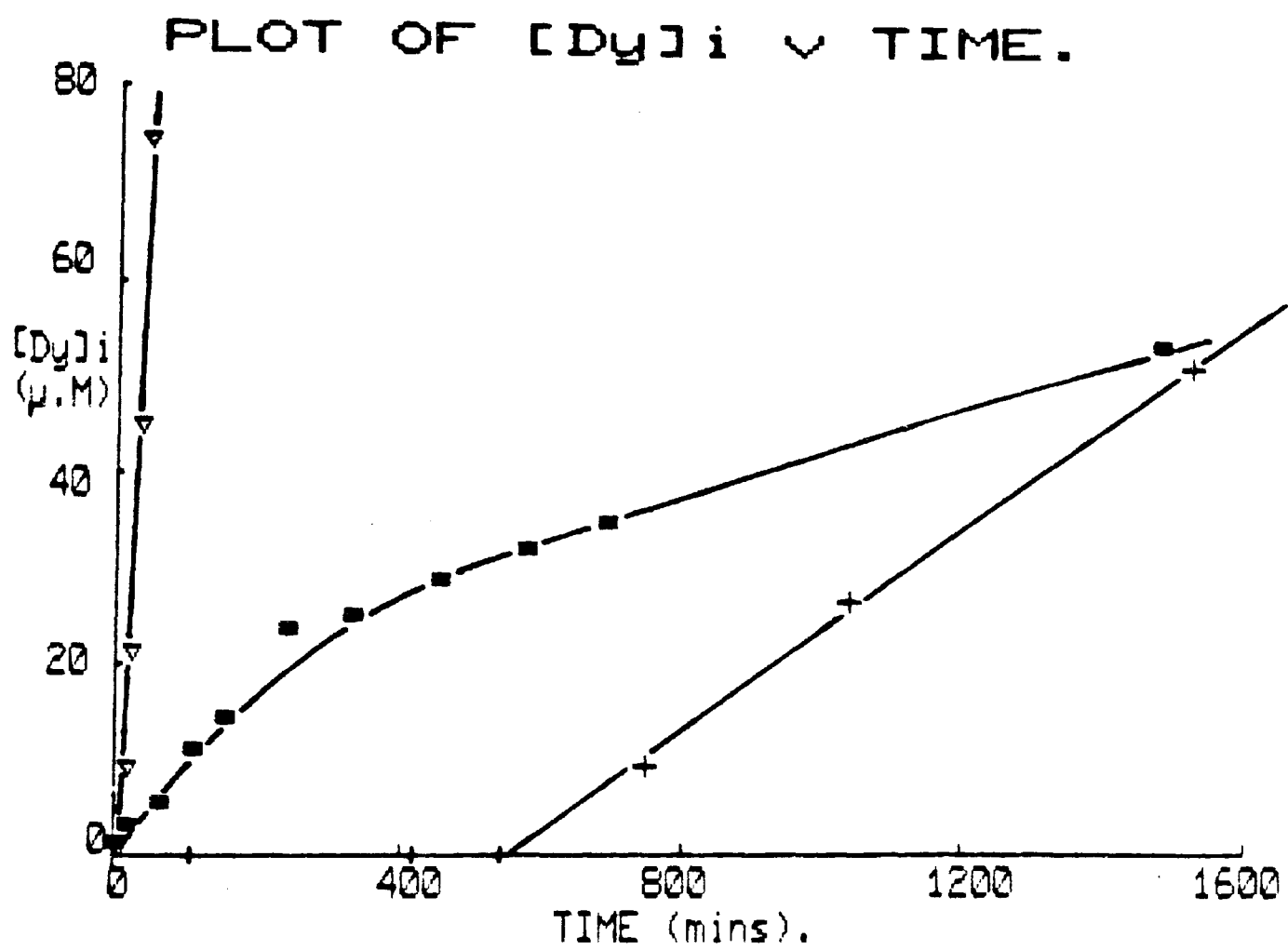


FIG 6

PHOSPHATIDIC ACID REGULATES THE ACTIVITY OF THE CHANNEL-FORMING
IONOPHORES ALAMETHICIN, MELITTIN AND NYSTATIN. A ¹H-NMR STUDY USING
PHOSPHOLIPID MEMBRANES.

G.R.A. Hunt , I.C. Jones and J.A. Veiro
The Department of science, The Polytechnic of Wales,
Pontypridd, CF37 1DL, U.K.

RUNNING TITLE: Channel regulation by phosphatidic acid.

KEYWORDS: ¹H-NMR, Phosphatidic acid, Alamethicin 30, Melittin,
Nystatin, Ion channel, Phosphatidylinositol effect, (phospholipid membranes).

ABSTRACT.

The regulation of ion channels by phosphatidic acid (a proposed active metabolite in the phosphatidylinositol effect) was investigated using ¹H-NMR spectroscopy and small unilamellar phospholipid vesicles. Transport across egg yolk phosphatidylcholine (egg PC) and dipalmitoyl phosphatidylcholine (DPPC) vesicular membranes in the presence of the channel forming ionophores alamethicin, melittin and nystatin, was monitored using the lanthanide probe ion Pr³⁺. In the absence of the ionophores, phosphatidic acid (PA) alone was found to have no ionophore properties, but in the presence of the ionophores the incorporation of 3 mole % phosphatidic acid in the bilayer markedly increased the rate of transport using melittin and nystatin, but decreased the rate using alamethicin, independent of the type of phosphatidylcholine used. The presence of PA in the bilayer also stimulated the production of lytic type channels, the extent of which were both ionophore and lipid dependent. These results are discussed in terms of possible molecular interactions between the PA, the individual ionophores and type of lipid used.

INTRODUCTION.

The link between Ca^{++} -dependent activation of cells and increased turnover of plasma membrane phosphoinositides is now well established [Michell and Kirk, 1981; Billah and Michell, 1979; Fain and Berridge, 1979]. However explanations of this PI effect in terms of the membrane activity of metabolites of phosphatidylinositol, such as phosphatidic acid (PA) and diacylglycerol (DAG) are still controversial. Thus ionophoretic properties of PA were demonstrated in model systems [Tyson et al. 1976; Serhan et al. 1981; Serhan et al. 1982] and this was claimed to be the mechanism of the PA-induced physiological responses observed [Salmon and Honeyman, 1980; Putney et al. 1980]. However recently Holmes and Yoss [1983] were unable to demonstrate transport of Ca^{++} across liposomal membranes and suggested that alternative mechanisms should be sought for the PI effect.

One such possibility is that PA could activate membrane proteins in a manner similar to DAG activation of protein kinase C [Nishizuka, 1983] or of phospholipases [Dawson et al. 1983]. A similar role can be postulated for PA, and in this report we demonstrate that physiological concentrations of phosphatidic acid in phosphatidylcholine unilamellar vesicular membranes can modulate the activity of the channel-forming polypeptides alamethicin 30 and melittin, and the polyene antibiotic nystatin.

Previous work in our laboratory [Hunt et al. 1978; Hunt, 1980] as well as that of other groups [Ting et al. 1981; Degani et al. 1978] demonstrated that NMR spectroscopy can be employed to study the transport of paramagnetic ions into phospholipid vesicles. These studies have shown that the lanthanide ion Pr^{3+} is a suitable probe ion for Ca^{++}

at least for carrier and channel-mediated transport using A23187 and alamethicin [Hunt and Jones 1982; Hunt and Jones 1983]. Voltage-dependent alamethicin channels have been extensively studied and reviewed [Rinehart, 1977; Boheim and Kolb, 1978]. Melittin-lipid interactions have been well investigated [Georghiou et al. 1982], but not the melittin channels [Tosteson and Tosteson, 1981]. Nystatin and other polyene antibiotic ionophores have been the subject of numerous studies due to the cholesterol requirement in their activity [Cass et al. 1970; Pierce et al. 1978].

In agreement with Holmes and Yoss [1983] we were unable to see any ionophore action by phosphatidic acid alone in phosphatidylcholine vesicular membranes. However, its presence in the bilayer selectively and significantly altered not only the rate of transport of Pr^{3+} via the above channel-forming ionophores but also the types of channel formed in the vesicles.

MATERIALS AND METHODS.

Egg yolk phosphatidylcholine (egg PC), synthetic dipalmitoyl phosphatidylcholine (DPPC), and egg yolk phosphatidic acid (PA) were obtained from Lipid Products, Redhill, Surrey, and were used without further purification. The ionophores melittin and nystatin were purchased from Sigma, and alamethicin 30 was obtained from the PHLS centre for Applied Microbiology and Research, Porton Down, Salisbury. Deuterium oxide (99.8%) was obtained from Aldrich, and praseodymium chloride from Lancaster Synthesis. All other chemicals were analytical grade or equivalent.

Sigma report that up to 20 units of phospholipase A have been found

per mg melittin (solid). Control experiments with bee venom phospholipase A₂ showed that 5mM Pr³⁺ inhibits phospholipase activity, which normally requires Ca⁺⁺ for enzyme activation. So that the transport observed is not due to phospholipase attack of the vesicles.

Single bilayer vesicles were prepared as previously reported [Hunt and Tipping, 1978], except that for egg PC the sonication was carried out at 4°C and under nitrogen. In all cases a final phospholipid concentration of 10 mg/ml was obtained. The incorporation of phosphatidic acid in the bilayer (3 mole % unless otherwise stated) was achieved by adding a known volume of a chloroform stock solution of the phosphatide, to the lipid chloroform solution and shaken. The solvent was then removed under a stream of nitrogen and the last traces by evacuation at 2mm Hg, and the vesicles were then prepared as above. Both alamethicin and melittin were introduced by pipetting a known volume of a ²H₂O stock solution into 1ml of vesicular solution in a 10mm NMR tube. The solution was then left to incubate for thirty minutes at 50°C. Transport was then initiated by adding the required quantity of a stock solution of praseodymium chloride in ²H₂O, to give an extravesicular Pr³⁺ concentration of 5mM. In the case of the polyene antibiotic ionophore nystatin, cholesterol is required for channel formation, as is the presence of the ionophore on both sides of the phospholipid bilayer [Cass et al. 1970]. The required amount of a stock chloroform solution of cholesterol was added to the lipid chloroform solution, in the same way as for phosphatidic acid, to give a cholesterol concentration of 10 mole %. The presence of nystatin both inside and outside the vesicles was achieved by adding the required amount of a stock solution of nystatin in ²H₂O to the dry lipid. This was shaken for sixty minutes at 50°C and then sonicated in the usual way.

The ^1H -NMR spectra were obtained on a JEOL FX90Q FT NMR spectrometer operating at 90MHz. Typically 10 pulse sequences (π - τ - $\pi/2$) were used with a pulse interval of approximately 2 seconds to minimise the $^2\text{H}^1\text{H}$ signal.

RESULTS.

The addition of 5mM praeodymium chloride to the external vesicular medium shifts the ^1H -NMR signal from the outer choline headgroups downfield. Such shifts are now well documented [Bergelson, 1978], and are caused by pseudocontact interaction of Pr^{3+} in rapid exchange between the $^2\text{H}_2\text{O}$ and phosphate sites on the headgroups of the outer monolayer. The apparent outside:inside signal ratio (O/I) is approximately 1.6 for sonications of both pure egg and dipalmitoyl phosphatidylcholine (figure 1a.), corresponding to a vesicular outer diameter of about 38nm [Hutton et al. 1977].

In the absence of ionophore the signal from the inner choline headgroup in egg PC and DPPC at 50°C is unaffected for up to several days after the addition of the Pr^{3+} to the external medium, indicating that the vesicles remained impermeable to Pr^{3+} . All transport experiments were carried out at 50°C in order to compare the effect of the two lipids (egg PC and DPPC) forming the vesicles. Even in the presence of 10 mole % cholesterol and 5mM Pr^{3+} this temperature is above the phase transition of the DPPC [Hunt and Tipping, 1978]. However in the presence of melittin, a time-dependent downfield movement of the inner choline resonance towards that of the outer resonance is observed (figure 1.e-h). This occurs as the ionophore transports Pr^{3+} ions uniformly for all the vesicles from the outer to the inner environment,

and is similar to that previously observed for alamethicin channels in vesicles [Hunt and Jones, 1982]. Since it can be calculated that these vesicles of internal diameter 25nm have an inner content of only 50 ions at 5mM, the slow movement of signal I must correspond to virtually single ion conduction across the channels.

The slight asymmetry of signal O (figure 1.c) occurs owing to the relatively high concentrations of melittin (300ug/ml) used with egg PC vesicles. The peptide will bind to some of the extravesicular phosphatidylcholine molecules, and in so doing may partly shield Pr^{3+} - headgroup interactions. Since it has been reported [Dufourcq and Faucon, 1977] that 1 melittin molecule requires 25 PC molecules for complete binding, we can readily calculate that at 300ug melittin : 10mg PC, approximately one third of the PC molecules in the outer monolayer of the vesicles will be bound to melittin. This is completely adequate to explain the shoulder observed. Asymmetry is not observed with DPPC vesicles due to the much lower concentration of melittin (40ug/ml) used.

Similar time-dependent spectra were obtained using egg PC and DPPC vesicles with the ionophores alamethicin (40ug/ml and 20ug/ml respectively) and nystatin (300ug/ml and 100ug/ml respectively), the latter experiments also including 10 mole % cholesterol in the egg PC and DPPC vesicles. However no asymmetry of the head-group signal is seen with these vesicles. Shifts of signal I are converted into intravesicular Pr^{3+} concentrations $[\text{Pr}^{3+}]_i$ using calibration graphs [Hunt, Tipping and Belmont, 1978]. Plots of $[\text{Pr}^{3+}]_i$ against time enable the rate of transport of the probe ion to be calculated from the gradients. As seen in figures 2, 3 and 4 the gradients of the plots obtained show that using the same concentrations of ionophores as for the controls, incorporation of phosphatidic acid into the vesicular

bilayer brings about an increase in the rate of mediated transport of Pr^{3+} by the ionophores melittin and nystatin (figs. 2 and 3) but a marked decrease in transport rate when alamethicin is used (fig. 4). This is consistent for both types of phosphatidylcholine vesicles.

The presence of phosphatidic acid in the bilayer also induces asymmetry of the outer choline signal. A shoulder is observed on the low field side of the signal (figure 1.b) which can be readily interpreted as arising from phosphatidylcholine molecules adjacent to phosphatidic acid molecules. The negative charge of phosphatidic acid enhances the binding of the metal ion to the adjacent phosphatidylcholine molecules, which would cause a greater downfield shift of the choline signal. The O/I ratio under these experimental conditions are slightly higher at 1.7, than for pure lipid without ionophores, probably due to asymmetry of the phosphatidate which shows preference for the inner monolayer of small vesicles [Berden et al. 1975]. Figure 1.d shows the combined effect of the presence of both melittin and PA on the symmetry of the outer choline signal in the presence of 5mM Pr^{3+} .

Additional features in the spectra obtained indicate that under certain of the experimental conditions channels are formed with different characteristics than those allowing the slow homogeneous passage of ions described above. Thus with egg PC/PA/cholesterol vesicles in the presence of nystatin the spectrum in fig. 5(b) shows not only the outer O and inner I headgroup signals on addition of 5mM extravesicular Pr^{3+} , but also an intermediate signal I'. From the calibration graphs it can be estimated that this signal originates from the inner headgroups of vesicles having $[\text{Pr}^{3+}]_i =$ to 0.5mM (or about 5 ions per vesicle). This behaviour is similar to that observed previously

using DPPC/cholesterol vesicles and bile salts as ionophores [Hunt and Jawaharlal, 1980]. With time, signal I is seen to shift downfield to a position under signal I' which has remained stationary up to this point. The combined inner signal then shifts and broadens with time (fig 5.b-f).

Using alamethicin in egg PC/PA vesicles a similar behaviour is observed, but here the intermediate signal I' is seen to develop with time rather than appear immediately after the Pr^{3+} addition, and the position of I' corresponds to vesicles which receive 2mM Pr^{3+} (20 ions per vesicles) intravesicularly. In the case of melittin and egg PC/PA vesicles, the uniform downfield shift of signal I is observed without the appearance of intermediate signals, so the effect of PA on melittin channels in egg PC vesicles is to increase the rate of slow transport without promoting additional channels which allow rapid passage of ions across the bilayer.

Finally, the spectra of DPPC/PA vesicles in the presence of alamethicin and melittin and of DPPC/PA/cholesterol vesicles with nystatin all show high O/I ratios on addition of the 5 mM Pr^{3+} , the values being 2.3 for melittin and nystatin, and 2.1 for alamethicin. Signal I, however, moves smoothly downfield with time showing only slight asymmetry. The increase in O/I ratio for these vesicles can be explained by the transfer of part of the intensity from the inner cholines to a position under the outer choline signal (i.e. a signal I' is now located under O). This corresponds to a process we have previously described as lysis [Hunt and Jones 1983] to indicate that a rapid equilibration of the 5mM Pr^{3+} takes place across the channels in the fraction of the vesicular population having inner headgroup signal I' . Thus the use of DPPC instead of egg PC in vesicles containing PA has

the effect of allowing complete equilibration of the 5mM Pr^{3+} across the lytic type channels, instead of the partial rise of $[\text{Pr}^{3+}]_i$ to 0.5mM or 2mM using nystatin and alamethicin in egg PC/PA vesicles. There is however complete absence of this type of channel using melittin in egg PC/PA vesicles, despite the larger quantities of melittin used compared to the DPPC vesicles.

DISCUSSION.

Experiments on the conductivity of planar lipid membrane indicates that the higher conducting alamethicin channels are formed by an increase in the average diameter of the channel rather than increases in channel life times [Eisenberg et al.1977]. The diameter of these channels clearly will be critical in determining whether a slow passage of ions (possibly partially desolvated of water molecules) occurs in narrow channels or a more rapid equilibration of the fully solvated ions in wider channels. We observed the former type behaviour in the case of alamethicin channels in DPPC vesicles [Hunt and Jones, 1982] where the stoichiometry was determined as four ionophore molecules per channel and hence a narrow channel is formed.

For alamethicin the effective channel diameter is probably dictated by the ring of glutamine 7 residues which are hydrogen bond linked [Fox and Richards, 1983]. While corresponding data is not available for melittin and nystatin channels, our results shown in figs. 2-4 indicate that the slow rate of transport deduced from the uniform downfield shift of signal I observed in alamethicin, melittin and nystatin channels in both types of lipid are likely to result from single ion transport in narrow channels. The effects of PA on these channels, as shown in

figs. 2-4, depends upon the ionophore in question. The incorporation of PA in the bilayer is expected to increase electrostatic and hydrogen bond interactions at the vesicular surface. The former will be particularly relevant in the case of melittin since the polypeptide has a large hydrophobic amino acid sequence but a terminal segment with four positively charged amino acids two lysines and two argenines [Hanke et al. 1983] So increased channel life-time should be expected for melittin in PA containing vesicles, due to favourable electrostatic interactions with the bilayer. The reduced rate of transport for alamethicin in PA can also be related to the negative charge carried on the peptide by the glutamic acid at position 18 [Fox and Richards, 1983]. In the case of nystatin one would not expect electrostatic interactions to be so significant, but hydrogen bonding effects via the hydroxyl group on cholesterol, which have recently been shown to be altered by changes in lipid composition [Chauhan et al. 1984] could be important.

Further examination of fig.5 enables us to interpret the remaining features of the results in terms of large diameter channels which will allow rapid equilibration of the Pr^{3+} ions across the vesicular bilayers. The fact that signal I' appears immediately after addition of the Pr^{3+} indicates that initially not all vesicles are behaving in the same way. This could well result from an initial non-homogeneous distribution of the ionophore during the preparation of the PA-containing vesicles, with those vesicles having most nystatin able to form large channels. Separate signals I' and I persisting for some time also implies a slow rate of exchange of ionophore between vesicles. The concentration of $[\text{Pr}^{3+}]_i = 0.5\text{mM}$ suggests that these large channels close under the influence of the transmembrane potential set up by the unequal concentrations of ions. After this initial opening and closing

of these large voltage dependent channels, the slow downfield movement of signal I (fig.5.b-f) indicates that the slow channels are still open and single ion conduction continues. Finally when I and I' merge they continue to move downfield together showing that all vesicles have formed the slow channels, which are not voltage dependent or allow transport of anions or counter transport of protons so that potentials are not set up.

In the case of melittin in egg PC/PA vesicles no large channels are formed even using 300 μ g ionophore per 10mg egg PC. However the effect of PA is to accelerate the rates of slow channel conduction probably by stabilising channel life-times as discussed above. It is interesting that one of the few planar bilayer conductivity studies of melittin channels indicate a stoichiometry of only four monomers per channel i.e. a narrow channel seems more stable [Tosteson and Tosteson, 1982].

For the PA/DPPC bilayers, all the ionophores show the lytic type of channel allowing complete equilibration of 5mM Pr^{3+} across the vesicular membranes. These channels do not seem to be closed by a transmembrane potential, or this potential may not be set up due to a co-equilibration of anions. DPPC therefore stabilises the formation of large channels and although comparisons are more difficult to make with egg PC (where different concentrations of ionophores were used) we also observe that DPPC accelerates the narrow channel transport. These effects would seem to be related to the lower fluidity and increased order of DPPC bilayers producing a favourable environment for the alignment of channel-forming ionophore monomers.

The above observations strongly suggest additional possible mechanisms for the importance of the role of phosphatidic acid in the

inositol effect which accompanies receptor mediated membrane phenomenon. Nayar et al [1981] have shown that the predilection of phosphatidylinositol for the bilayer organisation both in the presence and absence of calcium argues against a dynamic role of phosphatidylinositol per se in Ca^{2+} transport. They suggests that phosphatidylinositol primarily possesses a structural role, but its enzymatically generated derivatives play dynamic roles in transbilayer transport, not by acting as ionophores but by affecting the transport proteins themselves. A model for this behaviour is seen in the influence of phosphatidic acid on the antibiotic and polypeptides reported above.

ACKNOWLEDGEMENT.

We are grateful to Dr Hans Brockerhoff for communicating his results prior to publication, and to Mrs Morris, the departmental secretary, for assistance in preparing the manuscript.

REFERENCES.

- Berden JA, Baker RW, and Radda GK (1975) *Biochim. Biophys. Acta* 375, 186-208
- Bergelson LD (1978) in *Methods in Membrane Biology* (Korn E, ed.), vol. 9, pp 257-335
- Billah MM and Michell RH (1979) *Biochem. J.* 182, 661-681
- Boheim G and Kolb HA (1978) *J. membrane Biol.* 38, 99-150
- Cass A, Finkelstein A, and Krespi V (1970) *J. Gen. Physiol.* 56, 100-124
- Chauhan VPS, Ramsammy LS, and Brockerhoff H (1984) submitted to *Biochim. Biophys. Acta*
- Dawson RMC, Hemington NL, and Irvine RF (1983) *Biochim. Biophys. Res. Commun.* 117, 196-201
- Degani H, Simon S, and McLaughlin AC (1981) *Biochim. Biophys. Acta* 646, 320-328
- Dufourcq J and Faucon J-F (1977) *Biochim. Biophys. Acta* 467, 1-11
- Eisenberg M, Kleinberg ME and Shaper JH (1977) *Ann. N.Y. Acad. Sci.* 303, 281-291
- Fain JN and Berridge MJ (1979) *Biochem. J.* 180, 665-681
- Fox RO and Richards FM (1982) *Nature* 300, 325-330
- Georghiou s, Thompson M and Mukhopadhyay AK (1982) *Biophys. J.* 37, 159-161
- Hanke W, Methfessel C, Wilmsen H-U, Katz E, Jung G, and Boheim G (1983) *Biochim. Biophys. Acta* 727, 108-114
- Holmes RP and Yoss NL (1983) *Nature* 305, 637-638
- Hunt GRA (1980) *Phys. Chem. Lipids* 27, 353-364
- Hunt GRA and Jawahalal K (1980) *Biochim. Biophys. Acta* 601, 678-684
- Hunt GRA and Jones IC (1982) *Biosci. Rep.* 2, 921-928
- Hunt GRA and Jones IC (1983) *Biochim. Biophys. Acta* 736, 1-10
- Hunt GRA and Tipping LRH (1978) *Biochim. Biophys. Acta* 507, 242-261
- Hunt GRA, Tipping LRH, and Belmont MR (1978) *Biophysical Chem.* 8, 341-355
- Hutton WC, Yeagle PL and Martin RB (1977) *Chem. Phys. Lipids* 19, 255-265

- Michell RH and Kirk CJ (1981) Trends Pharmacol. Sci. 2, 86-89
- Nayar R, Schmid SL, Hope MJ, and Cullis PR (1982) Biochim. Biophys. Acta 688, 169-176
- Nishizuka Y (1983) Phil. Trans. R. Soc. Lond. B202, 101-112
- Pierce HD Jr., Unran AM, and Oehlschlager AC (1978) Can. J. Biochem. 56, 801-807
- Putney JW, Weiss SJ, Van DE Walle CM, and Haddas RA (1980) Nature 284, 345-347
- Salmon DM and Honeyman TW (1980) Nature 284, 344-345
- Serhan CN, Anderson P, Goodman E, Dunham PB, and Weissmann G (1981) J. Biol. Chem. 256, 2736-2741
- Serhan CN, Fridovich J, Goetzl EJ, Dunham PB, and Weissmann G (1982) J. Biol. Chem. 257, 4746-4752
- Ting TZ, Hagan PS, Chan SI, Doll JD, and Springer CS Jr. (1981) Biophys. J. 34, 189-216
- Tosteson MT and Tosteson DC (1981) Biophys. J. 36, 109-116
- Tyson CA, Zande HV, and Green DE (1976) J. Biol. Chem. 251, 1326-1332

CAPTIONS FOR FIGURES.

Figure. 1

a) 90 MHz ^1H -NMR spectrum of egg PC vesicles (10mg/ml) at 50°C in the presence of 5mM Pr^{3+} , showing signals from the extravesicular choline headgroups (O); the intravesicular choline headgroup (I); and the lipid acyl chain signals (H). Figures b-d, show the initial spectrum of signals O and I in the presence of; b) 3 mole % PA in the vesicular bilayer; c) 300 μg extravesicular melittin per 10mg egg PC.; d) Both PA and melittin at the above concentrations and conditions. Figures e-h, show the result of transport of Pr^{3+} from the outside to the inside of egg PC vesicles, mediated by melittin channels (300 μg /10mg egg PC). Shifts of signal I are measured with respect to signal H and are shown after the following time intervals, e) 11 mins. f) 32 mins. g) 103 mins. h) 245 mins.

Figure. 2

Increase in the intravesicular Pr^{3+} concentration as a function of time at 50°C , with an extravesicular Pr^{3+} concentration of 5mM using; a) $\nabla - \nabla$ 300 μg melittin per 10mg egg PC vesicles; b) $+ - +$ as a) but with the incorporation of 3 mole % PA in the vesicular bilayer; c) $\times - \times$ 40 μg melittin per 10mg DPPC; d) $\blacksquare - \blacksquare$ as c) but with the incorporation of 3 mole % PA in the bilayer.

Figure 3

Increase in the intravesicular concentration of Pr^{3+} as a function of time at 50°C using; a) $\times - \times$ 300 μg nystatin per 10mg egg PC; b) $\blacksquare - \blacksquare$ as a) but with the presence of 3 mole % Pa in the vesicular bilayer; c) $\nabla - \nabla$ 100 μg nystatin per 10mg DPPC vesicles; d) $+ - +$ as c) but with the

presence of 3 mole % PA in the bilayer. In each case the lipid was cosonicated with cholesterol (10 mole) % and the ionophore was present in both monolayers.

Figure. 4

Increase in the intravesicular concentration $[\text{Pr}^{3+}]_i$, of Pr^{3+} as a function of time at 50°C using; a) $+ - +$ 20 μg alamethicin 30 per 10mg DPPC vesicles; b) $\times - \times$ as a) but with the incorporation of 3 mole % PA in the phospholipid bilayer; c) $\blacksquare - \blacksquare$ 40 μg alamethicin 30 per 10mg egg PC vesicles; d) $\nabla - \nabla$ as c) but with the incorporation of 5 mole % PA in the bilayer. In each case an extravesicular Pr^{3+} concentration of 5mM is used.

Figure. 5

a) ^1H -NMR spectrum of egg PC vesicles cosonicated with cholesterol (10 mole %) and nystatin (300 μg per 10mg egg PC) in the presence of 5mM Pr^{3+} at 50°C . Spectra b-f show the signal brought about by the initial partial lysis I' , and transport of Pr^{3+} from the outer to inner vesicular environment mediated by nystatin with the inclusion of 3 mole % PA in the vesicular bilayer after; b) 105 mins. c) 305 mins. d) 485 mins. e) 1460 mins. f) 2790 mins.

FIG 1

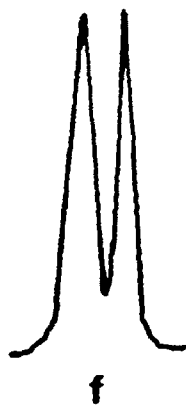
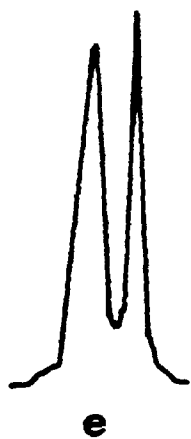
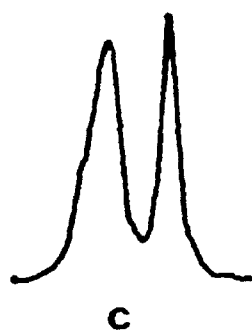
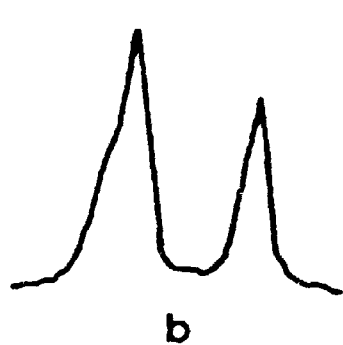
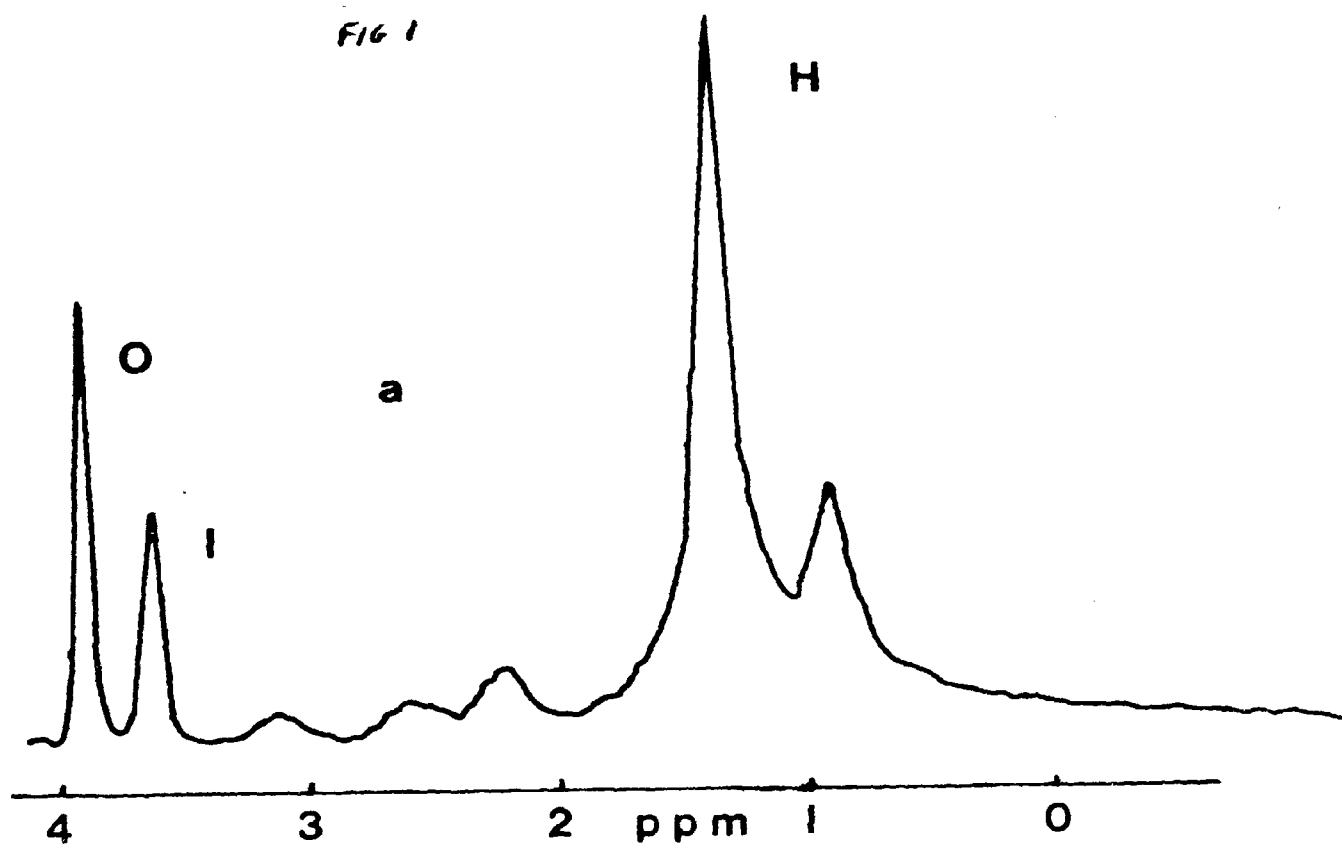


FIG. 2

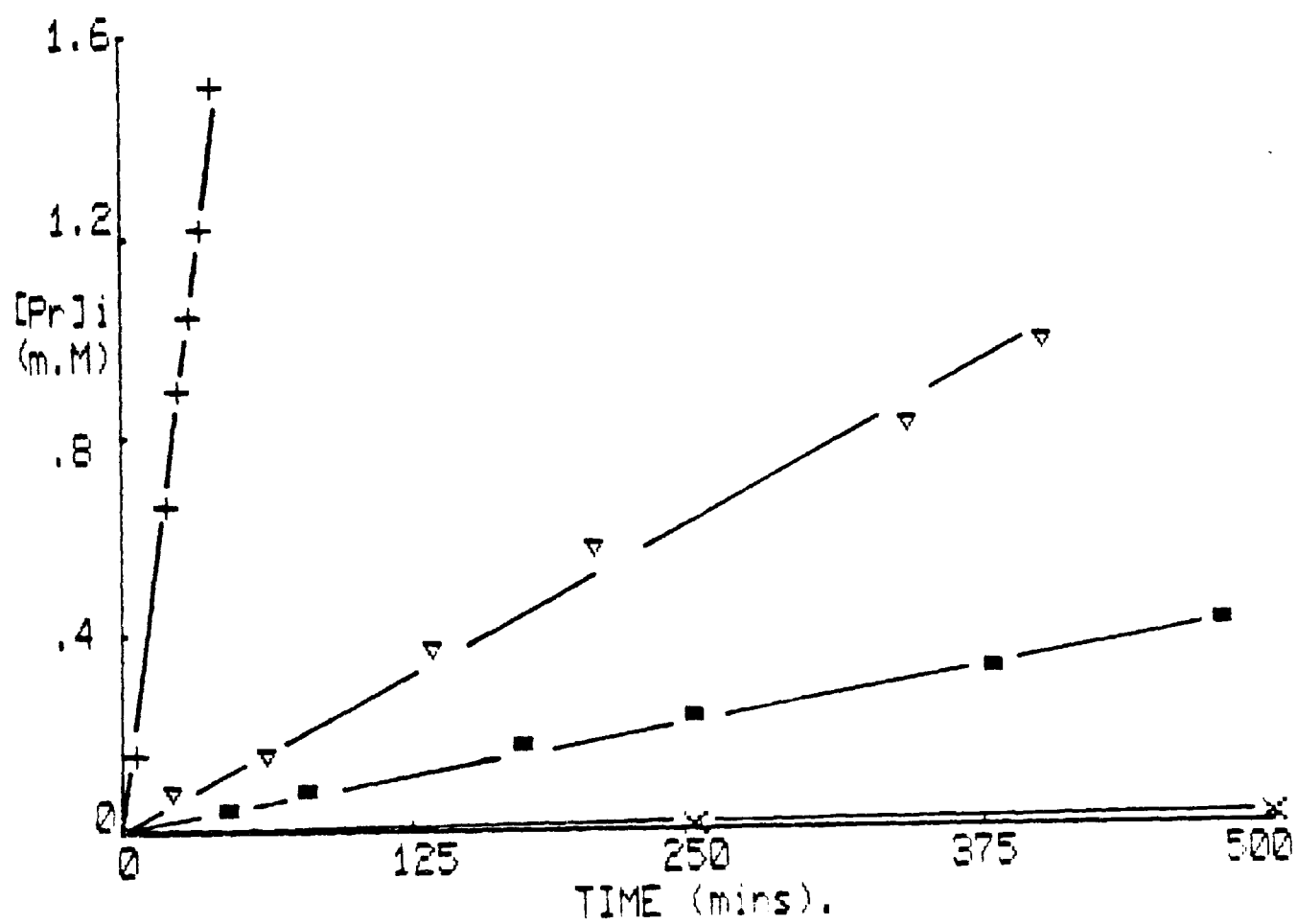


FIG. 3

